Microbial co-existence and stable equilibria in a mechanistic model of enteric methane production

A thesis presented in partial fulfillment of the requirements
for the degree of

Doctor of Philosophy
in
Mathematics

at Massey University, Manawatū Campus,
New Zealand

Yuancheng Wang
2016

Abstract

Globally, 14.5% of all anthropogenic greenhouse gases come from ruminants. One of these is methane, which is produced in the rumen of ruminant animals. Feed is degraded by microbes to produce volatile fatty acids (which are absorbed by the animal) and hydrogen (which is metabolized by methanogens to form methane). The dynamics of hydrogen production and metabolism are subject to thermodynamic control imposed by the hydrogen concentration. Existing models to estimate methane production are based on calculation of hydrogen balances without considering the presence of methanogens and do not include thermodynamic control. In this project, a model is developed based on glucose-hydrogen-methanogen dynamics to estimate methane production and illustrates a co-existence of microbes that employs different fermentation pathways competing for the same food source in the rumen. Glucose was chosen as an example of a fermentable feed component. A thermodynamic term was integrated into a Monod-type model to represent the thermodynamic control of hydrogen concentration on the rates of hydrogen generation and hydrogen metabolism. Results of this model suggest that the microbial community composition and the combination of the different pathways are determined by the rumen environment, biological parameters of the microbes and the feedback imposed by substrate and product concentrations. The mathematical enunciation of this model is therefore consistent with biological expectations. This model could be expanded to include plant polymer degradation rate, feeding level and feeding frequency to explore their effects on methane production. This model could also be integrated into models of whole rumen function to address more complex questions. It would also support experimentation

with animals for understanding factors that control methane formation and to explore methane mitigation strategies.

Acknowledgements

This project would not have been possible without the contributions of people along the journey of this research. My sincere thanks go to my parents for their continuous support. I would like to express my gratitude to my supervisors: Dr. Tammy A. Lynch, Associate Professor Bruce Van Brunt, Dr. Peter H. Janssen and Dr. David Pacheco, for their guidance and inspiration throughout this challenge. I enjoyed learning and working with this team. Thank you for your effort and time on proofreading reports, manuscripts, and this thesis. The visit of Dr. Mark I. Nelson, University of Wollongong, to discuss my works is greatly appreciated. Many thanks to Dr Indrakumar Vetharaniam and Dr Ronaldo Vibart, AgResearch, for valuable feedback on the manuscript. I would like to acknowledge the stipend from the New Zealand Agricultural Greenhouse Gas Research Centre (NZAGRC) and the combined methane mitigation program of the NZAGRC and the Pastoral Greenhouse Gas Research Consortium. Thanks to the Institute of Fundamental Sciences of Massey University, Manawatū Campus and AgResearch, Grassland Research Centre, for hosting my study. Thanks are also due to the IT, academic and administrative staff at the Institute of Fundamental Sciences and AgResearch for their direct and indirect assistance. The interactions with my office mates and other PhD students including: Ali Ashher Zaidi, Saima Gul, Yang Li, Nick Palevich and Preeti Raju are treasured. It is my privilege to present this work combining all these efforts to you.

Contents

List of Figures

List of Tables

Abbreviations

ADP	Adenosine diphosphate
ATP	Adenosine triphosphate (used by microbes for maintenance and reproduction)
VFA	Volatile fatty acids (e.g., acetate, propionate and butyrate)
HM	Hydrogen-methanogen dynamics
HM^{θ}	Hydrogen-methanogen dynamics with thermodynamic term
GHM^{θ}	Glucose-hydrogen-methanogen dynamics with thermodynamic term

Nomenclature

Subscript

Substrate	Description
h	hydrogen
g	glucose
A	acetate
P	propionate
B	butyrate

Microbe	Description
m	methanogens
i	glucose fermenters

Superscript

Notation	Description
$*$	equilibrium point (steady state solution) of variables

Variables

Notation	Description	Unit
t	time	s
S	substrate concentration	mol ml^{-1}
X	microbe population density	cell ml^{-1}
θ	thermodynamic term	unitless
M	estimated methane production	$rumen^{-1}$ d^{-1}

Parameters

Rumen environment	Description	Unit
α	passage rate through the rumen	s^{-1}
β	rate of substrate generation	mol ml^{-1} s^{-1}
γ	absorption rate of substrate	s^{-1}

Microbe	Description	Unit
q	maximal rate at which a microbe can metabolize substrate	mol $cell^{-1}$ s^{-1}
K	substrate concentration at half of q assuming no thermodynamic feedback	mol ml^{-1}
w	moles of product generated from metabolizing per mole of substrate	unitless
n	ATP gained by microbe from metabolizing per mole of substrate	mol_{ATP} mol^{-1}
m	maintenance requirement of a microbe	mol_{ATP} $cell^{-1}$ s^{-1}
Y	reproduction coefficient of microbe	cell mol_{ATP}^{-1}
μ	reproduction rate of microbe	s^{-1}
d	death coefficient of microbe	s^{-1}

Thermodynamic term	Description	Unit
T	temperature	K
$\mathcal{R}$	ideal gas constant	kJ mol^{-1} K^{-1}
ΔG_T^o	Gibbs free energy of a chemical reaction at T under standard conditions	kJ mol^{-1}
ΔG_{ATP}	energy required to generate one unit of ATP	kJ mol_{ATP}^{-1}

Chapter 1

Background

1.1 Methane

Methane comes from either natural systems (e.g., wetlands and lakes [176], [187]) or anthropogenic sources. These anthropogenic activities include some that are biological sources of methane and others that release methane through industrial processes. As the world's population passes seven billion [167], methane emissions due to anthropogenic activities are increasing. Major anthropogenic activities that produce methane and have a biological source include rice cultivation in paddies [20]; waste treatment, to maintain habitable surroundings [122] and ruminants-based agriculture (e.g., cattle, sheep and goats) [52], to meet food demand (e.g., rice, milk, meat and other animal products).

After carbon dioxide, methane is the next most abundant greenhouse gas (GHG) in the Earth's atmosphere, followed by nitrous oxide and ozone [11]. Over a 100-year time horizon, methane is 25 times more effective than carbon dioxide, by weight, at absorbing long-wave radiation [71]. This traps heat in the atmosphere resulting in global warming and climate change.

Worldwide, 14.5% of all anthropogenic GHG come from ruminants [137]. In 2013, ruminants-based agriculture produced about half of New Zealand's total anthropogenic GHG emissions [112]. Methane emissions from ruminants contribute about 40% of all of New Zealand's anthropogenic GHG emissions [112]. Meanwhile, in 2013, about a third of

New Zealand's export earnings (nearly NZ $20 billion) came from animal products [148]. New Zealand's government has committed to reducing GHG emissions to below their 1990 levels [111]. There is growing interest in reducing GHG emissions from ruminants, especially methane, while maintaining animal productivity and controlling global warming. Thus, the long-term sustainable prosperity of pastoral agriculture requires the development of strategies to reduce methane emissions, while maintaining and even increasing animal product output to meet the requirements of a growing human population.

1.2 Ruminants

1.2.1 Rumen, it's microbial ecosystem and passage rate

The digestive tract of ruminants has a four-compartment digestive forestomach and stomach that digests feed before it enters the lower gastrointestinal tract. The four compartments of forestomach are the rumen, reticulum, omasum, and abomasum (Figure 1.1). The first two compartments are often simply called the rumen, and are the major site of microbial digestion of the ingested feed. Together, these make up about 64–69% of the total volume of the four compartments [35]. The omasum serves to return large feed particles back to the reticulum, while smaller particles and liquid can enter the abomasum [174]. The abomasum is the true mammalian stomach in which food is broken down by enzymes and microbes. The temperature of the rumen is around 39°C and it is essentially anaerobic [67]. The rumen never empties, even during fasting. The pH of a normally functioning rumen is between 5.6 and 6.7 [85]. The rumen can contain 60–120 kg of contents in cattle and 4–8 kg in sheep [174], and its contents make up 8–15% of the total animal weight [70].

Ruminants in agricultural systems are normally fed forages and grains, both separately and as mixtures. The total daily feed intake of a ruminant is about 1–3 times the volume of the rumen [70]. Food ingested by ruminants is retained in the rumen, and there it undergoes microbial col-

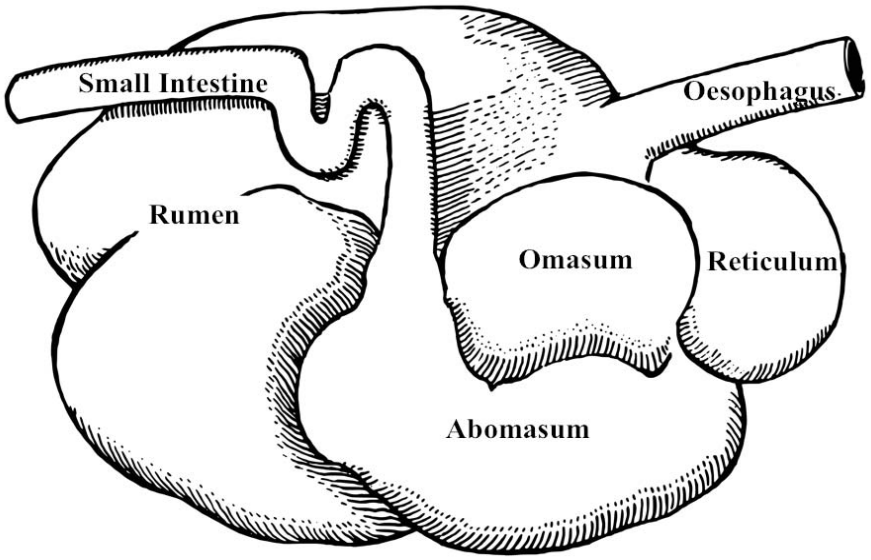

Figure 1.1: The gastrointestinal tract of an adult cattle. This figure was modified from a raw image from Wikimedia Commons, original donated by Pearson Scott Foresman.

onization, digestion and feed fermentation. The microbes in the rumen act on the fermentable plant components in the feed, much of which is not able to be digested by the mammalian digestive system. The particle size of the feed is reduced by mastication and then subsequent rumination. During rumination, digesta in the reticulum are regurgitated, re-chewed, and returned to the rumen. Each milliliter of rumen liquid contains 10^{10} to 10^{11} bacterial cells, 10^8 to 10^9 methanogens, and 10^5 to 10^6 protozoa [70]. These microbes make up a globally universal microbial ecosystem in the rumen [55]. They appear to be specialists found only in the rumen, and in a few other functionally and physiologically similar digestive systems, such as those found in camelids, macropods and hoatzin [55]. The proportions of the microbial species in the rumen change when different feeds are fed [43], [55]. Feed and microbes pass through the rumen as ruminants keep ingesting feed (and/or drinking liquid and secreting saliva), with the flow of material out of the rumen being commonly described as the (fractional) passage or outflow rate. Large particles are

retained in the rumen, while there is a preferential outflow of smaller particles. When smaller quantities or less digestible feeds are eaten, the passage rate is slower [105].

The microbes inhabiting the rumen need to reproduce at a rate that replaces those washed out from the rumen, otherwise their populations would be eliminated. Microbes gain energy from feed fermentation for maintenance and reproduction. The microbes grow using an energy source that is part of the feed ingested by the animal, or is derived by the actions of other microbes on that feed. This energy source is commonly referred to as the growth substrate or simply substrate. The steady state is a dynamic equilibrium state where the reproduction rate of the microbe (on average) matches the passage rate. For microbes, there is expected to be a dynamic but average steady state substrate concentration (assuming the animal has a similar feed intake over time) that ensures such an average growth rate [76], [133]. Microbial populations will also maintain a quasi-steady-state size while the same feed is ingested. On average, therefore, the rumen approximates a continuous culture system with a turnover that determines a substrate concentration and allows a microbial population that uses that substrate to reproduce at a rate that maintains its population size while undergoing a continuously constant fractional passage rate [133].

1.2.2 Hydrogen, methanogens and methane

The amount of feed consumed by ruminants is the major driver of methane formation: the correlation between the methane production and the amount of feed consumed is at least 90% [88]. Different combinations of feeds result in different mixtures of end products that lead to different amounts of methane production per unit of feed [7], [80], [114]. The main end products from the primary fermentation of feed (Figure 1.2) are volatile fatty acids (e.g., acetate, propionate and butyrate, listed in order of increasing carbon chain length), hydrogen (metabolized by methanogens to form methane), carbon dioxide, ammonia, and microbial cells. The result is that the feeds are transformed into products the

ruminants can use. For example, volatile fatty acids are absorbed across the rumen wall and either used as an energy source for the animal or converted into animal products, and the microbial cells are digested in the lower digestive tract as a source of protein for the ruminants [70]. Acetate is normally the main volatile fatty acid produced in the rumen [33]. The ratio of the different volatile fatty acids is important for animal agriculture: the volatile fatty acids profile is associated with milk production and milk fat content [33].

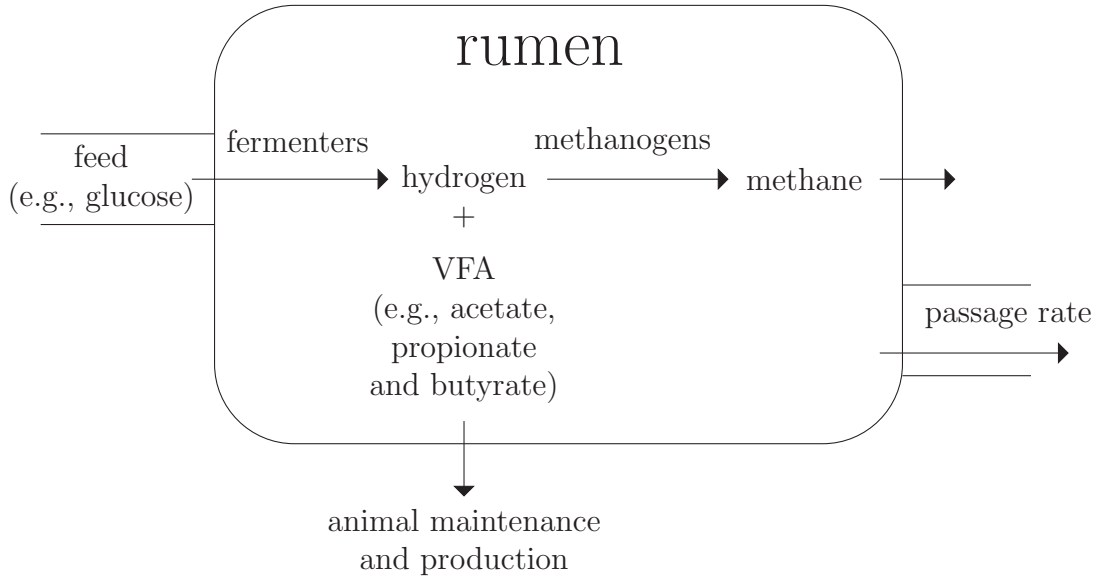

Figure 1.2: Rumen fermentation.

In the rumen, methane is produced biologically as a result of the activity of microbes called methanogens, which can use hydrogen, formate, methanol and other methyl donors, acetate, and a few alcohols as their energy sources. In contrast, in rice paddies [130] and waste treatment systems (wastewater treatment and landfill) [36],[56], methane is formed mainly from the breakdown of acetic acid (between 60 to 70%) and that formed from hydrogen is a smaller part (between 30 and 40%). Those microbes that degrade acetate cannot establish themselves in the rumen at high densities, because they grow too slowly to maintain a population due to the high passage rates in the rumen relative to rice

paddies and wastewater systems [76]. It is interesting to note that in high-passage-rate wastewater systems, acetate-using methanogens form large visible multi-cellular granules that are preferentially maintained against the flow [157]. This does not occur in the rumen. The hydrogen-using carbon-dioxide reducing methanogens can often also use formate, and appear to be the most abundant in the rumen, making up 78% of the rumen methanogens [55]. Those that use methanol or methyl groups can be hydrogen-dependent, meaning they require hydrogen plus the methyl donor, or hydrogen-independent, which can grow just using methyl donors. Worldwide, hydrogen-dependent methylotrophs make up about 22% of rumen methanogens, and hydrogen-independent methylotrophs are almost entirely absent [55]. Acetate-dependent methanogenesis is very important in most non-rumen methane-forming ecosystems (waste treatment [36], [56]; rice paddies [156]), but these methanogens appear to be very rare in the rumen [55]. The hydrogen-using carbon dioxide-reducing rumen methanogens, rather than the hydrogen-dependent methylotrophs, are the focus of this project, although the principles developed could be extended to include other methanogens as well.

The numerically-dominant hydrogen-using rumen methanogens use (dissolved) hydrogen formed from the primary feed fermentation in the rumen [76]. The chemical reaction describing their metabolism is

$$4H_2 + CO_2 \rightarrow CH_4 + 2H_2O \ . \tag{1.1}$$

Temperature variation has little impact on methane production in the rumen because the temperature is maintained at about 39°C ([67]). In contrast, methane production is linked to soil temperature in rice paddies [66], [94]. In certain rice paddies, it had been observed that some of the methane formed can be oxidized in the same soil where it was formed [60], [141], [144]. This oxidation is, however, spatially separated from the production, and occurs in zones where oxygen is available. Biological methane production is an anaerobic process in the rumen, meaning it occurs in the absence of oxygen. Thus, methane formed in the ru-

men is not biologically oxidized in *situ*. Ruminants and rumen microbes cannot use the methane, and it is emitted from the rumen to the atmosphere as a GHG, mostly through belching ($\approx 95\%$) with the remaining lost in flatus [119]. Individual cattle emit approximately 150–420 L of methane per day, while sheep emit approximately 25–55 L [27], [59], [103]. Typically, 2–12% of the total energy intake of ruminants is lost as methane produced and emitted to the atmosphere [80]. Therefore, it would be environmentally and economically beneficial to develop strategies that reduce methane emissions from ruminants-based agriculture, without decreasing animal productivity.

1.3 Methane mitigation strategies

Methane emissions that come from the enteric (in the rumen) fermentation are referred as enteric methane emissions. (See Figure 1.2). Ruminant enteric methane mitigation strategies have been reviewed extensively [16], [23], [26], [61], [77], [79], [90], [101], [107], [128]. From these review papers, approaches to reduce methane production in the rumen can be classified into three categories.

1. Interventions that reduce the net amount of hydrogen that is generated from fermentation pathways (because nearly all the hydrogen is rapidly converted to methane [68]).

2. Those that redirect the hydrogen elsewhere so that hydrogen is not metabolized by methanogens to form methane.

3. Interventions that inhibit (or remove) the methanogens themselves.

The latter is expected to result in increased dissolved hydrogen concentrations in the rumen, which in turn is expected to feed back on hydrogen-forming steps to result in less net hydrogen formation (i.e., hydrogen production becomes less favorable [76]). The dissolved hydrogen concentration in the rumen can influence the rate of hydrogen generation and volatile fatty acids production by differentially influencing the efficiency of the different fermentation pathways and microbes that are active [76],

[177]. Because different species of microbes that ferment feed components produce different amounts of hydrogen (and volatile fatty acids) per unit of feed fermented, selection for or against hydrogen-producers by low or high hydrogen concentrations would result in different mixes of species, and different net amounts of hydrogen (and hence methane) formed. Less methane production is associated with a greater propionate production relative to acetate and butyrate [76], because propionate is more reduced. Propionate production serves as an alternative hydrogen or electron sink (acceptor) in fermentation [166] and is associated with less hydrogen formation and hence less methane emissions.

1.3.1 Reducing hydrogen generation rate

One method to reduce the hydrogen generation rate in the rumen is to feed ruminants with cereal grain [93]. Grains, such as corn, contain larger amounts of rapidly degradable starch. When more digestible feed is eaten, the passage rate is greater [105]. A greater passage rate is associated with a greater hydrogen concentration that leads to reduce net hydrogen formation and hence less methane production [76]. This apparently paradoxical effect is a result of a requirement for a greater hydrogen concentration to allow for the greater growth rate needed by the methanogen population to match the passage rate, as predicted by Monod growth kinetics (Section 1.5) for microbes [115]. The greater hydrogen concentration is postulated to result in thermodynamic feedback that slows the rate of hydrogen formation [76]. By feeding forage brassicas (rape and swedes), the methane production from sheep was respectively 23% and 25% less than that of ryegrass [151]. Sun *et al.* [151], [152] concluded that this difference in methane production is due to rape and swedes being more rapidly degradable than ryegrass, that is, they behave like grain in the rumen.

Changing diet from forage to grain leads to lower rumen pH, even if it does not result in acidosis [154]. Reducing the activity of methanogens can be achieved by reducing pH. The growth rate and activity of rumen methanogens are inhibited by pH values of less than 6.5 [136], [168].

Thus, when grain is fed, the methane reducing effect is a composite of the way the feed is fermented and a direct methanogens inhibition via reduced pH. However, a pH of below 5.5 is life-threatening to ruminants, resulting in depression of feed intake and ruminal acidosis [123].

The passage rate is greater when the level of feed intake is greater [41]. From sheep trials, increasing the level of feed intake by one kg per day of dry matter intake reduced methane production by 4.5 grams per kg dry matter intake [54].

Blaxter and Clapperton [13] reported that there were differences in methane emissions from individual ruminants receiving the same diet, corrected for differences in intake. Pinares-Patiño *et al.* [132] reported that low methane emitting sheep had 11% less methane yield than high emitting sheep on a grass diet, whereas on a grain-rich pelleted diet the difference was 26%. The natural differences in methane production between these animals could be due to intrinsic animal characteristics such as retention time of particles in the rumen and/or to individual differences in rumen microorganisms associated with the rate of degradation processes and fermentation parameters. The rumen capacity of low methane emitting sheep is smaller, with shorter rumen retention times than those of high emitting sheep [50]. A smaller rumen and shorter rumen retention time leads to greater passage rate. Pinares-Patiño *et al.* [131] also observed that the passage rate of low methane emitting sheep was greater than in high methane emitting sheep. That is, a greater passage rate is associated with less methane production. Kittelmann *et al.* [83] reported that there was certain bacteria that were more dominant in low methane emitting sheep than in high emitting sheep. Such bacteria would ferment feed into less amounts of hydrogen (that leads to low methane production). There were no natural differences in densities of methanogens among low or high methane emitting sheep [83] but there were differences in methanogen gene expression which were interpreted as a response to lower dissolved hydrogen concentration in the rumen of high methane emitting sheep [145]. That is, a lower dissolved hydrogen concentrations leads to greater hydrogen production and then greater methane production.

Protozoa produces hydrogen and it has been estimated that 37% of methanogenesis is associated with methanogen attached to the exterior surface of protozoa in the rumen [44]. Removal of protozoa (e.g., defaunation by dietary treatment, starvation and chemical treatment with calcium peroxide [179]) is another approach to reduce the hydrogen generation rate. However, defaunation has not been used routinely because of toxicity problems to the rest of the rumen microbial population and the host animals [179].

1.3.2 Redirecting the hydrogen away from methanogens

An example of redirecting the hydrogen away from methanogens is dietary nitrate supplementation in dairy cows with corn silage-based feed [170]. Because nitrate reduction is more energetically favorable than methanogenesis [164], nitrate-reducing hydrogen-using bacteria can outcompete methanogens for hydrogen [24], decreasing the availability of hydrogen for methanogens (i.e., less methane production). Dietary nitrate supplementation or infused nitrate can, however, lead to nitrate toxicity [155], although this can be overcome or prevented by treatment (methylene blue [172]) or feed management (ruminants should be fed gradually with diets that contain dietary nitrate supplementation). Van Zijderveld *et al.* [170] reported that the energetic benefit from the reduced methane production did not benefit the ruminants because milk production was not affected.

So-called propionate enhancers (malate and fumarate) can be used to redirect the hydrogen away from methanogens. When malate was added in the diet of cattle, Foley *et al.* [45] reported that there was at most a 9% methane reduction per kg dry matter intake. However, using malate was associated with a lower dry matter intake [45] that could negatively affect animal production. By adding 1% fumarate in the diet of beef cattle, Beauchemin and McGinn [8] found that methane emissions were not reduced. However, Wallace *et al.* [175] observed that methane production from sheep was reduced by 75% with 10% fumarate in the

diet. Fumarate may be converted into acetate instead of propionate [165]. Acetate production from fumarate is thermodynamically feasible in ruminal conditions even at very low fumarate concentrations so that this may stoichiometrically increase methane production in the rumen [165].

Stimulation of (reductive) acetogens can act as an alternative hydrogen sink: acetogens compete with methanogens for hydrogen, redirecting the hydrogen away from methanogens. Lopez *et al.* [99] found that methane production was reduced (by 5% after one day) when acetogens (microbes) were added to rumen fluid *in vitro*. There was no persistence of decreasing methane production [99] because acetogens cannot compete for hydrogen against methanogens, without stimulating acetogens and suppressing the activity of methanogens. Fonty *et al.* [46] demonstrated that acetogens can only establish in the rumen when methanogens are inhibited. That is, stimulation of acetogens has the potential to use hydrogen in the rumen, only if reliable techniques for inhibiting methanogens can be implemented and such inhibition effects maintained.

1.3.3 Methanogens inhibition

Adding methanogen inhibitors can reduce the activity of methanogens [62], [95], [101]. Methanogen inhibitors are used to manipulate the methanogen population density and methane production pathways, which may increase hydrogen concentrations and cause a shift in fermentation pathways [76]. Inhibitors can be naturally occurring, e.g., lipids (dietary fat) such as linseed and fish oil, or synthetic compounds, e.g., 2-bromoethanesulfonate, chloroform and 3-nitrooxypropanol (3NOP) among others. These inhibitors can directly inhibit the methane formation pathway 1.1 or be toxic to methanogens to reduce methane production. Based on 67 studies, Martin *et al.* [101] concluded that there is a mean decrease of 3.8% in methane from ruminants for each 1% addition of lipids included in the diet. Goel *et al.* [48] reported that there was 78% decrease in methanogen population with saponin extracted from 5 grams of dried ground plant leaves (*Sesbania*). There was no consistent re-

sults of methane production being affected by saponin extract in *vitro* [127]. Some synthetic methanogen inhibitors (2-bromoethanesulfonate and chloroform) can also inhibit the activity of other bacteria and so may lead to lower animal productivity [95]. Hristov *et al.* [62] found that methane production of dairy cows was reduced by 25% per kg of dry matter intake when 3NOP was included in a prepared diet fed to lactating dairy cows. This inhibitory effect persisted over 12 weeks with no negative effect on feed intake or on milk production or composition [62].

Another technology for reducing methane formation from ruminants would be to vaccinate them with a vaccine that targets methanogens. A methanogen vaccine should stimulate the ruminant's immune system to produce antibodies against the methanogens [185]. These antibodies then could be transferred via saliva to the rumen where the activity of methanogens is diminished [185]. If such a vaccine can be developed and validated, then it would lead to smaller populations of rumen methanogens and higher hydrogen concentrations that can cause a shift in fermentation pathways [76]. There were severals attempts made by Williams *et al.* [180], Zhang *et al.* [186] and Subharat *et al.* [153]. However, to date, a successful vaccine targeting rumen methanogens has not been reported.

1.3.4 Mathematical models and mitigation strategies

It is expensive to run animal trials and laboratory experiments to develop and screen methane mitigation strategies. For example, it can take a month to conduct an animal trial; it is expensive to source, purchase and transport feed and it is labour-consuming to feed the ruminants and collect data [150]. All possible variables cannot be controlled, and the number of potential experiments even to test some simple hypothesis can be very large. Some experiments may be impossible to perform because factors cannot be varied independently in the animal system.

An example of this is that changing diet from forage to grain is usually associated with a change in passage rate and rumen pH, even if it does not result in acidosis. Thus, suitable mathematical models of rumen function can be effective tools to support experimentation with animals for exploring mitigation strategies. For example, by allowing exploration of a wide range of values for many variables (exploring ideas of what may and may not work), without having to do all the experiments, the results can be used to design more targeted experiments. Also, models allow an assessment of the size of an impact, and thus help to decide whether an experiment might give a measurable outcome.

1.4 Mathematical models of methane production from anthropogenic activities

In response to global concerns over climate change and its impact on people and the environment, there is a global interest in better understanding methane emissions from anthropogenic activities. As part of that quest for understanding, mathematical models have been developed for non-animal systems (rice paddies [65], [66], [94], [126] and waste treatment systems [6], [25], [36], [56], [161]) and ruminants-based agriculture (whole-farm [106], [149] and individual animal [39], [109], [114]). There are two types of mathematical models of ruminal methane production from individual ruminants: empirical and mechanistic. Empirical models are developed by fitting equations to experimental data and estimating methane production based on regression functions, e.g., Ellis *et al.* [39], Kriss [88], Moe and Tyrrell [114], Ramin and Huhtanen [135]. Mechanistic models, such as those developed by Baldwin [5], Benchaar *et al.* [10] and Mills *et al.* [109], estimate methane production as a stoichiometric function of the hydrogen balance of the rumen. The scope of this thesis is modelling of enteric methane production. We start by reviewing existing models of methane production from a whole-farm.

1.4.1 Models of a whole-farm

There are differences in farm-to-farm methane emissions due to soil organic matter and crops of the farm, type and number of cattle, feeding practices and manure management operations [149]. Stewart *et al.* [149] developed a whole-farm model of methane production for beef because cattle are significant sources of GHGs. These authors considered four farms to represent four diverse climatic (e.g., temperature) and soil conditions (e.g., soil type) of Canada. They estimated the methane production of a farm as a linear function of methane production from rumen and manure. That is, methane production from a farm is determined by the enteric methane production from individual ruminants and the numbers of ruminants in a farm. Both the methane production from rumen and manure [149] was estimated as a constant proportion (i.e., conversion factor) of gross energy intake for all the animals in the farm. McGinn and Beauchemin [106] applied a whole-farm model (commercial software using an inverse-dispersion technique) for three dairy farms (from 208 to 351 cows) in Canada. Methane emissions were estimated based on diet, type of animals (lactating and nonlactating), field measurements of methane concentration, and wind statistics (speed and direction). Despite the limited dataset (because of poor wind direction for the instrumentation orientation), for lactating cows, they found a mean methane production (363 gram per day) that was similar to other reported values. They also concluded that the enteric methane emission of individual animals (and the number of animals) is the main contribution to the methane emission of a farm. That it, the methane production of a whole-farm can be estimated by multiplying the enteric methane production from individual ruminants with the number of animals. Thus, in this thesis, we will focus on developing a model of enteric methane production from individual ruminants in an effort to fill the gaps in existing models for individual ruminants. To identify such gaps, existing models of methane production from individual ruminants will be reviewed in the following two sub-sections.

406 ## 1.4.2 Models of individual ruminants

407 ### 1.4.2.1 Existing empirical models

408 An early attempt to empirically model ruminal methane production from
409 individual ruminants was made by Kriss [88]. He found a linear relation-
410 ship between the amount of dry matter of feed consumed (DM) and
411 methane production based on experimental data. An empirical model
412 with a quadratic relationship of DM to methane formed was developed
413 by Axelsson [3]. The model of Kriss [88] overestimated mean methane
414 production, whereas the equation of Axelsson [3] underestimated it. In
415 another approach [135], dry matter intake, feeding level and dietary com-
416 position data were collected from 52 published papers (1960s to 2011 with
417 207 cattle and 91 sheep). Ramin and Huhtanen [135] developed linear
418 and quadratic functions of DM to calculate total methane production for
419 cattle. Methane production of this model [135] can also be estimated
420 as a linear function of acetate, propionate and butyrate, associated with
421 different coefficients based on volatile fatty acids stoichiometry. With
422 those collected datasets, there was 15% prediction error for their model
423 [135].

424 Blaxter and Clapperton [13] developed a linear model to describe
425 methane production as a function of digestibility of feed and feeding
426 level (expressed as dietary energy intake). They found that, with highly
427 digestible feeds, increasing feeding level (increasing passage rate) led to
428 less methane production per unit of feed. This is the case because a
429 greater passage rate is associated with less methane production [76].

430 A linear relationship between methane production and carbohydrate
431 digested (without explicit expressions of the hydrogen pool and methanogens)
432 was developed by Bratzler and Forbes [14]. They concluded that methane
433 production was closely related to the amount of carbohydrate digested.
434 Czerkawski and Breckenridge [28] demonstrated that methane produc-
435 tion in the rumen was not only related to the amount of carbohydrate
436 digested but to the nature of carbohydrate digested (e.g., hemicellulose
437 and cellulose). This observation was confirmed by Moe and Tyrrell [114]
438 with an extended range of dietary carbohydrate. From their model [114],

methane production per gram of cellulose digested was nearly three times more than that per gram of hemicellulose digested. These models all suggested that there are not simple relationships between the amount of DM ingested and the amount of methane formed. The chemical composition of the feed appears to influence methane production.

Moraes *et al.* [116] presented an empirical model of methane production using details such as gross energy intake, dietary level and animal information. Their linear model could be used for the evaluation of greenhouse gas inventories with different levels of details; e.g., animal information such as lactating cows, non-lactating cows, heifers and steers. They suggested that by including animal information it would be possible to improve model fitness and better match the data.

Non-linear empirical models of methane production, introduced by Mills *et al.* [110], adopted biologically sensible constraints, such as zero methane production with zero intake of feed and an upper limit of methane emission. An extensive database of methane production measurements made on beef cattle in northern USA and Canada was used by Ellis *et al.* [39] to develop both linear (ratio-based) and non-linear models without explicit expressions of hydrogen pool and methanogens. They suggested that the predictions of their models were better and could be more suitable for modern production conditions of North American beef cattle than for other ruminant-based agriculture systems outside North America.

The coefficients and parameters of empirical models for ruminant-based agriculture (reviewed in this section) need to be re-validated to predict methane production any time there is a new dataset representing different feed, microbes or animal type (cattle and sheep). A mechanistic model of rumen function is based on biological properties of the rumen that are universal across ruminants. Thus, in this project, a mechanistic model of enteric methane production from individual ruminants will be developed. The following section is a review of existing mechanistic models of enteric methane production based on rumen function.

1.4.2.2 Existing mechanistic models

Existing mechanistic models include/exclude different important features of ruminant methane production. In general, a representation of the microbe and/or hydrogen pool may or may not be included in any given model and methane production is then estimated based on different stoichiometric representations of feed fermentation pathways. In this section, to identify the gaps in mechanistic models for individual ruminants, existing mechanistic models are reviewed with a focus of these features.

Ulyatt *et al.* [163] developed a mechanistic model of cellulose digestion in the rumen for ten feed elements (e.g., soluble carbohydrate, starch, hemicellulose and cellulose) and a single microbe pool. Methane production was estimated based on a stoichiometric function of glucose. The methane production predicted by their model was 13% greater than literature data for sheep [69]. Because the equations of their model were not explicitly presented in [163], this comparison of methane production between their model and literature data, however, cannot be assessed.

The mechanistic model of (sheep) rumen function described by Black *et al.* [12] is a system of linear equations. The predicted microbial growth was estimated by total microbial mass with no distinction made among microbes. A single pathway of fermentation was used for each substrate considered. The assumption of this model [12] was that carbohydrates were fermented to yield methane. Methane production was estimated using stoichiometric functions [12]. To extend the model of rumen function from sheep to cows based on the model of Black *et al.* [12], Baldwin *et al.* [4] developed a dairy cow model [5] named Molly95. There are three options to estimate methane production in Molly95: the Blaxter and Clapperton [13] equation, the Moe and Tyrrell [114] equation (both of which have been described above), and an estimate based on a stoichiometric function of the hydrogen balance of the rumen without an explicit expression of methanogens. This hydrogen balance was defined as the difference between the amount of hydrogen produced and used in reactions occurring in the rumen. It is important to note that hydrogen consumption includes reactions that actually use electrons that could have been used for hydrogen formation, as pointed out by Janssen

[76]. From equation (1.1), the hydrogen balance in the rumen is simply divided by four to get the methane production. This third option to estimate methane production from the hydrogen balance in Molly95 was used in the mechanistic model of methane production described by Benchaar *et al.* [10]. The assumptions of this model [10] were that there was continuous feeding and that methane was formed solely by the reduction of carbon dioxide, which is present in excess, with residual hydrogen, i.e., it was controlled by hydrogen availability. Similar to Benchaar *et al.* [10], the hydrogen balance was divided by four to get the methane production in [109]. Such hydrogen balance is the difference between the amount of hydrogen produced and used in reactions occurring in the rumen based on a stoichiometric function. Mills *et al.* [109] used a rumen function [31] other than Molly95 that caused different stoichiometric values and so different methane estimation compared to Benchaar *et al.* [10]. The rumen model described by Dijkstra *et al.* [31] consisted of 17 variables (e.g., volatile fatty acids) without an explicit expression of methanogens. Volatile fatty acids stoichiometry developed by Bannink *et al.* (2006, 2008) were later integrated into this model [158]. However, there was no explicit expressions of hydrogen pool and methanogens in their model and no thermodynamic feedback of hydrogen on the volatile fatty acids stoichiometry. A key assumption of the approach of Mills *et al.* [109] is that the hydrogen remaining after feed fermentation is used solely and completely by methanogens. This assumption was also used by Vetharaniam *et al.* [173] to modify Molly95 [5]. The improvement of the model developed by Vetharaniam *et al.* [173] over Molly95 [5] included an explicit dissolved hydrogen pool and an adjustment on the stoichiometric function of hydrogen production under different sheep's rumen environments.

1.4.3 Summary

After reviewing existing models of enteric methane production from individual ruminants, the gaps in existing models can be identified. Methane production is directly related to the rate of hydrogen generation from

rumen fermentation [68] which is subjected to thermodynamic control imposed by substrate and product (e.g., volatile fatty acids and hydrogen) concentrations [84]. As concluded by Ellis *et al.* [38], a dynamical hydrogen pool was required for improving models of rumen fermentations. This dynamic hydrogen pool was implemented in the study of Vetharaniam *et al.* [173]. The dissolved hydrogen concentration is a key controller of fermentation pathways [76], [84]. However, most existing models for ruminant-based agriculture do not include an explicit expression of the hydrogen pool. Therefore, the feedback of hydrogen on the selection of the various fermentation pathways can not be represented in the model. A model that describes the interaction between methanogen growth and hydrogen has utility beyond the estimation of methane, as it provides an alternative approach to the current representation of fermentation based on stoichiometric profiles from feed components (e.g., [4], [31]). Such an approach could help overcome other known limitations of current models of rumen function, such as the prediction of volatile fatty acid profiles [38], [117]. The models of Baldwin [5] (Molly95), Benchaar *et al.* [10] and Mills *et al.* [109] include the concept of balancing hydrogen production and consumption, and Offner and Sauvant [124] developed models with an explicit dissolved hydrogen pool and methanogens, but their models do not directly describe the interactions between hydrogen and methanogens. That is, there is a gap in existing models of ruminal methane production: there is not a representation of the interaction between hydrogen and methanogen growth. Such interaction (i.e., hydrogen-methanogen dynamics) can be modelled by employing an explicit expressions of the hydrogen pool (for modeling hydrogen feedback on fermentation pathways) and the methanogens population pool (for exploring strategies that directly target methanogens activity, e.g., inhibitors). Furthermore, in current models of rumen function (e.g., [4], [31]), yield factors of volatile fatty acid profiles are predetermined for different types of feed components leading to poor estimation of volatile fatty acid profiles [38], [117]. Rather than predetermining stoichiometric profiles from feed components, we wish to develop a model where the microbial growth kinetics and the thermodynamic feedback on this growth

571 from the substrates and products of the fermentation (such as hydrogen
572 and volatile fatty acids) determine the composition of the rumen micro-
573 bial community, the fermentation pathway used, and the volatile fatty
574 acid profiles. The volatile fatty acid profiles can be calculated from the
575 population densities of the various microbes that use different fermen-
576 tation pathways leading to different ratios of end products (including
577 volatile fatty acids) and different yields of hydrogen per unit of ingested
578 feed. Thus, in this project, a bottom-up mechanistic modelling of enteric
579 methane production in the ruminants is developed starting with a base
580 of methanogens growth kinetics as a function of hydrogen concentration.

581 1.5 Methanogens growth kinetics

582 The change in the population density, as viable cells, of a microbial cul-
583 ture growing from a small number of cells under general laboratory con-
584 ditions that permits proliferation of the number of individuals has been
585 illustrated by Monod [115]. In this system, the cell number increases
586 because there is no removal of cells. The change in population density is
587 shown in Figure 1.3. Phases 1 and 2 are the lag and acceleration phase
588 that may be suppressed if the starting cells are from an already actively
589 growing culture. Phase 3 (the exponential phase) is the reproduction of
590 the population that can be described mathematically as follows. Let P_o
591 be the microbial population density (cell, i.e., cell numbers) at time t_o
592 of the exponential phase, and P_n be the population density (cell) after
593 time t still in the exponential phase. The doubling time, t_d is then

$$t_d = \frac{t - t_o}{(\log(P_n) - \log(P_o))/\log(2)} \ . \tag{1.2}$$

594 The reproduction rate of the microbes is

$$\mu = \frac{(\log(P_n) - \log(P_o))}{t - t_o} \ , \tag{1.3}$$

595 which is the slope of the curve (Log_2 Microbial density) in phase 3 of
596 Figure 1.3.

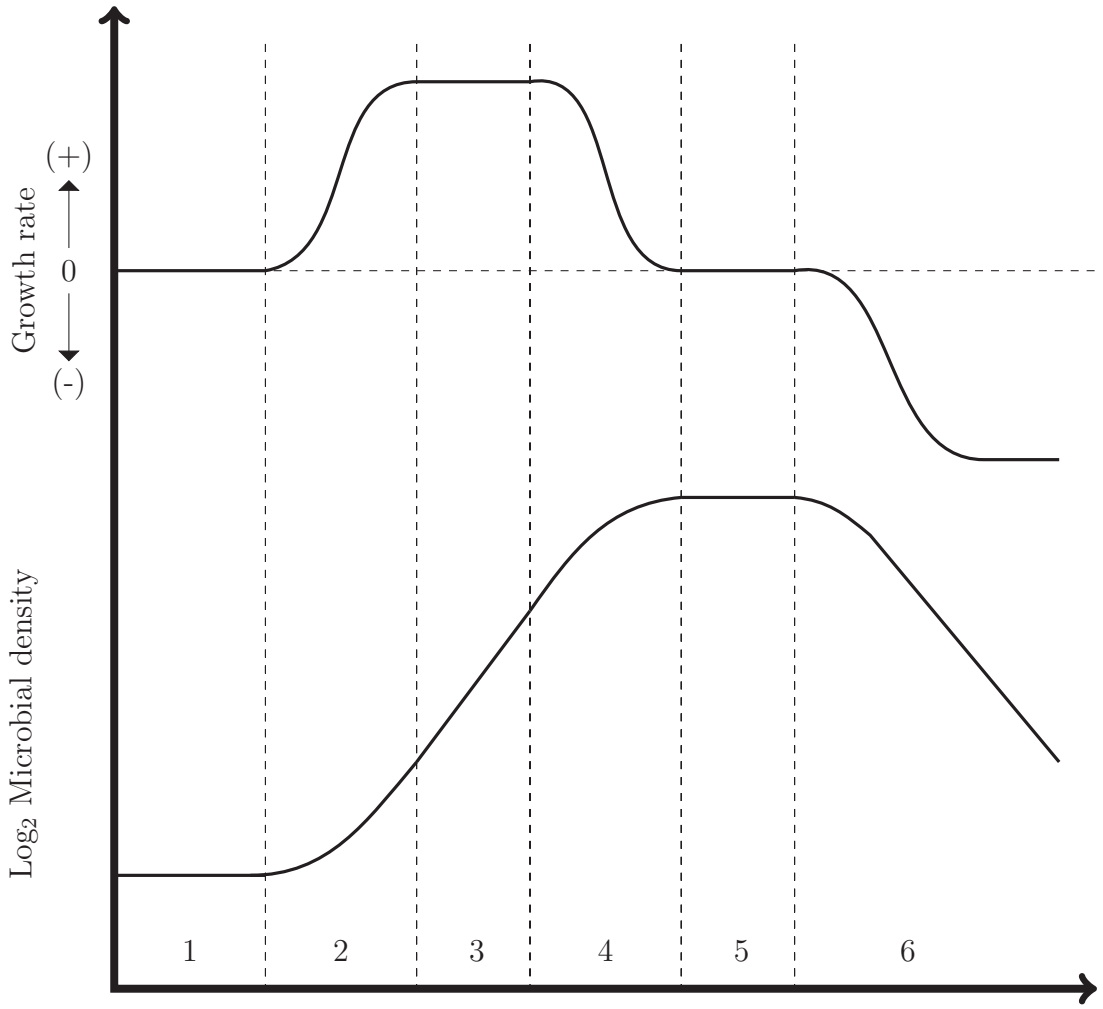

Figure 1.3: The phases of microbes growth based on Monod [115].

The rumen approximates a continuous culture system [133] so that the microbes are effectively continuously removed in phase 3. Because the microbial reproduction rate approximates the washout rate (the rate at which the microbes are removed from the system, also known as the fractional passage rate), the population density does not increase in the rumen, although in reality it can be expected that the reproduction and passage rates vary so that only on average they are equal. The retardation and stationary phases are sometimes too short to be noticed (phases 4 and 5). The last phase is decline, with a negative growth rate, attributed to cell death through some combination of factors like starvation

607 due to nutrient depletion or the accumulation of end products that make
608 the environment unfavorable for survival. These phases are expected to
609 be transient or absent in an environment that approximates a continuous
610 flow system, such as the rumen.

611 The energy source is often referred to as the limiting substrate for
612 growth. The reproduction rate of a microbe dependent on a single sub-
613 strate can be described by the Monod model [115].

$$\mu(S) = \frac{\mu_{\max} S}{K_s + S} \ . \tag{1.4}$$

614 Note that

$$\frac{d\mu}{dS} = \frac{\mu_{\max} K_s}{(K_s + S)^2} > 0 \ .$$

615 Mathematically, μ is strictly increasing: that is, the value of $\mu(S)$ is
always increasing with respect to S as shown in Figure (1.4). Equation

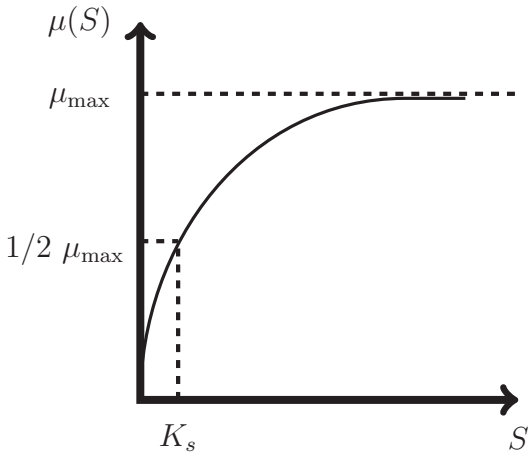

Figure 1.4: A plot of Monod model $\mu(S)$.

616

617 (1.4) indicates that the reproduction rate of the microbe increases rapidly
618 at smaller substrate concentrations, S, and slowly at greater substrate
619 concentrations. $\mu(S) \to \mu_{\max}$ as $S \to \infty$, therefore $\mu_{\max}$ is a horizontal
620 asymptote. The Monod constant, K_s, is the substrate concentration
621 that results in half of the maximum specific reproduction rate (Figure
622 1.4). The maximum specific reproduction rate is specific for each type

of microbe, substrate and environmental conditions such as temperature; and the lag phase is not included in the Monod model.

Initially, the Monod model, as it related to microbial growth, was found empirically. In enzyme kinetics, there is an equivalent specific growth rate function called the Michaelis-Menten equation. There is a standard mechanistic derivation of Michaelis-Menten enzyme kinetics provided by Campbell [19]. Liu *et al.* [97] provided a thermodynamic interpretation of the Monod model for microbial growth and proposed that the magnitude of the Monod constant was the chemical equilibrium position of a microbial growth process. Four theoretical approaches for derivation of the Monod model were reviewed by Liu [98]. Insights into the physical meaning of the Monod constant were also discussed by Liu [98]. The conclusion was that the Monod constant differed with different substrates for a single microbe.

Methane is produced by methanogens, using (dissolved) hydrogen produced from the feed fermentation in the rumen as their major energy source or substrate. Reproduction of any single methanogen cell occurs by an increase in cell size followed by fission into new equal daughter cells. The increase in size is fueled by energy gained from metabolic pathways coupled to the formation of methane. The reproduction of methanogens and hence growth of the methanogen population, is represented as dependent on a single substrate, hydrogen, since carbon dioxide is present in excess [104]. Typical concentrations are 5.9×10^{-5} (mol ml^{-1}) for carbon dioxide [76] and 1×10^{-9} (mol ml^{-1}) for hydrogen [70]. The Monod model of microbial growth can be adapted as methanogens growth kinetics to model the rate of hydrogen metabolism by methanogens as a function of the hydrogen concentration. The rumen approximates a continuous culture system [133]. A continuous culture system is a technique used for growing microbes in a vessel, into which limiting substrates for growth are continuously supplied at a constant rate, and from which liquid, microbes and end products are continuously removed [89]. A continuous culture is also known as a chemostat with a continuous input liquid (containing substrate) and output at the same rate to keep the volume constant [146]. One feature of the chemostat is that microbes

can be grown in a steady state under constant environmental parameters (e.g., washout). Another feature of chemostat and continuous culture systems is that they are well-mixed so that substrate and microbes are randomly and uniformly distributed in the liquid. The rate of change of the limiting substrate for growth for such chemostat can be modelled as [146]

rate of change of substrate = -(consumption + removal rate) + input ,

and that of microbes can be modelled as

rate of change of microbes = growth - removal rate .

The growth term in this 'standard' theoretical model [146] is generally based on the Monod model [115], expression (1.4), and the ratio of the specific growth rate to consumption of the substrate is generally modelled as a constant called the growth yield. The removal rate of the microbes from the system is a sum of the death rate and washout. The model presented in this thesis adapts the framework of this 'standard' theoretical model as described in Section 2.2.

Microbial growth can be influenced by inhibitors, pH and temperature, and therefore a number of modifications to the Monod model have been proposed [47]. The model presented in this thesis represents methanogen growth using functions (the Monod model) similar to those described for fermentative bacteria in the rumen models of Baldwin *et al.* [4] and Dijkstra *et al.* [31]. An advantage of representing methanogen growth using the Monod model [115] is that it allows a dynamic representation of the dissolved hydrogen pool in the rumen. Such an approach could help overcome other known limitations of current models of rumen function, such as the prediction of volatile fatty acid profiles [38], [173], because the hydrogen concentration influences, via thermodynamic feedback, the fermentation pathways that produce volatile fatty acids.

1.6 Research objectives and outlines

Globally, 14.5% of all anthropogenic GHG come from ruminants. Mathematical models of rumen function can be effective tools to support experimentation with animals for exploring methane mitigation strategies. Existing empirical and mechanistic mathematical models of methane production from rumen have 20% to 50% prediction errors (37% [37] for Baldwin *et al.* [4]; 20% [37] for Dijkstra *et al.* [31]; 50% [82] for Moe and Tyrrell [114]; 20% [82] for Baldwin [5]). For the models of Baldwin [5] and Ellis *et al.* [39], the differences in the prediction methane between these models was up to 35% when applied to data from the same production systems [92]. The prediction errors of existing empirical and mechanistic mathematical models of methane production are too large to explore methane mitigation strategies. A model of hydrogen-methanogen dynamics could be introduced into current models to provide the basis for both the prediction of methane and the representation of the feedback of hydrogen on fermentation pathways in the rumen. This model includes explicit expressions of the hydrogen pool (for modeling hydrogen feedback on fermentation pathways) and the methanogen population pool (for exploring strategies that target directly methanogen activity, e.g., inhibitors). These are two aspects which existing models are not capable of modeling and exploring. In this project, such a model and its expansions are described.

In Chapter 2, an individual rumen model is developed with an explicit representation of a dissolved hydrogen pool and methanogen population to allow for investigation of hydrogen-methanogen dynamics. It employs assumptions about rumen function such as that the methanogens and hydrogen are uniformly distributed in the rumen liquid contents; hydrogen is solely metabolized by methanogens to produce methane as shown in equation (1.1) and hydrogen is the limiting energy source for methanogens. This model is expanded to become a more comprehensive model in the later chapters. Namely, the feedback of products on substrate (e.g., hydrogen) metabolism is implemented in Chapter 3, and the feedback of hydrogen on fermentation pathways in the rumen is modeled

716 in Chapter 4. Co-existence of multiple types of microbes metabolizing
717 the same substrate but using different fermentation pathways are ex-
718 plored in Chapters 5. The mathematical enunciation of a model with an
719 explicit representation of a dissolved hydrogen pool, methanogens pop-
720 ulation and hydrogen-methanogen dynamics and its expansion is tested
721 for consistency with biological expectations described in the conceptual
722 framework proposed by Janssen [76].

Chapter 2

Hydrogen-methanogen dynamics

Based on the Monod model of microbial growth [115], we present a mechanistic system model of hydrogen-methanogen dynamics [1]. This model includes an explicit expression of the hydrogen pool and the methanogens population pool (for exploring strategies that target the methanogens activity directly, e.g., inhibitors). We first list the assumptions that are made for this model.

2.1 Assumptions

1. Methanogens and hydrogen are *uniformly distributed* in the rumen liquid contents.

2. Methanogens capture hydrogen *randomly with no competition* among methanogens for hydrogen.

3. *No other microbes compete* for hydrogen with the methanogens.

4. Hydrogen is the *only* energy source of methanogens, which *instantaneously* metabolize hydrogen to gain energy (i.e., adenosine triphosphate, ATP).

[1] This model has been published as Wang Y, Janssen PH, Lynch TA, van Brunt B, Pacheco D (2016) J Theor Biol 393, 75 – 81.

5. *Each methanogen cell* metabolizes hydrogen up to the *same maximum rate* to generate ATP and needs the *same* amount of ATP for maintenance.

6. The ATP gained is used either to maintain existing methanogens *or* to reproduce, and new methanogens are *biologically identical* to existing methanogens.

7. Methanogens cannot reproduce unless there is an *excess* of ATP beyond what is needed for their maintenance.

8. Hydrogen is lost through consumption by methanogens *or* exiting from the rumen (passage rate).

9. Methanogens are lost by exiting the rumen (passage) *or* "starvation" (i.e., there are no predators).

10. The passage rate in the rumen is *constant*.

11. The hydrogen generation rate in the rumen is *constant*.

These assumptions are simplifications of what actually occurs in the rumen. For example, methanogens can attach to epithelium and feed particles with different passage rate than liquids; there are multiple types of methanogens that compete for hydrogen and with different substrate requirements [38]; hydrogen can escape the rumen by eructation and absorption to blood; rates of passage and hydrogen generation are not constant. The aim of this chapter, however, is to develop a model with hydrogen-methanogen dynamics that can be expanded and implemented into models of whole rumen function to address more complex assumptions.

2.2 Model formulation

Equation

$$4H_2 + CO_2 \rightarrow CH_4 + 2H_2O \ ,$$

767 is the chemical reaction of methane production from carbon dioxide and
768 hydrogen. There is an excess of carbon dioxide in the rumen [104],
769 and hydrogen is the limiting nutrient source for methanogens. Thus,
770 in our model, the reproduction of methanogens and hence growth of
771 the methanogen population is represented as dependent on a single sub-
772 strate, hydrogen (H_2). The Monod model of microbial growth [115] can
773 be adapted to model the rate of hydrogen metabolism by methanogens
774 as a function of the hydrogen concentration.

775 Let S_h be the dissolved hydrogen concentration (mol ml^{-1}) and X_m
776 be the methanogen population density (cell ml^{-1}) in the rumen liquid at
777 time t. S_h' (mol ml^{-1} s^{-1}) and X_m' (cell ml^{-1} s^{-1}), are then the *rate of*
778 *change* of hydrogen concentration and methanogen population density,
779 respectively. Here $'$ denotes differentiation with respect to time. The
780 subscripts h and m indicate that the parameters are related to hydrogen
781 and methanogens, respectively. Let q (mol cell^{-1} s^{-1}) be the rate at
782 which a methanogen metabolizes hydrogen. From the Monod model, the
783 rate of hydrogen metabolism at a given hydrogen concentration is given
784 by

$$q = \frac{q_m S_h}{K_m + S_h} \text{ (mol cell}^{-1} \text{ s}^{-1}) \,, \tag{2.1}$$

785 where q_m (mol cell^{-1} s^{-1}) is the maximal rate at which a methanogen can
786 metabolize hydrogen and K_m (mol ml^{-1}) is the hydrogen concentration
787 at half of q_m. Under assumptions 1 – 5, the rate at which the hydrogen
788 is consumed by X_m methanogens is then

$$qX_m = \frac{q_m S_h}{K_m + S_h} X_m \text{ (mol ml}^{-1} \text{ s}^{-1}) \,.$$

789 Let α (s^{-1}) denote the (fractional) passage rate through the rumen.
790 Then, the hydrogen concentration will decrease by αS_h per unit of time.
791 Let β_h (mol ml^{-1} s^{-1}) denote the hydrogen generation rate. Thus, S_h' is
792 the sum of the rate at which hydrogen is metabolized by methanogens,
793 the rate at which hydrogen exits the rumen due to passage, and the rate

794 at which hydrogen is generated. This leads to the equation

$$S_h' = -\frac{q_m S_h}{K_m + S_h} X_m - \alpha S_h + \beta_h \text{ (mol ml}^{-1}\text{ s}^{-1}\text{)} .$$

795 Methanogens gain n_m (mol_{ATP} mol^{-1}) amount of ATP (energy) per
796 unit of hydrogen metabolized. The total ATP gained for the whole
797 methanogen population is

$$\frac{n_m q_m S_h}{K_m + S_h} X_m \text{ (mol}_{ATP}\text{ ml}^{-1}\text{ s}^{-1}\text{)} .$$

798 Let m_m (mol_{ATP} cell^{-1} s^{-1}) be the maintenance requirement for ATP of
799 a single methanogen per unit of time. Assumption 5 indicates that the
800 total maintenance requirement of X_m methanogens is $m_m X_m$. The net
801 ATP available, Δ, is thus

$$\Delta = \frac{n_m q_m S_h}{K_m + S_h} X_m - m_m X_m = \Delta_m X_m \text{ (mol}_{ATP}\text{ ml}^{-1}\text{ s}^{-1}\text{)} ,$$

802 where

$$\Delta_m = \frac{n_m q_m S_h}{K_m + S_h} - m_m \text{ (mol}_{ATP}\text{ cell}^{-1}\text{ s}^{-1}\text{)} .$$

803 The sign of Δ_m at a given hydrogen concentration, $\Delta_m(S_h)$, indicates if
804 the methanogen population meets the requirements for reproduction. If
805 $\Delta_m(S_h) > 0$, then methanogens can reproduce (assumptions 6 and 7).
806 Let Y_m (cell mol_{ATP}^{-1}) be the reproduction coefficient of a methanogen
807 cell i.e., the net apparent reproduction rate: the reproduction rate af-
808 ter deducting death due to natural causes (reproduction rate after non-
809 starvation death). Then

$$X_m' = \Delta_m Y_m X_m - \alpha X_m \text{ (cell ml}^{-1}\text{ s}^{-1}\text{)} . \tag{2.2}$$

810 If $\Delta_m(S_h) \leq 0$, the methanogens cannot reproduce. There is not
811 enough ATP available to meet the demand of maintenance and death
812 occurs in the population (assumption 9). The resulting shortage of ATP

is expressed as a proportion of m_m as follows

$$\frac{\Delta_m}{m_m} \text{ (unitless)} .$$

The rate of death among X_m methanogens is expressed as

$$\Delta_m \frac{d_m}{m_m} X_m \text{ (cell ml}^{-1} \text{ s}^{-1}) ,$$

where d_m (s^{-1}) denotes a death coefficient. By assumption 9, if $\Delta_m(S_h) \leq 0$,

$$X_m' = \Delta_m \frac{d_m}{m_m} X_m - \alpha X_m \text{ (cell ml}^{-1} \text{ s}^{-1}) . \tag{2.3}$$

The hydrogen-methanogen dynamics are thus modeled by the system

$$S_h' = -\frac{q_m S_h}{K_m + S_h} X_m - \alpha S_h + \beta_h \text{ (mol ml}^{-1} \text{ s}^{-1}) , \tag{2.4}$$

$$X_m' = \Delta_m E_m X_m - \alpha X_m \text{ (cell ml}^{-1} \text{ s}^{-1}) , \tag{2.5}$$

where

$$\Delta_m = \frac{n_m q_m S_h}{K_m + S_h} - m_m \text{ (mol}_{ATP} \text{ cell}^{-1} \text{ s}^{-1}) ,$$

and

$$E_m = \begin{cases} Y_m, & \text{if } \Delta_m(S_h) > 0 , \\ \frac{d_m}{m_m}, & \text{if } \Delta_m(S_h) \leq 0 . \end{cases}$$

The term Δ_m indicates the net ATP available after maintenance requirement of methanogens. If there is sufficient ATP over and above their maintenance requirement, methanogens are in the reproduction mode and otherwise they are in the decay mode as denoted by E_m. We shall refer to the system of equations given in (2.4) and (2.5) as the HM (hydrogen methanogen) model, where S_h is the hydrogen concentration and X_m is the methanogens population density.

Let S_h^{crit} denote the positive hydrogen concentration needed to ensure

828 that the maintenance requirement is met for the methanogen population.
829 In other words, it is the value of S_h at which $\Delta_m(S_h)$ changes sign, and
830 the right hand side of equation (2.5) changes. This critical concentration
831 is

$$S_h^{\text{crit}} = \frac{K_m m_m}{n_m q_m - m_m} > 0 \text{ (mol ml}^{-1}\text{)} . \tag{2.6}$$

832 There are two types of parameters in this model: ruminal parameters
833 related to rumen environment and biological parameters related to the
834 characteristics of methanogens. The ruminal parameters α and β_h are
835 non-negative. The biological parameters n_m, q_m, K_m, m_m, d_m and Y_m
836 reflect characteristics of methanogens. Although these parameters may
837 be variable, for simplicity we will assume they are positive constants.
838 Assumptions 5 and 6 indicate that the biological parameters are con-
839 sidered the same for each methanogen cell. This model could, however,
840 be modified to represent multiple types of methanogen populations with
841 different biological characteristics and substrate requirements [38].

842 2.2.1 Comparison of the HM model and the 'stan-
843 dard' theoretical approach

844 Using the notation of the HM model, the 'standard' theoretical approach
845 [146] (Section 1.5) to modelling the growth of microbes with a single
846 growth limiting substrate in a chemostat is

$$S_h' = -\frac{q_m S_h}{K_m + S_h} X_m - \alpha S_h + \beta_h \text{ (mol ml}^{-1}\text{ s}^{-1}\text{)} , \tag{2.7}$$

$$X_m' = \Delta_m Y_m X_m - \alpha X_m \text{ (cell ml}^{-1}\text{ s}^{-1}\text{)} , \tag{2.8}$$

$$\Delta_m = \left(\frac{q_m S_h}{K_m + S_h} - m_m \right) . \tag{2.9}$$

847 We refer to the system of equations (2.7), (2.8) and (2.9) as the 'standard'
848 model. Note that the term m_m in the 'standard' model is interpreted as
849 a decay or death coefficient, whereas, in the HM model, it is interpreted
850 as a maintenance requirement and d_m is the decay coefficient.
851 The 'standard' model has been adapted in our HM model to more

accurately represent the growth rate of methanogens. The reproduction rate of the microbes (e.g., methanogens) with sufficient substrate is known to be different than that of the decay rate with insufficient substrate [86]. From experiments, Konopha et al. [86] found that 50% to 90% of total cell population in a biomass reactor is eliminated after 32 days of starvation. For example, if we assume 50% of the total methanogen population is eliminated after 32 days of starvation, we obtain a death rate of $d_m = 2.50 \times 10^{-7}$ (s^{-1}). However, with sufficient growth limiting substrate, the apparent reproduction rate of methanogens can vary from 0.081 to 1.730×10^{-4} (s^{-1}) [129]. To account for this known difference in reproduction rate between starvation and non-starvation mode, a switching term E_m is used in the HM model. This switching term is new for modelling the growth rate of microbes on a single growth limiting substrate (e.g., modelling the growth rate of methanogens with respect to hydrogen in the rumen).

In the 'standard' model, it is assumed that death occurs at the same rate all the time. In the HM model, the switching term models death differently depending on whether or not the microbes have sufficient energy for maintenance or not. When the microbes have sufficient energy over and above their maintenance requirement (i.e., $\Delta_m > 0$) they go into reproductive mode (assumption 7). The term Y_m is the reproduction coefficient for methanogens (which includes natural death). Note that in the reproductive mode, the reproduction rate is greater than the natural death of cells and so the net reproduction coefficient of a methanogen cell, Y_m (cell mol_{ATP}^{-1}), is positive. When the microbes do not have sufficient energy to meet their maintenance requirements, they go into the decay mode where $\Delta_m \leq 0$. Here the reproduction coefficient is given by d_m/m_m, a death coefficient of a methanogen cell due to starvation and the unit of d_m/m_m is the same as Y_m so that the unit of equation (2.5) for $\Delta_m \leq 0$ matches up with that of when $\Delta_m > 0$. Note that the biological parameters (n_m, q_m, K_m, m_m, d_m and Y_m) and S_h are all positive. When $\Delta_m \leq 0$,

$$\left(\frac{n_m q_m S_h}{K_m + S_h} - m_m \right) \leq 0 \ .$$

From the HM model, equation (2.5) becomes

$$X'_m = \left(\frac{n_m q_m S_h}{K_m + S_h} - m_m \right) \frac{d_m}{m_m} X_m - \alpha X_m \ .$$

Essentially, when $\Delta_m \leq 0$, the amount of ATP gained from metabolizing hydrogen ($n_m q_m$) does not meet the maintenance requirement (m_m) for methanogens. That is, when $\Delta_m \leq 0$, by assumption 7, methanogens cannot reproduce and death occurs in the population due to starvation.

2.3 Steady state solutions

Mathematically, the long term hydrogen-methanogen dynamics can be characterized by the steady state solutions of the model. These solutions correspond to an equilibrium (critical) point for the dynamical system that can be used to explore the behaviors of this model.

An equilibrium point for equations (2.4) and (2.5) is a point (S_h^*, X_m^*) at which $S'_h = X'_m = 0$, i.e.,

$$-\frac{q_m S_h^*}{K_m + S_h^*} X_m^* - \alpha S_h^* + \beta_h = 0 \ , \tag{2.10}$$

$$\Delta_m E_m X_m^* - \alpha X_m^* = 0 \ . \tag{2.11}$$

Evidently, $(S_h^{*1}, X_m^{*1}) = (\beta_h/\alpha, 0)$ is a solution to equations (2.10) and (2.11). Suppose that $X_m^* \neq 0$. Then, equation (2.11) shows that $\Delta_m E_m = \alpha$, and since E_m and α are positive, we have $\Delta_m > 0$, i.e., $E_m = Y_m$, for any equilibrium point for which $X_m^* \neq 0$. In this case, $\Delta_m E_m = \alpha$ implies

$$(Y_m(n_m q_m - m_m) - \alpha) S_h^* = K_m(Y_m m_m + \alpha) \ . \tag{2.12}$$

If $Y_m(n_m q_m - m_m) - \alpha = 0$, then there are no solutions to equations (2.10) and (2.11) apart from (S_h^{*1}, X_m^{*1}). If $Y_m(n_m q_m - m_m) - \alpha \neq 0$, then, a second solution to equations (2.10) and (2.11) is

$$(S_h^{*2}, X_m^{*2}) = \left(\frac{K_m(Y_m m_m + \alpha)}{Y_m(n_m q_m - m_m) - \alpha}, \frac{(\beta_h - \alpha S_h^{*2}) Y_m n_m}{Y_m m_m + \alpha} \right) \ . \tag{2.13}$$

When the hydrogen concentration is smaller than S_h^{crit}, i.e., $\Delta_m < 0$, there is another equilibrium point, (S_h^{e3}, X_m^{e3})

$$(S_h^{*3}, X_m^{*3}) = \left(\frac{K_m m_m (d_m + \alpha)}{d_m(n_m q_m - m_m) - m_m \alpha} \, , \frac{(\beta_h - \alpha S_h^{*3}) d_m n_m}{m_m (d_m + \alpha)} \right) . \quad (2.14)$$

As shown in the next subsection, this point is useful for understanding some of the solution trajectories, it is not relevant to the long term dynamics of the system, since trajectories can not access it. Note that $S_h^{*2} > S_h^{\text{crit}}$ and $S_h^{*3} > S_h^{\text{crit}}$. It is possible that $S_h^{*2} < 0$ and/or $X_m^{*2} < 0$. In such cases (S_h^{*2}, X_m^{*2}) is of limited biological interest. Even if either of these quantities is negative, it is nonetheless useful to classify them because they do influence the geometry of solution curves that are in the biologically relevant positive quadrant.

2.3.1 Stability of steady state solutions

The solutions to the equations (2.4) and (2.5), for an initial condition $(S_h(0),\ X_m(0))$ can be represented by a trajectory, i.e., $(S_h(t),\ X_m(t))$, in the SX-plane. The family of trajectories formed by different initial conditions is the phase plane [57] that represents the interaction between the hydrogen concentration and the methanogen population geometrically. Equilibrium points dominate the long term behavior of solution trajectories. We are interested primarily in the steady state behavior of S_h and X_m. The dynamics of (S_h, X_m) are determined (at least locally) by the nature of the equilibrium points. Briefly, these points can be classified as stable or unstable. A stable steady state solution requires the equilibrium point to be stable in a sense that any $(S_h(0),\ X_m(0))$ near a stable equilibrium point will be drawn towards this point, and stay at the stable equilibrium point. In this sense, a stable equilibrium point represents a stable steady state solution of the model. If the initial condition happens to be an equilibrium point, i.e., $S_h(0) = S_h^*$, $X_m(0) = X_m^*$, then the solution is the constant solution $S_h = S_h^*$ and $X_m = X_m^*$ for all $t \geq 0$. The stability of an equilibrium point can be deduced from the eigenvalues associated with the point. Specifically, each equilibrium point has two

933 eigenvalues, λ_a and λ_b, and it is these values that determine the nature
934 of the equilibrium point. Let $\mathrm{Re}(\lambda_a)$ and $\mathrm{Re}(\lambda_b)$ denote the real part of
935 the eigenvalues, then (S_h^*, X_m^*) can be classified in the following way [9].

936 **A** stable, if both $\mathrm{Re}(\lambda_a)$ and $\mathrm{Re}(\lambda_b)$ are negative ;

937 **B** repelling, if both $\mathrm{Re}(\lambda_a)$ and $\mathrm{Re}(\lambda_b)$ are positive ;

938 **C** saddle, if $\mathrm{Re}(\lambda_a)$ and $\mathrm{Re}(\lambda_b)$ have opposite signs ;

939 **D** a centre or unknown, if both $\mathrm{Re}(\lambda_a)$ and $\mathrm{Re}(\lambda_b)$ are zero.

940 The equilibrium point of scenarios B or C is an example of an unstable
941 point. Solution trajectories near a centre will neither be attracted to it
942 nor be repelled from it.

943 The eigenvalues are evaluated at the steady state solutions from the
944 Jacobian matrix of the system equations. For the HM model, the eigen-
945 values, λ_a and λ_b are calculated by taking the partial derivatives of equa-
946 tions (2.4) and (2.5), and forming a 2 by 2 Jacobian matrix, J. Then,
947 the values of S_h and X_m at $(S_h^*,\ X_m^*)$ are substituted in the Jacobian,
948 and the equation $\det(J - \lambda I) = 0$ is solved to get λ_a and λ_b.

$$J = \begin{bmatrix} -\frac{q_m K_m X_m}{(K_m+S_h)^2} - \alpha & -\frac{q_m S_h}{K_m+S_h} \\ \\ \frac{E_m n_m q_m K_m X_m}{(K_m+S_h)^2} & E_m(\frac{n_m q_m S_h}{K_m+S_h} - m_m) - \alpha \end{bmatrix},$$

and

$$\det(J - \lambda I) = \begin{vmatrix} -\frac{q_m K_m X_m}{(K_m+S_h)^2} - \alpha - \lambda & -\frac{q_m S_h}{K_m+S_h} \\ \\ \frac{E_m n_m q_m K_m X_m}{(K_m+S_h)^2} & E_m(\frac{n_m q_m S_h}{K_m+S_h} - m_m) - \alpha - \lambda \end{vmatrix}.$$

949 At $(S_h^{*1},\ X_m^{*1})$ the eigenvalues are therefore

$$\lambda_{a1} = -\alpha\ ,$$
$$\lambda_{b1} = \left(\frac{E_m(n_m q_m - m_m) - \alpha}{\alpha K_m + \beta_h}\right)(\beta_h - \alpha S_h^{*2})\ .$$

950 At (S_h^{*2}, X_m^{*2}) and (S_h^{*3}, X_m^{*3}) the eigenvalues are

$$\lambda_{a2}, \lambda_{b2} = \frac{-(\alpha + \Xi) \pm \sqrt{(\alpha + \Xi)^2 - 4(E_m m_m + \alpha)\Xi}}{2} ,$$

951 where

$$\Xi = \frac{K_m(\beta_h - \alpha S_h^*)}{S_h^*(K_m + S_h^*)} ,$$

952 and S_h^* equals S_h^{*2} or S_h^{*3}. Notice that the nature of (S_h^{*2}, X_m^{*2}) and
953 (S_h^{*3}, X_m^{*3}) is the same: these two points are either both stable or both
954 unstable. The nature of the three equilibrium points are determined by

$$E_m(n_m q_m - m_m) - \alpha , \tag{2.15}$$

955 and

$$\beta_h - \alpha S_h^* . \tag{2.16}$$

956 Suppose first that $S_h^{*2} > 0$ and $X_m^{*2} > 0$. Then $E_m = Y_m$

$$Y_m(n_m q_m - m_m) - \alpha > 0 , \tag{2.17}$$

957 and

$$\beta_h - \alpha S_h^{*2} > 0 . \tag{2.18}$$

958 This makes (S_h^{*1}, X_m^{*1}) a saddle point. If $\Xi > 0$, and if

$$(\alpha + \Xi)^2 - 4(E_m m_m + \alpha)\Xi \geq 0 , \tag{2.19}$$

959 then the eigenvalues λ_{2a} and λ_{2b} are real. Since

$$\sqrt{(\alpha + \Xi)^2 - 4(E_m m_m + \alpha)\Xi} < (\alpha + \Xi) ,$$

960 we have

$$-(\alpha+\Xi) \pm \sqrt{(\alpha+\Xi)^2 - 4(E_m m_m + \alpha)\Xi} < 0 \ ,$$

961 and thus both λ_{2a} and λ_{2b} are negative. In this case, both (S_h^{*2}, X_m^{*2})
962 and (S_h^{*3}, X_m^{*3}) are stable equilibrium points. If inequality (2.19) is not
963 satisfied, then the eigenvalues are complex, but $\mathrm{Re}(\lambda_{2b}) = \mathrm{Re}(\lambda_{2b}) =$
964 $-(\alpha+\Xi)$, and thus (S_h^{*2}, X_m^{*2}) and (S_h^{*3}, X_m^{*3}) are stable.

965 Suppose both inequalities (2.17) and (2.18) are satisfied. When the
966 hydrogen concentration is below S_h^{crit}, the solution curve is attracted to
967 (S_h^{*3}, X_m^{*3}). Mathematically, the solution trajectories is affected geo-
968 metrically by the presence of (S_h^{*3}, X_m^{*3}). However, when the hydrogen
969 concentration is greater than S_h^{crit}, the solution trajectories are governed
970 by expressions (2.4) and (2.5) with $E_m = Y_m$ and thus attracted to (S_h^{*2},
971 X_m^{*2}). Thus, (S_h^{*3}, X_m^{*3}) cannot be accessed by the solution trajectories
972 so that (S_h^{*3}, X_m^{*3}) is omitted from further discussion. When both in-
973 equalities (2.17) and (2.18) are satisfied, the solution trajectories ($S_h(t)$,
974 $X_m(t)$) approach (S_h^{*2}, X_m^{*2}) as $t \geq 0$ with $S_h^{*2} > 0$ and $X_m^{*2} > 0$. Since
975 Y_m and α are positive, inequality (2.17) implies that

$$n_m q_m > m_m \ ,$$

976 i.e., methanogens must gain energy faster than their maintenance re-
977 quirement. Inequality (2.17) also implies that $S_h^{\mathrm{crit}} > 0$. Inequality (2.18)
978 requires the hydrogen generation rate to exceed the rate of hydrogen loss
979 near S_h^{*2}.

980 Let us plot phase plane diagrams for the system to investigate changes
981 in the stability of the steady state solutions for increasing values of pas-
982 sage rate. The nullclines representing $X_m' = 0$ are given by

$$X_m = 0 \ , \tag{2.20}$$

983 and

$$S_h = \frac{K_m(Y_m m_m + \alpha)}{Y_m(n_m q_m - m_m) - \alpha} \ . \tag{2.21}$$

The nullcline representing $S_h' = 0$ is

$$X_m = \frac{(K_m + S_h)(\beta_h - \alpha S_h)}{q_m S_h} \ , \tag{2.22}$$

assuming $S_h \neq 0$. (Note $S_h = 0$ and $S_h' = 0$ would require $\beta_h = 0$. We assume the hydrogen input into the system is greater than zero, i.e., there is a food intake by ruminants so that S_h is non-zero). An intersection of nullcline (2.20) and (2.22) requires $S_h = \beta_h/\alpha$. Note that the possibility of $S_h = -K_m$ is not in the domain of equations (2.4) and (2.5). An intersection of nullcline (2.21) and (2.22) requires

$$Y_m(n_m q_m - m_m) > \alpha \ ,$$

for positive substrate concentration. The intersection of the nullclines for $X_m' = 0$ and $S_h' = 0$ are the steady states of the system, e.g., there are two steady states in this example.

From equation (2.22),

$\beta_h < \alpha S_h = \frac{\alpha K_m}{\frac{Y_m n_m q_m}{Y_m + \alpha} - 1}$ gives $X_m < 0$;

$\beta_h = \alpha S_h$ gives $X_m = 0$ (which is the trivial solution already covered) ;

$\beta_h > \alpha S_h = \frac{\alpha K_m}{\frac{Y_m n_m q_m}{Y_m + \alpha} - 1}$ gives $X_m > 0$.

A bifurcation occurs at

$$\beta_h = \frac{\alpha K_m}{\frac{Y_m n_m q_m}{Y_m + \alpha} - 1} \ .$$

Solving for the positive root of α (passage rate must be positive), α_{sta}, the passage rate threshold value so that methanogens will be eliminated due to shortage of food, and we can find this bifurcation occurs at

$$\alpha_{\text{sta}} = \frac{-(\beta_h + Y_m m_m K_m) + \sqrt{(\beta_h + Y_m m_m K_m)^2 + 4\beta_h K_m (Y_m n_m q_m - Y_m m_m)}}{2K_m} \ . \tag{2.23}$$

Let $\alpha_{\text{tol}} = Y_m(n_m q_m - m_m)$. From equation (2.23), we obtain

$$\alpha_{\text{sta}} = \frac{\beta_h}{\beta_h + K_m\alpha_{\text{sta}} + Y_m m_m K_m}\alpha_{\text{tol}} \ . \tag{2.24}$$

Because all the parameter values are positive $0 < \alpha_{\text{sta}} < \alpha_{\text{tol}}$. We have for

(a) $0 < \alpha < \alpha_{\text{sta}}$
we have two steady states. The trivial solution is unstable, and the solution associated with non-trivial methanogen population density ($X_m > 0$) is stable;

(b) $\alpha_{\text{sta}} < \alpha < \alpha_{\text{tol}}$
both steady states again exist but the solution associated with non-trivial methanogen population is now unstable ($X_m < 0$) and the trivial solution is stable;

(c) $\alpha_{\text{tol}} < \alpha$
only the trivial steady state solution exists and is stable.

In Figure 2.1, each of the three scenarios is shown. Parameter values ($n_m = 1$, $q_m = 2$, $K_m = 1$, $m_m = 1$, $Y_m = 3$ and $\beta_h = 3$) have been arbitrarily chosen to illustrate each cases. For the given parameter values, and for positive substrate concentration, bifurcations occur at $\alpha_{\text{sta}} = 3(\sqrt{2} - 1)$ and again at $\alpha_{\text{tol}} = Y_m(n_m q_m - m_m) = 3$. In Figure 2.1(a), $\alpha = 0.9 < 3(\sqrt{2} - 1)$ and case (a) applies. In Figure 2.1(b), $\alpha = 1.5$ so that $3(\sqrt{2} - 1) < \alpha < 3$ and case (b) applies and in Figure 2.1(c) $\alpha = 6 > 3$ and case (c) applies. Dashed lines represent nullclines (2.20) and (2.21) and the solid line represents nullclines (2.22). The $S_h' = 0$ nullcline in the negative S_h quadrants is not shown as a negative substrate concentration is not relevant in the rumen context. The intersection of the nullclines for $X_m' = 0$ and $S_h' = 0$ are the equilibrium points of the HM model. Closed dot is a stable equilibrium point and open dot is an unstable equilibrium point. When both inequalities (2.17) and (2.18) are satisfied, ($S_h^{*2} > 0$, $X_m^{*2} > 0$) is a stable point as illustrated in Figure 2.1(a). If one of inequalities (2.17) and (2.18) is not satisfied, ($S_h^{*1} > 0$, $X_m^{*1} = 0$) is the only stable equilibrium point (Figure 2.1(b) and (c)).

For instance, suppose

$$Y_m(n_m q_m - m_m) < \alpha \ ,$$

then $S_h^* < 0$. Then, inequality (2.18) is satisfied because both β_h and α are non-negative. Then scenario where both inequalities (2.17) and (2.18) are not satisfied is not feasible.

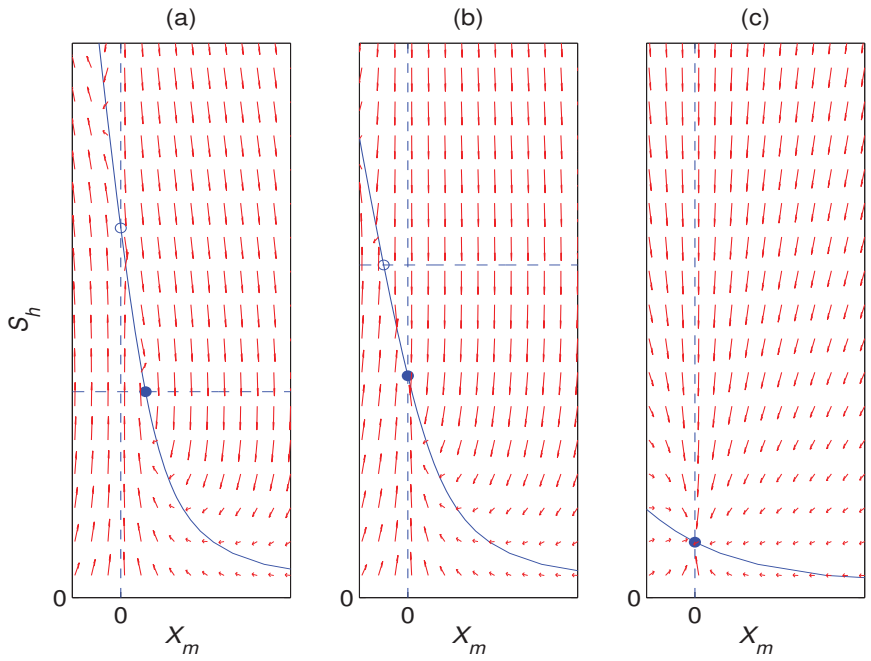

Figure 2.1: The steady state diagram and direction field of the HM model with parameter values ($n_m = 1$, $q_m = 2$, $K_m = 1$, $m_m = 1$, $Y_m = 3$ and $\beta_h = 3$ together with appropriate values of α) were chosen arbitrarily. (a) $\alpha = 0.9$ methanogens survive, $X^* > 0$. (b) $\alpha = 1.5 > \alpha_{\text{sta}}$ so that inequality (2.18) is not satisfied hence methanogens are eliminated, $X^* = 0$, due to insufficient food supply and (c) $\alpha = 6 > \alpha_{\text{tol}}$ so that inequality (2.17) is not satisfied hence methanogens are eliminated by washout.

In a nutshell, (S_h^{*1}, X_m^{*1}) is either a saddle or a stable point depending on parameter values and rumen environment. This is associated with (S_h^{*2}, X_m^{*2}) as a stable point (either a focus i.e., both eigenvalues of $(S_h^{*2},$

X_m^{*2}) are complex or a node i.e., both eigenvalues are real) or a saddle, respectively.

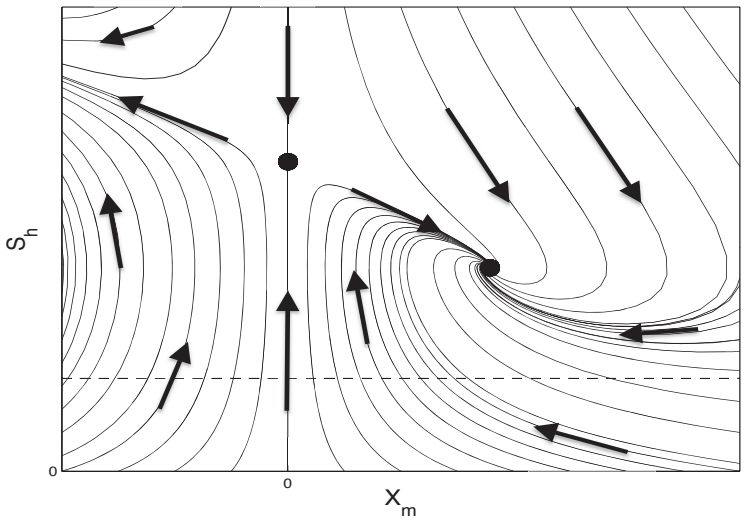

Figure 2.2: A typical phase plane for the system when $S_h^{*2} > 0$ and $X_m^{*2} > 0$.

Figure 2.2 is generated in MATLAB [102] and depicts a typical phase plane for the system with parameter values ($n_m = 1$, $q_m = 1$, $K_m = 0.8$, $m_m = 0.6$, $Y_m = 0.6$, $\alpha = 0.1$ and $\beta_h = 0.4$) were chosen arbitrarily so that $S_h^{*2} > 0$ and $X_m^{*2} > 0$, and both eigenvalues of (S_h^{*2}, X_m^{*2}) are complex so that (S_h^{*2}, X_m^{*2}) is a focus. In this figure the equilibrium points are represented by solid dots and each curve represents a solution to the system for different initial values of S_h and X_m. The horizontal dashed line is S_h^{crit}. The characteristics of the equilibrium points influence the solution curves, i.e., the arrows in Figure 2.2 show the evolution of hydrogen concentration and methanogen population over time. For any choice of initial conditions $(S_h(0), X_m(0))$, such that $S_h(0) \geq 0$ and $X_m(0) > 0$, the curve moves towards the steady state solution (S_h^{*2}, X_m^{*2}). A zero methanogen population is never achieved, unless $X_m(0) = 0$. In this case, the hydrogen concentration stabilizes at $S_h^{*1} = \beta_h/\alpha$. The phase plane includes curves outside the positive quadrant. Although such curves are not biologically relevant, they help to illustrate the global dynamics of the system. Mathematically, it is possible to have a negative methanogen population. The curves at the left of $X_m = 0$, however,

cannot cross the line $X_m = 0$ because (S_h^{*1}, X_m^{*1}) is a saddle point.

2.3.2 Estimation of methane production

As noted in Section 1.4.2.1, the existing mechanistic models use a net hydrogen balance, which is the difference between the amount of hydrogen produced and used in reactions occurring in the rumen on a daily basis. In contrast, our model uses the amount of hydrogen metabolized by the methanogens to calculate methane. Not all hydrogen generated becomes methane and the residual hydrogen contributes to a dynamic hydrogen pool, which in turn is expected to feed back on hydrogen-forming steps to result in less net hydrogen formation (i.e., hydrogen production becomes less favorable [76]). In contrast, for existing mechanistic models (Section 1.4.2.1), there is no explicit expression of a dynamic hydrogen pool because there is no residual hydrogen after estimating the methane production based on these models. From the chemical reaction (1.1), four moles of hydrogen metabolized yields one mole of methane so that the methane production rate, M, is

$$M = \frac{1}{4}\frac{q_m S_h}{K_m + S_h} X_m \ \ (\text{mol ml}^{-1}\ \text{s}^{-1}) \ . \tag{2.25}$$

In comparison to existing mechanistic models, there is an advantage to calculating methane production using expression (2.25). This expression allows one to calculate methane production for any time span with non-constant rates of passage and hydrogen generation.

In this model, it is assumed that there are constant rates of passage and hydrogen generation. If inequalities (2.17) and (2.18) are both satisfied, then there is only one stable, steady state solution, (S_h^{*2}, X_m^{*2}), and it is therefore reasonable to consider the steady state methane production, M^*, corresponding to this steady state solution. Substituting expression (2.13) into expression (2.25) yields

$$M^* = \frac{86400}{4}(\beta_h - \frac{\alpha K_m (Y_m m_m + \alpha)}{Y_m(n_m q_m - m_m) - \alpha}) r_c \ (\text{mol rumen}^{-1}\ \text{d}^{-1}) \ , \tag{2.26}$$

where there are 86400 seconds per day and r_c is the rumen liquid volume in ml. Notice that αS_h^{*2} is the proportion of hydrogen removed as part of the material passing out of the rumen at steady state. The biological expectation ([76], [68]) is that methane production is proportional to the net rate at which hydrogen is available in the rumen [68], i.e., $\beta_h - \alpha S_h^{*2}$ as in this model.

We evaluated the outputs of this model by using some typical parameter values found in the literature (Table 2.1). The death coefficient d_m (s^{-1}) was calculated by assuming 50% of methanogens cells are eliminated after 32 days of starvation [86]. Note that M^* does not depend on d_m. We estimated the hydrogen generation rate by conversion of the amount of methane production reported by Wolin [182]: we assume the rumen liquid volume is 82000 ml and the amount of methane produced in such a rumen is 8.3 mol rumen^{-1} d^{-1} (equivalent to about 200 L of methane production per rumen). Kaster *et al.* [81] reported a metabolism rate of hydrogen by methanogens of 8.461×10^{-5} (mol gram^{-1} s^{-1}), so with a cell mass of 4.44×10^{-13} (gram cell^{-1}) [74] we obtain $q_m = 3.76 \times 10^{-17}$ (mol cell^{-1} s^{-1}).

Note that inequalities (2.17) and (2.18) are satisfied with the typical parameter values. With these typical parameter values in Table 2.1, from equation (2.26), the methane production is 8.3 mol rumen^{-1} d^{-1}. The rate β_h is calculated from the methane production reported for a typical animal [181] and leads to the expected $M^* = 8.3$ mol rumen^{-1} d^{-1} with such β_h value. This exercise indicates that this model does not introduce any artefact that could change the magnitude of S_h^* and/or X_m^* and then M^*. With these typical parameter values, expression (2.13) indicates that

$$(S_h^{*2}, X_m^{*2}) = (1.1034 \times 10^{-10} \text{ mol ml}^{-1},\ 3.515 \times 10^{8} \text{ cell ml}^{-1}) .$$

The magnitudes of steady state hydrogen concentration and methanogens population are in agreement with those found in the literature ($1.9 - 11.7 \times 10^{-10}$ mol ml^{-1}, $1.42 - 13.4 \times 10^{8}$ cell [30], [68], [70], [121], [138]).

When (S_h^{*1}, X_m^{*1}) is a stable point, the corresponding estimated methane

Table 2.1: Parameter values used in the HM model.

Parameter	Description	Value
α	passage rate through the rumen	3.50×10^{-5} (s^{-1}) [150]
β_h	rate of hydrogen generation	4.70×10^{-9} (mol ml^{-1} s^{-1}) [182]
n_m	energy captured from metabolizing per mole of hydrogen	0.125 (mol_{ATP} mol^{-1}) [160]
q_m	maximal rate at which a methanogen can metabolize hydrogen	3.76×10^{-17} (mol $cell^{-1}$ s^{-1})
K_m	hydrogen concentration at half of q_m	2.00×10^{-10} (mol ml^{-1}) [87]
m_m	maintenance requirement of a methanogen	1.36×10^{-19} (mol_{ATP} $cell^{-1}$ s^{-1}) [42]
d_m	death coefficient of methanogen	2.50×10^{-7} (s^{-1})
Y_m	reproduction coefficient of methanogen	2.28×10^{13} (cell mol_{ATP}^{-1}) [160]

production is evidently zero. There is no hydrogen consumption when the methanogen population is absent and thus no methane production.

The term M contains a number of parameters some of which are difficult to measure accurately. It is thus useful to study the sensitivity of M to these parameters. A measure of the sensitivity of M to a parameter ϕ is given by [171]

$$\Theta(\phi) = \frac{\phi}{M}\frac{\partial M}{\partial \phi} \ .$$

This is called the relative sensitivity value. It represents the normalized influence on M to a small change in ϕ. By calculating Θ for all ϕ in M, we can determine the relative influence of a small change in ϕ on M_P. Using the parameter values in Table 2.1, we find that: M is least sensitive to m_m; M is, respectively, 7.9, 11.3, 12.3, 12.3 and 18.9 times more relatively sensitive to K_m, Y_m, n_m, q_m and α than it is to m_m; M is most sensitive to β_h, at 190 million times more relatively sensitive than it is to m_m.

Finding the change in M, the estimated methane production given in expression (2.25), with respect to a given increase in any of m_m, K_m, Y_m, n_m, q_m, α and β_h, yields the actual sensitivity of M with respect to that variable. Considering a 10% increase in each of m_m, K_m, Y_m, n_m, q_m, α and β_h we explore the actual sensitivity of M with respect

to each parameter. Using the parameter values in Table 2.1, the actual sensitivity of M is, respectively, -0.104$\times 10^{-7}$, -0.821$\times 10^{-7}$, 1.017$\times 10^{-7}$, 1.103×10^{-7}, 1.103×10^{-7}, -2.178$\times 10^{-7}$ and 1 with respect to m_m, K_m, Y_m, n_m, q_m, α and β_h. A negative magnitude in the actual sensitivity value of M with respect to a parameter indicates a decrease in estimated methane production by increasing that parameter value. For instance, increasing the maintenance requirement of a methanogen (m_m) and/or passage rate (α) will reduce the methanogen population density so that less methane is produced. In contrast, a positive magnitude in the actual sensitivity value of M with respect to a parameter indicates an increase in estimated methane production by increasing that parameter value. For example, doubling β_h, also doubles M with steady state solution, (S_h^{*2}, X_m^{*2}). The rate of methane production is proportional to the net rate of hydrogen generation from feed in the rumen [68], because nearly all the hydrogen is rapidly converted to methane. The implications of these findings are discussed next.

2.4 Effects of changes in hydrogen generation rate

In this section we consider the effect of β_h on X_m^* and hence M. We will regard all other parameters as fixed. With no consumption of hydrogen, $X_m^{*1} = 0$, and a larger hydrogen generation rate will result in a higher hydrogen concentration in the rumen. Note that X_m^{*2} depends on β_h, but S_h^{*2} does not. This indicates that the steady state hydrogen concentration is determined by the biological parameters associated with methanogens and passage rate, but not on the ruminal hydrogen generation rate itself. This observation is a consequence of using the Monod model [115] to describe the rate of hydrogen metabolism at a given hydrogen concentration, Equation (2.1) and, in fact, would also be true using any other per-capita kinetic law that is a function of the limiting growth substrate S_h only [140]. Suppose now that we consider X_m^{*2} for two different hydrogen generation rates, $c\beta_h$ and β_h, where c is a constant. We see that

the term αS_h^{*2} is much smaller than β_h, assuming that the number c is not too small relative to β_h; hence,

$$\frac{X_m^{*2}(c\beta_h)}{X_m^{*2}(\beta)} = \frac{c\beta_h - \alpha S_h^{*2}}{\beta_h - \alpha S_h^{*2}} \approx c \ . \tag{2.27}$$

This shows that, as long as methanogens can survive in the rumen, increasing the hydrogen generation rate by a factor of c roughly increases the methanogen population, and hence methane production, by a factor of c.

2.5 Effects of changes in passage rate

In this section, we discuss the predicted changes (based on the model) of the reproduction rate of methanogens, steady state hydrogen concentration and methane production in response to changes in ruminal passage rate. This is to test the mathematical enunciation of this model for consistency with biological expectations.

2.5.1 Effect of passage rate on the reproduction rate of methanogens

At the steady state (S_h^{*2}, X_m^{*2}), the reproduction rate of methanogens is

$$\mu_m = Y_m \left(n_m q_m \frac{S_h^{*2}}{K_m + S_h^{*2}} - m_m \right) = \alpha \ . \tag{2.28}$$

Biologically, this means that the methanogen population must reproduce at a rate that exactly replaces those methanogens removed from the rumen to maintain equilibrium. From equations (1.2) and (1.3),

$$t_d = \log(2)/\mu_m$$

with typical parameter values, the doubling time of methanogens is $t_d =$ 143.35 minutes. This value is within the interval (between 29 to 623 minutes) of the doubling time of different types of methanogens reported

by Pavlostathis and Giraldo-Gomez [129].

It is useful to explore the maximal passage rate that can be tolerated by methanogens as predicted by the model. Let us define the tolerance threshold as the maximum passage rate, α_{tol}, that methanogens can tolerate without being eliminated from the rumen, i.e., $X_m^{*2} > 0$. Using the typical parameter values in Table 2.1, expression (2.17) implies

$$\alpha_{\text{tol}} = Y_m(n_m q_m - m_m) = \ 1.04 \times 10^{-4} \text{ s}^{-1} \ (0.374 \text{ h}^{-1}) \ .$$

Note that the passage rate in Table 2.1 is $\alpha = 3.50 \times 10^{-5} < 1.04 \times 10^{-4}$ s^{-1} so methanogens can survive with a positive methane production in this setting. From equation (2.23), using the parameter values in Table 2.1, the passage rate threshold value so that methanogens will be eliminated due to shortage of food, α_{sta}, is 0.00046% less than α_{tol}, i.e., $\alpha_{\text{sta}} \approx \alpha_{\text{tol}}$. In Section 2.5, we explore the effect of varying the passage rate, α, between $0 < \alpha < \alpha_{\text{sta}}$ on the stable steady state methanogen population, hydrogen concentration and methane production.

With $\beta_h = 4.70 \times 10^{-9}$ mol ml^{-1} s^{-1}, if $0 < \alpha < \alpha_{\text{sta}}$, the only stable equilibrium point is (S_h^{*2}, X_m^{*2}) because both inequalities (2.17) and (2.18) are satisfied. As passage rate increases towards α_{sta}, a larger proportion of methanogens will be removed from the rumen so that the stable steady state methanogen population decreases (Figure 2.3). That is, the methanogen population could be reduced if their reproduction rate was made slower than the passage rate, which would reduce methane production because less hydrogen will be metabolized. This reduction in the reproduction rate could be achieved using chemical inhibitors or vaccines [91]. The whole methanogen population will be eliminated when $\alpha \geq \alpha_{\text{sta}}$. However, a typical range of passage rate is $1 \times 10^{-5} \leq \alpha \leq 5 \times 10^{-5}$ s^{-1} [150], [152]. Thus, practically the methanogen population will not be removed by increasing the passage rate because $\alpha_{\text{sta}} > 5 \times 10^{-5}$ s^{-1} is greater than typical passage rate values in the rumen. If $\alpha \geq \alpha_{\text{sta}}$, inequality (2.18) is not satisfied and there is a bifurcation at $\alpha \geq \alpha_{\text{sta}}$ where the only stable equilibrium point becomes (S_h^{*1}, X_m^{*1}) instead of the point (S_h^{*2}, X_m^{*2}), as predicted by the HM model.

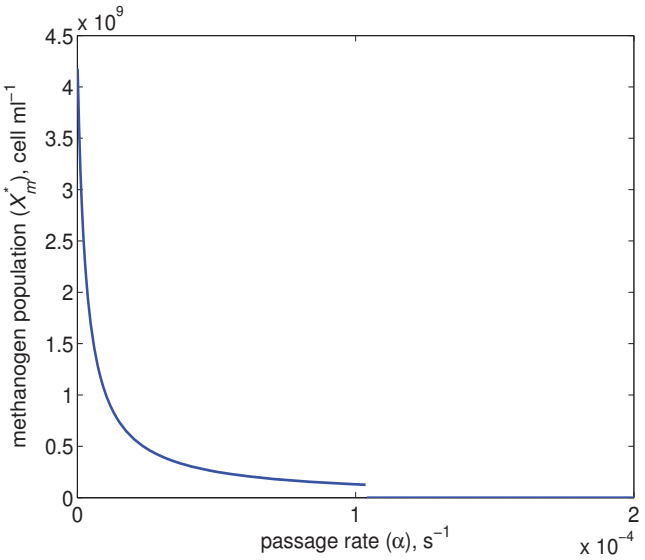

Figure 2.3: The stable steady state methanogen population for a range of passage rate values with other parameter values in Table 2.1. There is a discontinuity in the figure ($\alpha = \alpha_{\text{sta}} = 1.04 \times 10^{-4}$ s^{-1}). If $0 < \alpha < \alpha_{\text{sta}}$, there is a stable positive population density of methanogens. Otherwise, the methanogen population density is zero.

2.5.2 Effect of passage rate on steady state hydrogen concentration

When $\alpha = 0$,

$$S_h^{*2} = \frac{K_m m_m}{n_m q_m - m_m} = S_h^{\text{crit}} \ . \tag{2.29}$$

For fixed biological parameter values of methanogens in Table 2.1, as $\alpha \to \alpha_{\text{tol}}$, $S_h^{*2} \to \infty$. This seemingly counterintuitive observation can be explained from the Monod model. The Monod model requires a greater S_h^{*2} to allow a greater reproduction rate of methanogens. A greater passage rate leads to a greater reproduction rate of methanogens at steady state. The steady state hydrogen concentration thus increases with an increasing passage rate.

With the same β_h, as shown in expression (2.26)

$$\lim_{\alpha \to \alpha_{\text{tol}}} M^* \to 0 \ ,$$

because $S_h^{*2} \to \infty$. Indeed, biological experiments have provided evidence of increasing passage rate leads to less methane production. Sheep that naturally produced less methane per unit of feed eaten have been reported to have smaller rumens and faster ruminal passage rate [50]. Also, increasing feeding level results in increased rumen passage rate of solids and liquids, with a concomitant reduction in methane per unit of intake [54]. Ruminants fed with fresh forages produce less methane as the amount of water in the feed increases, presumably as an effect of acceleration of liquid passage rate in the rumen [125]. When developing methane mitigation strategies, particularly those targeted at reducing the activity of methanogens [91], this model could help us to understand the behavior of methane production in terms of the biological characteristics of methanogens, such as maintenance or reproduction rate, and rumen environment parameters, such as passage rate.

From equation (2.24), $\alpha_{\text{sta}} < \alpha_{\text{tol}}$. As α tends towards α_{sta} from the right, the only stable hydrogen concentration S_h^{*2} tends towards infinity (illustrated in Figure 2.4(a)) and X_m^{*2} tends towards zero (Figure 2.3). In this limit, $\alpha \to \alpha_{\text{sta}}$, the only physically meaningful stable solution is (S_h^{*2}, X_m^{*2}) because both inequalities (2.18) and (2.17) are both satisfied. For $\alpha \geq \alpha_{\text{sta}}$ or $\alpha \geq \alpha_{\text{tol}}$, the stable steady state solution will change from point (S_h^{*2}, X_m^{*2}) to $(S_h^{*1}, X_m^{*1} = 0)$. That is, when $\alpha \geq \alpha_{\text{sta}}$ or $\alpha \geq \alpha_{\text{tol}}$, the only stable steady state hydrogen concentration is S_h^{*1} because inequality (2.18) or inequality (2.17) is respectively not satisfied. S_h^{*1} decreases as α increases. In the absence of methanogens there is no consumption of hydrogen in the rumen, and a greater passage rate leads to a smaller steady state hydrogen concentration through dilution (Figure 2.4(b)). A typical range of passage rate is $1 \times 10^{-5} \leq \alpha \leq 5 \times 10^{-5}$ s^{-1} [150], [152]. Thus, in Figure 2.4, the hydrogen concentration associated with $\alpha > 6 \times 10^{-5}$ s^{-1} will not be observed in the rumen. Based on the HM model, the corresponding hydrogen concentration with respect

to $\alpha = 5 \times 10^{-5}$ s^{-1} is at most 0.2×10^{-9} mol ml^{-1}. In the rumen, the hydrogen concentration is approximately 1×10^{-9} mol ml^{-1} [68], [177].

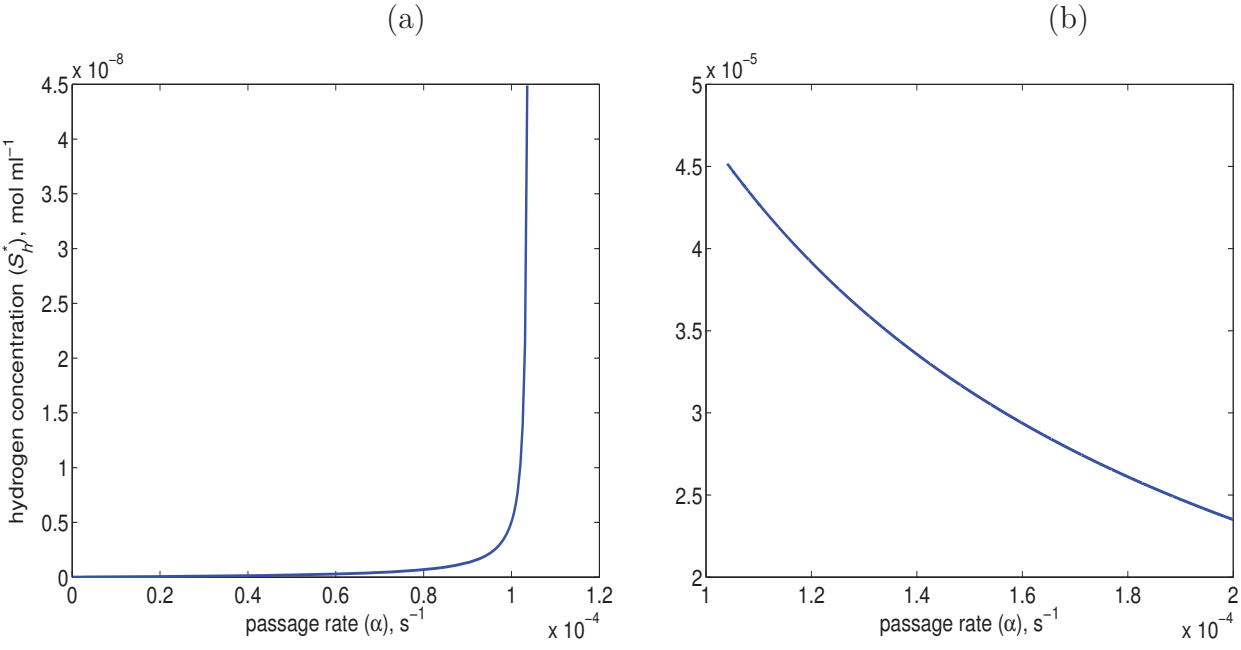

Figure 2.4: The stable steady state hydrogen concentration for a range of passage rate values with parameter values in Table 2.1. (a) for $0 < \alpha < \alpha_{\text{sta}}$. (b) for $\alpha_{\text{sta}} \leq \alpha \leq 2 \times 10^{-4}$ s^{-1}. There is approximately 1000 difference in the magnitude of the stable steady state hydrogen concentration between (a) and (b). Note that $S_h^{\text{crit}} = 5.959 \times 10^{-12}$ mol ml^{-1}.

2.5.3 Significance of passage rate

When (S_h^{*2}, X_m^{*2}) is the stable steady state, methane production (Figure 2.5) at double the typical parameter value of passage rate is only 0.0016% less than at the typical passage rate value. In contrast, the effect of passage rate on S_h^{*2} is more noticeable (Figure 2.4). It is 2.89 times greater at double the typical parameter value of passage rate. The rate of methane production is proportional to the net rate of hydrogen generation from fermentation pathways [68]. In the HM model the effect of passage rate on methane production is negligible. However, when thermodynamic control and feed fermentation pathways are introduced into the model, we will demonstrate in Chapter 5 that passage rate can shift fermentation

pathways leading to different hydrogen generation rates and the effect of changing passage rate on methane production is more noticeable than that of shown in Figure 2.5.

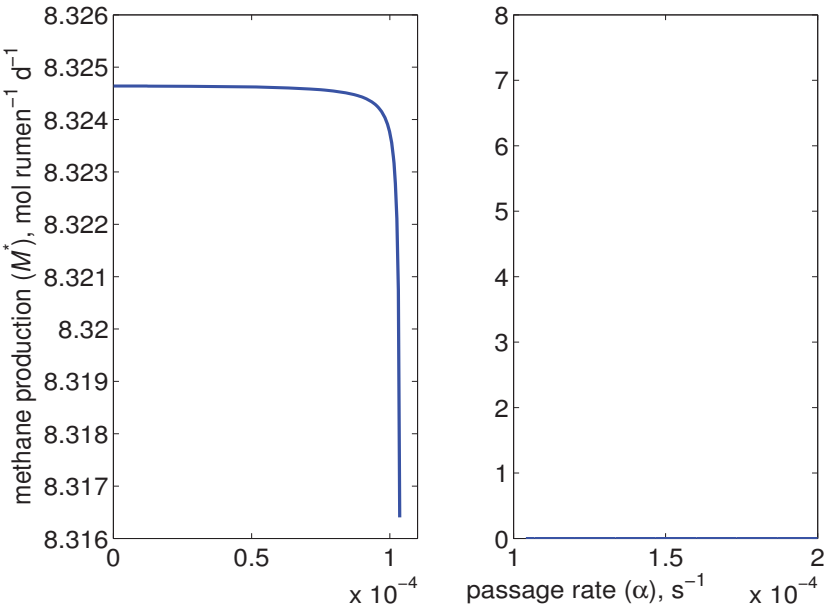

Figure 2.5: The methane production for a range of passage rate values with other parameter values in Table 2.1. There is essentially one value of methane production for $\alpha < \alpha_{\text{sta}}$ and another (0) for $\alpha \geq \alpha_{\text{sta}}$.

2.6 Passage and hydrogen generation rates

This HM model can be used to explore how different combinations of passage and hydrogen generation rates effect the dynamics system of the microbe and growth substrate. In reality in the rumen, the hydrogen generation rate depends on the ingested solid feed (and feed fermentation pathways). Feed and microbes pass through the rumen as ruminants keep ingesting solid feed, drinking liquid and secreting saliva, with the flow of material out of the rumen being commonly described as the passage rate. The passage is linked to solid feed, liquid and saliva in the rumen. That is, the hydrogen generation rate is not independent of the passage rate. However, in the HM model they are modelled as independent. In

an extension of this HM model in Chapter 4, the passage rate can shift feed fermentation pathways so that the passage rate directly affects the hydrogen generation rate through selection of feed fermentation pathways as demonstrated in Chapter 5. In Section 2.6, we investigate the effect of changing the passage rate and hydrogen generation rate independently on hydrogen-methanogen dynamics.

When $\beta_h = \alpha S_h^{*2}$, there is one stable solution

$$(S_h^*, X_m^*) = (\beta_h/\alpha, 0) \ .$$

When $\beta_h < \alpha S_h^{*2}$, inequality (2.18) is not satisfied, so that the methanogen population will be removed due to a shortage of their energy supply. This is illustrated in the phase plane, Figure 2.6, which has two equilibrium points: (S_h^{*1}, X_m^{*1}) is a stable steady state solution and (S_h^{*2}, X_m^{*2}) is a saddle point that cannot be accessed from the positive quadrant.

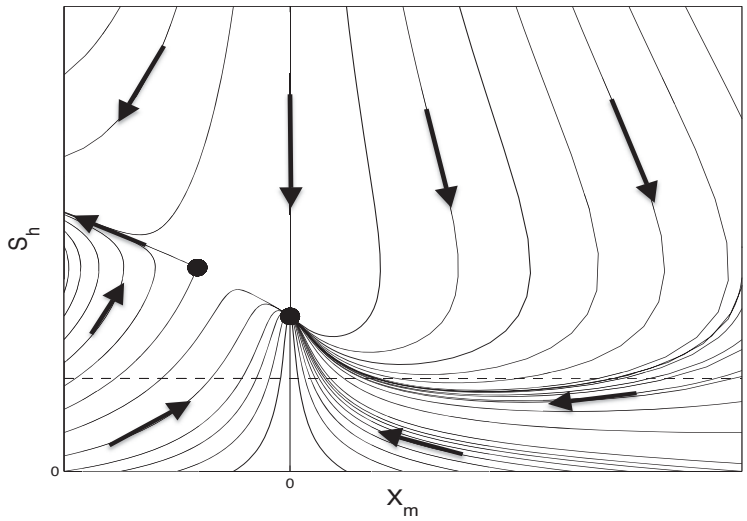

Figure 2.6: A typical phase plane for the system when $\beta_h < \alpha S_h^{e2}$.

2.7 Summary

In this chapter, a model of the hydrogen-methanogen dynamics is explored by phase planes which demonstrate the interaction between hydrogen concentration and methanogen population. Analytical results

show that (S_h^{*2}, X_m^{*2}) is the stable steady state solution of the model, if and only if inequalities (2.17) and (2.18) are both satisfied. Equivalently, there is a positive methanogen population, if and only if methanogens can tolerate the passage rate and there is sufficient food supply for reproduction. The predicted effects (based on the model) of passage rate agrees with the conceptual model postulated by Janssen [76]. That is, a greater passage rate is associated with a greater reproduction rate of methanogens (if $\alpha \geq \alpha_{\text{tol}}$, methanogens will be removed) and a greater steady state hydrogen concentration. Decreasing the maximal rate of hydrogen metabolism (q_m) or increasing the maintenance energy requirement (m_m), would lead to the methanogen population decreasing towards zero which reduces methane production as these approaches would result in the left hand side of inequality (2.17) becoming smaller. Similarly, other changes to ruminal parameters that lead to the left hand side of inequality (2.18) becoming smaller, such as increasing the passage rate or decreasing the hydrogen generation rate, would lead to less methane production.

This HM model could be used to improve our ability to model the dynamics of hydrogen in the rumen, which in turn influence aspects beyond methane formation, such as volatile fatty acid profiles. It could be employed as a basis for developing a more comprehensive model that includes thermodynamics (hydrogen concentration can thermodynamically affect the metabolism rate of hydrogen [76], see Chapter 3), and feed fermentation (see Chapter 4). Feed is degraded to produce hydrogen and volatile fatty acids and it is itself subject to thermodynamic control imposed by hydrogen concentration dynamics [76], [84]. This thermodynamic control causes a shift in production of volatile fatty acids that could be beneficial for the ruminants [72]. Ultimately, such a model could improve our ability to mathematically explore methane mitigation strategies in the rumen.

Chapter 3

Hydrogen-methanogen dynamics with thermodynamic term

In Chapter 2, K_m (i.e., K_s of the Monod model) is interpreted as a constant that describes the saturation of a cell's substrate transport capacity with increasing substrate concentrations [18]. The rate at which a cell can transform a substrate to products is limited by physical constraints of the cell. There is the rate at which the substrate can be transported into the cell, and the rate at which the cell can transform the substrate inside the cell. This physical limitation of substrate metabolism is described by q. The rate of substrate metabolism by the cell can also be limited by thermodynamic control [78]: the concentrations of substrates and products can limit the rate of substrate metabolism. Existing models (listed in [47]) described the substrate inhibition effect on metabolism rate by using functions of substrate concentration. In this chapter, a representation of thermodynamic control (a thermodynamic term) is developed that includes substrate and product concentration to describe the thermodynamic feedback on the rate of substrate transformation (e.g., the chemical reaction of substrate metabolized by a microbe to its products). This term is then introduced into the HM model to model the effects of thermodynamic feedback on the metabolism rate of hydrogen by a methanogen species in the rumen. The differences between the HM

model with and without the thermodynamic term are discussed.

3.1 Gibbs free energy and thermodynamic term

Consider a reaction,

$$a_1\mathrm{A}_1 + a_2\mathrm{A}_2 + a_3\mathrm{A}_3 \ ... \rightleftharpoons b_1\mathrm{B}_1 + b_2\mathrm{B}_2 + b_3\mathrm{B}_3 \ ... \ . \tag{3.1}$$

The forward reaction is where the substrates A_i are converted into products B_i. The backward reaction is where products are degraded into substrates. The coefficients a_i and b_i are, respectively, the amounts (moles) of $\mathrm{A_i}$ and $\mathrm{B_i}$ required to balance the chemical equation. The reaction quotient is

$$\mathcal{Q} = \frac{[\mathrm{B}_1]^{b_1}[\mathrm{B}_2]^{b_2}[\mathrm{B}_3]^{b_3}...}{[\mathrm{A}_1]^{a_1}[\mathrm{A}_2]^{a_2}[\mathrm{A}_3]^{a_3}...} = \frac{\mathcal{P}}{\mathcal{S}} \ , \tag{3.2}$$

where $[\mathrm{A_i}]$ and $[\mathrm{B_i}]$ denote the concentrations of A_i and B_i, respectively. The reaction quotient is calculated by substituting the **actual concentrations** of products and substrates, $\mathcal{P}$ and $\mathcal{S}$ into expression (3.2). At chemical equilibrium, the net change of substrate and product concentrations is zero. Substituting the **chemical equilibrium concentrations** into expression (3.2) yields the equilibrium constant, $\mathcal{K}$.

At a given temperature T, the Gibbs free energy change of a reaction, ΔG_T (kJ mol^{-1}), is [21]

$$\Delta G_T = \mathcal{R}T \ \ln(\mathcal{Q}/\mathcal{K}) \ ;$$

hence,

$$\mathcal{Q}/\mathcal{K} = \mathrm{e}^{\Delta G_T/(\mathcal{R}T)} \ \text{(unitless)} \ . \tag{3.3}$$

Here T is the ambient temperature (degrees Kelvin, K) at which the reaction occurs. In this project, this is the rumen temperature. $\mathcal{R}$

(kJ mol^{-1} K^{-1}) is the ideal gas constant. The ratio of $\mathcal{Q}/\mathcal{K}$ indicates the activity of a chemical reaction:

- If $\mathcal{Q}/\mathcal{K} = 1$, a reaction is at chemical equilibrium.
- If $\mathcal{Q}/\mathcal{K} < 1$, substrates convert into products.
- If $\mathcal{Q}/\mathcal{K} > 1$, products degrade into substrates.

Therefore, if $\mathcal{Q}/\mathcal{K} < 1$, a reaction is capable of happening without needing to be driven by an additional energy source (Similarly, work is required to make a reaction happen if $\mathcal{Q}/\mathcal{K} > 1$). Note that the unit of ΔG_T is the same as $\mathcal{R}T$, i.e., the unit of $\mathcal{Q}/\mathcal{K}$ is unitless. Also since $\mathcal{Q}$ and $\mathcal{K}$ describe the same chemical reaction, the units for $\mathcal{Q}$ and $\mathcal{K}$ in $\mathcal{Q}/\mathcal{K}$ cancel out such that $\mathcal{Q}/\mathcal{K}$ is unitless.

ΔG_T can also be defined as [21]

$$\Delta G_T = \Delta G_T^o + \mathcal{R}T \ln(\mathcal{Q}) \ ,$$

so that

$$\Delta G_T^o = -\mathcal{R}T \ln(\mathcal{K}) \ ,$$

where ΔG_T^o (kJ mol^{-1}) is the Gibbs free energy change at temperature T under standard conditions (one bar of atmospheric pressure of gases, dissolved substrates and products in units of one mole per liter, and solid and water at an activity of one). Thus, $\mathcal{Q}$ is calculated on the basis of moles per liter to match up with the units of ΔG_T^o. Rather than units of moles per milliliter used to describe microbial growth kinetics in Chapter 2, as we will see, the incorporation of the thermodynamic term into the microbial growth model will be in a unitless form, so that this difference in units is of no consequence. In living organisms, ATP (adenosine triphosphate) is one form in which energy from a reaction can be captured. Other forms, such as membrane gradients of protons or sodium can be converted stoichiometrically into ATP (or generated stoichiometrically from ATP). In this project, ATP will be used as the energy currency for organisms, without assuming exactly which form (actual

ATP or membrane gradients) is being used by the organism. Organisms such as methanogens generate ATP from ADP (adenosine diphosphate) to capture, temporarily, energy from a reaction (e.g., hydrogen metabolized by methanogens into methane in the rumen). The reaction of ATP formation is [1]

$$\mathrm{ADP}^{3-} + \mathrm{HPO}_4^{2-} + \mathrm{H}^+ \rightarrow \mathrm{ATP}^{4-} + \mathrm{H_2O} \ .$$

In order to do work, the concentration of ATP and ADP in the cell are maintained away from chemical equilibrium, and the difference from equilibrium can be described by a ΔG_{ATP} for ATP formation. The formation of ATP is driven by the energy released from the transformation of the energy source (or substrate) into products, and so the amount of ATP that can be formed is limited by the amount of energy released from the substrate transformation via a chemical reaction. As well as the thermodynamic effects of substrate and product concentrations, the coupling of ATP to the reaction of substrate transformation reduces the net free energy change, and ATP formation cannot require more energy than is available from the energy-yielding reaction. That is, energy is required to generate energy from a reaction and cannot generate more energy than the amount of energy input. Let ΔG_{ATP} (kJ mol_{ATP}^{-1}) denote the amount of energy required to form one mole of ATP. The total energy required to capture n (mol_{ATP} mol^{-1}) units of ATP per mole of substrate or product of interest is $n\ \Delta G_{ATP}$. The net Gibbs free energy for a reaction coupled to ATP formation is

$$\Delta G_T = \Delta G_T^o + \mathcal{R}T\ \ln(\mathcal{Q}) + n\ \Delta G_{ATP} \ . \tag{3.4}$$

Organisms couple the Gibbs free energy change of the transformation of their energy sources to the synthesis of ATP. These organisms then use this ATP to drive reactions required for cell maintenance and growth. The rate at which ATP is formed therefore determines the growth rate of a microbial population. ATP formation is considered as part of the overall chemical reaction, expression (3.1), of substrate transformation to product by the organisms, and the driving force governing the rate of

the transformation is the net Gibbs free energy change including ATP formation. Combining expressions (3.3) and (3.4), we can let θ denote a thermodynamic term for a reaction

$$\theta = \mathcal{Q}/\mathcal{K} = \mathrm{e}^{\Delta G_T/(\mathcal{R}T)} = \mathcal{Q}\ \mathrm{e}^{(\Delta G^o_T + n\ \Delta G_{ATP})/(\mathcal{R}T)}\ \text{(unitless)}\ . \qquad (3.5)$$

The equilibrium constant, $\mathcal{K}$, is required for the mathematical representation of thermodynamic control in rumen fermentation developed by Kohn and Boston [84] and Offner and Sauvant [124]. In the term θ, ΔG^o_T can be calculated from published data, for example from published tables, converting for temperature, as widely described in standard textbook. The actual concentration of a chemical reaction can be directly measured so that $\mathcal{Q}$ of a chemical reaction is more accessible than $\mathcal{K}$. Note that θ can be calculated without knowing $\mathcal{K}$ such that the thermodynamic term developed in this chapter is applicable to a wider ranges of chemical reactions than the approach to thermodynamic control developed by Kohn and Boston [84] and Offner and Sauvant [124]. Importantly, in addition, θ also accounts for the fact that living organisms need to use energy to capture ATP from a chemical reaction.

Transformation of substrates to products can only occur if the overall change of Gibbs free energy is negative. It is assumed that biochemical evolution does not favor true reversibility, i.e., products are not degraded into substrates, and that biochemical regulation does not allow true reversibility. That is, organisms do not transform products back into substrates with the use of ATP. Thus, if $\Delta G_T > 0$, ΔG_T is set to zero so that $0 \leq \theta \leq 1$. In the rumen, products (transformed from substrates) are absorbed (removed from the rumen) by the ruminants as energy source so that the backwards reaction is negligible.

3.2 HM model with thermodynamic term

One underlying assumption of the Monod model [115] for microbial growth is that the concentration of products is effectively zero [40]. As the reaction progresses, the accumulation of products could affect the rate

of chemical reaction. Thermodynamic control occurs when substrate metabolism is limited by the concentration of products. The thermodynamic feedback of a growth limiting substrate on the rate of its metabolism can be modelled by modifying the Monod model (examples listed in [47]) to fit with experimental data. Such models do not take into account thermodynamic feedback due to other substrates such as end products of fermentation. The thermodynamic feedback of products on the rates of substrate metabolism can be modelled by including a thermodynamic potential factor [78]. Using reaction rates from transition state theory, and average stoichiometric numbers of a chemical reaction, Jin and Bethke [78] developed a thermodynamic potential factor with a value between zero and unity. This factor can be multiplied by the Monod model [115] to model the thermodynamic feedback of products on the rates of substrate metabolism. van Lingen *et al.* [169] applied the thermodynamic potential factor developed by Jin and Bethke [78] in this way to explore the effect of hydrogen concentration on the rate of glucose metabolism. They did this by finding the value of the thermodynamic potential factor at different hydrogen concentrations. This allowed them to explore thermodynamic feedback without an explicit representation of the glucose fermenter population pools. However, we know that fermentation cannot take place without the microbes and changes in their population size changes the rate at which substrate are converted into products, and substrate and products inhibition in turn effects the growth rate of the microbes. So the size of the microbes pool, conversion of substrate to products, and production inhibition on microbial growth are all interconnected.

In this project, we develop a model that includes microbe population pool. Microbes can be considered analogues of enzymes because substrates are converted into products by microbes the same as enzymes do. The Gibbs free energy change affects the rate of transformation of substrates into products through a pathway catalyzed by multiple enzymes [2], and here we consider a microbe performing such a conversion to be an analogue of such a pathway. ATP is gained by microbes during such reaction but not for enzymes. The enzyme kinetics developed by

Haldane [53] and Plowman [134] and applied to microbial metabolism by Hoh and Cord-Ruwisch [58] has been modified for the work that follows in this thesis. As this thesis was being completed, Großkopf and Soyer [51] independently derived a thermodynamically controlled growth model based on the same basis of enzyme kinetics, but without explicitly incorporating ATP formation.

In this section, based on a symbolic scheme of theoretically reversible enzyme reactions proposed by Haldane [53], a growth kinetics model for rumen microbes with a thermodynamic term (including the energy used for the formation of ATP as part of the thermodynamic effect) is developed. This adaptation of Haldane growth kinetics model with thermodynamic term (θ) is the first of its kind in the literature. The inclusion of a thermodynamic term in the Monod model can be used to model the effect of substrate and product concentrations on the rate of energy source or substrate transformation via a chemical reaction. Based on the symbolic scheme [53], Plowman [134] and Hoh and Cord-Ruwisch [58] found the rate of transformation of a substrate with respect to the concentration of all substrates and products is

$$q = \frac{q_3(\mathcal{S} - \mathcal{P}/\mathcal{K})}{K_s + \mathcal{S} + q_3/q_2\mathcal{P}/\mathcal{K}} \ , \tag{3.6}$$

where q_3 is the maximal metabolism rate of substrate into products, q_2 is the maximal rate of transformation of products back to substrate and K_s is the Monod constant. Both Hoh and Cord-Ruwisch [58] and Plowman [134] assumed these two maximal rates are the same, i.e., $q_3 = q_2$, expression (3.6) reduces to

$$q = \frac{q_3(\mathcal{S} - \mathcal{P}/\mathcal{K})}{K_s + \mathcal{S} + \mathcal{P}/\mathcal{K}} \ , \tag{3.7}$$

and substituting $\mathcal{Q} = \mathcal{P}/\mathcal{S}$ and $\theta = \mathcal{Q}/\mathcal{K}$ into expression (3.7) yields

$$q = \frac{q_3\mathcal{S}(1-\theta)}{K_s + \mathcal{S}(1+\theta)} \ (\text{mol cell}^{-1}\ \text{s}^{-1}) \ . \tag{3.8}$$

Expression (3.8) can be used to model the rate transformation of

a substrate by a microbe and the effect of all substrate and product concentrations on the metabolism rate of that substrate. For example, as more hydrogen is metabolized by methanogens into methane, it leads to a higher concentration of products so that the concentration of products could limit hydrogen metabolism. In particular, expression (3.8) can be used to model the growth rate of methanogens subject to hydrogen and the thermodynamic control of hydrogen concentration and products on the rate of hydrogen metabolism. The HM model incorporates a dissolved hydrogen pool that allows thermodynamic control through the hydrogen concentration to be modeled in response to changes in the pool size. Using $\theta = \theta_m$, $q_3 = q_m$ and $K_s = K_m$, expression (3.8) is

$$q = \frac{q_m S_h (1 - \theta_m)}{K_m + S_h (1 + \theta_m)} \text{ (mol cell}^{-1} \text{ s}^{-1}) \, . \tag{3.9}$$

Note that the subscript m of θ_m denotes the calculation of θ for the chemical reaction of hydrogen metabolism to methane by the methanogens. Thus, in expression (3.5), $\Delta G_T^o = \Delta G_{T_m}^o$ and $n = n_m$ are used to calculate θ_m.

Using the same assumptions, notation and arguments for model formulation as for the HM model, equation (3.9) can be used instead of equation (2.1), and this leads to the HM$^\theta$ model, which is the HM model with a thermodynamic term

$$S_h' = -\frac{q_m S_h (1 - \theta_m)}{K_m + S_h (1 + \theta_m)} X_m - \alpha S_h + \beta_h \text{ (mol ml}^{-1} \text{ s}^{-1}) \, , \tag{3.10}$$

$$X_m' = \Delta_m E_m X_m - \alpha X_m \text{ (cell ml}^{-1} \text{ s}^{-1}) \, , \tag{3.11}$$

where

$$\Delta_m = \frac{n_m q_m S_h (1 - \theta_m)}{K_m + S_h (1 + \theta_m)} - m_m \text{ (mol}_{ATP} \text{ cell}^{-1} \text{ s}^{-1}) \, ,$$

is the net hydrogen concentration after the maintenance requirement of

methanogens have been met, and

$$E_m = \begin{cases} Y_m, & \text{if } \Delta_m(S_h) > 0 \ ; \\ \frac{d_m}{m_m}, & \text{if } \Delta_m(S_h) \leq 0 \ . \end{cases}$$

For the reaction of hydrogen metabolizing by methanogens to methane in the rumen, H_2 is used as the reference substrate to be consistent with the unit of n_m (per mole of hydrogen). Then, $\mathcal{Q}$ is calculated from

$$H_2 + \frac{1}{4}CO_2 \rightarrow \frac{1}{4}CH_4 + \frac{1}{2}H_2O \ , \tag{3.12}$$

and θ_m is given by

$$\theta_m = \frac{[H_2O]^{\frac{1}{2}}[CH_4]^{\frac{1}{4}}}{[H_2][CO_2]^{\frac{1}{4}}} \ e^{(\Delta G^o_{T_m} + n_m \ \Delta G_{ATP})/(\mathcal{R}T)} \ .$$

Note that $[H_2]$ denotes the hydrogen concentration. Concentration in mol ml^{-1} are reported in the HM$^\theta$ model and, these must be converted into mol L^{-1} to calculate θ_m. Expression (3.4) is used to calculate the net Gibbs free energy for an overall reaction (3.12) where hydrogen in the rumen liquid is converted to methane in the rumen liquid by a methanogen cell. For such overall reaction, there are three partial intermediate chemical reactions:

1. Hydrogen is transported from the rumen liquid into a cell
2. Hydrogen is converted to methane inside a cell
3. Formed methane is then released to the rumen liquid.

The net Gibbs free energy of an overall reaction is the sum of the net Gibbs free energy for the partial intermediate chemical reaction of that overall reaction. That is, the sum of the net Gibbs free energy for these three chemical reactions is the same as the net Gibbs free energy for the overall reaction (3.12) where hydrogen in the rumen liquid is converted to methane in the rumen liquid. Thus, the dissolved hydrogen, methane and carbon dioxide concentration in the rumen liquid, rather than those

inside a methanogen cell, is used to calculate expression (3.4) and θ_m. The parameters used to calculate θ_m are given in Table 3.1.

Table 3.1: Parameter values used to calculate θ_m for the HM$^\theta$ model.

Parameter	Description	Value
$[H_2O]$	water concentration	1.00 (activity)
$[CH_4]$	dissolved methane concentration in the rumen	3.56×10^{-7} (mol ml^{-1})
$[CO_2]$	dissolved carbon dioxide in the rumen	5.9×10^{-5} (mol ml^{-1}) [76]
$\Delta G^o_{T_m}$	Gibbs free energy of methane production at temperature T under standard conditions	-47.86 (kJ mol^{-1}) [21]
ΔG_{ATP}	energy required to generate one unit of ATP	75 (kJ mol$^{-1}_{ATP}$)
$\mathcal{R}$	ideal gas constant	8.314×10^{-3} (kJ mol^{-1} K^{-1}) [21]
T	rumen temperature	312 (K) [67]

The concentration of water is approximated by the water activity and assumed constant [21]. The solubility of methane at one atmosphere (i.e., 100% methane) and 312 K is 11.48×10^{-7} (mol ml^{-1}) [178]. It was reported by Moate *et al.* [113] that 31% of the rumen headspace gas is methane so that the dissolved methane concentration in the rumen is 3.56×10^{-7} (mol ml^{-1}). The thermodynamic term θ_m depends on the hydrogen concentration and this is certainly not constant in the HM$^\theta$ model. To explore the effect of hydrogen concentration on hydrogen metabolism, equation (3.9), the dissolved methane and carbon dioxide concentration are assumed to be constant although in reality they will vary over time. That could be included in future investigations using this model. Under standard conditions, $\Delta G_{ATP} = 32.5$ kJ mol$^{-1}_{ATP}$ [1]. The reported ΔG_{ATP} for 6 different microbes ranged from 60 to 80 kJ mol$^{-1}_{ATP}$, with a mean value of 75 kJ mol$^{-1}_{ATP}$ [15]. Although the concentrations of ADP and ATP in cells vary, the changes appear to result in constant values for ΔG_{ATP} even when the types of metabolism carried out is very different [162]. Simulation was used to explore the effect of different values of ΔG_{ATP} on the rate of hydrogen metabolism by a population of methanogens. With all other parameter values as in Table 3.1, the effect of ΔG_{ATP} on the rate of hydrogen metabolism was calculated and the results are depicted in Figure 3.1. There are differences in the rate of

hydrogen metabolism at low hydrogen concentration if different values of ΔG_{ATP} are used. This should be explored in future to determine its impact on the outcomes of the full model. For now, let us assume ΔG_{ATP} is a constant with a value of 75 kJ mol_{ATP}^{-1}.

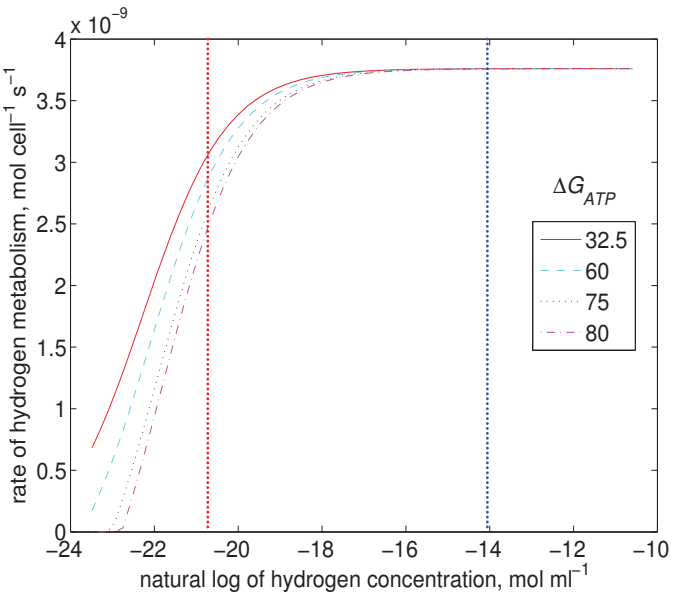

Figure 3.1: The effect of ΔG_{ATP} on the rate of hydrogen metabolism. The values for ΔG_{ATP} are in kJ mol_{ATP}^{-1}. The left vertical dotted line of the figure is a typical ruminal hydrogen concentration, 1×10^{-9} mol ml^{-1} [70]. The right vertical line is the maximal possible dissolved hydrogen concentration at one atmosphere and 312 K in the rumen [76].

Bearing in mind the reference concentration units we have that $S_h = [\text{H}_2]/1000$; thus, under the above assumptions

$$\theta_m = \frac{C_m}{S_h} \ , \tag{3.13}$$

where C_m (mol ml^{-1}) is given by

$$C_m = \frac{[\text{H}_2\text{O}]^{\frac{1}{2}}[\text{CH}_4]^{\frac{1}{4}}}{1000[\text{CO}_2]^{\frac{1}{4}}} \ \text{e}^{(\Delta G^o_{T_m} + n_m \ \Delta G_{ATP})/(\mathcal{R}T)} \tag{3.14}$$

is a positive constant that is independent of S_h. Finally, the estimated methane production of the HM$^\theta$ model is calculated based on the amount

of hydrogen metabolized by methanogens

$$M^\theta = \frac{1}{4}\frac{q_m S_h(1-\theta_m)}{K_m + S_h(1+\theta_m)} X_m \text{ (mol ml}^{-1}\text{ s}^{-1}\text{)} . \tag{3.15}$$

3.3 Effects of thermodynamic term

The effects of θ_m on the steady state solutions of the HM$^\theta$ model are discussed here. For the purpose of this discussion, α, β_h and the biological parameters of methanogens will be assumed to be fixed.

When the concentration of products is effectively zero, i.e., $\mathcal{P} = 0$ then $\theta_m = 0$ and equation (3.9) reduces to equation (2.1). In this case, the HM$^\theta$ model is the HM model. Suppose that methane production in the rumen reaches its chemical equilibrium: methanogens stop metabolizing hydrogen into methane even though there is sufficient hydrogen. This rumen environment can be captured by the HM$^\theta$ model, i.e., $\theta_m = 1$. However, without a thermodynamic term, the HM model cannot describe the rumen environment where there is any thermodynamic feedback at all, i.e., the HM model is only applicable to $\theta_m = 0$.

Substituting expression (3.13) into equations (3.10) and (3.11) yields the system

$$\begin{aligned}
\hat{S_h}' &= -\frac{q_m}{\hat{K_m} + \hat{S_h}} \hat{S_h} X_m - \alpha \hat{S_h} + \hat{\beta_h} \text{ (mol ml}^{-1}\text{ s}^{-1}\text{)} , \\
X_m' &= \Delta_m E_m X_m - \alpha X_m \text{ (cell ml}^{-1}\text{ s}^{-1}\text{)} ,
\end{aligned}$$

where

$$\begin{aligned}
\hat{S_h} &= S_h - C_m \text{ (mol ml}^{-1}\text{)} , \\
\hat{K_m} &= K_m + 2C_m \text{ (mol ml}^{-1}\text{)} , \\
\hat{\beta_h} &= \beta_h - \alpha C_m \text{ (mol ml}^{-1}\text{ s}^{-1}\text{)} .
\end{aligned}$$

If there is little impact of unfavorable thermodynamics (e.g., $C_m = \theta_m = 0$), the size of the apparent K_m, $\hat{K_m}$, will be largely determined by the capacity of the cell to transport substrate into the cell, i.e., $\hat{K_m}$ will tend to K_m. If the thermodynamic inhibition of substrate transformation

increases ($C_m > 0$), then the contribution of K_m will diminish and the thermodynamic control of substrate transformation will increase so that $\hat{K_m}$ will tend away from K_m. This is consistent with the expectations of Jin and Bethke [78], that under thermodynamically unfavorable rumen environment there will be a decrease in the affinity of microbes for their growth substrate and that thermodynamics rather than diffusion and cell envelope architecture will play a major role in determining the rate of substrate transformation.

Note that the form of the above system is the same as that for the HM model. The analytical results from Chapter 2 can thus be readily adapted to this system. By the same arguments given for systems (2.4) and (2.5), systems (3.10) and (3.11) has two equilibrium points, $(S_h^{\theta*}, X_m^{\theta*})$. Table 3.2 lists the equilibrium points for both systems. Note that $(S_h^{\theta*1}, X_m^{\theta*1}) = (S_h^{*1}, X_m^{*1})$. These points describe where the initial methanogen population is zero or methanogens cannot maintain themselves in the rumen so that no hydrogen is metabolized into methane in the long term. Hydrogen concentration thus has no effect on the rate of hydrogen metabolism (i.e., both points are independent of C_m). For the same parameters between the HM and the HM$^\theta$ models, because $S_h^{\theta*2} > S_h^{*2}$, less hydrogen is metabolized by methanogens so that $X^{\theta*2} < X^{*2}$ and $M^\theta < M$.

The eigenvalue of the HM$^\theta$ model, λ_a and λ_b are calculated from the Jacobian matrix, J, of the above system. From the analytical results of the HM model,

$$\det(J - \lambda I) = \begin{vmatrix} -\frac{q_m \hat{K_m} X_m}{(\hat{K_m}+\hat{S_h})^2} - \alpha - \lambda & -\frac{q_m \hat{S_h}}{\hat{K_m}+\hat{S_h}} \\ \frac{E_m n_m q_m \hat{K_m} X_m}{(\hat{K_m}+\hat{S_h})^2} & E_m(\frac{n_m q_m \hat{S_h}}{\hat{K_m}+\hat{S_h}} - m_m) - \alpha - \lambda \end{vmatrix} .$$

Then, the values of S_h and X_m at $(S_h^{\theta*},\ X_m^{\theta*})$ are substituted in the Jacobian, and the equation $\det(J - \lambda I) = 0$ is solved to get λ_a and λ_b. For the HM$^\theta$ model, at $(S_h^{\theta*1},\ X_m^{\theta*1})$ the eigenvalues are therefore

$$\lambda_{a1} = -\alpha \ ,$$
$$\lambda_{b1} = \left(\frac{E_m(n_m q_m - m_m) - \alpha}{\alpha(K_m + C_m) + \beta_h} \right) \left(\beta_h - \alpha S_h^{\theta*2} \right) \ .$$

1639 At $(S_h^{\theta*2}, X_m^{\theta*2})$ the eigenvalues are

$$\lambda_{a2}, \lambda_{b2} = \frac{-(\alpha + \Xi) \pm \sqrt{(\alpha + \Xi)^2 - 4(E_m m_m + \alpha)\Xi}}{2} ,$$

1640 where

$$\Xi = \frac{(K_m + 2C_m)(\beta_h - \alpha S_h^{\theta*2})}{(S_h^{\theta*2} - C_m)(K_m + S_h^{\theta*2} + C_m)} .$$

If the chemical reaction of methane production does not reach its chem-

Table 3.2: Equilibrium points of the HM and HM$^\theta$ models

	Equilibrium point one	Equilibrium point two
HM model	$S_h^{*1} = \beta_h/\alpha$	$S_h^{*2} = \frac{K_m(Y_m m_m+\alpha)}{Y_m(n_m q_m - m_m)-\alpha}$
	$X_m^{*1} = 0$	$X_m^{*2} = \frac{(\beta_h - \alpha S_h^{*2})Y_m n_m}{Y_m m_m + \alpha}$
HM$^\theta$ model	$S_h^{\theta*1} = \beta_h/\alpha$	$S_h^{\theta*2} = S_h^{*2} + \frac{(Y_m(n_m q_m + m_m)+\alpha)C_m}{Y_m(n_m q_m - m_m)-\alpha}$
	$X_m^{\theta*1} = 0$	$X_m^{\theta*2} = \frac{(\beta_h - \alpha S_h^{\theta*2})(K_m + S_h^{\theta*2} + C_m)}{q_m(S_h^{\theta*2} - C_m)}$

1641

1642 ical equilibrium, then

$$S_h^{\theta*2} > C_m \geq 0 . \tag{3.16}$$

1643 Suppose that $S_h^{\theta*2} > 0$ and $X_m^{\theta*2} > 0$. Then $E_m = Y_m$

$$Y_m(n_m q_m - m_m) - \alpha > 0 , \tag{3.17}$$

1644 and

$$\beta_h - \alpha S_h^{\theta*2} > 0 . \tag{3.18}$$

From inequalities (3.16) and (3.18), yield

$$\frac{\beta_h}{\alpha} > S_h^{\theta*2} > C_m \geq 0 \ . \tag{3.19}$$

If both inequalities (3.17) and (3.19) are satisfied, then $(S_h^{\theta*2}, X_m^{\theta*2})$ is the stable steady state solution of the HM$^{\theta}$ model.

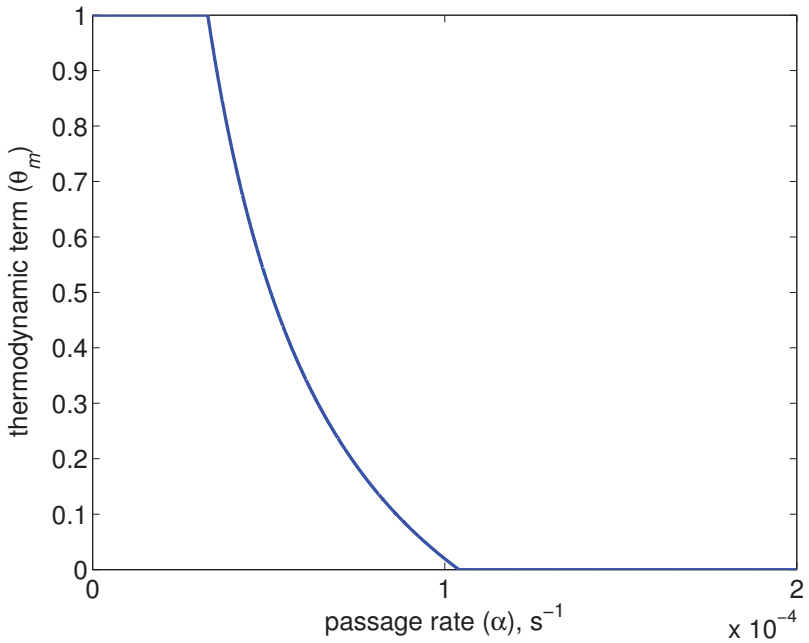

Figure 3.2: Thermodynamic term for a range of passage rate values and typical parameter values found in the literature (Tables 2.1 and 3.1).

From equation (3.13), the thermodynamic term is a function of hydrogen concentration, which is a function of passage rate. Thus, the thermodynamic term is a function of passage rate as illustrated in Figure 3.2. From Figure 3.2, for $0 < \alpha < 3.272 \times 10^{-5}$ s^{-1}, $\theta_m = 1$, and no hydrogen can be transformed to methane by methanogens due to the thermodynamic penalty. For $\alpha > 10.406 \times 10^{-5}$ s^{-1}, the whole methanogen population will be eliminated due to passage rate. Thus, no hydrogen is metabolized into methane by methanogens and so there is no thermodynamic feedback ($\theta_m = 0$). Each passage rate value is associated with a hydrogen concentration. That is, hydrogen can be metabolized by methanogens only when the hydrogen concentration is greater than a

hydrogen concentration threshold, i.e., $S_h > C_m$, so that $\theta_m < 1$ based on expression (3.13) and the chemical reaction occurs in the forward direction allowing substrate to be metabolized for methanogen growth and converted into products. With the same typical parameter values found in the literature (Tables 2.1 and 3.1), $C_m = 1.004 \times 10^{-10}$ mol ml^{-1}. Such hydrogen concentration threshold values have been measured for a range of methanogens in laboratory experiments. These range from 0.206×10^{-10} to 0.737×10^{-10} mol ml^{-1} [24], and are of the same order of magnitude as C_m. The differences in the magnitude of C_m versus results from Cord-Ruwisch *et al.* [24] could be the result of temperature (37^oC constant in the rumen versus $28 - 34^o$C), different biological characteristics of the methanogens, and environment (passage rate versus no passage rate when working with pure cultures in test tubes). One novelty of the HM$^\theta$ model is that the substrate threshold is an emergent property of the model. The HM model (and existing models, e.g., [51]) does not result in such hydrogen concentration thresholds. Substrate thresholds are a major decider of competitive success in anaerobic systems [24], [100].

For the same parameters values between the HM and the HM$^\theta$ models, it is possible that the stable steady state solutions of the HM model and the HM$^\theta$ model are different. That is, the predicted behavior of these two models could be different for the same rumen environmental condition. When $C_m \geq S_h^{\theta*2}$ and both inequalities (3.17) and (3.18) are satisfied, (S_h^{*2}, X_m^{*2}) is the stable steady state solution of the HM model. However, from the HM$^\theta$ model, $(S_h^{\theta*2}, X_m^{\theta*2})$ is a saddle point. When $C_m \geq S_h^{\theta*2}$, for the HM$^\theta$ model, $\Delta_m(S_h) \leq 0$ leads to

$$E_m = \frac{d_m}{m_m} \ ,$$

and

$$E_m(n_m q_m - m_m) - \alpha < 0 \ ,$$

such that $(S_h^{\theta*1}, X_m^{\theta*1})$ is the stable steady state solution of the HM$^\theta$ model instead of $(S_h^{\theta*2}, X_m^{\theta*2})$. That is, when the steady state hydrogen concentration is less than the critical hydrogen concentration threshold imposed

by thermodynamic control, no hydrogen is metabolized by methanogens to gain ATP. Therefore, methanogens cannot reproduce and are in the decay mode so that the methanogens population density becomes zero over time due to passage rate.

3.4 Summary

Substrate and product concentrations in the rumen can shift fermentation pathways, resulting in different microbial community composition, different amounts of volatile fatty acid (that are used by the ruminants to produce meat, wool and milk) and change in methane production [84]. For instance, the hydrogen concentration can influence the rate of hydrogen generation in the rumen, by differentially influencing the efficiency of the different fermentation pathways that are active [76].

In this chapter, a representation of thermodynamic control (by introducing a thermodynamic term θ) is developed to improve modeling of hydrogen dynamics. This is a proposed extension (listed in Section 2.7) of the HM model. This refinement allows for thermodynamic feedback using known values of ΔG for reactions, and accurate concentrations of substrates and products. It yields a substrate threshold, equation (3.14), below which a substrate cannot be metabolized; this threshold is dependent on the concentrations of substrate and products. From the HM model, there is a positive methanogen population, if and only if methanogens can tolerate the passage rate (they are not washed out) and there is sufficient food supply (they are not in starvation mode), i.e., inequalities (2.17) and (2.18) are both satisfied. In addition to these requirements, for the HM$^\theta$ model, there is a positive methanogen population, if and only if the substrate threshold is also satisfied, e.g., $S_h^{\theta *} > C_m$. By equation (3.13) this guarantees that $\theta < 1$ and the chemical reaction occurs in the forward direction allowing substrate to be metabolized for methanogen growth and converted into products.

The HM$^\theta$ model can be further extended by modifying it to include more microbes, including those that ferment the ingested feed to generate hydrogen via fermentation pathways. In such an extension, both

rates of hydrogen generation and hydrogen metabolism are influenced by the hydrogen concentration and products of other microbial fermentation pathways. The thermodynamic terms of each of the fermentation pathways would capture this behavior. Such an expansion of the HM$^\theta$ model would also be useful to explore methane mitigation strategies (i.e., strategies that lead to a smaller methane production, M) via the hydrogen-methanogen dynamics. In current models of rumen function (e.g., [4], [31]), yield factors of volatile fatty acid profiles are predetermined for different types of feed components leading to poor estimation of volatile fatty acid profiles [38], [117]. An extended HM$^\theta$ model, could provide an alternative to overcome these limitations of current models of rumen function, where the microbial growth kinetics and the thermodynamic feedback on this growth from the substrates and products of the fermentation (such as hydrogen and volatile fatty acids) determine the composition of the rumen microbial community, the fermentation pathway used, and the volatile fatty acid profiles. The volatile fatty acid profiles can be calculated from the population densities of the various microbes that use different fermentation pathways leading to different ratios of end products (including volatile fatty acids) and different yields of hydrogen per unit of ingested feed. Such a model is developed in Chapter 4.

Chapter 4

Glucose-hydrogen-methanogen dynamics

In the HM and HM$^{\theta}$ models (Chapters 2 and 3), the hydrogen generation rate is an input parameter acting as a direct hydrogen "hose" into the rumen. In reality, hydrogen is generated from feed ingested by ruminants. The microbes in the rumen ferment the plant structural material in the feed, much of which is not able to be digested by the mammalian digestive system. The main end products of the primary fermentation of feed are volatile fatty acids (e.g., acetate, propionate and butyrate, listed in order of increasing carbon chain length), ammonia, hydrogen, carbon dioxide and microbial cells. The volatile fatty acids are absorbed by the ruminants as energy sources for the animal or converted into animal products such as meat, milk and wool. The hydrogen is used by methanogens to produce methane, as modeled by the HM and HM$^{\theta}$ models. The amount and rate of methane production is proportional to the net amount and rate of hydrogen generation from fermentation pathways in the rumen [68], because nearly all the hydrogen is rapidly converted to methane. The rate of hydrogen production is determined by the activities of the different microbes using different fermentation pathways. Importantly, the amount of hydrogen formed from a given amount of feed depends on the chemical nature of the feed and on the metabolism of the mi-

crobes fermenting the feed. For the same type of feed, different feed fermentation pathways lead to different end products, including differing amounts of hydrogen, and so to differences in methane production [76]. Feed fermentation pathways are subject to thermodynamic control: if the hydrogen concentration decreases, then this leads to more hydrogen being generated from fermentation pathways and hence more methane production [76] and different microbial community composition [84]. In this chapter, the HM and HM$^\theta$ models are extended to a model that includes examples of feed fermentation pathways.

4.1 Glucose fermentation pathways and glucose fermenters

Ingested feed is first broken down to monomers such as glucose, which can then be fermented by multiple types of glucose fermenters. The following are two examples of glucose fermentation pathways. A more comprehensive discussion of glucose fermentation pathways can be found in Appendix B.

$$\begin{aligned} &C_6H_{12}O_6 \rightarrow CH_3CH_2CH_2COO^- + 2\ H_2 + 2\ CO_2 + H^+\ , \\ &C_6H_{12}O_6 \rightarrow CH_3COO^- + CH_3CH_2COO^- + H_2 + CO_2 + 2\ H^+\ . \end{aligned}$$

Here $C_6H_{12}O_6$ is glucose which comes from the feed and CH_3COO^-, $CH_3CH_2COO^-$ and $CH_3CH_2CH_2COO^-$ are the volatile fatty acids: acetate, propionate and butyrate, respectively. Let A, P and B represent acetate, propionate and butyrate, respectively. Then, these chemical equations can be written more concisely as

$$\begin{aligned} &\text{glucose} \rightarrow B + 2\ H_2 + 2\ CO_2 + H^+\ , \\ &\text{glucose} \rightarrow A + P + H_2 + CO_2 + 2\ H^+\ . \end{aligned}$$

Collectively, glucose fermenters are able to metabolize glucose using many different pathways, but individual types of glucose fermenters generally have a limited repertoire. For the purpose of this project, each type

of glucose fermenter is associated with one of the pathways. Let X_i (cell ml^{-1}) denote the population density of each type of glucose fermenter. These glucose fermenters gain ATP by metabolizing per mole of glucose, n_i (mol$_{ATP}$ mol^{-1}), and n_i can vary even for the same fermentation pathway (See Appendix C). Different glucose fermentation pathways yield different amounts of hydrogen that affect the hydrogen-methanogen dynamics [76], [84], which lead to different end product profiles and methane production.

Using glucose as a reference substrate, each glucose fermentation pathway can be generalized as

$$\text{glucose} + w_{wt_i}\text{H}_2\text{O} \rightarrow w_{A_i}A + w_{P_i}P + w_{B_i}B + w_{h_i}\text{H}_2 + w_{cd_i}\text{CO}_2 + w_{\text{H}^+{}_i}\text{H}^+ \ , \tag{4.1}$$

where the w are the unitless stoichiometric coefficients of the chemical equation and the subscript i indicates the glucose fermenter that uses this pathway. Namely, in every ml rumen liquid, glucose fermenter i converts each mole of glucose into w_{A_i} moles of A, w_{P_i} moles of P, w_{B_i} moles of B, w_{h_i} moles of hydrogen (H_2), w_{cd_i} moles of carbon dioxide and $w_{\text{H}^+{}_i}$ moles of hydrogen ions. Note that H_2 contributes to the hydrogen generation rate, β_h, and hydrogen ions contribute to the pH of the rumen. Not all fermentation pathways produce all of these end products so some of the stoichiometric coefficients could be zero. However, at least one of w_{A_i}, w_{P_i}, w_{B_i} must be positive because one or more of acetate, propionate or butyrate is always the main end products from glucose fermentation. Production of volatile fatty acid is subjected to thermodynamic control [84]. In each glucose fermentation pathway (chemical reaction), the concentration of the products could limit the substrate (glucose) metabolism. Just as a thermodynamic term, θ_m, was introduced to model thermodynamic control in the metabolism of methanogens with respect to chemical reaction (3.12), this thermodynamic term, θ_i, for glucose fermenter i is

$$\theta_i = \frac{[A]^{w_{A_i}}[P]^{w_{P_i}}[B]^{w_{B_i}}[\text{H}_2]^{w_{h_i}}[\text{CO}_2]^{w_{cd_i}}[\text{H}^+]^{w_{\text{H}^+{}_i}}}{[\text{glucose}][\text{H}_2\text{O}]^{w_{wt_i}}}\ \text{e}^{(\Delta G^o_{T_i} + n_i\ \Delta G_{ATP})/(\mathcal{R}T)}\ \text{(unitless)} \ .$$

Recall that $0 \leq \theta < 1$ (Section 3.2). A glucose fermentation path-

way with $\theta_i = 1$ is at its chemical equilibrium so metabolism of glucose through that pathway will stop. A pathway with a greater value of θ_i is thermodynamically less favorable than one with a smaller θ_i, as determined by the rumen environment. Through θ_i, a greater concentration of hydrogen, $[H_2]$, will thermodynamically favor glucose fermentation pathways that produce less hydrogen (those with a smaller magnitude of w_{h_i}). Note that $[H_2]$ is in the numerator of θ_i but is in the denominator of θ_m. A lower hydrogen concentration favors glucose fermenters that produce more hydrogen (i.e., those with a smaller θ_i) but disfavors methanogens (by increasing θ_m) so that more glucose will be fermented to produce more hydrogen for methanogens, which in turn favors the methanogens but disfavors glucose fermenters. This feedback mechanism can reach an equilibrium where the net hydrogen concentration is stabilized at the same level by methanogen population. This is where the amount of hydrogen generated from the glucose fermentation pathways is metabolized into methane at any instant. In a more realistic rumen model with temporal variation, the population of glucose fermenters and methanogens would interact through the hydrogen pool and the effects of substrate and product concentrations via θ_m and θ_i.

4.2 GHM$^\theta$ model

4.2.1 Objectives

A more comprehensive model of methane production in the rumen must include representations of the interaction between glucose fermenters, glucose, volatile fatty acids, methanogens and hydrogen. This is achieved by extending the HM$^\theta$ model to include fermentation pathways and glucose fermenters, to yield a mechanistic model of glucose-hydrogen-methanogen dynamics with thermodynamic terms (the GHM$^\theta$ model). Both rates of hydrogen generation and hydrogen metabolism are influenced by the hydrogen concentration and products of feed fermentation pathways, as captured by the thermodynamic terms. This GHM$^\theta$ model is developed in this chapter.

4.2.2 Assumptions

The assumptions of the GHM$^\theta$ model are adapted from the HM$^\theta$ model. Between the assumptions of these models, one of the main differences arises because the hydrogen generation rate is assumed to be a direct input parameter in the HM$^\theta$ model but not in the GHM$^\theta$ model. Instead, in the GHM$^\theta$ model, there is a glucose input parameter, which can be considered as a rate of generation from feed breakdown, and hydrogen is generated by the glucose fermenters. In the rumen, the glucose generation rate depends on the ingested solid feed. The breaking down of the feed into glucose does not occur instantaneously in the rumen (because of the nature of the feed). Feed and microbes pass through the rumen as ruminants keep ingesting solid feed, drinking liquid and secreting saliva, with the flow of material out of the rumen being commonly described as the passage rate. That is, both rates of glucose generation and passage are dependent on the amount and nature of solid feed. Also, glucose generation rate is not independent of the passage rate. However, the explicit relationship between rates of glucose generation and passage is not known for all the different amount and nature of feed digested. In this project, for simplicity, we choose the glucose generation rate is independent of the passage rate (i.e., the glucose generation rate and the passage rate are modelled as independent) and independently explore these rates on the effect of the microbial community and methane production against the conceptual model presented by Janssen [76] and a chemostat experiment conducted by Isaacson *et al.* [72] (Chapter 5). In future investigations, the amount and nature of feed digested can be integrated into the GHM$^\theta$ model, and both rates of glucose generation and passage can be estimated based on different arbitrarily selected functions with respect to the amount and nature of feed digested. That is, based on the amount and nature of feed digested, both rates of glucose generation and passage can be self-adjusted in such extension of the GHM$^\theta$ model.

1. Methanogens, hydrogen, glucose fermenters and glucose are *uniformly distributed* in the rumen liquid contents.

2. Methanogens *randomly* capture hydrogen, with *no* competition

among methanogens for hydrogen, and glucose fermenters *randomly* capture glucose, with *no* competition among glucose fermenters for glucose.

3. *No other microbes compete* for hydrogen with the methanogens or glucose with the glucose fermenters.

4. Hydrogen is the *only* energy source for methanogens, which *instantaneously* metabolize hydrogen to gain ATP, and glucose is the *only* energy source for glucose fermenters, which *instantaneously* metabolize glucose to gain ATP.

5. *Each* methanogen cell metabolizes hydrogen at the *same rate* to gain ATP and needs the *same* amount of ATP for maintenance, and *each* glucose fermenter cell metabolizes glucose at the *same rate* to gain ATP and needs the *same* amount of ATP for maintenance.

6. The gained ATP is used either to maintain existing cells *or* to reproduce, and new methanogens and glucose fermenters are *biologically identical* to their existing cells.

7. Methanogens and glucose fermenters cannot reproduce unless there is an *excess* of ATP beyond what is needed for their maintenance.

8. Hydrogen and glucose are lost through passage rate *or* consumption by methanogens and glucose fermenters.

9. Methanogens and glucose fermenters are lost only by existing the rumen (passage) *or* "starvation" (i.e., there are no predators).

10. The passage rate in the rumen is *constant*.

11. Hydrogen is *only* generated by glucose fermentation and there is *no* other source of hydrogen in the rumen.

12. The glucose generation rate in the rumen is *constant*.

13. The absorption rates of acetate, butyrate and propionate in the rumen are *constant* but do not have to be the same.

14. From metabolizing substrates, the energy required for one mole of ATP formation, ΔG_{ATP}, is *constant and the same* for both methanogens and glucose fermenters.

15. The pH value in the rumen is *constant*.

These assumptions are simplifications of what actually occurs in the rumen. For example, the absorption rates of acetate, butyrate and propionate in the rumen are not constant. The pH value in the rumen is not constant [22]. The amount of new cell material that is produced per unit of ATP is different for methanogens and glucose fermenters [147], [160]. As noted in Section 3.2., although the concentrations of ADP and ATP in cells vary, the changes appear to result in constant values for ΔG_{ATP} even when the types of metabolism carried out is very different [162]. We therefore make assumption 14 for modelling purposes. However, the GHM$^\theta$ model can be expanded and implemented into models of whole rumen function to address more complex assumptions. At this stage, these simplifications are introduced to explore the model here and analytically in the next chapter (Chapter 5).

4.2.3 Model formulation

Let subscript g, h, i and m, respectively, indicate the parameters and variables related to glucose, hydrogen, a type of glucose fermenter associated with a particular fermentation pathway and the methanogens. For instance, S_g (mol ml^{-1}) denotes the (dissolved) glucose concentration, S_h (mol ml^{-1}) denotes the (dissolved) hydrogen concentration, X_i (cell ml^{-1}) denotes the population density of a type of glucose fermenter i and X_m (cell ml^{-1}) denotes the methanogen population density. Methanogens and each type of glucose fermenter have the same set of biological parameters (n, q, K, m, d and Y) and these are distinguished for the different microbial populations by their subscripts. In addition to those listed in Tables 2.1 and 3.1, other parameters of the GHM$^\theta$ model are listed in Table 4.1. Ruminal parameters α, γ_A, γ_P, γ_B and β_g depend on the rumen environment, and are non-negative. The biological parame-

ters of glucose fermenters may be variable. For simplicity we will assume these parameters are positive constants.

Table 4.1: Additional parameters used in the GHM$^\theta$ model.

Parameter	Description	Unit
$\gamma_A\ \gamma_P\ \gamma_B$	absorption rate of acetate, propionate and butyrate	s^{-1}
β_g	rate of glucose generation	mol ml^{-1} s^{-1}
n_i	ATP gained by glucose fermenter i metabolizing per mole of glucose	mol_{ATP} mol^{-1}
q_i	maximal rate at which glucose fermenter i can metabolize glucose	mol $cell^{-1}$ s^{-1}
K_i	glucose concentration at half of q_i assuming no thermodynamic feedback	mol ml^{-1}
m_i	maintenance requirement of glucose fermenter i	mol_{ATP} $cell^{-1}$ s^{-1}
d_i	death coefficient of glucose fermenter i	s^{-1}
Y_i	reproduction coefficient of glucose fermenter	cell mol_{ATP}^{-1}
$[H^+]$	hydrogen ion concentration	mol ml^{-1}
$\Delta G^o_{T_i}$	Gibbs free energy of glucose fermentation at temperature T under standard conditions	kJ mol^{-1}
$w_{A_i}\ w_{P_i}\ w_{B_i}$	moles of acetate, propionate and butyrate generated from each mole of glucose fermented by glucose fermenter i	unitless
$w_{wt_i}\ w_{cd_i}\ w_{H^+{}_i}$	moles of water, carbon dioxide and hydrogen ions generated from each mole of glucose fermented by glucose fermenter i	unitless
w_{h_i}	moles of hydrogen generated from each mole of glucose fermented by glucose fermenter i	unitless

There is an excess of water (H_2O) in the rumen and the water activity is assumed constant at one. Glucose is the growth rate-limiting substrate for glucose fermenter i in glucose fermentation pathway (4.1). Thus equation (3.8) can be adapted to model the kinetics of glucose when glucose is significantly limited with respect to products (volatile fatty acid and hydrogen concentrations) or when the glucose fermentation pathway is at its chemical equilibrium state such that no glucose is converted into products. The interaction between glucose and multiple types of glucose

1948 fermenters can thus be described by

$$S'_g = -\sum_{i=1}^{nn} \frac{q_i S_g(1-\theta_i)}{K_i + S_g(1+\theta_i)} X_i - \alpha S_g + \beta_g \text{ (mol ml}^{-1}\text{ s}^{-1}) , \quad (4.2)$$

$$X'_i = \Delta_i E_i X_i - \alpha X_i \text{ (cell ml}^{-1}\text{ s}^{-1}) , \quad (4.3)$$

1949 where

$$\Delta_i = \frac{n_i q_i S_g(1-\theta_i)}{K_i + S_g(1+\theta_i)} - m_i \text{ (mol}_{ATP}\text{ cell}^{-1}\text{ s}^{-1}) ,$$

$$E_i = \begin{cases} Y_i, & \text{if } \Delta_i(S_g) > 0 , \\ \frac{d_i}{m_i}, & \text{if } \Delta_i(S_g) \leq 0 , \end{cases}$$

1950 For the volatile fatty acids (VFA): acetate, propionate and butyrate,
1951 let S_A (mol ml^{-1}) denote the acetate concentration, and S_P (mol ml^{-1})
1952 denote the propionate concentration, S_B (mol ml^{-1}) denote the butyrate
1953 concentration. That is, $S_A = [A]$, $S_P = [P]$ and $S_B = [B]$ for θ_i. The
1954 rate of change of acetate, propionate and butyrate are

$$S'_A = \sum_{i=1}^{nn} w_{A_i} \frac{q_i S_g(1-\theta_i)}{K_i + S_g(1+\theta_i)} X_i - \gamma_A S_A - \alpha S_A \text{ (mol ml}^{-1}\text{ s}^{-1}) , \quad (4.4)$$

$$S'_P = \sum_{i=1}^{nn} w_{P_i} \frac{q_i S_g(1-\theta_i)}{K_i + S_g(1+\theta_i)} X_i - \gamma_P S_P - \alpha S_P \text{ (mol ml}^{-1}\text{ s}^{-1}) , \quad (4.5)$$

$$S'_B = \sum_{i=1}^{nn} w_{B_i} \frac{q_i S_g(1-\theta_i)}{K_i + S_g(1+\theta_i)} X_i - \gamma_B S_B - \alpha S_B \text{ (mol ml}^{-1}\text{ s}^{-1}) . \quad (4.6)$$

1955 The interaction between hydrogen and methanogens is the same as
1956 the HM$^\theta$ model

$$S'_h = -\frac{q_m S_h(1-\theta_m)}{K_m + S_h(1+\theta_m)} X_m - \alpha S_h + \beta_h \text{ (mol ml}^{-1}\text{ s}^{-1}) , \quad (4.7)$$

$$X'_m = \Delta_m E_m X_m - \alpha X_m \text{ (cell ml}^{-1}\text{ s}^{-1}) , \quad (4.8)$$

1957 where

$$\Delta_m = \frac{n_m q_m S_h(1-\theta_m)}{K_m + S_h(1+\theta_m)} - m_m \text{ (mol}_{ATP}\text{ cell}^{-1}\text{ s}^{-1}) ,$$

$$E_m = \begin{cases} Y_m, & \text{if } \Delta_m(S_h) > 0 \ , \\ \frac{d_m}{m_m}, & \text{if } \Delta_m(S_h) \leq 0 \ . \end{cases}$$

Concentrations are reported as mol ml^{-1} in the GHM$^\theta$ model, so these must be converted into mol L^{-1} to calculate θ_i and θ_m. For methanogens, θ_m is the same as in the HM$^\theta$ model. In the HM$^\theta$ model, the hydrogen generation rate, β_h was a direct input parameter. In the GHM$^\theta$ model, the hydrogen generation rate is calculated from the glucose fermenter population density and glucose fermentation pathways as follows:

$$\beta_h = \sum_{i=1}^{nn} w_{h_i} \frac{q_i S_g (1-\theta_i)}{K_i + S_g(1+\theta_i)} X_i \text{ (mol ml}^{-1} \text{ s}^{-1}) \ .$$

From the HM model, the actual sensitivity value of methane production with respect to hydrogen generation rate is one. The rate of methane production is proportional to the net rate of hydrogen generation from feed in the rumen [68]. Glucose is fermented to hydrogen then metabolized to methane (equation 3.15). In this GHM$^\theta$ model, the ratio between the hydrogen generated rate and glucose generate rate at a time t, β_h/β_g, is used as a measure to compare methane production from different rumen environments: a lower ratio leads to less estimated methane production.

Let us refer to the five equations, (4.2), (4.3), (4.4), (4.5), and (4.6) as Part (1) of the GHM$^\theta$ model. Similarly, let us refer to the HM$^\theta$ model or the two equations (4.7) and (4.8) as Part (2) of the GHM$^\theta$ model. Part (1) models the processes associated with the glucose fermentation pathways that yields volatile fatty acids, hydrogen and other end products. Part (1) affects Part (2) via the hydrogen generation rate. Part (2) then influences Part (1) through the hydrogen concentration in the thermodynamic term θ_i. The GHM$^\theta$ model is new as no previous models in the literature included dynamic pools of all of: the glucose, hydrogen and volatile fatty acids substrate, multiple glucose fermenter populations each associated with different fermentation pathways, and the methanogen population. This GHM$^\theta$ model describes the interaction among glucose fermenters, glucose, volatile fatty acids, methanogens and hydrogen in the rumen, as

demonstrated in the flowchart Figure 4.1. The thermodynamic terms θ_i and θ_m link these variables and so model the effect of glucose and hydrogen concentration and other products of glucose fermentation pathways on the rates of glucose metabolism, hydrogen generation and hydrogen metabolism.

The GHM$^\theta$ model provides an alternative approach to current representation of fermentation based on stoichiometric profiles from feed components. In current models of rumen function (e.g., [4], [31]), volatile fatty acid profiles (S_A^*, S_P^* and S_B^*) are estimated based on yield factors for different types of feed components. However, such yield factors are not adequate in estimating the volatile fatty acid profiles for all feed components [38]. In contrast, the GHM$^\theta$ model could estimate the volatile fatty acids profiles from glucose fermentation pathways without predetermining yield factors. Changing rumen environments would have differing impacts on glucose fermenters and methanogens. If multiple types of glucose fermenters could co-exist as predicted by the GHM$^\theta$ model, but their activities and population size changed in response to changes in rumen environments, the GHM$^\theta$ model could respond by altering volatile fatty acid profiles and estimated methane production.

The next step is to examine the behavior of the GHM$^\theta$ model with one type of glucose fermenter. Then expand it to two or more types of glucose fermenters, to explore whether there is a stable co-existence of glucose fermenters that respond to changing rumen environments by altering the ratio of different products formed.

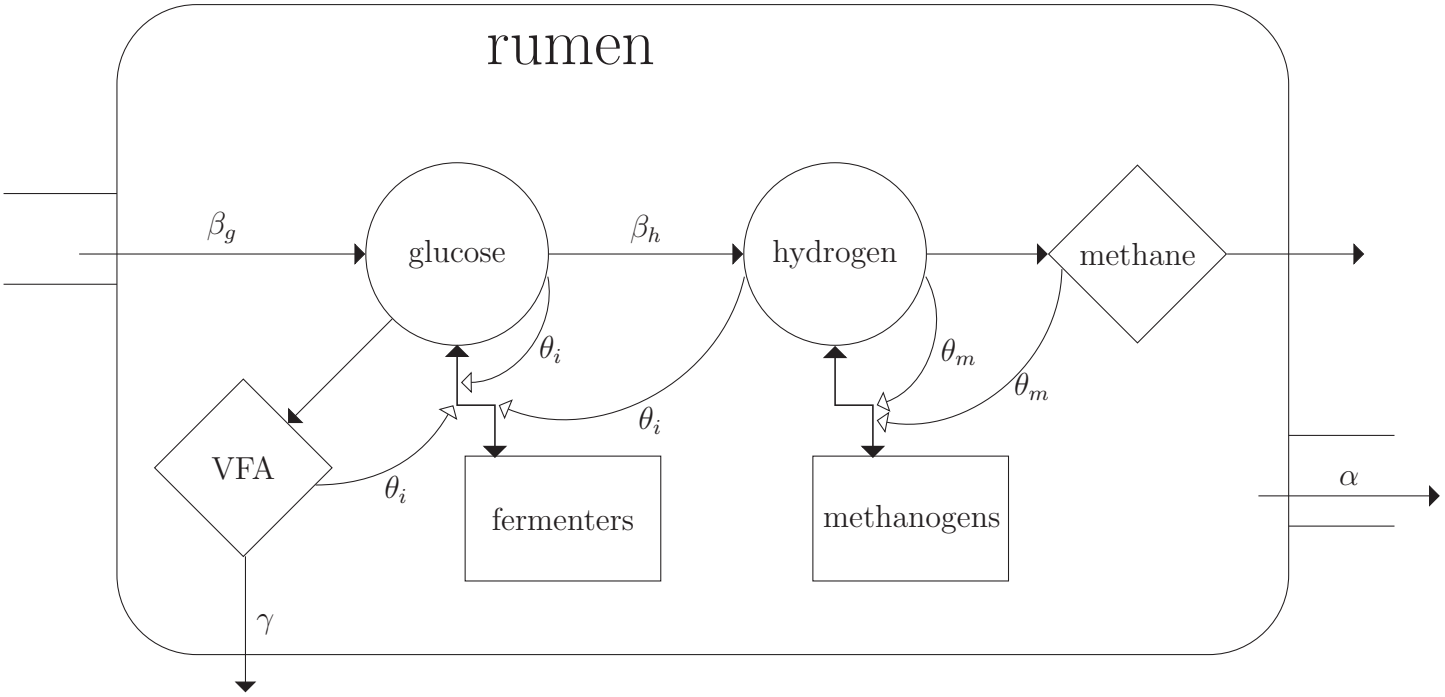

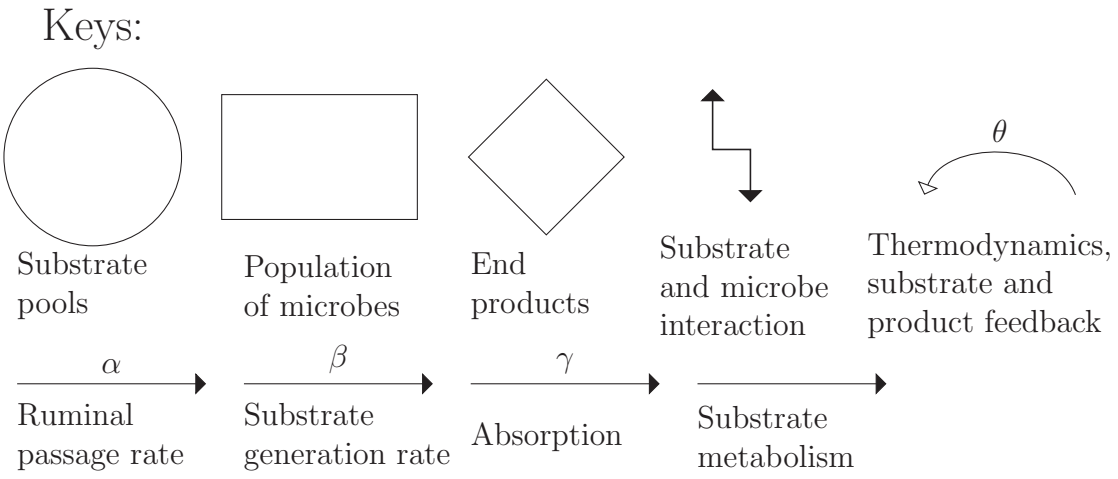

Subscript keys:

g - glucose
h - hydrogen

Figure 4.1: Flowchart of the GHM$^\theta$ model.

Chapter 5

Co-existence

5.1 Introduction

Multiple microbial populations are known to co-exist in the rumen. In this chapter we investigate co-existence of various glucose fermenter populations and methanogens. In this work the different glucose fermenter populations are associated with different feed fermentation pathways, but all have glucose as their growth limiting substrate. The methanogens are modeled as one population associated with one fermentation pathway (3.12) and hydrogen is their growth limiting substrate.

5.1.1 Competitive exclusion principle

The problem of co-existence of multiple fermenter populations competing for the same growth limiting substrate has been well studied in the chemostat literature ([17], [29], [96], [140], [146], [183], [184]). In this section, we summarize some of the results of this work rewritten in the context of multiple glucose fermenter populations competing for the substrate glucose. We use the notation established in Chapter 4. Note that the chemostat literature does not include a thermodynamic term, so $\theta_i = 0$ in the equations presented in this summary.

Let X_i denote the population density of one type of glucose fermenter. For the population to survive in the long term so that its steady state population, $X_i^* > 0$, it must long term be in its reproduction mode so

2032 that it can maintain itself in the rumen, i.e., $E_i = Y_i$. With $E_i = Y_i$ and
2033 $\theta_i = 0$, the equations (4.2) and (4.3) from Chapter 4 can be written as:

$$S_g' = -\frac{q_i S_g}{K_i + S_g} X_i - \alpha S_g + \beta_g \ ,$$
$$X_i' = \left(\frac{Y_i n_i q_i S_g}{K_i + S_g} - Y_i m_i - \alpha \right) X_i \ .$$

2034

2035 At steady state, (S_g^*, X_i^*), the reproduction rate of the glucose fer-
2036 menter, μ_i, is given by

$$\mu_i = \frac{Y_i n_i q_i S_g}{K_i + S_g} - Y_i m_i \ ,$$

2037 and is necessarily the same as the passage rate, i.e., $\mu_i = \alpha$, for $X_i > 0$.
2038 We refer to μ_i as the break-even reproduction rate of the glucose fer-
2039 menter population. For any positive value of passage rate α, there is ex-
2040 actly one positive value of steady state substrate concentration, denoted
2041 as $S_g^*(i)$, that guarantees glucose fermenter i survives at the steady state
2042 (Figure 5.1).

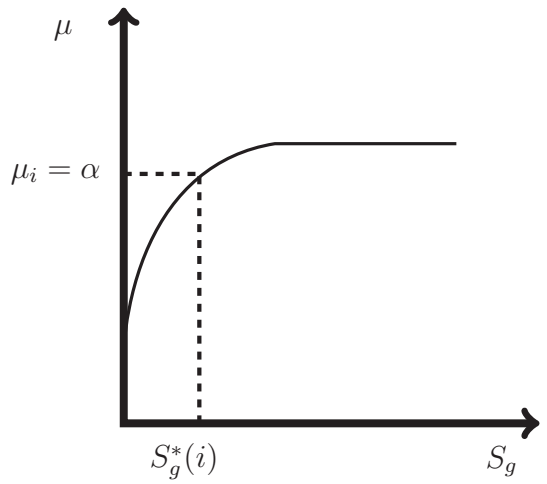

Figure 5.1: Growth rate of a type of glucose fermenter i with a single growth limiting substrate glucose (S_g).

2043 Suppose there is another type of glucose fermenter with population
2044 density denoted by X_j. For glucose fermenter populations i and j to

survive long term, they must be in their reproduction mode in the long term in order to maintain themselves in the rumen, i.e., $E_i = Y_i$ and $E_j = Y_j$. With $E_i = Y_i$, $E_j = Y_j$ and $\theta_i = \theta_j = 0$, equations (4.2) and (4.3) become:

$$
\begin{aligned}
S_g' &= -\frac{q_i S_g}{K_i + S_g} X_i - \alpha S_g + \beta_g \ , \\
X_i' &= \left(\frac{Y_i n_i q_i S_g}{K_i + S_g} - Y_i m_i - \alpha \right) X_i \ , \\
X_j' &= \left(\frac{Y_j n_j q_j S_g}{K_j + S_g} - Y_j m_j - \alpha \right) X_j \ .
\end{aligned}
$$

At steady state, the existence of each fermenter population requires its break-even reproduction rate, μ_i and μ_j, to be the same as the passage rate (i.e., $\mu_i = \mu_j = \alpha$). For any positive value of passage rate, there is exactly one positive value of steady state substrate concentration, denoted $S_g^*(i)$ and $S_g^*(j)$, that guarantees glucose fermenter i and j, respectively can survive. There is only one possibility for co-existence, when $S_g^*(i) = S_g^*(j)$, which is where the two curves in Figure 5.2(b) intersect such that $\mu_i = \mu_j = \alpha$. Otherwise, the glucose fermenter population that survives is the one that can grow at the lowest growth limiting steady state substrate concentration. Mathematically, the model predicts that the glucose fermenter with the best traits for the given environment (the one that can grow at the lowest growth limiting steady state substrate concentration) will survive. For instance, in Figure 5.2(a), because $S_g^*(i) < S_g^*(j)$, glucose fermenter i will survive and glucose fermenter j will die out. Note that we can add multiple types of microbes that all feed on the same single growth limiting substrate into the environment and this result will hold: the only possibility for co-existence of any two or more fermenter populations, is in the unlikely case that their break-even reproduction rates are the same and less than the break-even reproduction rates of the other fermenter population. Otherwise, the population that can grow at the lowest growth limiting steady state substrate concentration will win and the others will die out in the long term. This is known as the competitive exclusion principle [146]. The first mathe-

matical proof is provided by Hsu *et al.* [63] and a simpler, elegant proof using LaSalle's extension theorem from Lyapunov stability is given in [64]. Note that the competitive exclusion principle has been shown to hold for a variety of other specific growth rate functions (e.g., Monod and other monotone growth rate functions [17], [29], [96], [140], [146], [183], [184]). A common feature of the specific growth rate functions studied in each of these competitive exclusion studies is that they are functions of the growth limiting substrate S only.

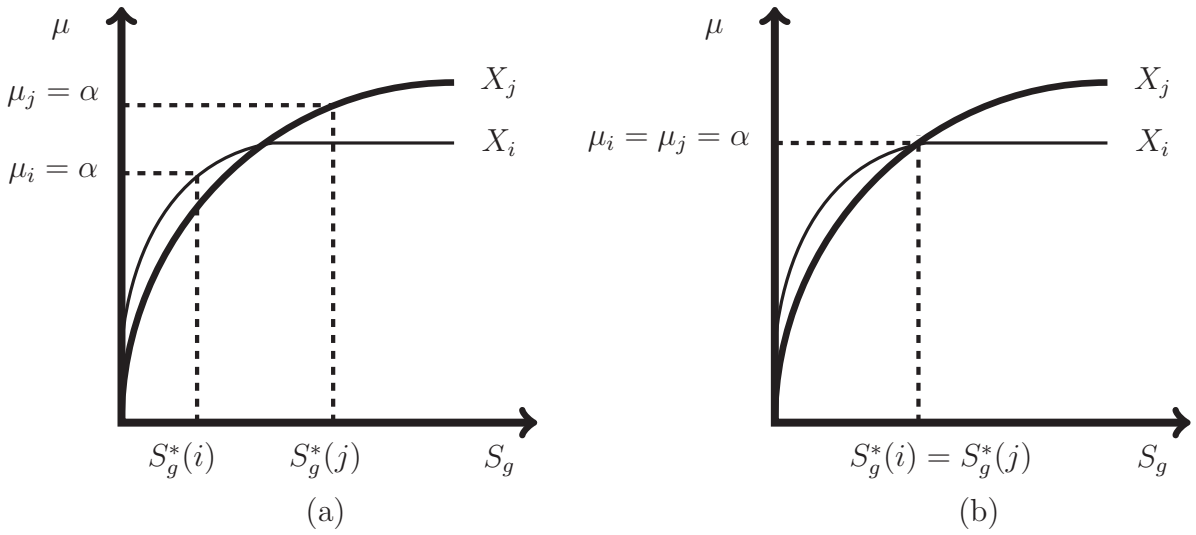

Figure 5.2: Growth rates of two types of glucose fermenter i and j that compete for the same single growth limiting substrate. (a) No co-existence of glucose fermenter i and j. (b) Co-existence.

For the GHM$^\theta$ model presented in Chapter 4, if we consider only the glucose fermenter populations (that is, the methanogen population is zero) and no thermodynamic feedback (so that the thermodynamic term, $\theta_i = 0$), then the work done by Hsu *et al.* [63] shows that one type of glucose fermenter will always win. That is, there can be no (stable) co-existence of glucose fermenters in the rumen (except in the highly unlikely case that all of the glucose fermenter populations grow at the same break-even reproduction rate for the steady state substrate concentration which can happen at most at one positive value of passage rate, α). However, it has been observed that co-existence of glucose fermenters does occur for more than one value of passage rate [70], [139]. Thus, the competitive

exclusion principle concluded from this model is paradoxical. It is then reasonable to ask if the inclusion of the thermodynamic term described in Chapter 4 is able to model co-existence of multiple types of glucose fermenters.

5.1.2 Thermodynamic term for co-existence

In the competitive exclusion models found in [29], [140], [146], the growth rate of microbes are modeled as a function of the growth limiting substrate (e.g., Monod model [115]). In the GHM$^{\theta}$ model, by including a thermodynamic term (θ), the specific growth rate of the microbe is modeled as a function of the end products (to capture the inhibition effects of end products on substrate metabolism) as well as the growth limiting substrate. So it is reasonable to ask if including this thermodynamic term in the GHM$^{\theta}$ model can model the co-existence of more than one type of glucose fermenter at more than one value of passage rate.

Note that changing the passage rate does not change the outcome of competitive exclusion when using the Monod growth rate model only (or any other specific growth rate function that is a function of substrate only) [146]. But different types of glucose fermenters are associated with different fermentation pathways that lead to different end products, including differing amounts of hydrogen, and so to differences in methane production [76]. Thus, a co-existence of different types of glucose fermenter causes different methane production with the same glucose generation rate (i.e., the amount of feed). So it is also interesting to ask if changing the passage rate in the GHM model with the thermodynamic term (and so growth rate dependent on substrate and end product concentration), can lead to co-existence of different types and/or mixture of glucose fermenters (and hence different methane production).

Note that as this thesis was being completed, Großkopf and Soyer [51] used a thermodynamic term to show co-existence of two types of microbes metabolizing the same single growth limiting substrate. However, they did not consider that energy is required to generate ATP (i.e., ΔG_{ATP} is not included in their model and thermodynamic term) and

they only demonstrated a co-existence of two microbes utilizing fermentation pathways that yield different end products without classifying the stability of such a co-existence. In this chapter, the co-existence of two types of glucose fermenters competing for glucose that share at least one common end product is explored using the GHM$^{\theta}$ model.

5.1.3 Outline of the chapter

We start by looking at the case of one type of glucose fermenter associated with the fermentation pathway

$$\text{glucose} \rightarrow B + 2\ \text{H}_2 + 2\ \text{CO}_2 + \text{H}^+ \ ,$$

and a methanogen population associated with pathway (3.12) to explore co-existence of one glucose fermenter population with the methanogens. As these two populations feed on different growth limiting substrates, co-existence is generally expected. We will then extend our analysis to explore co-existence for two types of glucose fermenters feeding on the same growth limiting substrate, but associated with different fermentation pathways. These pathways share at least one common end product:

$$\begin{aligned} &\text{glucose} \rightarrow B + 2\ \text{H}_2 + 2\ \text{CO}_2 + \text{H}^+ \ , \\ &\text{glucose} \rightarrow A + P + \text{H}_2 + \text{CO}_2 + 2\ \text{H}^+ \ . \end{aligned}$$

We will model these cases using the GHM$^{\theta}$ model (Chapter 4). In both cases, the stability of the equilibrium point(s) are examined from the eigenvalues of the Jacobian matrix. These two glucose fermentation pathways are used as an example to demonstrate and explore the mechanism of co-existence, as predicted by the GHM$^{\theta}$ model. The case of two generalized fermentation pathways is investigated in Section 5.4.1.

5.2 One type of glucose fermenter

5.2.1 Analytical results

Suppose there is a type of glucose fermenter population that is labelled as glucose fermenter 1. Let X_1 denote the population density of glucose fermenter 1 associated with the pathway

$$\text{glucose} \rightarrow B + 2\ \text{H}_2 + 2\ \text{CO}_2 + \text{H}^+ \ . \tag{5.1}$$

The thermodynamic term for this pathway is

$$\theta_1 = \frac{[B][\text{H}_2]^2[\text{CO}_2]^2[\text{H}^+]}{[\text{glucose}]}\ \text{e}^{(\Delta G^o_{T_1} + n_1\ \Delta G_{ATP})/(\mathcal{R}T)} = \frac{(S_B)(S_h)^2 C_1}{S_g}\ ,$$

where C_1 is a positive constant based on the assumptions that all the following are constant in the rumen: the pH value (i.e., $[\text{H}^+]$); the energy required for one mole of ATP formation by the glucose fermenter, ΔG_{ATP}; the dissolved carbon dioxide concentration, $[\text{CO}_2]$ and the rumen temperature, T. Let X_m denote the methanogen population associated with the pathway given by equation (3.12). The thermodynamic term for this pathway is equation (3.13). We are interested primarily in whether this glucose fermenter population and methanogens can co-exist in the long term (i.e., at their steady state population, X_1^* and X_m^*, $X_1^* > 0$ and $X_m^* > 0$). For this to occur, both glucose fermenter and methanogens must long term be in their reproduction mode so that they can maintain themselves in the rumen, i.e., $E_1 = Y_1$ and $E_m = Y_m$. Otherwise, they will be eliminated. The GHM$^\theta$ model for this scenario becomes

$$S_g' = -\frac{q_1(S_g - (S_B)(S_h)^2 C_1)}{K_1 + S_g + (S_B)(S_h)^2 C_1} X_1 - \alpha S_g + \beta_g\ , \tag{5.2}$$

$$X_1' = \left(\frac{Y_1 n_1 q_1(S_g - (S_B)(S_h)^2 C_1)}{K_1 + S_g + (S_B)(S_h)^2 C_1} - Y_1 m_1 - \alpha\right) X_1\ , \tag{5.3}$$

$$S_h' = -\frac{q_m(S_h - C_m)}{K_m + S_h + C_m} X_m - \alpha S_h + 2\frac{q_1(S_g - (S_B)(S_h)^2 C_1)}{K_1 + S_g + (S_B)(S_h)^2 C_1} X_1\ ,$$

$$X_m' = \left(\frac{Y_m n_m q_m(S_h - C_m)}{K_m + S_h + C_m} - Y_m m_m - \alpha\right) X_m\ ,$$

$$S'_B = \frac{q_1(S_g - (S_B)(S_h)^2 C_1)}{K_1 + S_g + (S_B)(S_h)^2 C_1} X_1 - \gamma_B S_B - \alpha S_B \ .$$

The long term behavior of solution trajectories is dominated by the equilibrium point(s). The equilibrium point describing co-existence of glucose fermenters and methanogens is

$$\begin{aligned}
&(S_g^*, X_1^*, S_h^*, X_m^*, S_B^*) = \\
&\Bigg(\frac{K_1(Y_1 m_1 + \alpha) + (Y_1 n_1 q_1 + Y_1 m_1 + \alpha)(S_B^*)(S_h^*)^2 C_1}{Y_1 n_1 q_1 - Y_1 m_1 - \alpha} \ , \\
&\frac{(\beta_g - \alpha S_g^*)(K_1 + S_g^* + (S_B^*)(S_h^*)^2 C_1)}{q_1(S_g^* - (S_B^*)(S_h^*)^2 C_1)} \ , \frac{K_m(Y_m m_m + \alpha) + (Y_m n_m q_m + Y_m m_m + \alpha) C_m}{Y_m n_m q_m - Y_m m_m - \alpha} \ , \\
&\frac{(2\frac{q_1(S_g^* - (S_B^*)(S_h^*)^2 C_1)}{K_1 + S_g^* + (S_B^*)(S_h^*)^2 C_1)} X_1^* - \alpha S_h^*)(K_m + S_h^* + C_m)}{q_m(S_h^* - C_m)}, \frac{\beta_g - \alpha S_g^*}{\gamma_B + \alpha} \Bigg) \ . \qquad (5.4)
\end{aligned}$$

By substituting

$$S_g^* = \frac{K_1(Y_1 m_1 + \alpha) + (Y_1 n_1 q_1 + Y_1 m_1 + \alpha)(S_B^*)(S_h^*)^2 C_1}{Y_1 n_1 q_1 - Y_1 m_1 - \alpha} \ ,$$

into

$$S_B^* = \frac{\beta_g - \alpha S_g^*}{\gamma_B + \alpha} \ ,$$

this yields

$$S_B^* = \frac{\beta_g(Y_1 n_1 q_1 - Y_1 m_1 - \alpha) - \alpha K_1(Y_1 m_1 + \alpha)}{\Big((\gamma_B + \alpha)(Y_1 n_1 q_1 - Y_1 m_1 - \alpha) + (Y_1 n_1 q_1 + Y_1 m_1 + \alpha)(S_h^*)^2 C_1\Big)} \ .$$

Note that S_h^* is a function of the biological parameter of methanogens, C_m (a constant that can be evaluated using expression (3.14)) and α. It is assumed that α, γ_B and β_g are all constant so S_B^* can be evaluated and $(S_g^*, X_1^*, S_h^*, X_m^*, S_B^*)$ can be determined given the biological parameters of the methanogens and fermenters and C_m, α, γ_B and β_g.

Suppose glucose fermenters can tolerate the passage rate and so are

not washed out, i.e., $Y_1(n_1q_1 - m_1) > \alpha$. Then,

$$\beta_g(Y_1n_1q_1 - Y_1m_1 - \alpha) - \alpha K_1(Y_1m_1 + \alpha) > 0 \ , \tag{5.5}$$

is required for a positive steady state butyrate concentration ($S_B^* > 0$). Solving for the positive root of α (passage rate must be positive) in expression (5.5), α_{bty}, we find the passage rate value that leads to zero steady state butyrate concentration ($\beta_g - \alpha_{\text{bty}} S_g^* = 0$). At this values, the glucose fermenter will also be eliminated due to shortage of food. This occurs at

$$\alpha_{\text{bty}} = \frac{-(\beta_g + Y_1m_1K_1) + \sqrt{(\beta_g + Y_1m_1K_1)^2 + 4\beta_g K_1(Y_1n_1q_1 - Y_1m_1)}}{2K_1} \ .$$

Similar to expression (2.24), $\alpha_{\text{bty}} < Y_1(n_1q_1 - m_1)$. Overall, a passage rate in the range $0 < \alpha < \alpha_{\text{bty}} < Y_1(n_1q_1 - m_1)$ is required so that the steady state butyrate concentration, glucose fermenter population density and glucose concentration are all positive.

Note that there are three other equilibrium points in addition to the one that describes co-existence. The first such point represents the scenario where glucose fermenters survive and methanogens die out (i.e., $X_1^* > 0$ and $X_m^* = 0$),

$$(S_g^*, X_1^*, S_h^*, X_m^*, S_B^*) =$$
$$\left(\frac{K_1(Y_1m_1 + \alpha) + (Y_1n_1q_1 + Y_1m_1 + \alpha)(S_B^*)(S_h^*)^2C_1}{Y_1n_1q_1 - Y_1m_1 - \alpha} \ , \right.$$
$$\left. \frac{(\beta_g - \alpha S_g^*)(K_1 + S_g^* + (S_B^*)(S_h^*)^2C_1)}{q_1(S_g^* - (S_B^*)(S_h^*)^2C_1)} \ , \frac{2\frac{q_1(S_g^* - (S_B^*)(S_h^*)^2C_1)}{K_1 + S_g^* + (S_B^*)(S_h^*)^2C_1)}X_1^*}{\alpha} \ , 0 \ , \frac{\beta_g - \alpha S_g^*}{\gamma_B + \alpha} \right).$$

The long term survival of glucose fermenters and death of methanogens can occur due to one or more of the following:

1. The hydrogen concentration threshold is not satisfied so no hydrogen can be metabolized by methanogens due to thermodynamic feedback, that is $S_h^* \leq C_m$;

2. There is insufficient supply of hydrogen to support methanogens,

$2\frac{q_1(S_g^*-(S_B^*)(S_h^*)^2C_1)}{K_1+S_g^*+(S_B^*)(S_h^*)^2C_1)}X_1^* < \alpha S_h^*$;

3. Methanogens cannot tolerate the passage rate and so are washed out, $Y_m(n_m q_m - m_m) < \alpha$.

Another equilibrium point is the trivial solution,

$$(S_g^*, X_1^*, S_h^*, X_m^*, S_B^*) = \left(\frac{\beta_g}{\alpha}\ ,0\ ,0\ ,0\ ,0\right).$$

This point represents the scenario where both glucose fermenters and methanogens are eliminated due to one or more of the following:

1. The glucose concentration threshold is not satisfied so no hydrogen can be metabolized by methanogens due to thermodynamic feedback, $S_g^* \leq (S_B^*)(S_h^*)^2C_1$;

2. There is insufficient supply of glucose to support the glucose fermenter population, $\beta_g < \alpha\frac{K_1(Y_1m_1+\alpha)+(Y_1n_1q_1+Y_1m_1+\alpha)(S_B^*)(S_h^*)^2C_1}{Y_1n_1q_1-Y_1m_1-\alpha}$;

3. Glucose fermenters cannot tolerate the passage rate and so are washed out, $Y_1(n_1q_1 - m_1) < \alpha$.

When glucose fermenters are eliminated, then no glucose is metabolized to produce hydrogen and methanogens are then also eliminated due to shortage of food supply.

The fourth equilibrium point is then

$$\begin{aligned}&(S_g^*, X_1^*, S_h^*, X_m^*, S_B^*) = \\ &\left(\frac{\beta_g}{\alpha}\ ,0\ ,\frac{K_m(Y_m m_m+\alpha)+(Y_m n_m q_m+Y_m m_m+\alpha)C_m}{Y_m n_m q_m - Y_m m_m - \alpha}\ ,\right. \\ &\left.-\alpha S_h^*\frac{K_m+S_h^*+C_m}{q_m(S_h^*-C_m)}\ ,0\right).\end{aligned}$$

As noted previously, no hydrogen is generated in the absence of glucose fermenters and yet this point suggests a zero glucose fermenter population and non-zero methanogen population. Furthermore, suppose only methanogens survive i.e., $X_m^* > 0$, so that the hydrogen concentration

threshold is satisfied and methanogens can tolerate the passage rate (are not washed out). This is presented mathematically by

$$S_h^* > C_m \ ,$$

and

$$Y_m(n_m q_m - m_m) > \alpha \ .$$

Because all the biological parameters are positive, these conditions yield a negative methanogen population (X_m^*) which is a contradiction to the assumption that there is a positive methanogen population. Thus, the fourth equilibrium point cannot occur and is omitted from further discussion.

5.2.2 Parameters

For numerical study, parameter values used are from the literature:

$$\begin{aligned}
m_1 &= 6.35 \times 10^{-20} \text{ mol}_{ATP} \text{ cell}^{-1} \text{ s}^{-1} \text{ [139]} \ , \\
q_1 &= 6.61 \times 10^{-19} \text{ mol cell}^{-1} \text{ s}^{-1} \text{ [143]} \ , \\
Y_1 &= 5.35 \times 10^{13} \text{ cell mol}_{ATP}^{-1} \text{ [120] [160]} \ , \\
K_1 &= 2 \times 10^{-10} \text{ mol ml}^{-1} \text{ [87]} \ , \\
n_1 &= 3 \text{ mol}_{ATP} \text{ mol}^{-1} \text{ [Appendix } C\text{]} \ , \\
\Delta G_{T_1}^o &= -191.963 \text{ kJ mol}^{-1} \text{ [21]} \ , \\
\gamma_B &= 1.30 \times 10^{-6} \text{ s}^{-1} \text{[32]} \ .
\end{aligned}$$

A theoretical glucose fermentation balance was calculated by Wolin [181]

$$57.5 \text{ glucose} \rightarrow 65A + 20P + 15B + 60\text{CO}_2 + 35\text{CH}_4 + 25\text{H}_2\text{O} \ .$$

As four moles of hydrogen are converted into one mole of methane, equivalently, 2.435 moles of hydrogen are produced for every mole of glucose

2231 fermented. Therefore, for the GHM$^\theta$ model, we assume β_g is given by:

$$\beta_g = \beta_h/2.435 = 1.930 \times 10^{-9} \text{ mol ml}^{-1}\text{s}^{-1} .$$

2232 The pH of the rumen is assumed to be constant at 6.5 [70], so

$$[\text{H}^+] = 10^{-6.5} \text{ mol L}^{-1} = 3.162 \times 10^{-10} \text{ mol ml}^{-1} .$$

2233 It is assumed that the glucose fermenters and methanogens both need
2234 the same amount of energy to gain one unit of ATP, i.e., $\Delta G_{ATP} =$
2235 75 kJ mol$^{-1}_{ATP}$ (assumption 14). Other parameters can be found in the
2236 HM and HM$^\theta$ models (Tables 2.1 and 3.1).

2237 5.2.3 Stability of equilibrium point

2238 The stability of the three physically meaningful equilibrium points of the
2239 GHM$^\theta$ model with one type of glucose fermenter can be explored numer-
2240 ically. With typical parameter values (Tables 2.1 and 3.1 and Section
2241 5.2.2), the only stable solution is

$$\begin{aligned}
&(S_g^*, X_1^*, S_h^*, X_m^*, S_B^*) = \\
&(1.134 \times 10^{-10} \text{ mol ml}^{-1},\ 8.067 \times 10^9 \text{ cell ml}^{-1}, \\
&3.215 \times 10^{-10} \text{ mol ml}^{-1},\ 0.288 \times 10^9 \text{ cell ml}^{-1}, \\
&5.316 \times 10^{-5} \text{ mol ml}^{-1}) .
\end{aligned}$$

2242 The corresponding eigenvalues of the Jacobian matrix of the model, J_1
2243 (page 98), are

$$-10.9,\ -3.84 \times 10^{-5},\ -11.2,\ -3.81 \times 10^{-5},\ -3.63 \times 10^{-5} .$$

2244 The real part of these five eigenvalues are all negative so that $(S_g^*, X_1^*, S_h^*,$
2245 $X_m^*, S_B^*)$ is a stable point: $(S_g^*, X_1^*, S_h^*, X_m^*, S_B^*)$ is the only stable steady
2246 state solution of the GHM$^\theta$ model and there is a stable co-existence of one
2247 type of glucose fermenter and the methanogens with typical parameter
2248 values.

Note that the eigenvalues associated with S_g^* and S_h^* are six orders of magnitude greater than those associated with X_1^*, X_m^* and S_B^* indicating that the glucose and hydrogen concentration will converge towards their corresponding steady state values relatively quickly compared to the glucose fermenters, methanogens and butyrate concentration. A closer look at the equation with the typical parameter values shows why this is the case. The eigenvalue of a matrix is solved at the equilibrium point from $\det(J_1 - \lambda I) = 0$. The eigenvalue associated with S_B is given by

$$-\frac{q_1(S_h)^2 C_1(K_1 + 2S_g)X_1}{(K_1 + S_g + (S_B)(S_h)^2 C_1)^2} - (\gamma_B + \alpha) \ .$$

At the point $(S_g^*, X_1^*, S_h^*, X_m^*, S_B^*)$, the magnitude of

$$\frac{q_1(S_h)^2 C_1(K_1 + 2S_g)X_1}{(K_1 + S_g + (S_B)(S_h)^2 C_1)^2} \ ,$$

is less than 1×10^{-10} and $-(\gamma_B + \alpha) = 3.63 \times 10^{-5}$, so that the eigenvalue associated with S_B is approximated by -$(\gamma_B + \alpha)$. Note that -$(\gamma_B + \alpha)$ is in S_B'. It can similarly be shown that $-(Y_1 m_1 + \alpha) = -3.84 \times 10^{-5}$ and $-(Y_m m_m + \alpha) = -3.81 \times 10^{-5}$ are, respectively, in X_1' and X_m', and dominate the eigenvalues associated with these variables.

$$J_1 = \begin{bmatrix} -\frac{q_1(K_1+2(S_B)(S_h)^2C_1)X_1}{(K_1+S_g+(S_B)(S_h)^2C_1)^2} - \alpha & -\frac{q_1(S_g-(S_B)(S_h)^2C_1)}{K_1+S_g+(S_B)(S_h)^2C_1} & \frac{2q_1S_BS_hC_1(K_1+2S_g)X_1}{(K_1+S_g+(S_B)(S_h)^2C_1)^2} & 0 & \frac{q_1(S_h)^2C_1(K_1+2S_g)X_1}{(K_1+S_g+(S_B)(S_h)^2C_1)^2} \\ \frac{Y_1n_1q_1(K_1+2(S_B)(S_h)^2C_1)X_1}{(K_1+S_g+(S_B)(S_h)^2C_1)^2} & \frac{Y_1n_1q_1(S_g-(S_B)(S_h)^2C_1)}{K_1+S_g+(S_B)(S_h)^2C_1} - Y_1m_1 - \alpha & \frac{2Y_1n_1q_1S_BS_hC_1(K_1+2S_g)X_1}{(K_1+S_g+(S_B)(S_h)^2C_1)^2} & 0 & \frac{Y_1n_1q_1(S_h)^2C_1(K_1+2S_g)X_1}{(K_1+S_g+(S_B)(S_h)^2C_1)^2} \\ \frac{2q_1(K_1+2(S_B)(S_h)^2C_1)X_1}{(K_1+S_g+(S_B)(S_h)^2C_1)^2} & \frac{2q_1(S_g-(S_B)(S_h)^2C_1)}{K_1+S_g+(S_B)(S_h)^2C_1} & -\frac{q_m(K_m+2C_m)X_m}{(K_m+S_h+C_m)^2} - \alpha + \frac{4q_1S_BS_hC_1(K_1+2S_g)X_1}{(K_1+S_g+(S_B)(S_h)^2C_1)^2} & -\frac{q_m(S_h-C_m)}{K_m+S_h+C_m} & \frac{2q_1(S_h)^2C_1(K_1+2S_g)X_1}{(K_1+S_g+(S_B)(S_h)^2C_1)^2} \\ 0 & 0 & \frac{Y_mn_mq_m(K_m+2C_m)X_m}{(K_m+S_h+C_m)^2} & \frac{Y_mn_mq_m(S_h-C_m)}{K_m+S_h+C_m} - Y_mm_m - \alpha & 0 \\ \frac{q_1(K_1+2(S_B)(S_h)^2C_1)X_1}{(K_1+S_g+(S_B)(S_h)^2C_1)^2} & \frac{q_1(S_g-(S_B)(S_h)^2C_1)}{K_1+S_g+(S_B)(S_h)^2C_1} & -\frac{2q_1S_BS_hC_1(K_1+2S_g)X_1}{(K_1+S_g+(S_B)(S_h)^2C_1)^2} & 0 & -\frac{q_1(S_h)^2C_1(K_1+2S_g)X_1}{(K_1+S_g+(S_B)(S_h)^2C_1)^2} - \gamma_B - \alpha \end{bmatrix}$$

2263

Suppose the initial value, $(S_g, X_1, S_h, X_m, S_B)$, is in the neighborhood of $(S_g^*, X_1^*, S_h^*, X_m^*, S_B^*)$ such that the order of X_1 is of the same magnitude as X_1^*, i.e., 1×10^9 cell ml^{-1}. Using the listed parameter values (Section 5.2.2), from equation (5.2), the metabolism of S_g by glucose fermenters X_1, is given by

$$-\frac{q_1(S_g - (S_B)(S_h)^2 C_1)}{K_1 + S_g + (S_B)(S_h)^2 C_1} X_1 \ ,$$

and is of the same magnitude as S_g^* (1×10^{-10} mol ml^{-1}). The magnitude of β_g is 1×10^{-9} mol ml^{-1} s^{-1} which is ten times greater than the magnitude of S_g^*. Then, in one second, the rate of change in glucose concentration, S_g', is about the same magnitude as S_g^*. In contrast, from equation (5.3), the change in the glucose fermenter population is determined by

$$\frac{Y_1 n_1 q_1(S_g - (S_B)(S_h)^2 C_1)}{K_1 + S_g + (S_B)(S_h)^2 C_1} - Y_1 m_1 - \alpha \ ,$$

which is of magnitude as 1×10^{-5} s^{-1}. Then, in one second, the rate of change of the glucose fermenter population, X_1', is about 1×10^4, five orders of magnitude smaller than the magnitude of X_1^*. Because the rate of change in glucose concentration is relatively quick (10^5 faster) as compared to the glucose fermenters, the glucose concentration will converge towards its corresponding steady state value relatively quickly as compared to the glucose fermenters. This difference in the rates of change is also shown in the difference in magnitudes of their corresponding eigenvalues. It can be similarly shown that, the hydrogen concentration converges towards its corresponding steady state values relatively quickly as compared to the methanogen population. Using the listed parameter values, glucose and hydrogen could be metabolized instantaneously (in one second) by glucose fermenters and methanogens, respectively. That is in agreement with assumption 4 of the GHM$^\theta$ model. However, glucose fermenters and methanogens cannot be removed by the passage rate in one second, unless the passage rate is increased from a typical passage rate value of 3.5×10^{-5} s^{-1} by a factor of at least 10^5. Such a passage

rate (1 s^{-1}) is, however, beyond the range of passage rates observed in the rumen ($1 \times 10^{-5} \leq \alpha \leq 5 \times 10^{-5}$ s^{-1} [150], [152]).

From equation (4.6), the rate of change in butyrate concentration is determined by the term $-(\gamma_B + \alpha)$ with a magnitude of 10^{-5}. In one second, the rate of change in butyrate concentration, S'_B, is about 10^{-10} which is five orders of magnitude smaller than the magnitude of the steady state butyrate concentration, S^*_B. Similar to glucose fermenters and methanogens, there are no realistic absorption and passage rate values that would allow all the butyrate to be removed from the rumen in one second. Note that the butyrate concentration will converge towards its corresponding steady state value relatively slowly (10^5 slower) as compared to the glucose and hydrogen concentration. Unlike glucose and hydrogen, butyrate is an end product that is not metabolized by other microbes so that the rate of change in butyrate concentration is similar to that of the glucose fermenters and methanogens that are also not consumed by other microbes in the GHM$^\theta$ model.

5.2.4 Simulation

Recall that there are three physically meaningful equilibrium points representing: co-existence of glucose fermenters and methanogens; survival of glucose fermenters and methanogen extinction; and the trivial solution. For $0 < \alpha < 1.026 \times 10^{-4}$ $s^{-1} = Y_1(n_1 q_1 - m_1)$, the glucose fermenters can survive without being eliminated by washout. In addition, glucose fermenters can survive with sufficient food supply when (see discussion in Section 5.2.1)

$$\alpha < \alpha_{\text{bty}} = \frac{-(\beta_g + Y_1 m_1 K_1) + \sqrt{(\beta_g + Y_1 m_1 K_1)^2 + 4\beta_g K_1 (Y_1 n_1 q_1 - Y_1 m_1)}}{2K_1} .$$

Using parameter values listed in Section 5.2.2, $\alpha_{\text{bty}} = 1.026 \times 10^{-4}$ $s^{-1} \approx Y_1(n_1 q_1 - m_1)$. Overall, using typical parameter values (Tables 2.1 and 3.1 and Section 5.2.2), for $0 < \alpha < 1.026 \times 10^{-4}$ s^{-1}, the only stable equilibrium point is where there is a stable co-existence of glucose fermenters and methanogens. In this section we examine changes stability of in

equilibrium point for varying passage rates, α, $0 < \alpha \leq 1.2 \times 10^{-4}$ s^{-1}.

When using typical parameter values (Tables 2.1 and 3.1 and Section 5.2.2), if $\alpha \geq 1.026 \times 10^{-4}$ s$^{-1} = Y_1(n_1 q_1 - m_1)$, the reproduction rate of the glucose fermenters is insufficient to tolerate the passage rate so that glucose fermenters are eliminated due to washout (see point 3, page 94) or glucose fermenters are eliminated due to insufficient food supply. The maximal passage rate that the methanogens can tolerate without being eliminated from the rumen is 1.04×10^{-4} s^{-1} (Section 2.5). However, when $\alpha \geq 1.026 \times 10^{-4}$ s^{-1}, methanogens are also eliminated because there is no hydrogen generated from glucose fermentation in the absence of glucose fermenters (i.e., lack of food source). Thus, the scenario where there is stable survival of glucose fermenters without methanogens is not feasible, when using typical parameter values.

For each value of passage rate, there is only one stable equilibrium point. When $0 < \alpha < 1.026 \times 10^{-4}$ s^{-1}, there is stable co-existence of glucose fermenters and methanogens. For $\alpha \geq 1.026 \times 10^{-4}$ s^{-1}, the trivial solution is the only stable steady state solution. Figure 5.3 illustrates the stable steady state population densities for glucose fermenters and methanogens. By increasing the passage rate, a larger proportion of each population is removed so that the stable population size decreases, until both glucose fermenters and methanogens are removed by the passage rate when $\alpha \geq 1.026 \times 10^{-4}$ s^{-1} (Figure 5.3). This leads to less butyrate production and eventually no butyrate production when $\alpha \geq 1.026 \times 10^{-4}$ s^{-1} as illustrated in Figure 5.5. When there is a stable co-existence of glucose fermenters and methanogens, increasing the passage rate leads to an increase in both the steady state glucose and hydrogen concentrations (S_g^* and S_h^*), and a decrease in the steady state butyrate concentration, S_B^*, which is negatively proportional to S_g^* (Figure 5.5 and the left panel of Figure 5.4). When the glucose fermenters and methanogens have been washed out and the trivial solution is the only steady state, the steady state glucose concentration is given by $S_g^* = \beta_g/\alpha$ and the steady state hydrogen concentration is zero as there are no glucose fermenters to produce hydrogen (right panel of Figure 5.4).

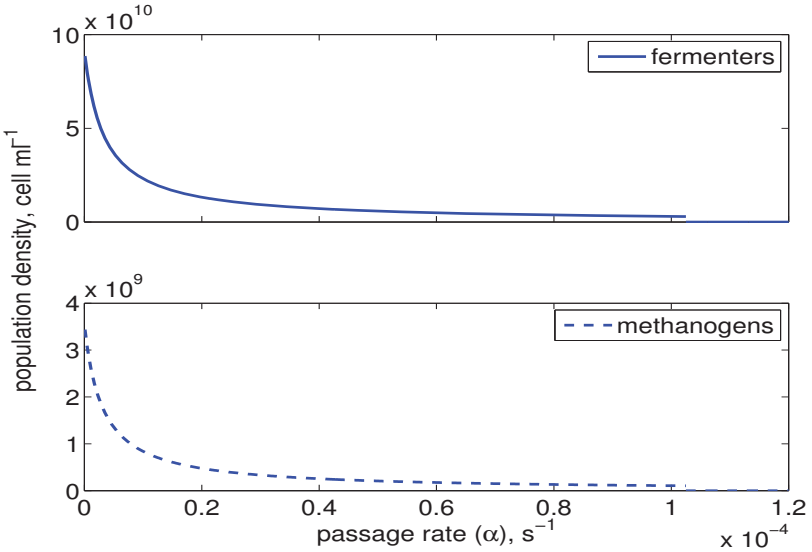

Figure 5.3: The stable population densities of glucose fermenters and methanogens for a range of passage rate values. There is a discontinuity in the figure ($\alpha = 1.026 \times 10^{-4}$ s^{-1} $= \alpha_{\text{bty}} \approx Y_1(n_1 q_1 - m_1)$).

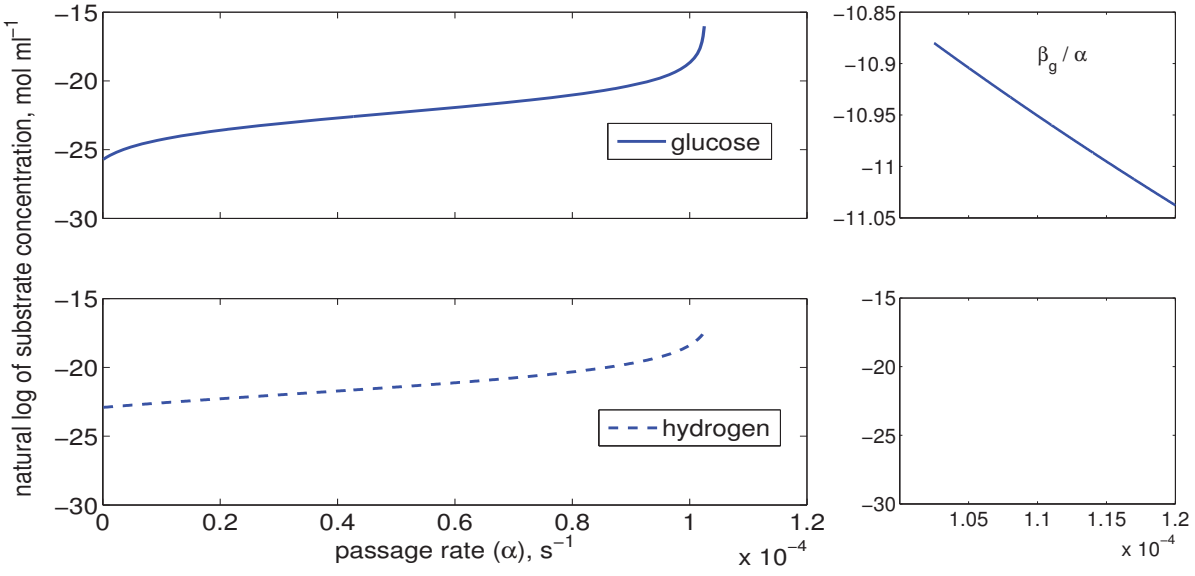

Figure 5.4: The stable steady state substrate (glucose and hydrogen) concentration for a range of passage rate values. The left panel is associated with a stable co-existence of glucose fermenters and methanogens and right panel is where both populations are eliminated.

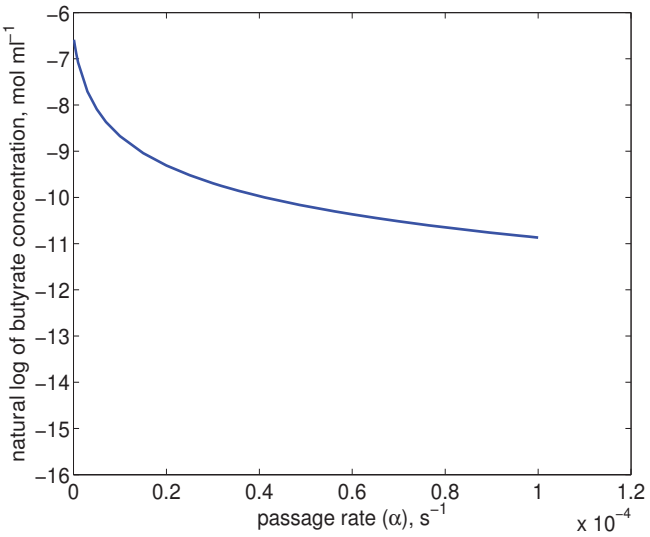

Figure 5.5: The stable steady state butyrate concentration for a range of passage rate values. When the glucose fermenters are eliminated by increasing the passage rate, there is no butyrate production so that the corresponding steady state butyrate concentration is zero when $\alpha \geq 1.026 \times 10^{-4}$ s^{-1}. Note log(0) is negative infinity so zero concentration is not shown on graph.

From the HM model, the actual sensitivity value of methane production with respect to the hydrogen generation rate is one. The rate of methane production is proportional to the net rate of hydrogen generation from feed in the rumen [68]. Glucose is fermented to hydrogen then metabolized to methane (equation 3.15). In this GHM$^{\theta}$ model, the ratio between the hydrogen generation rate and the glucose generation rate at time t, β_h/β_g, is used as a measure to compare methane production from different rumen environments: a lower ratio leads to less estimated methane production. Because there is only one type of glucose fermenter, when $X_1^* > 0$ and $\theta_1 = 0$ each mole of glucose fermented yields two moles of hydrogen that are metabolized by methanogens to form methane. By increasing the passage rate, the hydrogen generation rate decreases due to thermodynamic feedback ($\theta_1 > 0$) so that β_h/β_g decreases and, consequently, so does methane production. By increasing the passage rate up to $\alpha = 1.026 \times 10^{-4}$ s^{-1}, $\beta_h/\beta_g = 1.9884$ so that methane production is

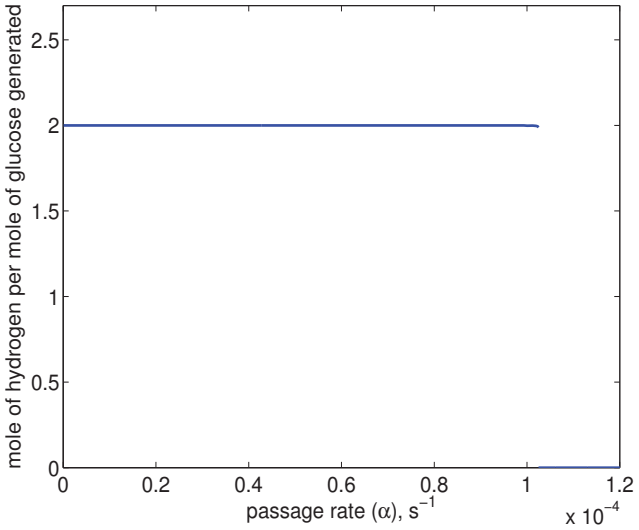

Figure 5.6: With a constant $\beta_g = 1.930 \times 10^{-9}$ mol ml^{-1} s^{-1}, β_h/β_g of the stable steady state is calculated over a range of passage rate values. There is essentially one value of β_h/β_g for $0 < \alpha < 1.026 \times 10^{-4}$ s^{-1} and another (0) for $\alpha \geq 1.026 \times 10^{-4}$ s^{-1}.

reduced by at most $(2 - 1.9884)/2 = 0.583\%$, as shown in the left panel of Figure 5.6. In the HM model, from Figure 2.5, methane is reduced by at most 0.099%. The effect of increasing the passage rate on methane production becomes more significant when a glucose fermenter population and its associated pathway is included in the HM model that yields the GHM$^\theta$ model. In experiments on sheep, by increasing the passage rate, the observed reduction in methane production was about 11% [132]. Note that there is only one glucose fermenter population associated with one fermentation pathway in this GHM$^\theta$ model. A reasonable question to ask is, would including more fermentation pathways and associated glucose fermenters lead to greater than 0.583% reduction in methane production when increasing the passage rate? To explore this, and the potential stable co-existence of different types and mixtures of glucose fermentation populations, the next step is to introduce a second type of glucose fermenter associated with a different fermentation pathway. This will also allow us to explore the mechanism for shifts in glucose fermentation pathways, as predicted by the GHM$^\theta$ model.

5.3 Two types of glucose fermenters

In this section, two types of glucose fermenter populations, each associated with a different fermentation pathway, and methanogens, associated with pathway (3.12), are modeled using the GHM$^\theta$ model. This is done in an effort to explore the potential for co-existence of fermenter populations competing for the same substrate (glucose) as well as the mechanism for such a co-existence as predicted by the GHM$^\theta$ model. The conclusions of this section can be applied to any two types of glucose fermenter populations that are associated with different fermentation pathways taking the form given in equation (4.1).

5.3.1 Analytical results

Let X_1 denote the population density of the glucose fermenter population 1 given in Section (5.2) associated with the pathway (5.1). Let us introduce another type of glucose fermenter population 2 with a population density of X_2 that is associated with the pathway

$$\text{glucose} \rightarrow A + P + \text{H}_2 + \text{CO}_2 + 2\ \text{H}^+ \ .$$

The thermodynamic term for this pathway is

$$\theta_2 = \frac{[A][P][\text{H}_2][\text{CO}_2][\text{H}^+]^2}{[\text{glucose}]}\ \text{e}^{(\Delta G^o_{T_2} + n_2\ \Delta G_{ATP})/(\mathcal{R}T)} = \frac{(S_A)(S_P)(S_h)C_2}{S_g}\ ,$$

where C_2 is a positive constant based on the same assumptions stated in Section 5.2. In other words, the following are constant in the rumen: the pH value (i.e., $[\text{H}^+]$); the energy required for one mole of ATP formation by the glucose fermenter, ΔG_{ATP}; the dissolved carbon dioxide concentration, $[\text{CO}_2]$ and the rumen temperature, T. The GHM$^\theta$ model becomes

$$\begin{aligned} S_g' &= -\frac{q_1(S_g(1-\theta_1)}{K_1 + S_g(1+\theta_1)}X_1 - \frac{q_2 S_g(1-\theta_2)}{K_2 + S_g(1+\theta_2)}X_2 - \alpha S_g + \beta_g\ , \qquad (5.6)\\ X_1' &= \left(\frac{Y_1 n_1 q_1 S_g(1-\theta_1)}{K_1 + S_g(1+\theta_1)} - Y_1 m_1 - \alpha\right) X_1\ , \end{aligned}$$

$$X_2' = \left(\frac{Y_2 n_2 q_2 S_g (1-\theta_2)}{K_2 + S_g(1+\theta_2)} - Y_2 m_2 - \alpha \right) X_2 \ ,$$

$$S_h' = -\frac{q_m S_h (1-\theta_m)}{K_m + S_h(1+\theta_m)} X_m - \alpha S_h + 2\frac{q_1 S_g (1-\theta_1)}{K_1 + S_g(1+\theta_1)} X_1 + \frac{q_2 S_g (1-\theta_2)}{K_2 + S_g(1+\theta_2)} X_2 \ , \tag{5.7}$$

$$X_m' = \left(\frac{Y_m n_m q_m S_h (1-\theta_m)}{K_m + S_h(1+\theta_m)} - Y_m m_m - \alpha \right) X_m \ , \tag{5.8}$$

$$S_A' = \frac{q_2 S_g (1-\theta_2)}{K_2 + S_g(1+\theta_2)} X_2 - \gamma_A S_A - \alpha S_A \ ,$$

$$S_P' = \frac{q_2 S_g (1-\theta_2)}{K_2 + S_g(1+\theta_2)} X_2 - \gamma_P S_P - \alpha S_P \ ,$$

$$S_B' = \frac{q_1 S_g (1-\theta_1)}{K_1 + S_g(1+\theta_1)} X_1 - \gamma_B S_B - \alpha S_B \ .$$

For this system of equations, we are interested primarily under what conditions there is co-existence of the two types of glucose fermenters 1 and 2 in the long term (i.e., at their steady state population, X_1^* and X_2^*, $X_1^* > 0$ and $X_2^* > 0$) and if this co-existence is stable. We denote this equilibrium point by $(S_g^*, X_1^*, X_2^*, S_h^*, X_m^*, S_A^*, S_P^*, S_B^*)$. This steady state, or equilibrium, occurs where $S_g' = X_1' = X_2' = X_h' = X_m' = S_A' = S_P' = S_B' = 0$.

$S_g' = 0$ yields

$$\beta_g - \alpha S_g^* = \frac{q_1 (S_g (1-\theta_1)}{K_1 + S_g(1+\theta_1)} X_1 + \frac{q_2 S_g (1-\theta_2)}{K_2 + S_g(1+\theta_2)} X_2 \ .$$

A physically meaningful population density cannot be negative, i.e., X_1 or X_2 cannot be negative. We also have $0 \leq \theta_1 \leq 1$ and $0 \leq \theta_2 \leq 1$ and all the biological parameters are positive. Therefore, the term

$$\frac{q_1 (S_g (1-\theta_1)}{K_1 + S_g(1+\theta_1)} X_1 \ ,$$

and

$$\frac{q_2 S_g (1-\theta_2)}{K_2 + S_g(1+\theta_2)} X_2$$

are non-negative. Therefore, a sufficient glucose supply, $\beta_g > \alpha S_g^*$, is

required to guarantee at least one type of glucose fermenters can survive. If there is insufficient glucose supply both types of glucose fermenters will be eliminated, for instance, if $\beta_g = \alpha S_g^*$, then $X_1 = X_2 = 0$ and/or $\theta_1 = \theta_2 = 1$. Note that $\theta_1 = \theta_2 = 1$ indicates no glucose can be metabolized by either type of glucose fermenter due to thermodynamic feedback so that both types of glucose fermenters cannot reproduce and will therefore eventually be eliminated by the passage rate. Thus, $(\beta_g/\alpha, 0, 0, 0, 0, 0, 0, 0)$ is the only solution of the GHM$^\theta$ model under this condition.

$X_1' = 0$, and $X_1^* > 0$ yields

$$S_g^* = \frac{K_1(Y_1 m_1 + \alpha)}{Y_1 n_1 q_1 (1 - \theta_1) - (Y_1 m_1 + \alpha)(1 + \theta_1)} \ . \tag{5.9}$$

$X_2' = 0$, and $X_2^* > 0$ yields

$$S_g^* = \frac{K_2(Y_2 m_2 + \alpha)}{Y_2 n_2 q_2 (1 - \theta_2) - (Y_2 m_2 + \alpha)(1 + \theta_2)} \ . \tag{5.10}$$

For either type of fermenter to survive, the feed intake must be positive, and so the substrate concentration, $S_g^* > 0$, must be positive. The numerators of equations (5.9) and (5.10) are positive. From the denominators we have the following conditions for positivity of S_g^*.

$$Y_1 n_1 q_1 (1 - \theta_1) - (Y_1 m_1 + \alpha)(1 + \theta_1) > 0 \ ,$$

or

$$Y_2 n_2 q_2 (1 - \theta_2) - (Y_2 m_2 + \alpha)(1 + \theta_2) > 0 \ .$$

These conditions ensure the individual fermenter populations are not eliminated by passage rate and fermenter population 1 and 2, respectively, can reproduce and maintain themselves in the rumen. For X_1 to exist, $\theta_1^* \neq 1$ and for X_2 to exist, $\theta_2^* \neq 1$.

Note that S_g^* in equation (5.9) is a function of the biological parameters of the glucose fermenter population 1. Similarly, S_g^* in equation (5.10) is a function of the biological parameters of the glucose fermenter

population 2. We denote the steady state glucose concentration given in equation (5.9) as $S_g^*(1)$ and that in equation (5.10) as $S_g^*(2)$ to indicate its dependence on the parameters of glucose fermenter population 1 and 2, respectively. If $S_g^*(1) < 0$, then $X_1^* = 0$ because glucose fermenters 1 cannot reproduce fast enough to match up with the passage rate and/or $\theta_1^* = 1$. Similarly, if $S_g^*(2) < 0$, then $X_2^* = 0$. As shown later in this chapter, when $S_g^*(1) > 0$ and $S_g^*(2) > 0$, the comparison of $S_g^*(1)$ and $S_g^*(2)$ determines whether $X_1^* > 0$ and $X_2^* > 0$.

At such an equilibrium point, from $X_1' = 0$, and $X_1^* > 0$

$$\frac{q_1 S_g^*(1-\theta_1)}{K_1 + S_g^*(1+\theta_1)} = \frac{Y_1 m_1 + \alpha}{Y_1 n_1} = \delta_1 \ ,$$

and from $X_2' = 0$, and $X_2^* > 0$

$$\frac{q_2 S_g^*(1-\theta_2)}{K_2 + S_g^*(1+\theta_2)} = \frac{Y_2 m_2 + \alpha}{Y_2 n_2} = \delta_2 \ ,$$

where δ_1 and δ_2 represent a ratio of ATP used by a cell for overcoming maintenance requirements and passage rate to reproduction. Note that δ_1 and δ_2 are determined by the passage rate and biological parameters for glucose fermenters 1 and 2, respectively.

$S_g' = 0$ yields

$$\delta_1 X_1^* + \delta_2 X_2^* = \beta_g - \alpha S_g^* \ ,$$

and the conditions $S_A' = S_P' = S_B' = 0$ lead to

$$(\gamma_B + \alpha) S_B^* = \delta_1 X_1^* \ , \tag{5.11}$$

$$(\gamma_A + \alpha) S_A^* = \delta_2 X_2^* \ , \tag{5.12}$$

$$(\gamma_P + \alpha) S_P^* = \delta_2 X_2^* \ ,$$

such that

$$(\gamma_A + \alpha) S_A^* = (\gamma_P + \alpha) S_P^* \ , \tag{5.13}$$

and

$$(\gamma_B + \alpha)S_B^* + (\gamma_A + \alpha)S_A^* = \beta_g - \alpha S_g^* \ . \tag{5.14}$$

$S_h' = 0$, and $X_m^* > 0$ yields

$$\delta_m X_m^* = 2(\gamma_B + \alpha)S_B^* + (\gamma_A + \alpha)S_A^* - \alpha S_h^* \ , \tag{5.15}$$

where

$$\delta_m = \frac{Y_m m_m + \alpha}{Y_m n_m} \ .$$

$X_m' = 0$, and $X_m^* > 0$ yields

$$S_h^* = \frac{K_m \delta_m + (q_m + \delta_m)C_m}{q_m - \delta_m} \ , \tag{5.16}$$

provided

$$\theta_m = \frac{C_m}{S_h} \ .$$

Note that δ_m represents a ratio of ATP used by a methanogen cell for overcoming maintenance requirements and passage rate to reproduction. If $q_m > \delta_m$, then $S_h^* > 0$ and $X_m^* > 0$. Otherwise, methanogens are eliminated in the long term ($X_m^* = 0$) because the required substrate metabolism rate for a cell to survive is greater than its maximal substrate metabolism rate. There are three other cases where $X_m^* = 0$: either

$$S_h^* \leq C_m \ ,$$

where the steady state hydrogen concentration is less than the hydrogen concentration threshold imposed by thermodynamic control such that $\theta_m^* = 1$; or

$$2(\gamma_B + \alpha)S_B^* + (\gamma_A + \alpha)S_A^* - \alpha S_h^* \leq 0 \ ,$$

where there is insufficient hydrogen supply from glucose fermentation for

methanogens; or methanogens cannot reproduce faster than the passage rate. If $X_m^* = 0$, then

$$S_h^* = \frac{2(\gamma_B + \alpha)S_B^* + (\gamma_A + \alpha)S_A^*}{\alpha} \ .$$

Because $S_B^* \geq 0$, $S_A^* \geq 0$ and $\alpha > 0$, $S_h^* \geq 0$. Overall, $S_h^* \geq 0$.

With S_A^*, S_P^*, S_B^*, and S_g^*, the steady state thermodynamic terms are

$$\theta_1^* = \frac{(S_B^*)(S_h^*)^2 C_1}{S_g^*} \ ,$$
$$\theta_2^* = \frac{(S_A^*)(S_P^*)(S_h^*)C_2}{S_g^*} \ .$$

$S_g^*(1)$ and $S_g^*(2)$ become

$$S_g^*(1) = \frac{K_1\delta_1 + (q_1 + \delta_1)(S_B^*)(S_h^*)^2 C_1}{q_1 - \delta_1} \ , \tag{5.17}$$
$$S_g^*(2) = \frac{K_2\delta_2 + (q_2 + \delta_2)(S_A^*)(S_P^*)(S_h^*)C_2}{q_2 - \delta_2} \ . \tag{5.18}$$

In equations (5.14), (5.17) and (5.18), there are three unknowns: S_g^*, S_B^* and S_A^* because S_P^* can be determined from S_A^*. Equations (5.14), (5.17) and (5.18) can be re-written as

$$S_g^* = \frac{\beta_g}{\alpha} - \frac{\gamma_B + \alpha}{\alpha} S_B^* - \frac{\gamma_A + \alpha}{\alpha} S_A^* \ ,$$
$$S_g^* = \xi_1 + \eta_1 S_B^* = S_g^*(1) \ ,$$
$$S_g^* = \xi_2 + \eta_2 (S_A^*)^2 = S_g^*(2) \ .$$

where

$$\xi_1 = \frac{K_1\delta_1}{q_1 - \delta_1} \ ,$$
$$\eta_1 = \frac{(q_1 + \delta_1)(S_h^*)^2 C_1}{q_1 - \delta_1} \ ,$$
$$\xi_2 = \frac{K_2\delta_2}{q_2 - \delta_2} \ ,$$
$$\eta_2 = \frac{(q_2 + \delta_2)(\gamma_A + \alpha)(S_h^*)C_2}{(q_2 - \delta_2)(\gamma_P + \alpha)} \ ,$$

are all positive and are combinations of the passage rate and biological parameters for these two types of glucose fermenters 1 and 2. Note that ξ_1 is the predicted steady state glucose concentration determined by the biological parameters of glucose fermenter 1 and passage rate in the absence of glucose fermenter 2 and without thermodynamic control. $\eta_1 S_B^*$ is the shift to that steady state glucose concentration caused by thermodynamic control. Similarly, ξ_2 and $\eta_2 (S_A^*)^2$ are the corresponding terms for glucose fermenter 2. Note that $S_g^* = \xi_2 + \eta_2 (S_A^*)^2 > 0$. Glucose concentration can only be one value regardless of whether there is co-existence of glucose fermenters or not. If there is a co-existence of glucose fermenters, then

$$\xi_1 + \eta_1 S_B^* = S_g^* = \xi_2 + \eta_2 (S_A^*)^2 \ ,$$

or

$$S_g^*(1) = S_g^*(2) \ ,$$

is required. Because S_B is only generated by glucose fermenter 1 and S_A is only generated by glucose fermenter 2, if S_B^* and S_A^* are both positive there is a co-existence of glucose fermenters 1 and 2 in the long term (i.e., $X_1^* > 0$ and $X_2^* > 0$). Thus, we now need to determine under what conditions S_B^* and S_A^* are positive. Since

$$\xi_1 + \eta_1 S_B^* = S_g^* = \xi_2 + \eta_2 (S_A^*)^2 \ ,$$

S_B^* is given by

$$S_B^* = \frac{\xi_2 - \xi_1 + \eta_2 (S_A^*)^2}{\eta_1} \ .$$

Then, $S_B^* > 0$ if

$$\eta_2 (S_A^*)^2 > \xi_1 - \xi_2 \ . \tag{5.19}$$

Since

$$\eta_2(S_A^*)^2 + \xi_2 = S_g^* = \frac{\beta_g}{\alpha} - \frac{\gamma_B + \alpha}{\alpha}\left(\frac{\xi_2 - \xi_1 + \eta_2(S_A^*)^2}{\eta_1}\right) - \frac{\gamma_A + \alpha}{\alpha}S_A^* \ ,$$

this yields

$$\eta_2(S_A^*)^2\left(1 + \frac{\gamma_B + \alpha}{\alpha\eta_1}\right) + \frac{\gamma_A + \alpha}{\alpha}S_A^* + \frac{(\gamma_B + \alpha)(\xi_2 - \xi_1)}{\alpha\eta_1} + \xi_2 - \frac{\beta_g}{\alpha} = 0 \ .$$

Note that the quadratic and linear coefficients of S_A^* are positive. If $S_A^* > 0$, this requires

$$\frac{\beta_g}{\alpha} > \frac{(\gamma_B + \alpha)}{\alpha}\frac{(\xi_2 - \xi_1)}{\eta_1} + \xi_2 \ . \tag{5.20}$$

Expressions (5.19) and (5.20) can be satisfied with a range of values of α and β_g that lead to $X_1^* > 0$ and $X_2^* > 0$. Thus, this example illustrates that the inclusion of a thermodynamic term in the GHM model leads to the co-existence of two types of glucose fermenters for more than one value of passage rate, unlike what is predicted by the Monod specific growth rate model. The inclusion of end product concentrations in the specific growth rate has allowed for co-existence of fermenter populations competing for the same growth limiting substrate and competitive exclusion is no longer the only outcome.

Suppose $X_1^* = 0$, then we will explore what conditions lead to $X_2^* > 0$ and vice versa. With $X_2^* > 0$, $X_2' = 0$ the steady state glucose concentration is given by expression (5.18), i.e., $S_g^* = \xi_2 + \eta_2(S_A^*)^2 > 0$. From

$$\eta_2(S_A^*)^2 + \xi_2 = S_g^* = \frac{\beta_g}{\alpha} - \frac{\gamma_B + \alpha}{\alpha}S_B^* - \frac{\gamma_A + \alpha}{\alpha}S_A^* \ ,$$

this yields

$$\eta_2(S_A^*)^2 + \frac{\gamma_A + \alpha}{\alpha}S_A^* + \xi_2 - \frac{\beta_g}{\alpha} = 0 \ ,$$

because $X_1^* = 0$ so that $S_B^* = 0$. If $S_A^* > 0$ so that $X_2^* > 0$, this requires

$$\frac{\beta_g}{\alpha} > \xi_2 \ . \tag{5.21}$$

In a similar manner, when $X_1^* > 0$ and $X_2^* = 0$, the steady state glucose concentration is given by expression (5.17) and

$$(\eta_1 + \frac{\gamma_B + \alpha}{\alpha})S_B^* + \xi_1 - \frac{\beta_g}{\alpha} = 0 \ ,$$

because $X_2^* = 0$ so that $S_A^* = 0$. If $S_B^* > 0$ so that $X_1^* > 0$, this requires

$$\frac{\beta_g}{\alpha} > \xi_1 \ . \tag{5.22}$$

When expressions (5.19), (5.20), (5.21) and (5.22) are all not satisfied then the only possible scenario is where both types of glucose fermenters 1 and 2 are eliminated

$$(S_g^*, X_1^*, X_2^*, S_h^*, X_m^*, S_A^*, S_P^*, S_B^*) = (\beta_g/\alpha, 0, 0, 0, 0, 0, 0, 0) \ .$$

Note that glucose fermenters 1 and 2 can all be eliminated by increasing the passage rate so that $q_1 < \delta_1$ and $q_2 < \delta_2$. That is, the required substrate metabolism rate for a cell to survive is greater than its maximal substrate metabolism rate.

The stability of an equilibrium point is determined by the eigenvalues of the dynamical system of equations. For $(S_g^*, 0, X_2^*, S_h^*, X_m^*, S_A^*, S_P^*, S_B^*)$, $X_1' = 0$ $X_1^* = 0$ and $X_2^* > 0$, all the elements in the second row of the Jacobian matrix, J_2 (page 116), are zero except the diagonal element, $J_2(2,2)$.

The eigenvalue of a matrix is found by solving $\det(J_2 - \lambda I) = 0$. Thus, one eigenvalue of $(S_g^*, 0, X_2^*, S_h^*, X_m^*, S_A^*, S_P^*, S_B^*)$ is

$$\frac{Y_1 n_1 q_1 (S_g^* - (S_B^*)(S_h^*)^2 C_1)}{K_1 + S_g^* + (S_B^*)(S_h^*)^2 C_1} - Y_1 m_1 - \alpha \ ,$$

or

$$\frac{Y_1 n_1 q_1 S_g^* (1 - \theta_1^*)}{K_1 + S_g^* (1 + \theta_1^*)} - Y_1 m_1 - \alpha \ . \tag{5.23}$$

Because glucose fermenters 1 and 2 do not have exactly the same end products and $X_1^* = 0$ (i.e., there is no thermodynamic feedback from

the glucose fermentation pathway associated with X_1 so that $\theta_1^* = 0$), expression (5.23) becomes

$$\frac{Y_1 n_1 q_1 S_g^*}{K_1 + S_g^*} - Y_1 m_1 - \alpha \ .$$

If

$$\frac{Y_1 n_1 q_1 S_g^*}{K_1 + S_g^*} - Y_1 m_1 - \alpha > 0 \ ,$$

then one of the eigenvalues of $(S_g^*, 0, X_2^*, S_h^*, X_m^*, S_A^*, S_P^*, S_B^*)$ is positive and $(S_g^*, 0, X_2^*, S_h^*, X_m^*, S_A^*, S_P^*, S_B^*)$ is an unstable point. Thus,

$$\frac{Y_1 n_1 q_1 S_g^*}{K_1 + S_g^*} - Y_1 m_1 - \alpha < 0 \ , \tag{5.24}$$

is required for $(S_g^*, 0, X_2^*, S_h^*, X_m^*, S_A^*, S_P^*, S_B^*)$ to be a stable equilibrium point.

Solving expression (5.24) for S_g^* yields

$$S_g^* < \frac{K_1(Y_1 m_1 + \alpha)}{Y_1 n_1 q_1 - Y_1 m_1 - \alpha} \ .$$

From $X_2' = 0$ and $X_2^* > 0$, the positive steady state glucose concentration is given by

$$S_g^* = \frac{K_2(Y_2 m_2 + \alpha) + (Y_2 n_2 q_2 + Y_2 m_2 + \alpha)(S_A^*)(S_P^*)(S_h^*)C_2}{Y_2 n_2 q_2 - Y_2 m_2 - \alpha} = S_g^*(2) \ .$$

Thus,

$$\frac{K_2(Y_2 m_2 + \alpha) + (Y_2 n_2 q_2 + Y_2 m_2 + \alpha)(S_A^*)(S_P^*)(S_h^*)C_2}{Y_2 n_2 q_2 - Y_2 m_2 - \alpha} < \frac{K_1(Y_1 m_1 + \alpha)}{Y_1 n_1 q_1 - Y_1 m_1 - \alpha} \ , \tag{5.25}$$

is required for $(S_g^*, 0, X_2^*, S_h^*, X_m^*, S_A^*, S_P^*, S_B^*)$, where $X_2^* > 0$, to be stable.

Similarly, for the steady state equilibrium point where X_1 exists and X_2 is eliminated, i.e., $X_1^* > 0$ and $X_2^* = 0$, $(S_g^*, X_1^*, 0, S_h^*, X_m^*, S_A^*, S_P^*, S_B^*)$,

from the third equation of the GHM$^{\theta}$ model, one eigenvalue is

$$\frac{Y_2 n_2 q_2 S_g^*}{K_2 + S_g^*} - Y_2 m_2 - \alpha \ ,$$

and

$$S_g^* = \frac{K_1(Y_1 m_1 + \alpha) + (Y_1 n_1 q_1 + Y_1 m_1 + \alpha)(S_B^*)(S_h^*)^2 C_1}{Y_1 n_1 q_1 - Y_1 m_1 - \alpha} = S_g^*(1) \ .$$

Then,

$$\frac{K_1(Y_1 m_1 + \alpha) + (Y_1 n_1 q_1 + Y_1 m_1 + \alpha)(S_B^*)(S_h^*)^2 C_1}{Y_1 n_1 q_1 - Y_1 m_1 - \alpha} < \frac{K_2(Y_2 m_2 + \alpha)}{Y_2 n_2 q_2 - Y_2 m_2 - \alpha} \ , \tag{5.26}$$

is required for $(S_g^*, X_1^*, 0, S_h^*, X_m^*, S_A^*, S_P^*, S_B^*)$ to be stable.

$$
J_2 = \begin{bmatrix}
-\frac{g_1(K_1+2kS_2)(S_2)^2C_1)X_1}{(K_1+S_2+(kg_1)(S_2)^2C_1)^2} - \frac{g_2(K_2+2kS_1)(S_1)^2C_2)X_2}{(K_2+S_1+(kg_2)(S_1)^2C_2)^2} - \alpha & -\frac{g_1(S_1-(S_1)(S_2)(S_1)C_1)}{(K_1+S_2+(kg_1)(S_2)^2C_1)} & -\frac{g_2(S_2-(S_1)(S_2)(S_2)C_2)}{(K_2+S_1+(kg_2)(S_1)^2C_2)} & \frac{2g_1S_2S_1C_1(K_1+2S_1)X_1}{(K_1+S_2+(kg_1)(S_2)^2C_1)^2} + \frac{g_2(S_2)(S_2)C_2(K_2+2S_2)X_2}{(K_2+S_1+(kg_2)(S_1)^2C_2)^2} & 0 & \frac{g_1(S_2)(S_1)C_1(K_1+2S_1)X_1}{(K_1+S_2+(kg_1)(S_2)^2C_1)^2} & \frac{g_2(S_1)(S_2)C_2(K_2+2S_2)X_2}{(K_2+S_1+(kg_2)(S_1)^2C_2)^2} & \frac{g_1(S_2)^2C_1(K_1+2S_1)X_1}{(K_1+S_2+(kg_1)(S_2)^2C_1)^2} \\
\frac{Y_1n_1g_1(K_1+2S_2)(S_2)^2C_1)X_1}{(K_1+S_2+(kg_1)(S_2)^2C_1)^2} & \frac{Y_1n_1g_1(S_2-(S_2)(S_2)^2C_1)}{(K_1+S_2+(kg_1)(S_2)^2C_1)} - Y_1m_1 - \alpha & 0 & \frac{2Y_1n_1g_1S_2S_1C_1(K_1+2S_1)X_1}{(K_1+S_2+(kg_1)(S_2)^2C_1)^2} & 0 & 0 & 0 & \frac{Y_1n_1g_1(S_2)^2C_1(K_1+2S_1)X_1}{(K_1+S_2+(kg_1)(S_2)^2C_1)^2} \\
\frac{Y_2n_2g_2(K_2+2S_1)(S_1)^2C_2)X_2}{(K_2+S_1+(S_1)(S_2)(S_1)C_2)^2} & 0 & \frac{Y_2n_2g_2(S_1-(S_1)(S_2)(S_1)C_2)}{(K_2+S_1+(S_1)(S_2)(S_1)C_2)} - Y_2m_2 - \alpha & \frac{Y_2n_2g_2S_2S_1C_2(K_2+2S_2)X_2}{(K_2+S_1+(S_1)(S_2)(S_1)C_2)^2} & 0 & \frac{Y_2n_2g_2(S_2)(S_1)C_2(K_2+2S_2)X_2}{(K_2+S_1+(S_1)(S_2)(S_1)C_2)^2} & \frac{Y_2n_2g_2(S_1)(S_2)C_2(K_2+2S_2)X_2}{(K_2+S_1+(S_1)(S_2)(S_1)C_2)^2} & 0 \\
\frac{2g_1(K_1+2kS_2)(S_2)^2C_1)X_1}{(K_1+S_2+(kg_1)(S_2)^2C_1)^2} + \frac{g_2(K_2+2kS_1)(S_2)(S_1)C_2)X_2}{(K_2+S_1+(kg_2)(S_2)^2C_2)^2} & \frac{2g_1(S_2-(S_2)(S_2)^2C_1)}{(K_1+S_2+(kg_1)(S_2)^2C_1)} & \frac{g_2(S_2-(S_2)(S_2)(S_1)C_2)}{(K_2+S_1+(S_1)(S_2)(S_1)C_2)} & -\frac{g_{m1}(K_{m1}+2C_{m1})X_{m1}}{(K_{m1}+S_2+C_{m1})^2} - \alpha + \frac{2g_1S_2S_1C_1(K_1+2S_1)X_1}{(K_1+S_2+(kg_1)(S_2)^2C_1)^2} + \frac{g_2(S_2)(S_2)C_2(K_2+2S_2)X_2}{(K_2+S_1+(S_1)(S_2)(S_1)C_2)^2} & -\frac{g_{m1}(S_2-C_{m1})}{K_{m1}+S_2+C_{m1}} & 0 & \frac{g_1(S_2)(S_1)C_1(K_1+2S_1)X_1}{(K_1+S_2+(kg_1)(S_2)^2C_1)^2} & \frac{g_2(S_1)(S_2)C_2(K_2+2S_2)X_2}{(K_2+S_1+(kg_2)(S_1)^2C_2)^2} & \frac{2g_1(S_2)^2C_1(K_1+2S_1)X_1}{(K_1+S_2+(kg_1)(S_2)^2C_1)^2} \\
0 & 0 & 0 & \frac{Y_{m1}n_{m1}g_{m1}(K_{m1}+2C_{m1})X_{m1}}{(K_{m1}+S_2+C_{m1})^2} & \frac{Y_{m1}n_{m1}g_{m1}(S_2-C_{m1})}{K_{m1}+S_2+C_{m1}} - Y_{m}m_m - \alpha & 0 & 0 & 0 & 0 \\
\frac{g_1(K_1+2S_2)(S_2)(S_2)C_2)X_2}{(K_2+S_2+(S_2)(S_2)(S_2)C_2)^2} & 0 & \frac{g_2(S_2-(S_2)(S_2)(S_2)C_2)}{K_2+S_2+(S_2)(S_2)(S_2)K_2} & -\frac{g_2(S_2)(S_2)C_2(K_2+2S_2)X_2}{(K_2+S_2+(S_2)(S_2)(S_2)K_2)^2} & 0 & -\frac{g_2(S_2)(S_2)C_2(K_2+2S_2)X_2}{(K_2+S_2+(S_2)(S_2)(S_2)K_2)^2} - \gamma_A - \alpha & -\frac{g_2(S_2)(S_2)C_2(K_2+2S_2)X_2}{(K_2+S_2+(S_2)(S_2)(S_2)K_2)^2} & 0 \\
\frac{g_1(K_2+2S_2)(S_2)(S_2)C_2)X_2}{(K_2+S_2+(S_2)(S_2)(S_2)K_2)^2} & 0 & \frac{g_2(S_2-(S_2)(S_2)(S_2)C_2)}{K_2+S_2+(S_2)(S_2)(S_2)K_2} & -\frac{g_2(S_2)(S_2)C_2(K_2+2S_2)X_2}{(K_2+S_2+(S_2)(S_2)(S_2)K_2)^2} & 0 & -\frac{g_2(S_2)(S_2)C_2(K_2+2S_2)X_2}{(K_2+S_2+(S_2)(S_2)(S_2)K_2)^2} - \gamma_P - \alpha & -\frac{g_2(S_2)(S_2)C_2(K_2+2S_2)X_2}{(K_2+S_2+(S_2)(S_2)(S_2)K_2)^2} & 0 \\
\frac{g_1(K_1+2kS_2)(S_2)^2C_1)X_1}{(K_1+S_2+(kg_1)(S_2)^2C_1)^2} & 0 & \frac{g_2(S_2-(S_2)(S_2)^2C_1)}{K_1+S_2+(kg_1)(S_2)^2C_1} & -\frac{g_1S_2S_1C_1(K_1+2S_1)X_1}{(K_1+S_2+(kg_1)(S_2)^2C_1)^2} & 0 & 0 & 0 & -\frac{g_1(S_2)^2C_1(K_1+2S_1)X_1}{(K_1+S_2+(kg_1)(S_2)^2C_1)^2} - \gamma_B - \alpha
\end{bmatrix}
$$

For $X_1^* > 0$ and $X_2^* > 0$

$$\xi_1 + \eta_1 S_B^* = S_g^* = \xi_2 + \eta_2 (S_A^*)^2 \ , \tag{5.27}$$

is required. At the steady state, expressions (5.25) and (5.26) become

$$\begin{aligned} \xi_2 + \eta_2 (S_A^*)^2 &< \xi_1 \ , \\ \xi_1 + \eta_1 S_B^* &< \xi_2 \ . \end{aligned}$$

Recall that η_1, ξ_1, η_2, ξ_2, S_A^* and S_B^* are all positive. Therefore

$$\begin{aligned} 0 < &\xi_2 + \eta_2 (S_A^*)^2 < \xi_1 + \eta_1 S_B^* \ , \\ 0 < &\xi_1 + \eta_1 S_B^* < \xi_2 + \eta_2 (S_A^*)^2 \ , \end{aligned}$$

or

$$0 < S_g^*(2) < S_g^*(1) \ , \tag{5.28}$$

$$0 < S_g^*(1) < S_g^*(2) \ . \tag{5.29}$$

Expressions (5.28) and (5.29) are, respectively, mutually exclusive with each other and expression (5.27). Therefore, exactly one of $(S_g^*, X_1^*, X_2^*, S_h^*, X_m^*, S_A^*, S_P^*, S_B^*)$ where $X_1^* > 0$ and $X_2^* > 0$, $(S_g^*, 0, X_2^*, S_h^*, X_m^*, S_A^*, S_P^*, S_B^*)$ where $X_2^* > 0$ or $(S_g^*, X_1^*, 0, S_h^*, X_m^*, S_A^*, S_P^*, S_B^*)$ where $X_1^* > 0$ is stable.

As shown, the stability of $(S_g^*, X_1^*, X_2^*, S_h^*, X_m^*, S_A^*, S_P^*, S_B^*)$, $(S_g^*, 0, X_2^*, S_h^*, X_m^*, S_A^*, S_P^*, S_B^*)$ or $(S_g^*, X_1^*, 0, S_h^*, X_m^*, S_A^*, S_P^*, S_B^*)$ is determined by comparing $S_g^*(1)$ and $S_g^*(2)$. Recall that there are two components for each of $S_g^*(1)$ and $S_g^*(2)$: the steady state glucose concentrations found by solving the systems without thermodynamic control, ξ_1 and ξ_2, and the shift to that steady state glucose concentration caused by thermodynamic control, $\eta_1 S_B^*$ and $\eta_2 (S_A^*)^2$. If there is no thermodynamic term, i.e., $\eta_2 (S_A^*)^2 = \eta_2 S_B^* = 0$, then this yields the same analytical result of Hsu [64]: the glucose fermenter with the lowest positive predicted steady state glucose concentration will outcompete the other one. In this case, there

is a co-existence of two types of glucose fermenters 1 and 2 if $\xi_1 = \xi_2$

$$\frac{K_1(Y_1 m_1 + \alpha)}{Y_1 n_1 q_1 - Y_1 m_1 - \alpha} = \frac{K_2(Y_2 m_2 + \alpha)}{Y_2 n_2 q_2 - Y_2 m_2 - \alpha} \ .$$

Equivalently, for the same set of biological parameters, there is exactly one positive passage rate that allows co-existence (same as the conclusion from Hsu *et al.* [63]). If $S_g^*(1) < 0$, then $X_1^* = 0$ because glucose fermenters 1 cannot reproduce fast enough to match up with the passage rate and/or $\theta_1^* = 1$. Similarly, if $S_g^*(2) < 0$, then $X_2^* = 0$. For a co-existence of glucose fermenters,

$$0 < S_g^*(1) = S_g^*(2) \ , \tag{5.30}$$

is required. By including a thermodynamic term, there is a range of positive passage rates (and biological and ruminal parameters) that allow stable co-existence of glucose fermenters 1 and 2. This is achieved because

$$\xi_1 + \eta_1 S_B^* = S_g^* = \xi_2 + \eta_2 (S_A^*)^2 \ ,$$

can be satisfied with infinitely many combinations of $\xi_1 + \eta_1 S_B^*$ and $\xi_2 + \eta_2 (S_A^*)^2$. When this is satisfied, there is a stable co-existence. Großkopf and Soyer [51] reported co-existence of two types of microbes metabolizing the same single substrate that yield different end products without classifying the stability of such co-existence. In contrast, there is a stable co-existence of two types of glucose fermenters that are competing for the same substrate and sharing at least one common end product (S_h) from different fermentation pathways, as predicted by the GHM$^\theta$ model for a range of biological and ruminal parameters.

Figure 5.7 indicates the region of stability for each of the four possible steady state solutions.

1. $X_1^* = 0$ and $X_2^* = 0$,
2. $X_1^* = 0$ and $X_2^* > 0$,
3. $X_1^* > 0$ and $X_2^* = 0$,

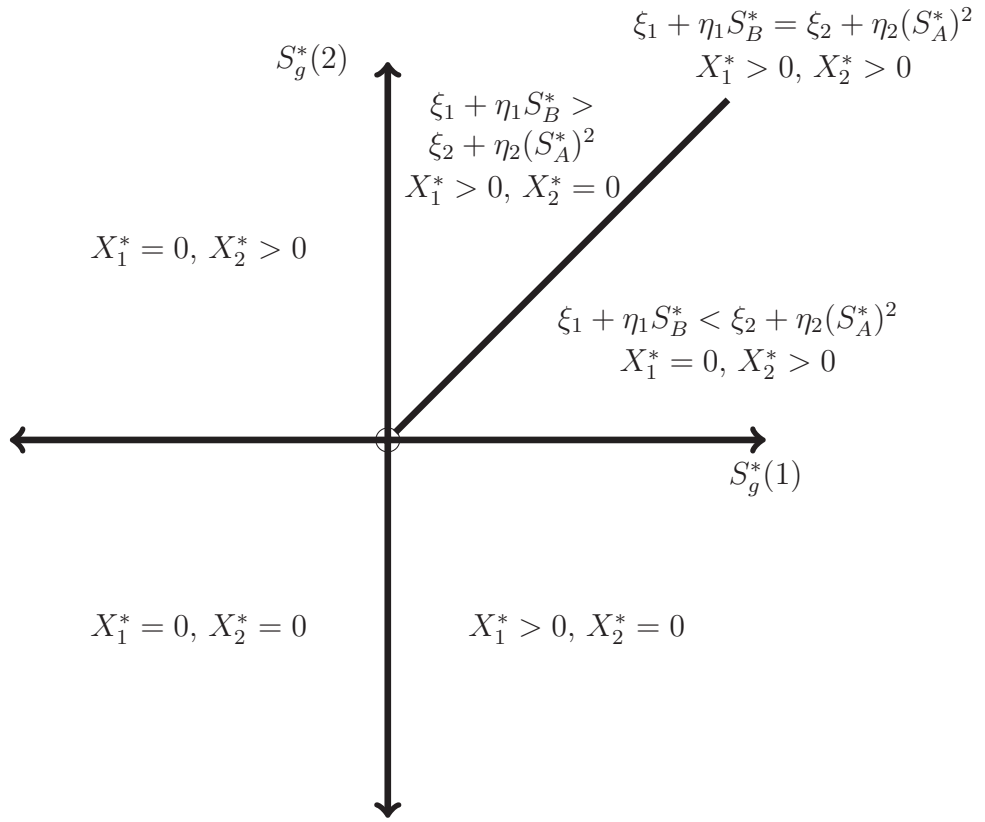

Figure 5.7: Regions of stable survival of glucose fermenter 1 or 2 or both. Note that $S_g^*(1) = \xi_1 + \eta_1 S_B^*$ and $S_g^*(2) = \xi_2 + \eta_2 (S_A^*)^2$.

4. $X_1^* > 0$ and $X_2^* > 0$.

In the first quadrant of the Figure 5.7, any point on the diagonal except the origin is where the steady state glucose concentration, as predicted by the biological parameters of both types of glucose fermenters 1 and 2 and the rumen environment, are the same and positive. That is, this diagonal line is where there is a stable co-existence of two types of glucose fermenters (i.e., $X_1^* > 0$ and $X_2^* > 0$). Above this line is the region where only glucose fermenter 1 will survive (i.e., $X_1^* > 0$ and $X_2^* = 0$). Below this line is where only glucose fermenter 2 will survive (i.e., $X_1^* = 0$ and $X_2^* > 0$). With insufficient glucose supply, both types of glucose fermenters will be unable to reproduce and maintain themselves in the rumen at a rate that prevents them from being eliminated due to

passage, equivalently $S_g^*(1) < 0$ and $S_g^*(2) < 0$. If $\theta_1^* = 1$ and $\theta_2^* = 1$, $S_g^*(1) < 0$ by equation (5.9) and $S_g^*(2) < 0$ by equation (5.10). In either of these cases, the only stable steady state scenario is $(\beta_g/\alpha, 0, 0, 0, 0, 0, 0, 0)$, i.e., the third quadrant of Figure 5.7. If $S_g^*(1) < 0$ and $S_g^*(2) > 0$ (the second quadrant), then $X_1^* = 0$ and $X_2^* > 0$. In this case glucose fermenter 1 cannot reproduce at a rate fast enough to maintain itself in the rumen so that it is eliminated due to passage, and/or $\theta_1^* = 1$. Similarly, If $S_g^*(1) > 0$ and $S_g^*(2) < 0$ (the fourth quadrant), then $X_1^* = 0$ and $X_2^* > 0$.

In summary, there are four physically meaningful steady state equilibrium points in the GHM$^\theta$ model with two types of glucose fermenters. Given any combination of biological (n, q, K, m, d and Y) and ruminal (α, β_g, γ_A, γ_P and γ_B) parameter values, there is exactly one stable equilibrium point, $(S_g^*, X_1^*, X_2^*, S_h^*, X_m^*, S_A^*, S_P^*, S_B^*)$. Which of the four points is stable is determined by comparison of $S_g^*(1)$ and $S_g^*(2)$.

1. $X_1^* = 0$ and $X_2^* = 0$,
   if $S_g^*(1) < 0$ and $S_g^*(2) < 0$ (both are washed out) ;

2. $X_1^* = 0$ and $X_2^* > 0$,
   if $S_g^*(1) < 0$ and $S_g^*(2) > 0$ (X_1 is washed out) or
   if $0 < S_g^*(2) < S_g^*(1)$ (X_2 outcompetes X_1) ;

3. $X_1^* > 0$ and $X_2^* = 0$,
   if $S_g^*(1) > 0$ and $S_g^*(2) < 0$ (X_2 is washed out) or
   if $0 < S_g^*(1) < S_g^*(2)$ (X_1 outcompetes X_2) ;

4. $X_1^* > 0$ and $X_2^* > 0$, if $0 < S_g^*(1) = S_g^*(2)$.

5.3.2 Simulation

The stability of co-existence of two types of glucose fermenters 1 and 2 and methanogens can also be explored numerically. For simplicity, we let the biological parameters of both types of glucose fermenters 1 and 2 be the same in the rest of this Section 5.2, i.e., $m_1 = m_2$,

$q_1 = q_2$, $Y_1 = Y_2$, $K_1 = K_2$, $n_1 = n_2$. Then, $\xi_1 = \xi_2$ so that expressions (5.20), (5.21) and (5.22) are the same. This implies that the minimum value of β_g/α required for each of (a) co-existence, (b) X_2 to survive without X_1, and (c) X_1 to survive without X_2, is equivalent. With $\xi_1 = \xi_2$, expression (5.20) must be satisfied for either or both types of glucose fermenters to survive in the long term. With a typical passage rate $\alpha = 3.5 \times 10^{-5}$ s^{-1}, and other typical values given in Section 5.2.2, expression (5.20) is satisfied when $\beta_g > 3.970 \times 10^{-15}$ mol ml^{-1} s^{-1}. For $\beta_g \leq 3.970 \times 10^{-15}$ mol ml^{-1} s^{-1}, the only stable point is $(\beta_g/\alpha, 0, 0, 0, 0, 0, 0, 0)$. A typical glucose generation rate in the rumen is about 1×10^{-9} mol ml^{-1} s^{-1} (Section 5.2.2). Hence, with realistic parameters values and passage rate, $(\beta_g/\alpha, 0, 0, 0, 0, 0, 0, 0)$ is always unstable.

The absorption rates of acetate and propionate are respectively [32]

$$\gamma_A = 9.20 \times 10^{-7} \text{ s}^{-1} ,$$
$$\gamma_P = 1.40 \times 10^{-6} \text{ s}^{-1} .$$

It is assumed that all types of glucose fermenters need the same amount of energy to gain one unit of ATP, i.e., $\Delta G_{ATP} = 75$ kJ mol$^{-1}_{ATP}$. Note that X_1 and X_2 are distinguished by

$$\Delta G^o_{T_1} = -198.306 \text{ kJ mol}^{-1} \text{ [21]} ,$$
$$\Delta G^o_{T_2} = -187.516 \text{ kJ mol}^{-1} \text{ [21]} ,$$

values that are associated with their glucose fermentation pathways. Other parameter values used in this section can be found in Tables 2.1 and 3.1 and Section 5.2.2.

Note that S^*_h can be evaluated numerically using equation (5.16) and Tables 2.1 and 3.1. Because the glucose concentration can only be one value, i.e., $S^*_g(1) = S^*_g(2)$, from equations (5.17) and (5.18)

$$(S^*_B)(S^*_h)C_1 = (S^*_A)(S^*_P)C_2 .$$

Substituting in for S_P^*, equation (5.13), and rearranging, we find

$$S_A^* = \sqrt{\frac{(S_B^*)(S_h^*)C_1(\gamma_P + \alpha)}{C_2(\gamma_A + \alpha)}} \ . \tag{5.31}$$

By substituting expressions (5.17) and (5.31) into expression (5.14), S_B^* can be found, and then S_g^*, S_A^*, S_P^*, X_1^*, X_2^* and X_m^* can be evaluated numerically using equations (5.17), (5.31), (5.13), (5.11), (5.12) and (5.15)

With $\xi_1 = \xi_2$, the same values of $\alpha = 3.5 \times 10^{-5}$ s^{-1} and $\beta_g = 1.930 \times 10^{-9}$ mol ml^{-1} s^{-1} and other typical parameter values used in Section 5.2.4, expression (5.20) is satisfied. Thus, there are three long term possible scenarios under this rumen environment:

$$\begin{aligned}
&(S_g^*, X_1^*, X_2^*, S_h^*, X_m^*, S_A^*, S_P^*, S_B^*) = \\
&(1.134 \times 10^{-10} \text{ mol ml}^{-1},\ 7.068 \times 10^{9} \text{ cell ml}^{-1},\ 0.998 \times 10^{9} \text{ cell ml}^{-1}, \\
&3.215 \times 10^{-10} \text{ mol ml}^{-1},\ 0.270 \times 10^{9} \text{ cell ml}^{-1}, \\
&0.665 \times 10^{-5} \text{ mol ml}^{-1},\ 0.656 \times 10^{-6} \text{ mol ml}^{-1},\ 4.658 \times 10^{-5} \text{ mol ml}^{-1}) \ .
\end{aligned}$$

The corresponding eigenvalues of the Jacobian matrix, J_2 (page 116), are

$$\begin{aligned}
&-10.9,\ -0.263 \times 10^{-20},\ -3.84 \times 10^{-5},\ -10.6,\ -3.81 \times 10^{-5}, \\
&\qquad -3.59 \times 10^{-5},\ -3.64 \times 10^{-5},\ -3.63 \times 10^{-5} \ .
\end{aligned}$$

Thus, $(S_g^*, X_1^*, X_2^*, S_h^*, X_m^*, S_A^*, S_P^*, S_B^*)$ is a stable point because the real part of these eigenvalues are all negative.

$$\begin{aligned}
&(S_g^*, 0, X_2^*, S_h^*, X_m^*, S_A^*, S_P^*, S_B^*) = \\
&(1.134 \times 10^{-10} \text{ mol ml}^{-1},\ 0,\ 8.067 \times 10^{9} \text{ cell ml}^{-1}, \\
&3.215 \times 10^{-10} \text{ mol ml}^{-1},\ 0.144 \times 10^{9} \text{ cell ml}^{-1}, \\
&5.373 \times 10^{-5} \text{ mol ml}^{-1},\ 5.302 \times 10^{-5} \text{ mol ml}^{-1},\ 0) \ ,
\end{aligned}$$

and the corresponding eigenvalues of the Jacobian matrix are

$$\begin{aligned}
&-5.62,\ -3.84 \times 10^{-5},\ 6.46 \times 10^{-20},\ -10.9,\ -3.81 \times 10^{-5}, \\
\end{aligned}$$

$$-3.59 \times 10^{-5},\ -3.64 \times 10^{-5},\ -3.63 \times 10^{-5}\ .$$

Thus, $(S_g^*, 0, X_2^*, S_h^*, X_m^*, S_A^*, S_P^*, S_B^*)$ is an unstable point because one of the eigenvalues has a positive real part. Also,

$$\begin{aligned}&(S_g^*, X_1^*, 0, S_h^*, X_m^*, S_A^*, S_P^*, S_B^*) = \\ &(1.134 \times 10^{-10} \text{ mol ml}^{-1},\ 8.067 \times 10^{9} \text{ cell ml}^{-1},\ 0,\\ &3.215 \times 10^{-10} \text{ mol ml}^{-1},\ 0.288 \times 10^{9} \text{ cell ml}^{-1},\\ &0,\ 0,\ 5.316 \times 10^{-5} \text{ mol ml}^{-1})\ ,\end{aligned}$$

and the corresponding eigenvalues of the Jacobian matrix of the model are

$$\begin{aligned}-10.9,\ 0.0380 \times 10^{-20},\ -3.84 \times 10^{-5}\ , -11.2,\ -3.81 \times 10^{-5},\\ -3.59 \times 10^{-5},\ -3.64 \times 10^{-5},\ -3.63 \times 10^{-5}\ .\end{aligned}$$

Thus, $(S_g^*, X_1^*, 0, S_h^*, X_m^*, S_A^*, S_P^*, S_B^*)$ is an unstable point because one of the eigenvalues has a positive real part.

In equilibrium point $(S_g^*, X_1^*, X_2^*, S_h^*, X_m^*, S_A^*, S_P^*, S_B^*)$, $X_1^* > X_2^*$ and X_1^* is associated with a smaller eigenvalue than that of X_2^*. That is, the glucose fermenter population 1 will converge towards its corresponding steady state value slowly as compared to the glucose fermenter population 2. This observations is the same for points $(S_g^*, 0, X_2^*, S_h^*, X_m^*, S_A^*, S_P^*, S_B^*)$ and $(S_g^*, X_1^*, 0, S_h^*, X_m^*, S_A^*, S_P^*, S_B^*)$.

Note that the eigenvalues associated with S_h^* are six orders of magnitude greater than those associated with X_m^*, S_A^*, S_P^* and S_B^* indicating that the glucose and hydrogen concentration will converge towards their corresponding steady state values relatively quickly compared to the methanogens, acetate, propionate and butyrate concentration. Suppose the initial value, $(S_g, X_1, X_2, S_h, X_m, S_A, S_P, S_B)$, is in the neighborhood of $(S_g^*, X_1^*, X_2^*, S_h^*, X_m^*, S_A^*, S_P^*, S_B^*)$ such that the order of X_1 and X_2 is of the same magnitude as X_1^* and X_2^*, i.e., 1×10^9 cell ml^{-1}, and the order of X_m is of the same magnitude as X_m^*, i.e., 1×10^8 cell ml^{-1}. Using the typical parameter values, from equation (5.7), the metabolism of S_h by

methanogens, is given by

$$-\frac{q_m(S_h - C_m)}{K_m + S_h + C_m} X_m \ ,$$

and is of the magnitude of (1×10^{-9} mol ml^{-1}). The magnitude of the hydrogen generation rate from glucose fermentation pathway is 1×10^{-9} mol ml^{-1} s^{-1} which is ten times greater than the magnitude of S_h^*. Then, in one second, the rate of change in hydrogen concentration, S_h', is about the same magnitude as S_h^*. Similarly, from equation (5.8), the change in the methanogen population is of magnitude as 1×10^{-5} s^{-1}. Because the rate of change in hydrogen concentration is relatively quick (10^5 faster) as compared to that of the methanogens, the hydrogen concentration will converge towards its corresponding steady state value relatively quickly as compared to the methanogens. This difference in the rates of change is also shown in the difference in magnitudes of their corresponding eigenvalues.

Similar to the GHM$^\theta$ model with one type of glucose fermenter (Section 5.2.3),

$$\begin{aligned} -(\gamma_A + \alpha) &= -3.592 \times 10^{-5} \ , \\ -(\gamma_P + \alpha) &= -3.640 \times 10^{-5} \ , \\ -(\gamma_B + \alpha) &= -3.630 \times 10^{-5} \ , \end{aligned}$$

are, respectively, in the equations for S_A', S_P' and S_B' of the GHM$^\theta$ model with two types of glucose fermenter, and dominate the eigenvalues associated with these variables. For example, the rate of change in butyrate concentration is determined by the term $-(\gamma_B + \alpha)$ so that in one second, the rate of change in butyrate concentration, S_B', is about 10^{-10} which is five orders of magnitude smaller than the magnitude of the steady state butyrate concentration, S_B^*. Similar differences hold for acetate and propionate rates of change and concentration. Thus, the acetate, propionate and butyrate concentration will converge towards their corresponding steady state values relatively slowly (10^5 slower) as compared to the hydrogen concentration.

From equation (5.6), the metabolism of S_g by either or both types of glucose fermenters is of the same magnitude as S_g^* (1×10^{-10} mol ml^{-1}). The magnitude of β_g is 1×10^{-9} mol ml^{-1} s^{-1} which is ten times greater than the magnitude of S_g^*. Similarly to hydrogen concentration, in one second, the rate of change in glucose concentration is about the same magnitude as S_g^*. That is, the glucose concentration will converge towards its corresponding steady state value at about the same rate as compared to the hydrogen concentration so that there is no difference in magnitudes of their corresponding eigenvalues. Unlike glucose and hydrogen, all of acetate, propionate and butyrate are end products that are not metabolized by other microbes so that the rate of change in acetate, propionate and butyrate concentrations are similar to that of the glucose fermenters and methanogens that are also not consumed by other microbes in the GHM$^\theta$ model. By changing biological and ruminal parameters, this could leads to a new $(S_g^*, X_1^*, X_2^*, S_h^*, X_m^*, S_A^*, S_P^*, S_B^*)$ and the glucose and hydrogen concentration will also converge towards their new corresponding steady state values relatively quickly as compared to the other variables. That is, by changing parameters, glucose and hydrogen concentration will response more quickly as compared to the other variables.

Recall that η_1, ξ_1, η_2, ξ_2, S_A^* and S_B^* are all positive. Also, we have assumed that the biological parameters of the two types of glucose fermenters are the same which gives $\xi_1 = \xi_2$. Then if $\alpha = 3.5 \times 10^{-5}$ s^{-1} and $\beta_g = 1.930 \times 10^{-9}$ mol ml^{-1} s^{-1}, there are four possible steady state solutions: $(S_g^*, 0, 0, S_h^*, X_m^*, S_A^*, S_P^*, S_B^*)$, $(S_g^*, X_1^*, X_2^*, S_h^*, X_m^*, S_A^*, S_P^*, S_B^*)$, $(S_g^*, 0, X_2^*, S_h^*, X_m^*, S_A^*, S_P^*, S_B^*)$ and $(S_g^*, X_1^*, 0, S_h^*, X_m^*, S_A^*, S_P^*, S_B^*)$. At the beginning of this section we determined that the trivial solution is always unstable. It remains to determine the stability of the other three steady state solutions. Because $\xi_1 = \xi_2$, the inequalities

$$\xi_2 + \eta_2 (S_A^*)^2 < \xi_1 \ ,$$
$$\xi_1 + \eta_1 S_B^* < \xi_2 \ ,$$

cannot both be satisfied so that expressions (5.28) and (5.29) cannot both

be satisfied. Therefore, the equilibrium points $(S_g^*, 0, X_2^*, S_h^*, X_m^*, S_A^*, S_P^*, S_B^*)$ and $(S_g^*, X_1^*, 0, S_h^*, X_m^*, S_A^*, S_P^*, S_B^*)$ are both unstable. Then there must be a stable co-existence of two types of glucose fermenters 1 and 2, i.e., $(S_g^*, X_1^*, X_2^*, S_h^*, X_m^*, S_A^*, S_P^*, S_B^*)$ with $X_1^* > 0$ and $X_2^* > 0$ is a stable steady state under the given assumptions. Note also that the simulation values for $S_g^* = S_g^*(1) = S_g^*(2) = 1.134 \times 10^{-10}$ mol ml^{-1} which is a confirmation that there is a stable co-existence of glucose fermenters 1 and 2 as expected from the analytical results (see equation (5.30)). The magnitudes of X_1^* and X_2^* are near the observed microbe densities in the rumen [70], when using $\beta_g = 1.930 \times 10^{-9}$ mol ml^{-1} s^{-1} that is calculated from a theoretical glucose fermentation based on measured product formation in the rumen [181], [182]. We have assumed that the biological parameters of the two types of glucose fermenters are the same which gives $\xi_1 = \xi_2$. With $\beta_g = 1.930 \times 10^{-9}$ mol ml^{-1} s^{-1} and a typical range of passage rate values $1 \times 10^{-5} \leq \alpha \leq 5 \times 10^{-5}$ s^{-1} [150], [152], it can be shown numerically that $(S_g^*, X_1^*, X_2^*, S_h^*, X_m^*, S_A^*, S_P^*, S_B^*)$ with $X_1^* > 0$ and $X_2^* > 0$ is a node because its eigenvalues have no imaginary part and the real part of the eigenvalues are all negative.

The effect of a feed and/or passage rate change in the rumen environment on the population densities of X_1 and X_2 is explored numerically through simulations with different combinations of β_g and α. Ruminants keep ingesting feed so that the passage rate is never zero. A typical range of passage rate values, $1 \times 10^{-5} \leq \alpha \leq 5 \times 10^{-5}$ s^{-1} [150], [152] is explored. As shown in the above example, if $\beta_g = 1.930 \times 10^{-9}$ mol ml^{-1} s^{-1}, this leads to glucose fermenter 1 becoming the dominant microbe. A range of values of glucose generation rates is then used to examine whether glucose fermenter 2 can dominate. Glucose generation rates that allow fermenters 2 to dominate are lower that 2×10^{-9} mol ml^{-1} s^{-1} but expression (5.20) is satisfied. Figure 5.8 illustrates the simulation result.

Figure 5.8 indicates that increasing the passage rate reduces the proportion of X_1^*. Importantly, over these realistic ranges of α and β_g, there is a stable co-existence of both types of glucose fermenters and methanogens. Remember that the other rumen environment parameters and the biological parameters of the microbes were obtained from the

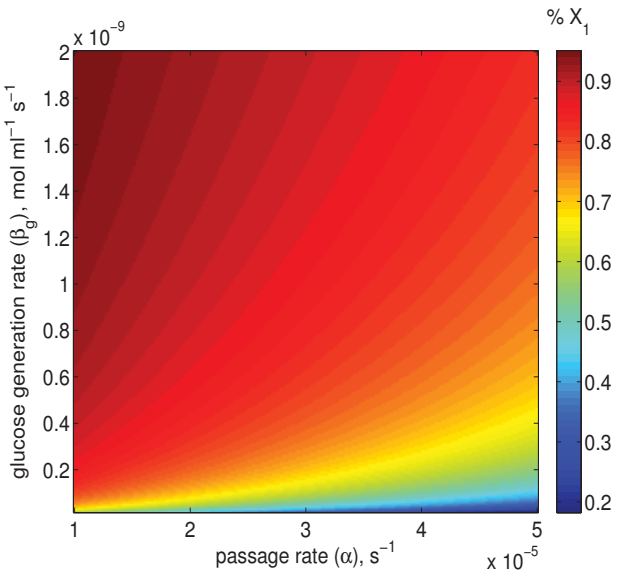

Figure 5.8: Proportion of X_1^* to total glucose fermenter population ($X_1^* + X_2^*$) with different combinations of β_g and α.

literature and not fitted to yield co-existence.

Increasing the passage rate reduces the proportion of X_1 (Figure 5.8). Equivalently, the fermentation pathways are shifted from the pathway associated with glucose fermenter 1

$$\text{glucose} \rightarrow B + 2\ \text{H}_2 + 2\ \text{CO}_2 + \text{H}^+\ , \tag{5.32}$$

to the pathway associated with glucose fermenter 2

$$\text{glucose} \rightarrow A + P + \text{H}_2 + \text{CO}_2 + 2\ \text{H}^+\ . \tag{5.33}$$

For the same amount of glucose fermented (β_g), this shift in fermentation leads to a greater propionate production, i.e., an increase in the proportion of the steady state propionate concentration to the total volatile fatty acids concentrations (Figure 5.9). This observation meets with the conceptual model presented by Janssen [76] and a chemostat experiment conducted by Isaacson *et al.* [72].

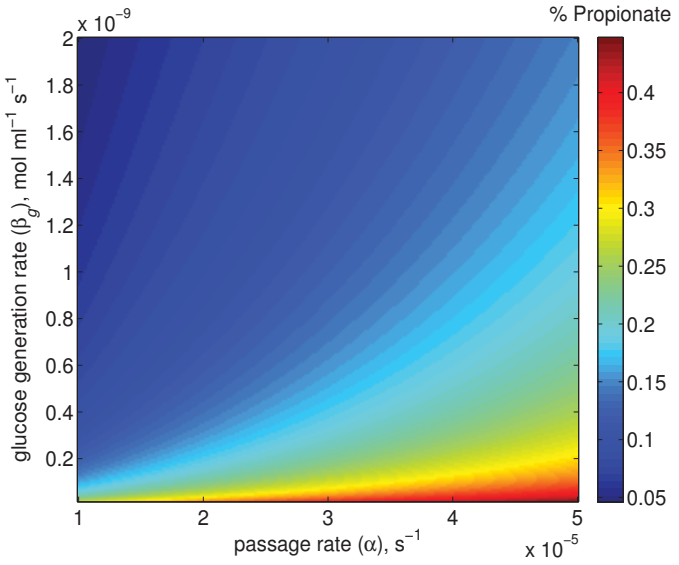

Figure 5.9: Proportion of the steady state propionate concentration (S_P^*) to the total volatile fatty acids concentrations ($S_A^* + S_B^* + S_P^*$) with different combinations of β_g and α.

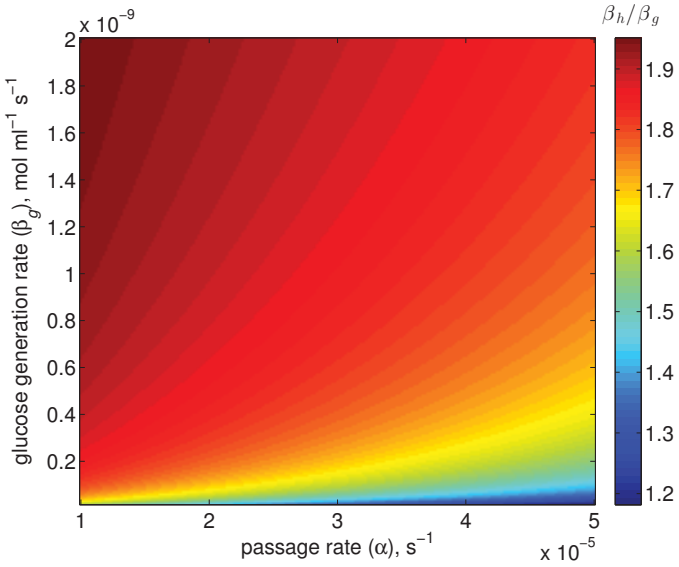

Figure 5.10: Mole of hydrogen generated per mole of glucose generated with different combinations of β_g and α.

From pathway (5.32), each mole of glucose is converted into two moles of hydrogen by glucose fermenter X_1. At small values of passage rate,

there is an abundance of X_1 (Figure 5.8) and $\beta_h/\beta_g \approx 2$. For instance, in Figure 5.10, with $\beta_g = 2 \times 10^{-9}$ mol ml^{-1} s^{-1} and $\alpha = 1 \times 10^{-5}$ s^{-1}, the corresponding β_h/β_g is

$$\begin{aligned}\frac{\beta_h}{\beta_g} &= \frac{2X_1^* + X_2^*}{\beta_g} \\ &= 2 \times 0.95 + 1 \times 0.05 \\ &= 1.95 \ .\end{aligned}$$

A greater passage rate is associated with a greater hydrogen concentration. Increasing the passage rate causes a decrease in X_1 (Figure 5.8) and a shift in glucose fermentation pathways from pathway (5.32) to pathway (5.33) due to the thermodynamic feedbacks imposed by the hydrogen concentration (and other end products). This leads to a reduced net hydrogen-formation (reduce β_h) and hence less estimated methane production [76] because methane production is most sensitive to the amount of hydrogen generated from fermentation [68]. That is, in the GHM$^\theta$ model, methane production (measured by β_h/β_g as illustrated in Figure 5.10) is reduced by increasing passage rate values. This observation meets with the conceptual model presented by Janssen [76] and a chemostat experiment conducted by Isaacson *et al.* [72].

Recall from the HM model where no glucose fermentation pathways are included: with $\beta_h = 4.70 \times 10^{-9}$ mol ml^{-1} s^{-1} ($\beta_g = 1.930 \times 10^{-9}$ mol ml^{-1} s^{-1} equivalent), at double of $\alpha = 3.5 \times 10^{-5}$ s^{-1}, estimated methane production is reduced by 0.0016%. However, given the same $\beta_g = 1.930 \times 10^{-9}$ mol ml^{-1} s^{-1}, from Figure 5.10, by increasing passage rate from $\alpha = 3.5 \times 10^{-5}$ s^{-1} to $\alpha = 5 \times 10^{-5}$ s^{-1}, β_h/β_g reduces from 1.9232 to 1.8684 (≈ 2.74 % reduction in estimated methane production). This reduction of estimated methane production from the GHM$^\theta$ model is greater than that of the HM model. A greater passage rate is associated with an increasing dissolved hydrogen concentrations in the rumen, which in turn is expected to feed back on hydrogen-forming steps to result in less net hydrogen formation and methane production (i.e., hydrogen production becomes less favorable [76]). Thus, passage rate indirectly

affects methane production by directly affecting the amount of hydrogen generated from glucose fermentation pathways. By increasing the passage rate, this also reduces the population densities of X_1 and X_2 that further reduces the hydrogen generation rate and estimated methane production. With an increasing passage rate (sheep with smaller rumens), the observed reduction in methane production from animal experiment [132] was about 11%. Such differences in methane production from animal experiments are greater than this simulation example ($\approx$ 2.74 % reduction in methane production). However, if more types of glucose fermenters and glucose fermentation pathways were to be introduced, greater effects of α and β_g on the methane formation could be achieved so that the GHM$^{\theta}$ model could potentially approximate realistic rumen function. This remains to be verified in the future work.

Next we will explore the steady state changes of glucose fermenters and methanogens population densities (Figure 5.11), volatile fatty acids (VFA) concentrations (Figure 5.12) and β_h/β_g ratio (Figure 5.13), over a range of passage rate values ($0 < \alpha \leq 1.2\times10^{-4}$ s^{-1}) at three specific values of glucose generation rate ($\beta_g = 1.930 \times 10^{-9}$, 1×10^{-9} mol ml^{-1} s^{-1} and 0.5×10^{-9} mol ml^{-1} s^{-1}). Because there is a co-existence of glucose fermenters 1 and 2 so that $S_g^* = S_g^*(1) = S_g^*(2)$, i.e., the steady state glucose and hydrogen concentrations over this range of passage rate values for both glucose generation rates is the same as in Section 5.2.4 (Figure 5.4). Because the Monod model [115] is used in the GHM$^{\theta}$ model to describe the rate of substrate (glucose and hydrogen) metabolism at a given substrate concentration, the steady state glucose and hydrogen concentrations are independent of the ruminal glucose and hydrogen generation rate (section 2.4). That is, the steady state glucose and hydrogen concentrations are determined by the biological parameters associated with glucose fermenters and methanogens and passage rate. Each value of passage rate is associated with one value of steady state substrate concentration regardless how many types of glucose fermenters co-exist in the rumen.

Note that the biological parameters of both types of glucose fermenters 1 and 2 have been assumed to be the same, and are the same

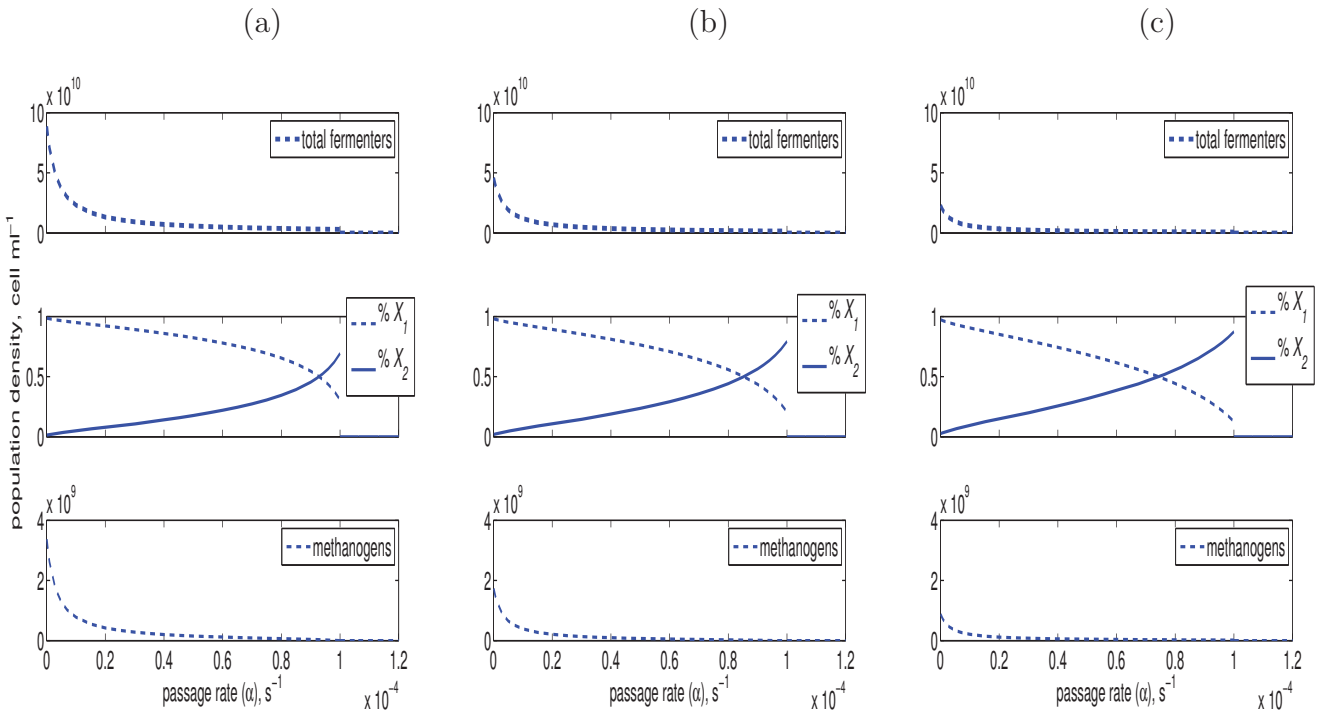

Figure 5.11: The stable steady state population densities of two types of glucose fermenters and methanogens for a constant β_g and a range of passage rate values. (a) $\beta_g = 1.930 \times 10^{-9}$ mol ml^{-1} s^{-1}. (b) $\beta_g = 1 \times 10^{-9}$ mol ml^{-1} s^{-1}. (c) $\beta_g = 0.5 \times 10^{-9}$ mol ml^{-1} s^{-1}. A bifurcation occurs in all cases when $\alpha = 1.026 \times 10^{-4}$ s^{-1} after which the stable steady state changes from co-existence of both glucose fermenter populations and methanogens to the trivial solution.

as presented in Figure 5.3. In Figure 5.11, we can see that increasing the passage rate beyond $\alpha = 1.026 \times 10^{-4}$ s^{-1} $= Y_1(n_1q_1 - m_1) = Y_2(n_2q_2 - m_2)$, eliminates both types of glucose fermenters as they cannot reproduce fast enough to match the passage rate, which in turn eliminates methanogens due to no hydrogen being produced from fermentation. This is illustrated in the discontinuity in Figure 5.11. If $\alpha > 1.026 \times 10^{-4}$ s^{-1}, the only stable equilibrium point is the trivial solution. Otherwise, there is a stable co-existence of both types of glucose fermenters and methanogens. That is, for each value of passage rate, there is only one stable equilibrium point and there is a bifurcation at $\alpha = 1.026 \times 10^{-4}$ s^{-1}. As noted before, in the rumen, the typical range of passage rate values is $1 \times 10^{-5} \leq \alpha \leq 5 \times 10^{-5}$ s^{-1} [150], [152]. In this

range for typical β_g values, the two fermenters in our example always co-exist.

The effect of changing β_g on the stable co-existence of two types of glucose fermenters and methanogens is illustrated in Figure 5.11. At a lower value of β_g (Figure 5.11(b)), glucose fermenter 2 becomes dominate more quickly with increasing the passage rate than it does for greater value of β_g (Figure 5.11(a)). With a 1.93 times lower ($1.930 \times 10^{-9}/1 \times 10^{-9} = 1.93$) value of β_g (food supply) a lower glucose fermenter population density yields a roughly 1.93 times lower hydrogen generation rate so that the methanogen population density is reduced roughly by a factor of 1.93 (Figure 5.11(a), (b)). Similar differences hold for Figure 5.11(b), (c). This observation of differences in methanogen population density for different values of glucose generation rate is in agreement with the conclusion from the HM model (Section 2.4) that as long as methanogens can survive in the rumen, decreasing the hydrogen generation rate by a factor of c roughly decreases the methanogen population density by a factor of c.

With a lower feed intake, it is expected that the animal products (e.g., meat, milk) are reduced (by the same factor). The volatile fatty acids (VFA) are absorbed by the ruminants as energy sources for the animal or converted into animal products. With a 1.93 times lower ($1.930 \times 10^{-9}/1 \times 10^{-9} = 1.93$) value of β_g, i.e., 1.93 times lower feed intake, the steady state volatile fatty acids concentrations are (roughly) reduced by the same factor. This is illustrated by the differences in Figures 5.12(a), (b). Similar differences hold for Figure 5.12(b), (c).

By decreasing $\beta_g = 1.930 \times 10^{-9}$ mol ml^{-1} s^{-1} to $\beta_g = 1 \times 10^{-9}$ mol ml^{-1} s^{-1}, there is a factor of 1.93 decrease in the glucose generation rate. This leads to a decrease in the hydrogen generation rate, β_h, by a factor of roughly 1.93 such that β_h/β_g in Figure 5.13(a) is approximately the same (at most 9% greater) as that in Figure 5.13(b). Similar differences hold for Figure 5.13(b), (c).

Although reducing the amount of feed (i.e., reducing β_g) consumed by ruminants can reduce methane production, this is not economical because this will also reduce VFA concentration (Figure 5.12(a), (b), (c))

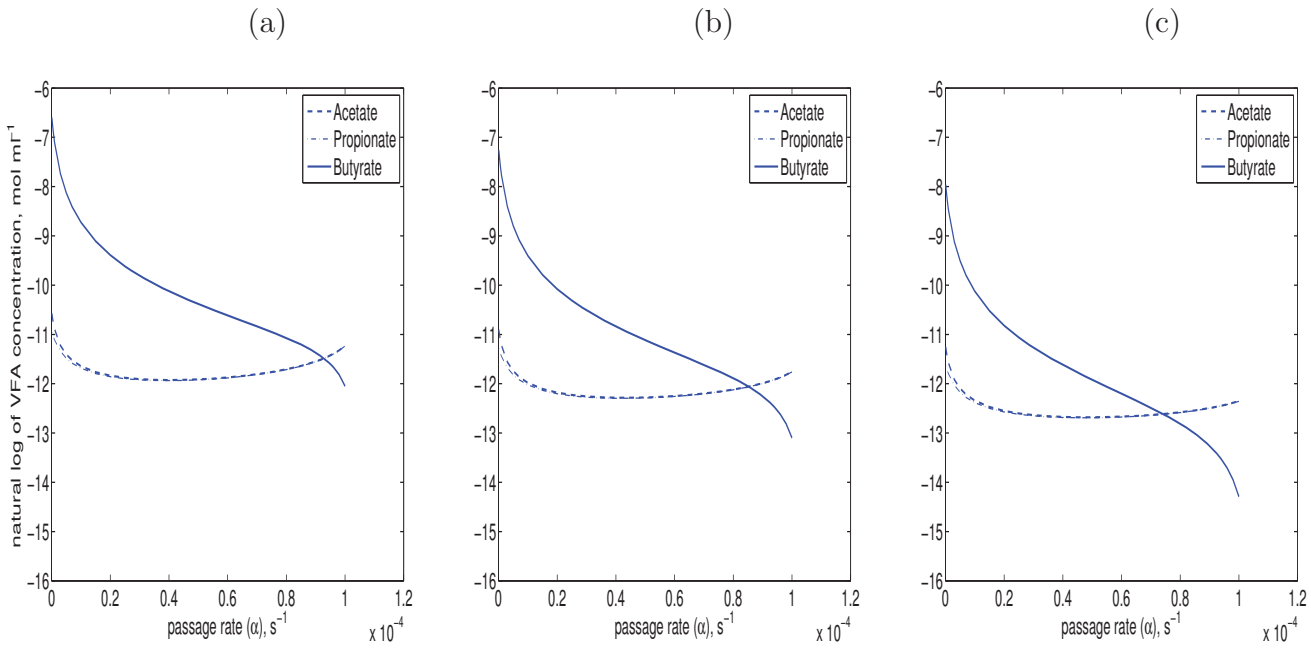

Figure 5.12: The stable steady state VFA concentration with a constant β_g and a range of passage rate values. (a) $\beta_g = 1.930 \times 10^{-9}$ mol ml^{-1} s^{-1}. (b) $\beta_g = 1 \times 10^{-9}$ mol ml^{-1} s^{-1}. (c) $\beta_g = 0.5 \times 10^{-9}$ mol ml^{-1} s^{-1}. The VFA concentration becomes zero (note log(0) is negative infinity so zero concentration is not shown on graph) when both types of glucose fermenters are eliminated, that is when $\alpha > 1.026 \times 10^{-4}$ s^{-1}.

and hence reduce animal productivity because the VFA are converted by the ruminants into animal products. The more economical approach to reduce methane production without reducing animal productivity is to increase the passage rate, as illustrated in Figure 5.13. A greater passage rate is associated with a greater hydrogen concentration. As illustrated in Figure 5.8, increasing the passage rate causes a decrease in X_1 and so a shift in glucose fermentation pathways from pathway (5.32) to pathway (5.33) due to the thermodynamic feedback imposed by the hydrogen concentration (and other end products). This leads to a reduced net hydrogen-formation (reduced β_h and β_h/β_g Figure 5.13) and hence less estimated methane production [76]. That is, increasing the passage rate leads to a shift in glucose fermentation pathways that produce less hydrogen: the passage rate indirectly affects methane production by directly affecting the amount of hydrogen generated from fermentation pathways.

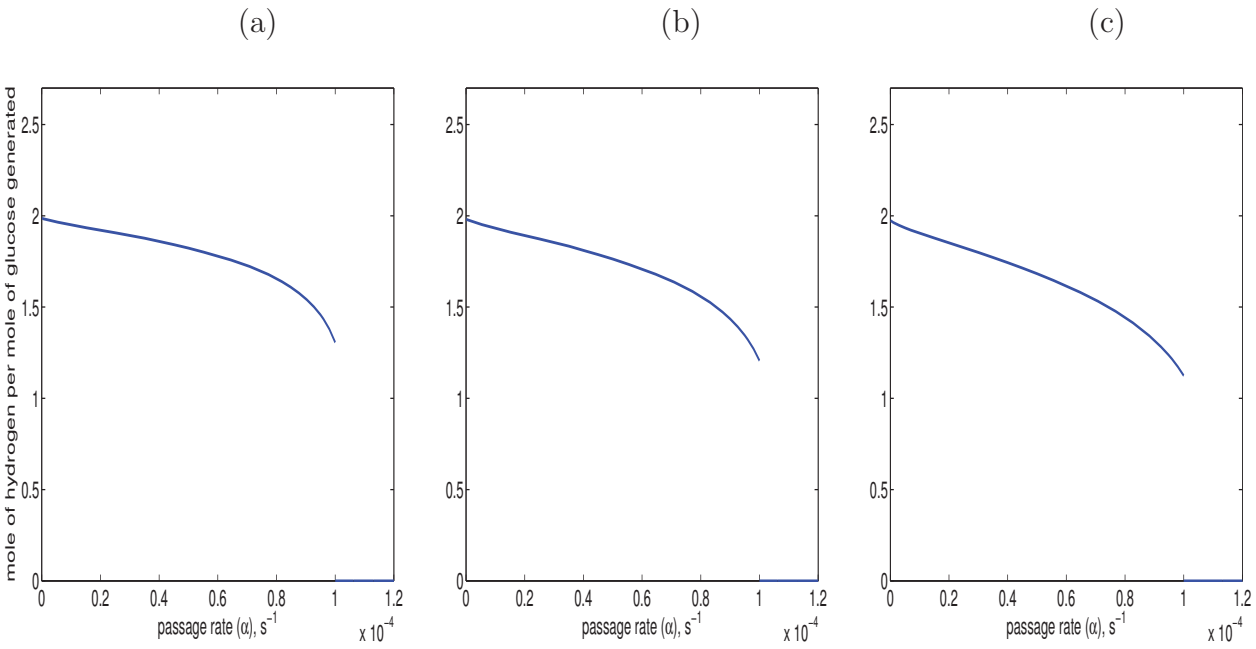

Figure 5.13: The steady state β_h/β_g ratio with a constant β_g and a range of passage rate values. (a) $\beta_g = 1.930 \times 10^{-9}$ mol ml^{-1} s^{-1}. (b) $\beta_g = 1 \times 10^{-9}$ mol ml^{-1} s^{-1}. (c) $\beta_g = 0.5 \times 10^{-9}$ mol ml^{-1} s^{-1}. There is essentially one value of β_h/β_g for $0 < \alpha < 1.026 \times 10^{-4}$ s^{-1} and another (0) for $\alpha > 1.026 \times 10^{-4}$ s^{-1} where glucose fermenters are eliminated by the passage rate so that no glucose is fermented to hydrogen, i.e., $\beta_h = 0$.

This observation from the GHM$^\theta$ model has been confirmed by theory and animal experiment. In theory, one method to reduce the hydrogen generation rate in the rumen is to feed ruminants with cereal grain [93]. Grains, such as corn, contain larger amounts of rapidly degradable starch. When more digestible feed is eaten, the passage rate is greater [105]. A greater passage rate is associated with a greater hydrogen concentration that leads to a shift in fermentation pathways towards more propionate production and reduce hydrogen generation rate and hence less methane production [76]. From animal experiment, by feeding forage brassicas (rape and swedes), the methane production from sheep was respectively 23% and 25% less than that of ryegrass [151]. Sun *et al.* [151], [152] concluded that this difference in methane production is due to rape and swedes being more rapidly degradable than ryegrass, that is, they behave like grain in the rumen.

By including glucose fermenters that can co-exist, the methane production (measured by β_h/β_g) can be reduced by increasing the passage rate that leads to shift glucose fermentation pathways towards less hydrogen generation rate, as shown in the differences in Figures 5.6 and 5.13. There are more than two types of glucose fermenters in the rumen. Therefore, the analytical results for the co-existence of two types of glucose fermenters are generalized to explore the mechanism of how more than two types of glucose fermenter can co-exist, as predicted by the GHM$^{\theta}$ model. Also, by including co-existence of more than two types of glucose fermenters, whether this can yield a lower β_h/β_g.

5.4 Generalization

In this section, we explore the possibility of whether or not more than two types of glucose fermenters can co-exist in the rumen and if so what is the mechanism leads to co-exist, as predicted by the GHM$^{\theta}$ model. Whether or not the methanogens can also survive is determined by the hydrogen generation rate (food source) from glucose fermentation, the rumen environment and biological parameters of methanogens, as modelled by the GHM$^{\theta}$ model.

5.4.1 Two types of glucose fermenters with generalized glucose fermentation pathways

Before exploring the co-existence of more than two types of glucose fermenters, let us examine the stability of equilibrium points where there are two types of glucose fermenters i and j that are associated with generalized glucose fermentation pathways, taking the form given in equation (4.1).

$$\text{glucose} + w_{wt_i}\text{H}_2\text{O} \rightarrow w_{A_i}A + w_{P_i}P + w_{B_i}B + w_{h_i}\text{H}_2 + w_{cd_i}\text{CO}_2 + w_{\text{H}^+{}_i}\text{H}^+ \ , \tag{5.34}$$

$$\text{glucose} + w_{wt_j}\text{H}_2\text{O} \rightarrow w_{A_j}A + w_{P_j}P + w_{B_j}B + w_{h_j}\text{H}_2 + w_{cd_j}\text{CO}_2 + w_{\text{H}^+{}_j}\text{H}^+ \ . \tag{5.35}$$

Then

$$\theta_i = \frac{[A]^{w_{A_i}}[P]^{w_{P_i}}[B]^{w_{B_i}}[\mathrm{H_2}]^{w_{h_i}}[\mathrm{CO_2}]^{w_{cd_i}}[\mathrm{H^+}]^{w_{\mathrm{H^+}_i}}}{[\text{glucose}][\mathrm{H_2O}]^{w_{wt_i}}}\ \mathrm{e}^{(\Delta G^o_{T_i}+n_i\ \Delta G_{ATP})/(\mathcal{R}T)}\ ,$$
$$\theta_j = \frac{[A]^{w_{A_j}}[P]^{w_{P_j}}[B]^{w_{B_j}}[\mathrm{H_2}]^{w_{h_j}}[\mathrm{CO_2}]^{w_{cd_j}}[\mathrm{H^+}]^{w_{\mathrm{H^+}_j}}}{[\text{glucose}][\mathrm{H_2O}]^{w_{wt_j}}}\ \mathrm{e}^{(\Delta G^o_{T_j}+n_j\ \Delta G_{ATP})/(\mathcal{R}T)}\ .$$

The w are the unitless stoichiometric coefficients of the chemical equation and the subscript indicates the glucose fermenter that uses this pathway. So, for example, in every millilitre of rumen liquid, glucose fermenter i converts each mole of glucose into w_{A_i} moles of acetate, A, w_{P_i} moles of propionate, P, w_{B_i} moles of butyrate, B, w_{h_i} moles of hydrogen, $\mathrm{H_2}$, w_{cd_i} moles of carbon dioxide, $\mathrm{CO_2}$, and $w_{\mathrm{H^+}_i}$ moles of hydrogen ions, H^+. Not all fermentation pathways produce all of these end products so some of the stoichiometric coefficients could be zero. However, at least one of w_{A_i}, w_{P_i}, w_{B_i}, must be positive because one or more of acetate, propionate or butyrate is always an end product from glucose fermentation. In Section 5.3, the assumption was made that glucose fermenters 1 and 2 had at least one common end product. In this Section, importantly, we do not assume that the glucose fermentation pathways have a common end product. Rather, glucose fermenter i and j are only required to be associated with glucose fermentation pathways where the value of stoichiometric coefficients balance the chemical equations (5.34) and (5.35).

We are interested primarily in whether glucose fermenter i and j can co-exist long term (i.e., $X_i^* > 0$ and $X_j^* > 0$). For this to occur, both types of glucose fermenter must be in their reproduction mode so that they can maintain themselves in the rumen, i.e., $E_i = Y_i$ and $E_j = Y_j$. The GHM$^\theta$ model then becomes

$$S_g' = -\frac{q_i S_g(1-\theta_i)}{K_i + S_g(1+\theta_i)}X_i - \frac{q_j S_g(1-\theta_j)}{K_j + S_g(1+\theta_j)}X_j - \alpha S_g + \beta_g\ ,$$
$$X_i' = \left(\frac{Y_i n_i q_i S_g(1-\theta_i)}{K_i + S_g(1+\theta_i)} - Y_i m_i - \alpha\right)X_i\ ,$$
$$X_j' = \left(\frac{Y_j n_j q_j S_g(1-\theta_j)}{K_j + S_g(1+\theta_j)} - Y_j m_j - \alpha\right)X_j\ ,$$

$$
\begin{aligned}
S'_h &= -\frac{q_m S_h(1-\theta_m)}{K_m + S_h(1+\theta_m)} X_m - \alpha S_h + w_{h_i} \frac{q_i S_g(1-\theta_i)}{K_i + S_g(1+\theta_i)} X_i + w_{h_j} \frac{q_j S_g(1-\theta_j)}{K_j + S_g(1+\theta_j)} X_j \ , \\
X'_m &= \left(\frac{E_m n_m q_m S_h(1-\theta_m)}{K_m + S_h(1+\theta_m)} - E_m m_m - \alpha \right) X_m \ , \\
S'_A &= w_{A_i} \frac{q_i S_g(1-\theta_i)}{K_i + S_g(1+\theta_i)} X_i + w_{A_j} \frac{q_j S_g(1-\theta_j)}{K_j + S_g(1+\theta_j)} X_j - \gamma_A S_A - \alpha S_A \ , \\
S'_P &= w_{P_i} \frac{q_i S_g(1-\theta_i)}{K_i + S_g(1+\theta_i)} X_i + w_{P_j} \frac{q_j S_g(1-\theta_j)}{K_j + S_g(1+\theta_j)} X_j - \gamma_P S_P - \alpha S_P \ , \\
S'_B &= w_{B_i} \frac{q_i S_g(1-\theta_i)}{K_i + S_g(1+\theta_i)} X_i + w_{B_j} \frac{q_j S_g(1-\theta_j)}{K_j + S_g(1+\theta_j)} X_j - \gamma_B S_B - \alpha S_B \ .
\end{aligned}
$$

This GHM$^\theta$ model with two types of glucose fermenters i and j is in the same form as the GHM$^\theta$ model with two types of glucose fermenters 1 and 2 in Section 5.3.

From $X'_i = 0$, in the absence of glucose fermenter j, the steady state glucose concentration, S^*_g, is given by the biological parameters of glucose fermenter i and the rumen environment

$$
S^*_g = \frac{K_i(Y_i m_i + \alpha)}{Y_i n_i q_i (1-\theta^*_i) - (Y_i m_i + \alpha)(1+\theta^*_i)} \ .
$$

By substituting the steady state thermodynamic term, θ^*_i,

$$
\theta^*_i = \frac{(S^*_A)^{w_{A_i}} (S^*_P)^{w_{P_i}} (S^*_B)^{w_{B_i}} (S^*_h)^{w_{h_i}} C_i}{S^*_g} \ ,
$$

into S^*_g so the steady state glucose concentration can be divided into two components: the first is the steady state glucose concentration found when there is no thermodynamic control (that is when $\theta_i = 0$), ξ_i; and the second is the shift in this value due to thermodynamic control, σ_i. There are given by

$$
\begin{aligned}
\xi_i &= \frac{K_i(Y_i m_i + \alpha)}{Y_i n_i q_i - Y_i m_i - \alpha} \ , \\
\sigma_i &= \frac{(Y_i n_i q_i + Y_i m_i + \alpha)(S^*_A)^{w_{A_i}} (S^*_P)^{w_{P_i}} (S^*_B)^{w_{B_i}} (S^*_h)^{w_{h_i}} C_i}{Y_i n_i q_i - Y_i m_i - \alpha} \ ,
\end{aligned}
$$

where

$$S_g^*(i) = \xi_i + \sigma_i \ .$$

Note that the concentration of water is approximated by the water activity and assumed constant [21] and C_i is a constant based on the same assumptions as stated in Section 5.2 that the following are constant in the rumen: the pH value (i.e., $[H^+]$); the energy required for one mole of ATP formation by the glucose fermenter, ΔG_{ATP}; the dissolved carbon dioxide concentration, $[CO_2]$ and the rumen temperature, T.

Similarly, in the absence of glucose fermenter i, we can determine the corresponding terms ξ_j and σ_j for glucose fermenter j and C_j is a constant.

$$\begin{aligned}
\xi_j &= \frac{K_j(Y_j m_j + \alpha)}{Y_j n_j q_j - Y_j m_j - \alpha} \ , \\
\sigma_j &= \frac{(Y_j n_j q_j + Y_j m_j + \alpha)(S_A^*)^{w_{A_j}}(S_P^*)^{w_{P_j}}(S_B^*)^{w_{B_j}}(S_h^*)^{w_{h_j}} C_j}{Y_j n_j q_j - Y_j m_j - \alpha} \ , \\
S_g^*(j) &= \xi_j + \sigma_j \ .
\end{aligned}$$

In Section 5.3, the comparison of $S_g^*(1)$ and $S_g^*(2)$ determined whether there was a stable co-existence of glucose fermenter 1 and 2 in the long term, e.g., expressions (5.28) and (5.29). Similarly, in this generalized example with glucose fermenter i and j, it is the comparison of $S_g^*(i)$ and $S_g^*(j)$ that determines whether there is a stable co-existence of glucose fermenter i and j in the long term. That is,

$$0 < S_g^*(i) < S_g^*(j) \ , \tag{5.36}$$

is required for $(S_g^*, X_i^*, 0, S_h^*, X_m^*, S_A^*, \ S_P^*, S_B^*)$, where $X_i^* > 0$, to be a stable equilibrium point;

$$0 < S_g^*(j) < S_g^*(i) \ , \tag{5.37}$$

is required for $(S_g^*, 0, X_j^*, S_h^*, X_m^*, S_A^*, \ S_P^*, S_B^*)$, where $X_j^* > 0$, to be a

stable equilibrium point; and

$$0 < S_g^*(i) = S_g^*(j) \ , \tag{5.38}$$

is required for $(S_g^*, X_i^*, X_j^*, S_h^*, X_m^*, S_A^*, S_P^*, S_B^*)$, where $X_i^* > 0$ and $X_j^* > 0$, to be a stable equilibrium point and therefore for a co-existence of X_i and X_j. Because only one of expression (5.36), (5.37) or (5.38) can be satisfied only one of $(S_g^*, X_i^*, 0, S_h^*, X_m^*, S_A^*, S_P^*, S_B^*)$ where $X_i^* > 0$, $(S_g^*, 0, X_j^*, S_h^*, X_m^*, S_A^*, S_P^*, S_B^*)$ where $X_j^* > 0$ or $(S_g^*, X_i^*, X_j^*, S_h^*, X_m^*, S_A^*, S_P^*, S_B^*)$ where $X_i^* > 0$ and $X_j^* > 0$ is a stable equilibrium. If either $S_g^*(i)$ or $S_g^*(j)$ is negative, the respective glucose fermenter cannot survive in the long term (i.e., it's steady state population, X_i^* or X_j^*, is zero). This could occur due to washout from the passage rate or the glucose fermentation pathways reaching chemical equilibrium (and therefore no glucose is fermented). As at least one of the populations is wiped out, there is not co-existence of glucose fermenter i and j when either or both of their S_g^* values is negative. In summary, there are four possible steady state scenarios and there is exactly one stable equilibrium point, $(S_g^*, X_i^*, X_j^*, S_h^*, X_m^*, S_A^*, S_P^*, S_B^*)$, for any combination of biological (n, q, K, m, d and Y) and ruminal (α, β_g, γ_A, γ_P and γ_B) parameter values.

1. $X_i^* = 0$ and $X_j^* = 0$,
   if $S_g^*(i) < 0$ and $S_g^*(j) < 0$ (both are washed out) ;

2. $X_i^* = 0$ and $X_j^* > 0$,
   if $S_g^*(i) < 0$ and $S_g^*(j) > 0$ (X_i is washed out) or
   if $0 < S_g^*(j) < S_g^*(i)$ (X_j outcompetes X_i) ;

3. $X_i^* > 0$ and $X_j^* = 0$,
   if $S_g^*(i) > 0$ and $S_g^*(j) < 0$ (X_j is washed out) or
   if $0 < S_g^*(i) < S_g^*(j)$ (X_i outcompetes X_j) ;

4. $X_i^* > 0$ and $X_j^* > 0$, if $0 < S_g^*(i) = S_g^*(j)$.

5.4.2 Three types of glucose fermenter

By introducing another type of glucose fermenter, the analytical results of the GHM$^{\theta}$ model with two types of glucose fermenters i and j can be expanded. Suppose now there is another glucose fermenter k associated with the generalized glucose fermentation pathway

$$\text{glucose} + w_{wt_k}\text{H}_2\text{O} \rightarrow w_{A_k}A + w_{P_k}P + w_{B_k}B + w_{h_k}\text{H}_2 + w_{cd_k}\text{CO}_2 + w_{\text{H}^+{}_k}\text{H}^+ \ ,$$

with the thermodynamic term

$$\theta_k = \frac{[A]^{w_{A_k}}[P]^{w_{P_k}}[B]^{w_{B_k}}[\text{H}_2]^{w_{h_k}}[\text{CO}_2]^{w_{cd_k}}[\text{H}^+]^{w_{\text{H}^+{}_k}}}{[\text{glucose}][\text{H}_2\text{O}]^{w_{wt_k}}}\ \text{e}^{(\Delta G^o_{T_k} + n_k\ \Delta G_{ATP})/(\mathcal{R}T)} \ .$$

Again, importantly, the glucose fermentation pathways of glucose fermenters i, j and k are generalised and do not assume required a common end product. The only requirement for each glucose fermenter is that it is associated with a generalized fermentation pathway in the form of equation (4.1), with stoichiometric coefficients that balance the chemical equations of the fermentation pathway.

In the absence of glucose fermenter i and j, the steady state glucose concentration, S_g^*, predicted by the biological parameters of glucose fermenter k and the rumen environment can be divided into two components as before:

$$\begin{aligned}
\xi_k &= \frac{K_k(Y_k m_k + \alpha)}{Y_k n_k q_k - Y_k m_k - \alpha} \ , \\
\sigma_k &= \frac{(Y_k n_k q_k + Y_k m_k + \alpha)(S_A^*)^{w_{A_k}}(S_P^*)^{w_{P_k}}(S_B^*)^{w_{B_k}}(S_h^*)^{w_{h_k}} C_k}{Y_k n_k q_k - Y_k m_k - \alpha} \ , \\
S_g^*(k) &= \xi_k + \sigma_k \ .
\end{aligned}$$

Note again that the concentration of water is approximated by the water activity and assumed constant [21] and C_k is a constant based on the same assumptions as stated in Section 5.2.

We are interested primarily in whether glucose fermenter i, j and k can co-exist in the long term (i.e., their steady state populations, X_i^*, X_j^* and X_k^* are all greater than zero). For this to occur, all three types

of glucose fermenters must long term be in their reproduction mode so that they can maintain themselves in the rumen, i.e., $E_i = Y_i$, $E_j = Y_j$ and $E_k = Y_k$. The GHM$^\theta$ model with three types of glucose fermenters then becomes

$$
\begin{aligned}
S_g' &= -\frac{q_i S_g(1-\theta_i)}{K_i + S_g(1+\theta_i)} X_i - \frac{q_j S_g(1-\theta_j)}{K_j + S_g(1+\theta_j)} X_j - \frac{q_k S_g(1-\theta_k)}{K_k + S_g(1+\theta_k)} X_k - \alpha S_g + \beta_g \ , \\
X_i' &= \left(\frac{Y_i n_i q_i S_g(1-\theta_i)}{K_i + S_g(1+\theta_i)} - Y_i m_i - \alpha \right) X_i \ , \\
X_j' &= \left(\frac{Y_j n_j q_j S_g(1-\theta_j)}{K_j + S_g(1+\theta_j)} - Y_j m_j - \alpha \right) X_j \ , \\
X_k' &= \left(\frac{Y_k n_k q_k S_g(1-\theta_k)}{K_k + S_g(1+\theta_k)} - Y_k m_k - \alpha \right) X_k \ , \\
S_h' &= -\frac{q_m S_h(1-\theta_m)}{K_m + S_h(1+\theta_m)} X_m - \alpha S_h \\
&\quad + w_{h_i} \frac{q_i S_g(1-\theta_i)}{K_i + S_g(1+\theta_i)} X_i + w_{h_j} \frac{q_j S_g(1-\theta_j)}{K_j + S_g(1+\theta_j)} X_j + w_{h_k} \frac{q_k S_g(1-\theta_k)}{K_k + S_g(1+\theta_k)} X_k \ , \\
X_m' &= \left(\frac{E_m n_m q_m S_h(1-\theta_m)}{K_m + S_h(1+\theta_m)} - E_m m_m - \alpha \right) X_m \ , \\
S_A' &= w_{A_i} \frac{q_i S_g(1-\theta_i)}{K_i + S_g(1+\theta_i)} X_i + w_{A_j} \frac{q_j S_g(1-\theta_j)}{K_j + S_g(1+\theta_j)} X_j + w_{A_k} \frac{q_k S_g(1-\theta_k)}{K_k + S_g(1+\theta_k)} X_k \\
&\quad - \gamma_A S_A - \alpha S_A \ , \\
S_P' &= w_{P_i} \frac{q_i S_g(1-\theta_i)}{K_i + S_g(1+\theta_i)} X_i + w_{P_j} \frac{q_j S_g(1-\theta_j)}{K_j + S_g(1+\theta_j)} X_j + w_{P_k} \frac{q_k S_g(1-\theta_k)}{K_k + S_g(1+\theta_k)} X_k \\
&\quad - \gamma_P S_P - \alpha S_P \ , \\
S_B' &= w_{B_i} \frac{q_i S_g(1-\theta_i)}{K_i + S_g(1+\theta_i)} X_i + w_{B_j} \frac{q_j S_g(1-\theta_j)}{K_j + S_g(1+\theta_j)} X_j + w_{B_k} \frac{q_k S_g(1-\theta_k)}{K_k + S_g(1+\theta_k)} X_k \\
&\quad - \gamma_B S_B - \alpha S_B \ .
\end{aligned}
$$

There are eight possible stable scenarios that can be represented by the equilibrium point, $(S_g^*, X_i^*, X_j^*, X_k^*, S_h^*, X_m^*, S_A^*, S_P^*, S_B^*)$, where

$$
\begin{aligned}
X_i^* = 0, X_j^* = 0, X_k^* = 0 \ , \\
X_i^* > 0, X_j^* = 0, X_k^* = 0 \ , \\
X_i^* = 0, X_j^* > 0, X_k^* = 0 \ ,
\end{aligned}
$$

$$
\begin{aligned}
X_i^* = 0, X_j^* = 0, X_k^* > 0 \ , \\
X_i^* > 0, X_j^* > 0, X_k^* = 0 \ , \\
X_i^* > 0, X_j^* = 0, X_k^* > 0 \ , \\
X_i^* = 0, X_j^* > 0, X_k^* > 0 \ , \\
X_i^* > 0, X_j^* > 0, X_k^* > 0 \ .
\end{aligned}
$$

The stability of these equilibrium points is determined by the corresponding eigenvalues of the Jacobian matrix for the dynamical system. For $(S_g^*, X_i^*, 0, 0, S_h^*, X_m^*, S_A^*, S_P^*, S_B^*)$, $X_j' = 0$, $X_k' = 0$, $X_i^* > 0$, $X_j^* = 0$ and $X_k^* = 0$. When this is true, all the elements of the third and fourth rows of the Jacobian matrix, J_3 (page 144), are zero except the diagonal elements, $J_3(3,3)$ and $J_3(4,4)$. The eigenvalue of this matrix is solved from $\det(J_3 - \lambda I) = 0$. There are two eigenvalues that can be determined from X_j' and X_k' with $X_j^* = X_k^* = 0$ and $X_i^* > 0$.

$$
\begin{aligned}
\frac{Y_j n_j q_j S_g^*(1-\theta_j^*)}{K_j + S_g^*(1+\theta_j^*)} - Y_j m_j - \alpha \ , \\
\frac{Y_k n_k q_k S_g^*(1-\theta_k^*)}{K_k + S_g^*(1+\theta_k^*)} - Y_k m_k - \alpha \ .
\end{aligned}
$$

At least these two eigenvalues must be negative to guarantee $(S_g^*, X_i^*, 0, 0, S_h^*, X_m^*, S_A^*, S_P^*, S_B^*)$ is a stable point. That is,

$$
\begin{aligned}
\frac{Y_j n_j q_j S_g^*(1-\theta_j^*)}{K_j + S_g^*(1+\theta_j^*)} - Y_j m_j - \alpha < 0 \ , \\
\frac{Y_k n_k q_k S_g^*(1-\theta_k^*)}{K_k + S_g^*(1+\theta_k^*)} - Y_k m_k - \alpha < 0 \ ,
\end{aligned}
$$

or equivalently

$$
\begin{aligned}
S_g^* < S_g^*(j) \ , \\
S_g^* < S_g^*(k) \ ,
\end{aligned}
$$

are both required to guarantee $(S_g^*, X_i^*, 0, 0, S_h^*, X_m^*, S_A^*, S_P^*, S_B^*)$ is a stable point.

Recall that in the absence of glucose fermenter j and k, (i.e., $X_j^* = X_k^* = 0$) the steady state glucose concentration, S_g^*, is predicted by $S_g^*(i)$, i.e., $S_g^* = S_g^*(i)$. Note that $S_g^*(i)$ is calculated based on the biological parameters of glucose fermenter i and the rumen environment. Similar to the GHM$^\theta$ model with glucose fermenter i and j, if any of $S_g^*(i)$, $S_g^*(j)$ or $S_g^*(k)$ is negative, then the corresponding glucose fermenter cannot survive in the long term (i.e., $X_i^* = 0$, $X_j^* = 0$ or $X_k^* = 0$). This could occur due to washout from the passage rate or the glucose fermentation pathway reaching chemical equilibrium (and hence no glucose is fermented). Overall,

$$0 < S_g^*(i) < S_g^*(j) \leq S_g^*(k) \ ,$$

is required to guarantee $(S_g^*, X_i^*, 0, 0, S_h^*, X_m^*, S_A^*, S_P^*, S_B^*)$, where $X_i^* > 0$, is a stable point, i.e., only glucose fermenter i will survive in the long term. If this inequality is not satisfied, then $(S_g^*, X_i^*, 0, 0,\ S_h^*, X_m^*, S_A^*, S_P^*, S_B^*)$, where $X_i^* > 0$, is unstable.

Similarly, if

$$0 < S_g^*(j) < S_g^*(i) \leq S_g^*(k) \ ,$$

then $(S_g^*, 0, X_j^*, 0,\ S_h^*, X_m^*, S_A^*, S_P^*, S_B^*)$, where $X_j^* > 0$, is a stable equilibrium point i.e., only glucose fermenter j will survive in the long term. If

$$0 < S_g^*(k) < S_g^*(i) \leq S_g^*(j) \ ,$$

then $(S_g^*, 0, 0, X_k^*,\ S_h^*, X_m^*, S_A^*, S_P^*, S_B^*)$, where $X_k^* > 0$, is a stable equilibrium point. In this case, only glucose fermenter k will survive in the long term.

$$
J_3 = \begin{bmatrix}
\frac{\partial S_g(S_g,X_i,X_j,X_k,S_h,S_A,S_P,S_B)}{\partial S_g} & \frac{\partial S_g(S_g,X_i,X_j,X_k,S_h,S_A,S_P,S_B)}{\partial X_i} & \frac{\partial S_g(S_g,X_i,X_j,X_k,S_h,S_A,S_P,S_B)}{\partial X_j} & \frac{\partial S_g(S_g,X_i,X_j,X_k,S_h,S_A,S_P,S_B)}{\partial X_k} & \frac{\partial S_g(S_g,X_i,X_j,X_k,S_h,S_A,S_P,S_B)}{\partial S_h} & 0 & \frac{\partial S_g(S_g,X_i,X_j,X_k,S_h,S_A,S_P,S_B)}{\partial S_A} & \frac{\partial S_g(S_g,X_i,X_j,X_k,S_h,S_A,S_P,S_B)}{\partial S_P} & \frac{\partial S_g(S_g,X_i,X_j,X_k,S_h,S_A,S_P,S_B)}{\partial S_B} \\
\frac{\partial\left(\frac{Y_i r_i q_i S_g(1-\theta_g)}{K_i+S_g(1+\theta_g)}-Y_i m_i-\alpha\right)}{\partial S_g}X_i & \frac{Y_i r_i q_i S_g(1-\theta_g)}{K_i+S_g(1+\theta_g)}-Y_i m_i-\alpha & 0 & 0 & 0 & 0 & \frac{\partial\left(\frac{Y_i r_i q_i S_g(1-\theta_g)}{K_i+S_g(1+\theta_g)}-Y_i m_i-\alpha\right)}{\partial S_A}X_i & \frac{\partial\left(\frac{Y_i r_i q_i S_g(1-\theta_g)}{K_i+S_g(1+\theta_g)}-Y_i m_i-\alpha\right)}{\partial S_P}X_i & \frac{\partial\left(\frac{Y_i r_i q_i S_g(1-\theta_g)}{K_i+S_g(1+\theta_g)}-Y_i m_i-\alpha\right)}{\partial S_B}X_i \\
\frac{\partial\left(\frac{Y_j r_j q_j S_g(1-\theta_g)}{K_j+S_g(1+\theta_g)}-Y_j m_j-\alpha\right)}{\partial S_g}X_j & 0 & \frac{Y_j r_j q_j S_g(1-\theta_g)}{K_j+S_g(1+\theta_g)}-Y_j m_j-\alpha & 0 & \frac{\partial\left(\frac{Y_j r_j q_j S_g(1-\theta_g)}{K_j+S_g(1+\theta_g)}-Y_j m_j-\alpha\right)}{\partial S_h} & 0 & \frac{\partial\left(\frac{Y_j r_j q_j S_g(1-\theta_g)}{K_j+S_g(1+\theta_g)}-Y_j m_j-\alpha\right)}{\partial S_A}X_j & \frac{\partial\left(\frac{Y_j r_j q_j S_g(1-\theta_g)}{K_j+S_g(1+\theta_g)}-Y_j m_j-\alpha\right)}{\partial S_P}X_j & \frac{\partial\left(\frac{Y_j r_j q_j S_g(1-\theta_g)}{K_j+S_g(1+\theta_g)}-Y_j m_j-\alpha\right)}{\partial S_B}X_j \\
\frac{\partial\left(\frac{Y_k r_k q_k S_g(1-\theta_g)}{K_k+S_g(1+\theta_g)}-Y_k m_k-\alpha\right)}{\partial S_g}X_k & 0 & 0 & \frac{Y_k r_k q_k S_g(1-\theta_g)}{K_k+S_g(1+\theta_g)}-Y_k m_k-\alpha & \frac{\partial\left(\frac{Y_k r_k q_k S_g(1-\theta_g)}{K_k+S_g(1+\theta_g)}-Y_k m_k-\alpha\right)}{\partial S_h} & 0 & \frac{\partial\left(\frac{Y_k r_k q_k S_g(1-\theta_g)}{K_k+S_g(1+\theta_g)}-Y_k m_k-\alpha\right)}{\partial S_A}X_k & \frac{\partial\left(\frac{Y_k r_k q_k S_g(1-\theta_g)}{K_k+S_g(1+\theta_g)}-Y_k m_k-\alpha\right)}{\partial S_P}X_k & \frac{\partial\left(\frac{Y_k r_k q_k S_g(1-\theta_g)}{K_k+S_g(1+\theta_g)}-Y_k m_k-\alpha\right)}{\partial S_B}X_k \\
\frac{\partial S_h(S_g,X_i,X_j,X_k,S_h,S_m,S_A,S_P,S_B)}{\partial S_g} & w_{h_i}\frac{q_i S_h(1-\theta_g)}{K_i+S_g(1+\theta_g)} & w_{h_j}\frac{q_j S_h(1-\theta_g)}{K_j+S_g(1+\theta_g)} & w_{h_k}\frac{q_k S_h(1-\theta_g)}{K_k+S_g(1+\theta_g)} & \frac{\partial S_h(S_g,X_i,X_j,X_k,S_h,S_m,S_A,S_P,S_B)}{\partial S_h} & -\frac{q_m S_h(1-\theta_g)}{K_m+S_h(1+\theta_m)} & \frac{\partial S_h(S_g,X_i,X_j,X_k,S_h,S_m,S_A,S_P,S_B)}{\partial S_A} & \frac{\partial S_h(S_g,X_i,X_j,X_k,S_h,S_m,S_A,S_P,S_B)}{\partial S_P} & \frac{\partial S_h(S_g,X_i,X_j,X_k,S_h,S_m,S_A,S_P,S_B)}{\partial S_B} \\
0 & 0 & 0 & 0 & \frac{Y_m r_m q_m (K_m+2C_m) X_m}{(K_m+S_h+C_m)^2} & \frac{Y_m r_m q_m (S_h-C_m)}{K_m+S_h+C_m}-Y_m m_m-\alpha & 0 & 0 & 0 \\
\frac{\partial S_A(S_g,X_i,X_j,X_k,S_h,S_A,S_P,S_B)}{\partial S_g} & \frac{\partial S_A(S_g,X_i,X_j,X_k,S_h,S_A,S_P,S_B)}{\partial X_i} & \frac{\partial S_A(S_g,X_i,X_j,X_k,S_h,S_A,S_P,S_B)}{\partial X_j} & \frac{\partial S_A(S_g,X_i,X_j,X_k,S_h,S_A,S_P,S_B)}{\partial X_k} & \frac{\partial S_A(S_g,X_i,X_j,X_k,S_h,S_A,S_P,S_B)}{\partial S_h} & 0 & \frac{\partial S_A(S_g,X_i,X_j,X_k,S_h,S_A,S_P,S_B)}{\partial S_A} & \frac{\partial S_A(S_g,X_i,X_j,X_k,S_h,S_A,S_P,S_B)}{\partial S_P} & \frac{\partial S_A(S_g,X_i,X_j,X_k,S_h,S_A,S_P,S_B)}{\partial S_B} \\
\frac{\partial S_P(S_g,X_i,X_j,X_k,S_h,S_A,S_P,S_B)}{\partial S_g} & \frac{\partial S_P(S_g,X_i,X_j,X_k,S_h,S_A,S_P,S_B)}{\partial X_i} & \frac{\partial S_P(S_g,X_i,X_j,X_k,S_h,S_A,S_P,S_B)}{\partial X_j} & \frac{\partial S_P(S_g,X_i,X_j,X_k,S_h,S_A,S_P,S_B)}{\partial X_k} & \frac{\partial S_P(S_g,X_i,X_j,X_k,S_h,S_A,S_P,S_B)}{\partial S_h} & 0 & \frac{\partial S_P(S_g,X_i,X_j,X_k,S_h,S_A,S_P,S_B)}{\partial S_A} & \frac{\partial S_P(S_g,X_i,X_j,X_k,S_h,S_A,S_P,S_B)}{\partial S_P} & \frac{\partial S_P(S_g,X_i,X_j,X_k,S_h,S_A,S_P,S_B)}{\partial S_B} \\
\frac{\partial S_B(S_g,X_i,X_j,X_k,S_h,S_A,S_P,S_B)}{\partial S_g} & \frac{\partial S_B(S_g,X_i,X_j,X_k,S_h,S_A,S_P,S_B)}{\partial X_i} & \frac{\partial S_B(S_g,X_i,X_j,X_k,S_h,S_A,S_P,S_B)}{\partial X_j} & \frac{\partial S_B(S_g,X_i,X_j,X_k,S_h,S_A,S_P,S_B)}{\partial X_k} & \frac{\partial S_B(S_g,X_i,X_j,X_k,S_h,S_A,S_P,S_B)}{\partial S_h} & 0 & \frac{\partial S_B(S_g,X_i,X_j,X_k,S_h,S_A,S_P,S_B)}{\partial S_A} & \frac{\partial S_B(S_g,X_i,X_j,X_k,S_h,S_A,S_P,S_B)}{\partial S_P} & \frac{\partial S_B(S_g,X_i,X_j,X_k,S_h,S_A,S_P,S_B)}{\partial S_B} \\
\end{bmatrix}
$$

For any two types of glucose fermenters to co-exist (Section 5.4.1), equation (5.38) is required. Similarly, if

$$0 < S_g^*(i) = S_g^*(j) = S_g^*(k) \ , \tag{5.39}$$

then there is a co-existence of glucose fermenters i, j and k in the long term, which is represented by the equilibrium point $(S_g^*, X_i^*, X_j^*, X_k^*, S_h^*, X_m^*, S_A^*, S_P^*, S_B^*)$ with $X_i^* > 0$, $X_j^* > 0$ and $X_k^* > 0$.

Again, similar to the GHM$^\theta$ model with glucose fermenter i and j, for the GHM$^\theta$ model with three types of glucose fermenter i, j and k, it is the comparison among

$$\begin{aligned} S_g^*(i) &= \xi_i + \sigma_i \ , \\ S_g^*(j) &= \xi_j + \sigma_j \ , \\ S_g^*(k) &= \xi_k + \sigma_k \ , \end{aligned}$$

that determines whether there is a stable co-existence of glucose fermenters and if so which types of glucose fermenters can co-exist. For instance, suppose

$$0 < S_g^*(i) = S_g^*(j) < S_g^*(k) \ .$$

Then, each of

$$0 < S_g^*(i) < S_g^*(j) \ , \tag{5.40}$$
$$0 < S_g^*(j) < S_g^*(i) \ , \tag{5.41}$$
$$0 < S_g^*(k) < S_g^*(i) \ , \tag{5.42}$$
$$0 < S_g^*(k) < S_g^*(j) \ , \tag{5.43}$$
$$0 < S_g^*(i) = S_g^*(k) \ , \tag{5.44}$$
$$0 < S_g^*(j) = S_g^*(k) \ , \tag{5.45}$$

and inequality (5.39) is not satisfied. Consequently,

Steady state $(S_g^*, X_i^*, X_j^*, X_k^*, S_h^*, X_m^*, S_A^*, S_P^*, S_B^*)$	Reason of instability
$X_i^* = 0,\ X_j^* = 0,\ X_k^* = 0$	$S_g^*(i) > 0,\ S_g^*(j) > 0$ and $S_g^*(k) > 0$
$X_i^* > 0,\ X_j^* = 0,\ X_k^* = 0$	inequality (5.40) is not satisfied
$X_i^* = 0,\ X_j^* > 0,\ X_k^* = 0$	inequality (5.41) is not satisfied
$X_i^* = 0,\ X_j^* = 0,\ X_k^* > 0$	inequalities (5.42) and (5.43) are not satisfied
$X_i^* > 0,\ X_j^* = 0,\ X_k^* > 0$	inequality (5.44) is not satisfied
$X_i^* = 0,\ X_j^* > 0,\ X_k^* > 0$	inequality (5.45) is not satisfied
$X_i^* > 0,\ X_j^* > 0,\ X_k^* > 0$	inequality (5.39) is not satisfied

Thus, if

$$0 < S_g^*(i) = S_g^*(j) < S_g^*(k) \ ,$$

then there is a stable co-existence of glucose fermenters i and j, and glucose fermenter k die out long term, i.e., $X_i^* > 0$, $X_j^* > 0$, $X_k^* = 0$ and $(S_g^*, X_i^*, X_j^*, 0, S_h^*, X_m^*, S_A^*, S_P^*, S_B^*)$, for co-existence of glucose fermenters i and j is the only stable point.

In summary, with any combination of biological (n, q, K, m, d and Y) and ruminal (α, β_g, γ_A, γ_P and γ_B) parameter values, there is exactly one stable equilibrium point that is determined by comparison of $S_g^*(i)$, $S_g^*(j)$ and $S_g^*(k)$.

1. $X_i^* = 0$, $X_j^* = 0$ and $X_k^* = 0$,
   if $S_g^*(i) < 0$, $S_g^*(j) < 0$ and $S_g^*(k) < 0$ (all are washed out) ;

2. $X_i^* > 0$, $X_j^* = 0$ and $X_k^* = 0$,
   if $S_g^*(i) > 0$, $S_g^*(j) < 0$ and $S_g^*(k) < 0$ (X_j and X_k are washed out)
   or if $0 < S_g^*(i) < S_g^*(j) \leq S_g^*(k)$
   (X_i outcompetes X_j and X_k) ;

3. $X_i^* = 0$, $X_j^* > 0$ and $X_k^* = 0$,
   if $S_g^*(j) > 0$, $S_g^*(i) < 0$ and $S_g^*(k) < 0$ (X_i and X_k are washed out)
   or if $0 < S_g^*(j) < S_g^*(i) \leq S_g^*(k)$
   (X_j outcompetes X_i and X_k) ;

4. $X_i^* = 0$, $X_j^* = 0$ and $X_k^* > 0$,
   if $S_g^*(k) > 0$, $S_g^*(i) < 0$ and $S_g^*(j) < 0$ (X_i and X_j are washed out)
   or if $0 < S_g^*(k) < S_g^*(i) \leq S_g^*(j)$
   (X_k outcompetes X_i and X_j) ;

5. $X_i^* > 0$, $X_j^* > 0$ and $X_k^* = 0$,
   if $S_g^*(k) < 0 < S_g^*(i) = S_g^*(j)$ (X_k is washed out) or
   if $0 < S_g^*(i) = S_g^*(j) < S_g^*(k)$ (X_i and X_j outcompete X_k) ;

6. $X_i^* > 0$, $X_j^* = 0$ and $X_k^* > 0$,
   if $S_g^*(j) < 0 < S_g^*(i) = S_g^*(k)$ (X_j is washed out) or
   if $0 < S_g^*(i) = S_g^*(k) < S_g^*(j)$ (X_i and X_k outcompete X_j) ;

7. $X_i^* = 0$, $X_j^* > 0$ and $X_k^* > 0$,
   if $S_g^*(i) < 0 < S_g^*(j) = S_g^*(k)$ (X_i is washed out) or
   if $0 < S_g^*(j) = S_g^*(k) < S_g^*(i)$ (X_j and X_j outcompete X_i) ;

8. $X_i^* > 0$, $X_j^* > 0$ and $X_k^* > 0$,
   if $0 < S_g^*(i) = S_g^*(j) = S_g^*(k)$.

From the analytical results of the GHM$^\theta$ model with two types of glucose fermenter i and j; and the GHM$^\theta$ model with three types of glucose fermenter i, j and k, there is a stable co-existence of glucose fermenters, if and only if these types of glucose fermenters are associated with the same lowest positive steady state glucose concentration. Such steady state glucose concentration is found from the biological parameters of all these types of glucose fermenters and the rumen environment. This analytical result can be extended to any number of types of glucose fermenters.

5.4.3 Multiple types of glucose fermenters

Suppose there are nn types of glucose fermenters, $i \in \{1, ..., nn\}$. Each type of glucose fermenter is associated with a glucose fermentation pathway given in the form of equation (4.1). It is not assumed that these pathways must (or necessarily) have or not have a common end product. The GHM$^\theta$ model with nn types of glucose fermenters is given in Section

4.2. Different combinations of glucose fermenters and/or rumen environment leads to co-existence of different types of glucose fermenters. In this section, we extend the analytical results of the GHM$^{\theta}$ model with three types of glucose fermenter to any number of types of glucose fermenters.

With $S_g' = 0$, equation (4.2) becomes

$$\beta_g - \alpha S_g^* = \sum_{i=1}^{nn} \frac{q_i S_g(1-\theta_i)}{K_i + S_g(1+\theta_i)} X_i \ .$$

Population density cannot be negative, i.e., $X_i \geq 0, \forall i \in \{1, ..., nn\}$. The thermodynamic term, θ_i, $0 \leq \theta_i \leq 1$ and all the biological parameters are positive so that

$$\frac{q_i (S_g(1-\theta_i)}{K_i + S_g(1+\theta_i)} X_i \ ,$$

is non-negative for all i. Therefore, a sufficient glucose supply, $\beta_g > \alpha S_g^*$, is required to guarantee at least one type of glucose fermenter can survive. So if there is insufficient glucose supply all types of glucose fermenters will be eliminated. If $\beta_g = \alpha S_g^*$, then $X_i = 0$ and/or $\theta_i = 1$, $\forall i \in \{1, ..., nn\}$. Note that $\theta_i = 1$ indicates no glucose can be metabolized by either type of glucose fermenter due to thermodynamic feedback so that all types of glucose fermenters cannot reproduce and will therefore be eliminated by the passage rate. Thus, $(\beta_g/\alpha, 0, ..., 0, 0, 0, 0, 0, 0)$ is the only solution of the GHM$^{\theta}$ model with nn types of glucose fermenters, if there is insufficient glucose supply, $\beta_g \leq \alpha S_g^*$.

With $X_i' = 0$, from equation (4.3), in the absence of all types of glucose fermenter except i, based on the biological parameters and a given rumen environment, the steady state glucose concentration predicted by glucose fermenter i is

$$S_g^* = \frac{K_i(Y_i m_i + \alpha)}{Y_i n_i q_i (1-\theta_i^*) - (Y_i m_i + \alpha)(1+\theta_i^*)} = S_g^*(i), \ i \in \{1, ..., nn\} \ .$$

The term $S_g^*(i)$ can be expressed as

$$S_g^*(i) = \xi_i + \sigma_i, \ i \in \{1, ..., nn\} \ .$$

Similarly to the GHM$^{\theta}$ model with two types of glucose fermenters (Section 5.3), those types of glucose fermenters i associated with negative $S_g^*(i)$ cannot survive, i.e., $X_i' < 0$ such that $X_i^* \to 0$, as determined by a given rumen environment. This would occur when the glucose fermentation pathways associated with glucose fermenter i are always at chemical equilibrium ($\theta_i^* = 1$) and/or glucose fermenter i cannot tolerate the passage rate. Then the types of glucose fermenters i which could survive are those with $\xi_i > 0$, $\sigma_i > 0$ and $0 \leq \theta_i^* < 1$, so that $S_g^*(i) > 0$ $\forall i \in (\{1, ..., mm\} \subseteq \{1, ..., nn\})$.

From the analytical results of three types of glucose fermenters, it is the comparison among $S_g^*(i)$, $S_g^*(j)$ and $S_g^*(k)$ that determines which type of glucose fermenters can co-exist. By induction, for the GHM$^{\theta}$ model with nn types of glucose fermenters, it is the comparison of $S_g^*(i)$, $i \in \{1, ..., nn\}$ that determines which type of glucose fermenters can co-exist. Specifically, there is a co-existence of glucose fermenters and the corresponding equilibrium point is the only stable point, if and only if these types of glucose fermenters are associated with the same lowest positive steady state glucose concentration.

$$S_g^*(mm+1) \leq ... \leq S_g^*(nn) < 0 < S_g^*(1) = ... = S_g^*(ll) < S_g^*(ll+1) \leq ... \leq S_g^*(mm) \ . \tag{5.46}$$

From the analytical results of three types of glucose fermenter, there is exactly one stable equilibrium point for any number of glucose fermenters with any combination of biological (n, q, K, m, d and Y) and ruminal (α, β_g, γ_A, γ_P and γ_B) parameter values. If there is insufficient substrate supply, i.e., $\beta_g - \alpha S_g^* \leq 0$, then the only stable equilibrium point is where all the types of glucose fermenters cannot survive. Suppose the biological parameters of each type of glucose fermenter are known. With sufficient glucose supply, i.e., $\beta_g - \alpha S_g^* > 0$, the only stable equilibrium point is then either there is a stable co-existence of glucose fermenters where expression (5.46) is satisfied so $X_i^* > 0$, $i \in \{1, ..., ll\}$ are those types of glucose fermenters that co-exist among nn types of glucose fermenters or only one type of glucose fermenter can survive in the long term, as

predicted by the GHM$^{\theta}$ model.

From $i \in \{1, ..., nn\}$ to $i \in \{1, ..., ll\}$, there are two situations in which a type of glucose fermenter i can be eliminated: either by passage rate and/or thermodynamic feedback of substrates and products or by competition among glucose fermenters. Note that both situations are related to $S_g^*(i)$, which is determined by both the biological and rumen environment parameters (passage rate and thermodynamic control imposed by substrate and product concentrations that is captured by θ_i). Each type of glucose fermenter is associated with a $S_g^*(i)$. From expression (5.46), $i \in \{mm + 1, ..., nn\}$ are those types of glucose fermenters be eliminated by passage rate and/or thermodynamic feedback so that $S_g^*(mm + 1) \leq ... \leq S_g^*(nn) < 0$ and

$$0 < S_g^*(1) = ... = S_g^*(ll) < S_g^*(ll + 1) \leq ... \leq S_g^*(mm) \ ,$$

indicates that $i \in \{1, ..., ll\}$ types of glucose fermenters co-exist and also outcompete $i \in \{ll + 1, ..., mm\}$ types of glucose fermenters. That is, $X_i^* > 0 \ \forall i \in \{1, ..., ll\}$ otherwise $X_i^* = 0$ long term, as predicted by the GHM$^{\theta}$ model based on the given biological parameters of all types of glucose fermenters and the rumen environment. For different combinations of initial glucose fermenters, it could mean that different types of glucose fermenters can co-exist, i.e., the elements in the set $\{1, ..., ll\}$ could be different. If a new type of glucose fermenter $nn + 1$ is introduced to the rumen, and/or there is a change in the rumen environment, expression (5.46) can be used to determine whether this allows different types of glucose fermenters to co-exist, i.e., whether those elements in the set $\{1, ..., ll\}$ will change. This observation can be demonstrated by the following simulation example.

Note that glucose fermenters X_1 and X_2 are introduced in Section 5.3. Let X_3 denote the population density of a type of glucose fermenter 3 associated with the pathway

$$\text{glucose} + 2 \ H_2O \rightarrow 2 \ A + 4 \ H_2 + 2 \ CO_2 + 2 \ H^+ \ .$$

Let X_4 denote the population density of a type of glucose fermenter 4

associated with the pathway

$$\text{glucose} + 2/3\ \text{H}_2\text{O} \rightarrow 2/3\ A + 2/3\ B + 8/3\ \text{H}_2 + 2\ \text{CO}_2 + 4/3\ \text{H}^+\ .$$

Let X_5 denote the population density of a type of glucose fermenter 5 associated with the pathway

$$\text{glucose} \rightarrow 2/3\ A + 4/3\ P + 2/3\ \text{CO}_2 + 2/3\ \text{H}_2\text{O} + 2\ \text{H}^+\ .$$

For simplicity, we let the biological parameters (m_i, q_i, Y_i, K_i, n_i) of these five types of glucose fermenters, X_i, $i \in \{1, ..., 5\}$ be the same and these five types of glucose fermenters need the same amount of energy to gain one unit of ATP, i.e., $\Delta G_{ATP} = 75$ kJ mol_{ATP}^{-1}. These five types of glucose fermenters are distinguished by n_i

$$\begin{aligned}
n_1 &= 3\ \text{mol}_{ATP}\ \text{mol}^{-1}\ [\text{Appendix } C]\ ,\\
n_2 &= 3\ \text{mol}_{ATP}\ \text{mol}^{-1}\ [\text{Appendix } C]\ ,\\
n_3 &= 4\ \text{mol}_{ATP}\ \text{mol}^{-1}\ [\text{Appendix } C]\ ,\\
n_4 &= 3.33\ \text{mol}_{ATP}\ \text{mol}^{-1}\ [\text{Appendix } C]\ ,\\
n_5 &= 2.67\ \text{mol}_{ATP}\ \text{mol}^{-1}\ [\text{Appendix } C]\ ,
\end{aligned}$$

and $\Delta G^o_{T_i}$

$$\begin{aligned}
\Delta G^o_{T_1} &= -198.306\ \text{kJ mol}^{-1}\ [21]\ ,\\
\Delta G^o_{T_2} &= -187.516\ \text{kJ mol}^{-1}\ [21]\ ,\\
\Delta G^o_{T_3} &= -52.435\ \text{kJ mol}^{-1}\ [21]\ ,\\
\Delta G^o_{T_4} &= -148.124\ \text{kJ mol}^{-1}\ [21]\ ,\\
\Delta G^o_{T_5} &= -229.748\ \text{kJ mol}^{-1}\ [21]\ .
\end{aligned}$$

Let $0 < \alpha \leq 1.2 \times 10^{-4}$ s^{-1} and $\beta_g = 1.930 \times 10^{-9}$ mol ml^{-1} s^{-1}. All the ruminal parameters are the same as listed in Section 5.2.2 and used in Section 5.3.2. Suppose initially only fermenters 1 and 2 exist. We consider introducing one of glucose fermenters 3, 4 or 5 into the model in the following three cases:

Scenario A. We start with X_1, X_2 and X_3 (Figure 5.14).

Scenario B. We start with X_1, X_2 and X_4 (Figure 5.15).

Scenario C. We start with X_1, X_2 and X_5 (Figure 5.19).

Scenario A: Recall that X_i (cell ml^{-1}) denotes the population density of a type of glucose fermenter i. For any value of passage rate $0 < \alpha \leq 1.380 \times 10^{-4}$ s^{-1} $= Y_3(n_3q_3 - m_3)$, X_3 cannot survive because its thermodynamic term is always one so that $S_g^*(3) < 0$. That is, X_3 is eliminated by the thermodynamic feedback imposed by the rumen environment and its biological parameters until it is eliminated by the passage rate. For $0 < \alpha < 1.026 \times 10^{-4}$ s^{-1}, there is a co-existence of glucose fermenters 1 and 2, i.e., $S_g^*(3) < 0 < S_g^*(1) = S_g^*(2)$, as predicted by the GHM$^{\theta}$ model (see Figure 5.14). For passage rates α greater than 1.026×10^{-4} s^{-1} $= Y_1(n_1q_1 - m_1) = Y_2(n_2q_2 - m_2)$, the glucose fermenters X_1 and X_2 are eliminated as they cannot reproduce fast enough to match the passage rate, which in turn eliminates methanogens due to no hydrogen being produced from fermentation. This is illustrated in the discontinuity in Figure 5.14. If $\alpha > 1.026 \times 10^{-4}$ s^{-1}, the only stable equilibrium point is the trivial solution ($S_g^*(3) < S_g^*(1) = S_g^*(2) < 0$). Otherwise, there is a stable co-existence of glucose fermenters X_1 and X_2 and methanogens. For each value of passage rate, there is only one stable equilibrium point and there is a bifurcation at $\alpha = 1.026 \times 10^{-4}$ s^{-1}. These results are summaried in Table 5.1.

Table 5.1: Competition among X_1, X_2 and X_3.

Passage rate (α) (s^{-1})	Reason for stability	Stable steady state population densities
$0 < \alpha < 1.026 \times 10^{-4}$	$S_g^*(3) < 0 < S_g^*(1) = S_g^*(2)$	$X_1^* > 0$, $X_2^* > 0$, $X_3^* = 0$
$1.026 \times 10^{-4} \leq \alpha \leq 1.2 \times 10^{-4}$	$S_g^*(3) < S_g^*(1) = S_g^*(2) < 0$	$X_1^* = 0$, $X_2^* = 0$, $X_3^* = 0$

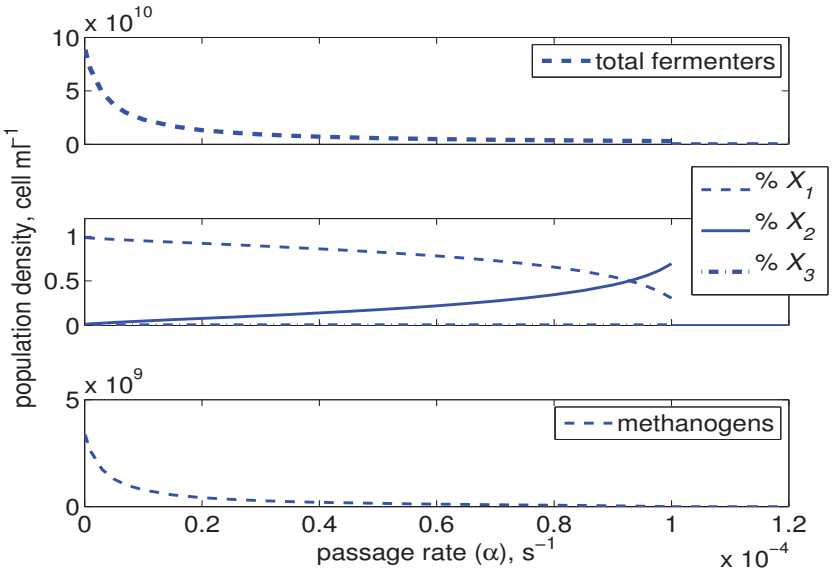

Figure 5.14: The stable steady state population densities of glucose fermenters 1, 2 and 3 and methanogens for a constant $\beta_g = 1.930 \times 10^{-9}$ mol ml^{-1} s^{-1} and a range of passage rate values. A bifurcation occurs when $\alpha = 1.026 \times 10^{-4}$ s^{-1} $= Y_1(n_1q_1 - m_1) = Y_2(n_2q_2 - m_2)$ after which the stable steady state changes from co-existence of glucose fermenter populations X_1 and X_2 and methanogens to the trivial solution.

Note that the population densities of glucose fermenters 1 and 2 in Figure 5.14 are the same as Figure 5.11(a) as expected due to the elimination of population X_3. Figures 5.4, 5.12(a), 5.13(a) are, respectively, the stable steady state substrate (glucose and hydrogen) concentration, VFA concentrations and the β_h/β_g ratio for scenario A.

Scenario B: For $0 < \alpha < 1.026 \times 10^{-4}$ s^{-1}, $S_g^*(1)$, $S_g^*(2)$ and $S_g^*(4)$ are all positive (and are therefore not eliminated due to thermodynamic feedback or washout), however, X_1 and X_2 are out competed by X_4, as determined by the rumen environment and its biological parameters,

$$0 < S_g^*(4) < S_g^*(1) = S_g^*(2) \ ,$$

and hence, there is no co-existence of X_1 and X_2 and X_4. That is, the glucose fermenter 4 will survive because it is the one with the best

traits for the given environment (the one that can grow at the lowest growth limiting steady state substrate concentration will survive and the others will die out in the long term). If $\alpha > 1.026 \times 10^{-4}$ s^{-1} = $Y_1(n_1q_1 - m_1) = Y_2(n_2q_2 - m_2)$, this eliminates both glucose fermenters 1 and 2 ($S_g^*(1) = S_g^*(2) < 0$) and only glucose fermenter 4 will survive for $1.026 \times 10^{-4} \leq \alpha < 1.143 \times 10^{-4}$ s^{-1} = $Y_4(n_4q_4 - m_4)$. A bifurcation occurs when $\alpha = 1.143 \times 10^{-4}$ s^{-1} after which the stable steady state changes from survival of glucose fermenter 4 and methanogens to the trivial solution (Figure 5.15). These results are summaried in Table 5.2.

Table 5.2: Competition among X_1, X_2 and X_4.

Passage rate (α) (s^{-1})	Reason for stability	Stable steady state population densities
$0 < \alpha < 1.026 \times 10^{-4}$	$0 < S_g^*(4) < S_g^*(1) = S_g^*(2)$	$X_1^* = 0$, $X_2^* = 0$, $X_4^* > 0$
$1.026 \times 10^{-4} \leq \alpha < 1.143 \times 10^{-4}$	$S_g^*(1) = S_g^*(2) < 0 < S_g^*(4)$	$X_1^* = 0$, $X_2^* = 0$, $X_4^* > 0$
$1.143 \times 10^{-4} \leq \alpha \leq 1.2 \times 10^{-4}$	$S_g^*(1) = S_g^*(2) < S_g^*(4) < 0$	$X_1^* = 0$, $X_2^* = 0$, $X_4^* = 0$

In scenario B, glucose fermenter 4 is associated with a fermentation pathway that yields 2.66 moles of hydrogen per mole of glucose fermented leading to more hydrogen production (a greater hydrogen generation rate) than in scenario A (which yields between one to two moles of hydrogen per mole of glucose fermented) for the same amount of glucose generation rate. The greater hydrogen generation rate for scenario B can support a greater methanogen population than that of scenario A (as discussed in Section 2.4) and is illustrated in the difference between Figures 5.15 and 5.14. In Figure 5.15, at $\alpha \geq 1.04 \times 10^{-4}$ s^{-1} = $Y_m(n_mq_m - m_m)$, methanogens are eliminated due to not being able to reproduce fast enough to match the passage rate, even though there is sufficient food supply. This is in contrast to Figure 5.14, scenario A where at $\alpha \geq 1.026 \times 10^{-4}$ s^{-1} = $Y_1(n_1q_1 - m_1)$, methanogens are eliminated because of insufficient food supply due to both type of glucose fermenters 1 and 2 being eliminated and hence no hydrogen being produced from fermentation. Figures 5.16, 5.17 and 5.18 are, respectively, the stable steady state substrate concentration, VFA concentrations and β_h/β_g ratios for scenario B.

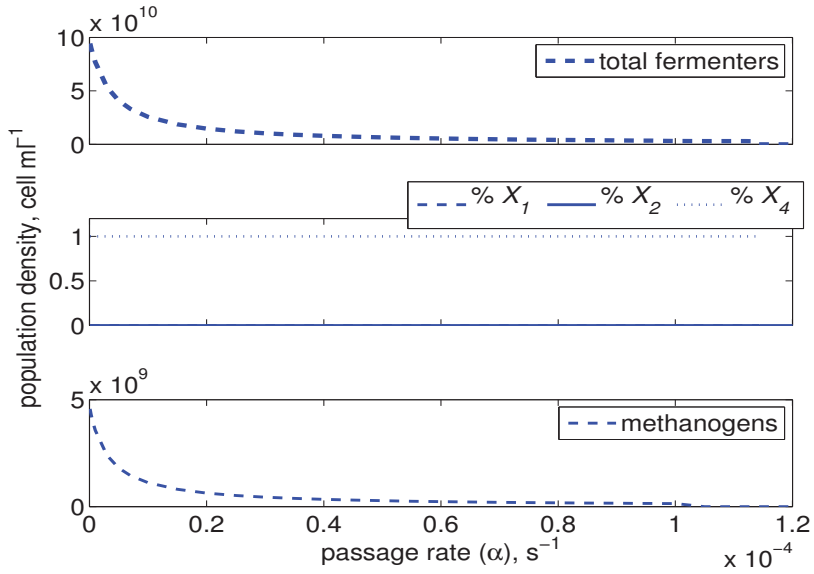

Figure 5.15: The stable steady state population densities of glucose fermenters 1, 2 and 4 and methanogens for a constant β_g and a range of passage rate values. A bifurcation occurs when $\alpha = 1.143 \times 10^{-4}$ s^{-1} = $Y_4(n_4q_4 - m_4)$ after which the stable steady state changes from co-existence of glucose fermenter populations and methanogens to the trivial solution.

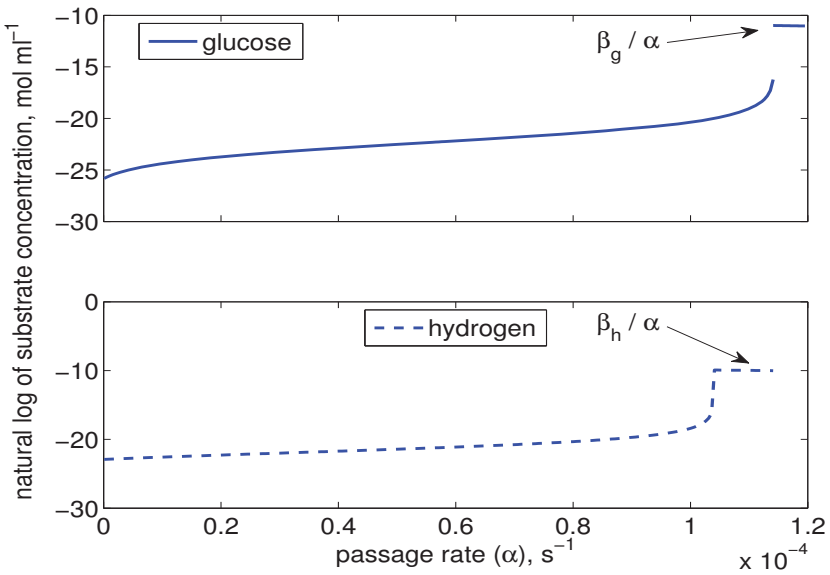

Figure 5.16: The stable steady state substrate (glucose and hydrogen) concentration for a range of passage rate values. For 1.04×10^{-4} s^{-1} $\leq$ $\alpha < 1.143 \times 10^{-4}$ s^{-1}, methanogens are eliminated by the passage rate so that the stable steady state hydrogen concentration is β_h/α. For 1.143×10^{-4} s^{-1} $\leq \alpha$, glucose fermenter 4 is eliminated by the passage rate so that the stable steady state glucose concentration is β_g/α.

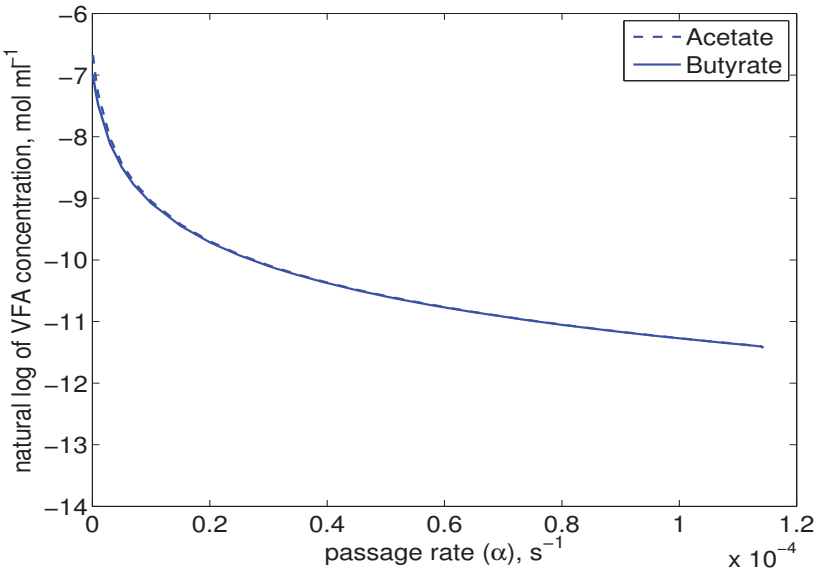

Figure 5.17: The stable steady state acetate and butyrate concentrations for a range of passage rate values. When the glucose fermenters are eliminated by increasing the passage rate, there is no acetate and butyrate production so that the corresponding steady state butyrate concentration is zero when $\alpha \geq 1.143 \times 10^{-4}$ s^{-1}. Note log(0) is negative infinity so zero concentration is not shown on graph.

Scenario C: For $0 < \alpha < 0.910 \times 10^{-4}$ s^{-1} $= Y_5(n_5 q_5 - m_5)$, the thermodynamic term of X_5 is not one, however, X_5 is out competed by X_1 and X_2 and there is a co-existence of X_1 and X_2 because X_1 and X_2 are the one with the best traits for the given environment (the one that can grow at the lowest growth limiting steady state substrate concentration will survive and the others will die out in the long term). In terms of expression (5.46), this is where $0 < S_g^*(1) = S_g^*(2) < S_g^*(5)$. For $0.910 \times 10^{-4} \leq \alpha < 1.026 \times 10^{-4}$ s^{-1}, X_5 cannot reproduce fast enough to match the passage rate and is eliminated due to passage, i.e., $S_g^*(5) < 0 < S_g^*(1) = S_g^*(2)$. Similar to scenario A (Figure 5.14), in scenario C (Figure 5.19), for 1.026×10^{-4} s^{-1} $\geq \alpha$, the stable steady state changes from co-existence of glucose fermenter populations and methanogens to the trivial solution. These results are summaried in Table 5.3. Note that the population densities of glucose fermenters 1

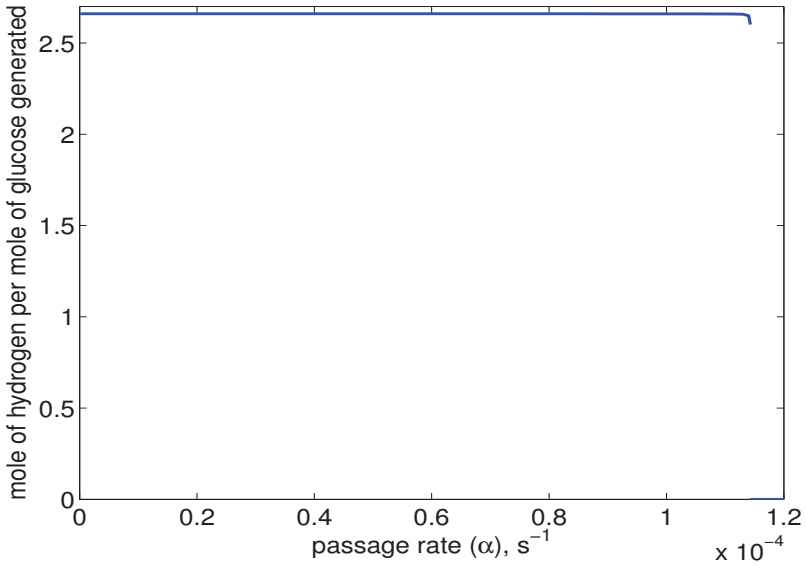

Figure 5.18: With a constant $\beta_g = 1.930 \times 10^{-9}$ mol ml^{-1} s^{-1}, β_h/β_g of the stable steady state with glucose fermenters 1, 2 and 4 is calculated over a range of passage rate values. There is essentially one value of β_h/β_g for $0 < \alpha < 1.143 \times 10^{-4}$ s^{-1} and another (0) for $\alpha \geq 1.143 \times 10^{-4}$ s^{-1}.

and 2 in Figure 5.19 is same as Figure 5.11(a). Figures 5.4, 5.12(a), 5.13(a) are, respectively, the stable steady state substrate (glucose and hydrogen) concentration, VFA concentrations and the β_h/β_g ratio for scenario C.

Table 5.3: Competition among X_1, X_2 and X_5.

Passage rate (α) (s^{-1})	Reason for stability	Stable steady state population densities
$0 < \alpha < 0.910 \times 10^{-4}$	$0 < S_g^*(1) = S_g^*(2) < S_g^*(5)$	$X_1^* > 0$, $X_2^* > 0$, $X_5^* = 0$
$0.910 \times 10^{-4} \leq \alpha < 1.026 \times 10^{-4}$	$S_g^*(5) < 0 < S_g^*(1) = S_g^*(2)$	$X_1^* > 0$, $X_2^* > 0$, $X_5^* = 0$
$1.026 \times 10^{-4} \leq \alpha \leq 1.2 \times 10^{-4}$	$S_g^*(5) < S_g^*(1) = S_g^*(2) < 0$	$X_1^* = 0$, $X_2^* = 0$, $X_5^* = 0$

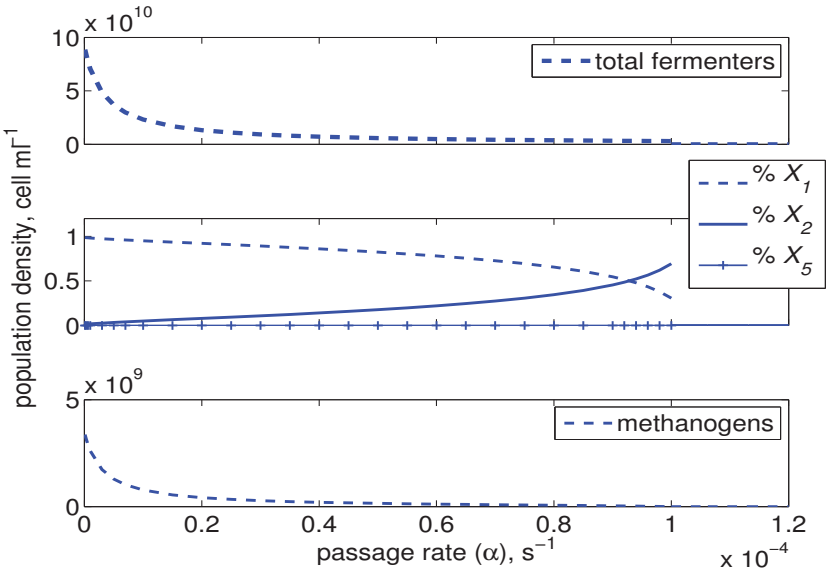

Figure 5.19: The stable steady state population densities of glucose fermenters 1, 2 and 5 and methanogens for a constant $\beta_g = 1.930 \times 10^{-9}$ mol ml^{-1} s^{-1} and a range of passage rate values. A bifurcation occurs when $\alpha = 1.026 \times 10^{-4}$ s^{-1} $= Y_1(n_1q_1 - m_1) = Y_2(n_2q_2 - m_2)$ after which the stable steady state changes from co-existence of glucose fermenter populations and methanogens to the trivial solution.

Now we explore the interaction among four types of glucose fermenters. Let $0 < \alpha \leq 1.2 \times 10^{-4}$ s^{-1} and $\beta_g = 1.930 \times 10^{-9}$ mol ml^{-1} s^{-1}. All the ruminal parameters are the same as used in Section 5.3.2. Suppose initially only fermenters 1 and 2 exist. Introducing two of glucose fermenter 3, 4 or 5 into the model with glucose fermenters 1 and 2 leads to one of three scenarios.

Scenario D. We start with X_1, X_2, X_3 and X_4.

Scenario E. We start with X_1, X_2, X_3 and X_5.

Scenario F. We start with X_1, X_2, X_4 and X_5.

Scenario D: Note that for any value of passage rate $0 < \alpha \leq 1.2 \times 10^{-4}$ s^{-1}, X_3 cannot survive because its thermodynamic term is always one so that $S_g^*(3) < 0$. As noted in Table 5.4. From Table 5.4, there is no survivor except glucose fermenter 4 ($X_4^* > 0$) for

$0 < \alpha < 1.143 \times 10^{-4}$ s^{-1}. Otherwise, the trivial solution is the stable steady state solution. The stable steady state population densities for glucose fermenters in scenario D are the same as in Figure 5.15 with $X_3^* = 0$.

Table 5.4: Competition among X_1, X_2, X_3 and X_4.

Passage rate (α) (s^{-1})	Reason for stability	Stable steady state population densities
$0 < \alpha < 1.026 \times 10^{-4}$	$S_g^*(3) < 0 < S_g^*(4) < S_g^*(1) = S_g^*(2)$	$X_1^* = X_2^* = X_3^* = 0$, $X_4^* > 0$
$1.026 \times 10^{-4} \leq \alpha < 1.143 \times 10^{-4}$ s^{-1}	$S_g^*(3) < S_g^*(1) = S_g^*(2) < 0 < S_g^*(4)$	$X_1^* = X_2^* = X_3^* = 0$, $X_4^* > 0$
1.143×10^{-4} s$^{-1} \leq \alpha \leq 1.2 \times 10^{-4}$	$S_g^*(3) < S_g^*(1) = S_g^*(2) < S_g^*(4) < 0$	$X_1^* = X_2^* = X_3^* = X_4^* = 0$

Scenario E: As noted in Table 5.5. the only survivors for $0 < \alpha < 1.026 \times 10^{-4}$ s^{-1} are glucose fermenters 1 and 2 ($X_1^* > 0$ and $X_2^* > 0$). Otherwise, the trivial solution is the stable steady state solution. The stable steady state population densities for glucose fermenters for scenario E are the same as in Figure 5.19 with $X_3^* = 0$.

Table 5.5: Competition among X_1, X_2, X_3 and X_5.

Passage rate (α) (s^{-1})	Reason for stability	Stable steady state population densities
$0 < \alpha < 0.910 \times 10^{-4}$	$S_g^*(3) < 0 < S_g^*(1) = S_g^*(2) < S_g^*(5)$	$X_1^* = 0$, $X_2^* > 0$, $X_3^* > 0$, $X_5^* = 0$
$0.910 \times 10^{-4} \leq \alpha < 1.026 \times 10^{-4}$ s^{-1}	$S_g^*(3) < S_g^*(5) < 0 < S_g^*(1) = S_g^*(2)$	$X_1^* = 0$, $X_2^* > 0$, $X_3^* > 0$, $X_5^* = 0$
1.026×10^{-4} s$^{-1} \leq \alpha \leq 1.2 \times 10^{-4}$	$S_g^*(3) < S_g^*(5) < S_g^*(1) = S_g^*(2) < 0$	$X_1^* = X_2^* = X_3^* = X_5^* = 0$

Scenario F: If $0 < \alpha < 0.910 \times 10^{-4}$ s^{-1} $= Y_5(n_5 q_5 - m_5)$, X_5 is out competed by X_1, X_2 and X_4. Also, X_1 and X_2 are out competed by X_4. That is, $0 < S_g^*(4) < S_g^*(1) = S_g^*(2) < S_g^*(5)$. If $0.910 \times 10^{-4} \leq \alpha < 1.026 \times 10^{-4}$ s^{-1} $= Y_1(n_1 q_1 - m_1) = Y_2(n_2 q_2 - m_2)$, X_5 is eliminated due washout, $S_g^*(5) < 0$, and X_1 and X_2 are out competed by X_4, i.e., $S_g^*(5) < 0 < S_g^*(4) < S_g^*(1) = S_g^*(2)$. For $1.026 \times 10^{-4} \leq \alpha < 1.143 \times 10^{-4}$ s^{-1}, glucose fermenters 1, 2 and 5 are all eliminated by the passage rate, i.e., $S_g^*(5) < S_g^*(1) = S_g^*(2) < 0$, and only glucose fermenter 4 remiants, i.e.,

$0 < S_g^*(4)$. If 1.143×10^{-4} s$^{-1} \leq \alpha$, glucose fermenters 1, 2, 4 and 5 are all eliminated by the passage rate. Table 5.6 is the summary for scenario F. From Table 5.6, there is no survivor except glucose fermenter 4 ($X_4^* > 0$) for $0 < \alpha < 1.143 \times 10^{-4}$ s^{-1}. Otherwise, the trivial solution is the stable steady state solution. The stable steady state population densities for glucose fermenters for scenario F are the same as in Figure 5.15 with $X_5^* = 0$.

Table 5.6: Competition among X_1, X_2, X_4 and X_5.

Passage rate (α) (s^{-1})	Reason for stability	Stable steady state population densities
$0 < \alpha < 0.910 \times 10^{-4}$ s^{-1}	$0 < S_g^*(4) < S_g^*(1) = S_g^*(2) < S_g^*(5)$	$X_1^* = X_2^* = X_5^* = 0$, $X_4^* > 0$
$0.910 \times 10^{-4} \leq \alpha < 1.026 \times 10^{-4}$	$S_g^*(5) < 0 < S_g^*(4) < S_g^*(1) = S_g^*(2)$	$X_1^* = X_2^* = X_5^* = 0$, $X_4^* > 0$
$1.026 \times 10^{-4} \leq \alpha < 1.143 \times 10^{-4}$	$S_g^*(5) < S_g^*(1) = S_g^*(2) < 0 < S_g^*(4)$	$X_1^* = X_2^* = X_5^* = 0$, $X_4^* > 0$
1.143×10^{-4} s$^{-1} \leq \alpha \leq 1.2 \times 10^{-4}$	$S_g^*(5) < S_g^*(1) = S_g^*(2) < S_g^*(4) < 0$	$X_1^* = X_2^* = X_3^* = X_4^* = 0$

Now we explore the interaction among five types of glucose fermenters. Note that for any value of passage rate $0 < \alpha \leq 1.2 \times 10^{-4}$ s^{-1}, X_3 cannot survive because its thermodynamic term is always one so that $S_g^*(3) < 0$. For glucose fermenters 1, 2, 3, 4 and 5, by combining $S_g^*(3) < 0$ with the second column of Table 5.6, this indicates that there is no survivor except glucose fermenter 4 ($X_4^* > 0$) for $0 < \alpha < 1.143 \times 10^{-4}$ s^{-1}. Otherwise, the trivial solution is the stable steady state solution. That is, the stable steady state population densities of glucose fermenter for five glucose fermenters in our example is same as in Figure 5.15 with $X_3^* = X_5^* = 0$.

These seven scenarios indicate that the GHM$^\theta$ model allows the system to select which types of fermenters survive (based on rumen environment and biological parameters). While for these five types of glucose fermenters at most two co-exist, by considering more types of glucose fermenters and/or different parameters, it is theoretically possible to construct/observe a stable co-existence of three or more types of glucose fermenters because a greater numbers of lowest positive equal steady state glucose concentration in expression (5.46) is more likely to be satisfied with a wider range of biological and ruminal parameter values provid-

ing more scenarios for co-existence of multiple glucose fermenters. For instance, for the GHM$^{\theta}$ model with 30 types of glucose fermenters, by sampling without replacement there are

$$\frac{30!}{2!(30-2)!} = 435$$

scenarios where there is a possible co-existence of any two types of fermenters. Similarly, there are 4060 scenarios for any three types of fermenters to potentially co-exist; 27405 scenarios for any four types and so on. That is, there is a total of 1.0737×10^9 scenarios for at least any two types of glucose fermenters to co-exist and only 31 where no co-existence occurs (one scenario where all 30 types are eliminated and 30 scenarios with sole survival of a single type of glucose fermenter) under any biological and ruminal parameters. In contrast, there are only four out of the eight possible scenarios that result in co-existence of at least two types of glucose fermenters when starting with three types of glucose fermenters.

Recall that changing the passage rate does not change the outcome of competitive exclusion when using the Monod growth rate model (or any other specific growth rate function that is a function of substrate only) [146]. However, by including a thermodynamic term, in the GHM$^{\theta}$ model, changing the passage rate (α) and/or other rumen environment parameters, (i.e., β_g, γ_A, γ_P and γ_B), substrate and product concentrations can change which in turn change θ_i and $S_g^*(i)$ which in turn may lead to a co-existence of different types of glucose fermenters based on expression (5.46). Remember that each type of glucose fermenter is associated with a $S_g^*(i)$. That is, when including a thermodynamic term, co-existence becomes possible for more than one value of passage rate, and changing the passage rate can potentially change the outcome of how many and which types of fermenters co-exist. This observation should be explored in future by simulations. A co-existence of different types of glucose fermenters could cause a shift in glucose fermentation pathways that can lead to differences in volatile fatty acids profiles, hydrogen generation rate, methanogens population density and methane production per mole of glucose. Such differences in methane could be explored using

the GHM$^{\theta}$ model with more types of glucose fermenters where the GHM$^{\theta}$ model will approximate a realistic rumen function.

If there is no thermodynamic term, $\sigma_i = 0$, $i \in 1, ..., nn$, and there is exactly one passage rate that allows co-existence. For any other value of passage rate, there is at most one type of glucose fermenter that can survive, which is the one with the lowest steady state glucose concentration as predicted by its biological parameters and rumen environment. That is the same analytical result presented by Hsu [64]. Under the Monod model (without thermodynamic control), for multiple types of microbes (e.g., glucose fermenters) competing for the same growth limiting substrate, at most one of them will survive [63]. However, from expression (5.46), by including a thermodynamic term, the GHM$^{\theta}$ model demonstrates a mechanism of a stable co-existence and/or competition among glucose fermenters for the same limiting substrate for growth under any given rumen environment. That is, by including a thermodynamic term, a stable co-existence of microbes competing for the same growth limiting substrate can be constructed/observed. This analytical result of stable co-existence is a breakthrough in theory. Essentially, the thermodynamic term restrains the ability of any single fermenter to use all of the glucose, giving a niche space for others with different end product leading to potential co-existence. This analytical result can be extended to explain the microbial diversity observed in other anaerobic microbial systems in which microbes compete for the same limiting substrate. Essentially, co-existence of microbes is determined by their biological parameters and the environment parameters of these biological systems. There is a stable co-existence of microbes if and only if the same lowest positive steady state substrate concentration is predicted by their biological parameters and the environment parameters (temperature, pH, etc). By considering more types of microbes, it is more likely to construct/observe a stable co-existence of microbes because expression (5.46) is more likely to be satisfied with a greater number of lowest positive equal steady state substrate concentration.

Chapter 6

Discussion and conclusions

6.1 Thesis summary

In this project, a hydrogen-methanogen dynamic model, the HM model (Chapter 2), was formulated to provide the basis for both the prediction of methane formation and a representation of the feedback of hydrogen on fermentation pathways in the rumen. The rate of hydrogen generation and volatile fatty acids production in the rumen can be differentially influenced by the efficiency of the different fermentation pathways and microbes that are active [76], [177] through the thermodynamic control imposed by the hydrogen concentration. A thermodynamic term, θ_m, with respect to the chemical reaction of metabolizing hydrogen into methane by methanogens is derived. The HM$^\theta$ model (Chapter 3) was formed by integrating θ_m into the HM model, for modeling the growth rate of methanogens with respect to hydrogen, including the inhibition effect of hydrogen concentration and products of hydrogen transformation on the rate of hydrogen metabolism. This HM$^\theta$ model was expanded by adding in glucose fermentation pathways and their associated thermodynamic control, θ_i, to model glucose-hydrogen-methanogen dynamics, the GHM$^\theta$ model (Chapter 4). The hierarchy of equations for these models (the HM, the HM$^\theta$ and the GHM$^\theta$ models) can be found in Appendix A. These models describe the interactions among substrate and product concentrations (hydrogen, glucose, acetate, propionate, butyrate) and microbes (methanogens and glucose fermenters) under different rumen

environments.

Existing mechanistic models (Section 1.4.2.1) use a net hydrogen balance, which is the difference between the amount of hydrogen produced and used in reactions occurring in the rumen on a daily basis. For existing mechanistic models, there is no explicit expression of a dynamic hydrogen pool (a net hydrogen balance is used to estimate methane production based on these models so there is no residual hydrogen after estimating the methane production). In contrast, the amount of hydrogen metabolized by the methanogen population is used to calculate methane production for any time span in the HM, the HM$^{\theta}$ and the GHM$^{\theta}$ models. That is, not all hydrogen generated becomes methane and the residual hydrogen contributes to a dynamic hydrogen pool. Importantly, the model explicitly contains a dynamic hydrogen pool and the hydrogen concentration controls the rate of methanogen growth through the Monod growth model and feedback on hydrogen production and metabolism through the thermodynamic term.

6.1.1 The HM model

Without an explicit expression of the methanogen population pool, existing mechanistic models are not capable of exploring methane mitigation strategies that target methanogens activity directly, e.g., using inhibitors. In Chapter 2, the HM model includes explicit expressions of both a dynamic hydrogen pool and methanogen population pool. The estimated methane production of the HM model is most sensitive to the hydrogen generation rate. That is expected because the rate of methane production is proportional to the net rate of hydrogen generation from feed in the rumen [68] and nearly all the hydrogen is rapidly converted to methane.

The HM model suggests that the steady state hydrogen concentration is determined by the biological parameters associated with methanogens and the passage rate, but not on the ruminal hydrogen generation rate itself. This observation is a consequence of using the Monod model [115] to describe the rate of hydrogen metabolism at a given hydrogen concentration, equation (2.1), in the HM model. The predicted effects of passage

rate on the HM model agree with the conceptual model postulated by Janssen [76]. A greater passage rate leads to a greater reproduction rate of methanogens and a greater hydrogen concentration at steady state. If the passage rate is greater than the maximal passage rate that can be tolerated by methanogens, then methanogens will be removed because they cannot reproduce fast enough to maintain themselves in the rumen. A greater hydrogen concentration is required to allow a greater reproduction rate of methanogens. The steady state hydrogen concentration thus increases with an increasing passage rate.

The HM model can potentially be used to study two approaches to reducing methane production: those targeting the activity of methanogens, i.e., those that change the biological parameters of methanogens through the use of inhibitors, and those that change the rumen environment. Inhibitors have the potential to decrease the maximal rate of hydrogen metabolism and/or increase the maintenance energy requirement of methanogens both of which lead to the methanogen population decreasing towards zero leading to less methane production. The HM model can be used to model such potential changes, both of which would result in the left hand side of inequality (2.17) becoming smaller resulting in a smaller population density of methanogens and hence less methane production. Similarly, changing the rumen environment by, for example, increasing the passage rate or decreasing the hydrogen generation rate, by for example changing the composition of the feed, leads to less methane production. The HM model can again be used to investigate the effects of such changes. In the model these changes would lead to the left hand side of inequality (2.18) becoming smaller so less hydrogen will be metabolized into methane by methanogens. Biological experiments have provided evidence that increasing passage rate leads to less methane production. Sheep that naturally produced less methane per unit of feed eaten have been reported to have smaller rumens and faster ruminal passage rate [50]. Also, increasing feeding level results in increased rumen passage rate of solids and liquids, with a concomitant reduction in methane per unit of intake [54]. Ruminants fed with fresh forages produce less methane as the amount of water in the feed

increases, presumably as an effect of acceleration of liquid passage rate in the rumen [125].

6.1.2 The HM$^{\theta}$ model

The rate at which a cell can transform a substrate to products is limited by physical constraints of the cell. These are the rate at which the substrate can be transported into the cell represented by K_m, and the rate at which the cell can transform the substrate inside the cell represented by q_m. The rate of substrate metabolism by the cell can also be limited by thermodynamic control [78]: the concentrations of substrates and products can limit the rate of substrate metabolism. The HM model (as a function of K_m and q_m) can only be used to describe the kinetic control of substrate metabolism. In Chapter 3, a representation of thermodynamic control (a thermodynamic term, θ) is developed to describe the thermodynamic feedback on the rate of substrate transformation.

The thermodynamic term developed in Chapter 3 is applicable to a wider ranges of chemical reactions than the approach to thermodynamic control developed by Kohn and Boston [84] and Offner and Sauvant [124] because θ can be calculated from the actual concentration of a chemical reaction without knowing the chemical equilibrium concentrations. Importantly, θ also accounts for the fact that living organisms need to use energy to capture ATP from a chemical reaction. As this thesis was being completed, Großkopf and Soyer [51] independently derived a representation of thermodynamic control, but without explicitly incorporating ATP formation.

The HM model incorporates a dissolved hydrogen pool that allows thermodynamic control through the hydrogen concentration to be modeled in response to changes in the pool size. The HM$^{\theta}$ model, which is the HM model with a thermodynamic term, can model the effects of thermodynamic feedback on the metabolism rate of hydrogen by a methanogen species in the rumen. When there is no thermodynamic feedback on the rate of substrate transformation, i.e., $\theta_m = 0$, the HM$^{\theta}$ model is the HM model.

From the HM$^{\theta}$ model, if the thermodynamic inhibition of substrate transformation increases ($0 < \theta_m < 1$), then the contribution of K_m will diminish and the thermodynamic control of substrate transformation will increase so that the apparent Monod constant will tend away from K_m. When there is little impact of unfavorable thermodynamics (e.g., $\theta_m = 0$), the size of the apparent Monod constant will be largely determined by the capacity of the cell to transport substrate into the cell, i.e., the apparent Monod constant will tend to K_m. This is consistent with the expectations of Jin and Bethke [78], that under thermodynamically unfavorable condition there will be a decrease in the affinity of microbes for their growth substrate and that thermodynamics rather than diffusion and cell envelope architecture will play a major role in determining the rate of substrate transformation.

One difference between the HM model and HM$^{\theta}$ model is that the HM$^{\theta}$ model can capture when methane production in the rumen reaches its chemical equilibrium, i.e., $\theta_m = 1$. However, the HM model cannot describe conditions where there is any kind of thermodynamic feedback, i.e., the HM model is only applicable to $\theta_m = 0$.

Another difference between the models is that hydrogen can be metabolized by methanogens only when the hydrogen concentration is greater than a hydrogen concentration threshold, as predicted by the HM$^{\theta}$ model. This hydrogen concentration threshold is an emergent property of the HM$^{\theta}$ model and has been measured for a range of methanogens in laboratory experiments [24]. The HM$^{\theta}$ model predicts hydrogen threshold concentrations that are of the same order of magnitude as those reported for methanogens. In contrast, in the HM model hydrogen can be metabolized by methanogens at any hydrogen concentration, meaning that the hydrogen threshold observed experimentally are not predicted by the HM model. As a result, the predicted methanogens population density of the HM model is greater than that of the HM$^{\theta}$ model and the predicted steady state hydrogen concentration of the HM model is smaller than that of the HM$^{\theta}$ model. Thus, the estimated methane production of the HM model is greater than that of the HM$^{\theta}$ model. In theory, a decreased steady state hydrogen concentration in the rumen would be

expected to feed back on hydrogen-forming steps to result in greater net hydrogen formation and methane production (i.e., hydrogen production becomes more favorable [76]). This thermodynamic feedback of hydrogen concentration on hydrogen-forming steps (i.e., hydrogen generation rate) is explored in the expansion of the HM$^\theta$ model.

6.1.3 The GHM$^\theta$ model

In the HM and HM$^\theta$ models, the hydrogen generation rate is an input parameter acting as a direct hydrogen "hose" into the rumen. In reality, hydrogen is generated from feed ingested by ruminants. The microbes in the rumen ferment the plant structural material in the feed, much of which is not able to be digested by the mammalian digestive system. The main end products of the primary fermentation of feed (Figure 1.2) are volatile fatty acids (e.g., acetate, propionate and butyrate, listed in order of increasing carbon chain length), ammonia, hydrogen, carbon dioxide and microbial cells. The volatile fatty acids are absorbed by the ruminants as energy sources for the animal or converted into animal products such as meat, milk and wool. The hydrogen is used by methanogens to produce methane, as modeled by the HM and HM$^\theta$ models. The amount and rate of methane production is proportional to the net amount and rate of hydrogen generation from fermentation pathways in the rumen [68], because nearly all the hydrogen is rapidly converted to methane. The rate of hydrogen production is determined by the activities of the different microbes using different fermentation pathways. Importantly, the amount of hydrogen formed from a given amount of feed depends on the chemical nature of the feed and on the metabolism of the microbes fermenting the feed. For the same type of feed, different feed fermentation pathways lead to different end products, including differing amounts of hydrogen, and so to differences in methane production [76]. Feed fermentation pathways are subject to thermodynamic control: if the hydrogen concentration decreases, then this leads to more hydrogen being generated from fermentation pathways and hence more methane production [76] and different microbial community composition [84]. The

GHM$^\theta$ model (Chapter 4) is an extension of the HM$^\theta$ model that includes glucose fermentation pathways (an example of feed fermentation), a thermodynamic term with respect to each of the glucose fermentation pathways and glucose fermenters.

The main three results of the GHM$^\theta$ model are demonstrated in Chapter 5. Under a GHM model based on the Monod model, there is at most one positive value of passage rate such that different types of glucose fermenters can co-exist. Otherwise, the type of glucose fermenter with the lowest positive steady state glucose concentration predicted by its biological parameters and rumen environment will outcompete the others. This analytical result, known as competitive exclusion, has previously been proved by Hsu *et al.* [63] and [64]. In contrast, the GHM$^\theta$ model which includes a thermodynamic term, predicts a range of values of passage rates that allow for a co-existence. This analytical result agrees with biological observations in the rumen [70] and has not be demonstrated in the existing mechanistic models.

Großkopf and Soyer [51] recently reported co-existence of two types of microbes metabolizing the same growth limiting substrate yielding different end products without classifying the stability of such a co-existence. In contrast, the GHM$^\theta$ model presented in this thesis demonstrates a stable co-existence of two types of glucose fermenters associated with different pathways that share at least one common end product for a range of values of passage rate and glucose generation rate. This analytical result can be generalized for infinitely many different types of glucose fermenters and could be used to explore and explain some of the observed microbial diversity in other anaerobic microbial systems in which microbes compete for the same growth limiting substrate. Also, with the same growth limiting substrate, co-existence of glucose fermenters is determined by the biological parameters (n, q, K, m, d and Y) of the glucose fermenters and the rumen environment (α, β_g, γ_A, γ_P and γ_B). That is, which types of glucose fermenters can survive associated with thermodynamically favorable fermentation pathways are effectively selected by the GHM$^\theta$ model based on biological and rumen parameters. In contrast, there was no population pools or pre-detetmined population

density for a feed type in existing models (Section 1.4.2.1).

There is exactly one stable equilibrium point for the GHM$^{\theta}$ model for any combination of biological (n, q, K, m, d and Y) and ruminal (α, β_g, γ_A, γ_P and γ_B) parameter values. If there is insufficient substrate supply, i.e., $\beta_g - \alpha S_g^* \leq 0$, then the only stable equilibrium point is where all the types of glucose fermenters cannot survive. With sufficient substrate supply, i.e., $\beta_g - \alpha S_g^* > 0$, the stable equilibrium point is then either one for which there is a stable co-existence of glucose fermenters among any number of glucose fermenters or one in which there is a competitive exclusion such that there is an extinction of all but one competitor, i.e., only one type of glucose fermenter can survive in the long term.

Under the Monod model (without thermodynamic control), for multiple types of microbes (e.g., glucose fermenters) competing for the same growth limiting substrate, only one of them will survive [63], regardless of the number of competitors [146]. However, by considering more types of glucose fermenters, it is more likely that there is a stable co-existence of multiple glucose fermenters as predicted by the GHM$^{\theta}$ model. That is, by considering more types of glucose fermenters, it is more likely to construct/observe a stable co-existence of multiple glucose fermenters from the GHM$^{\theta}$ model because there are wider ranges of biological parameters (n, q, K, m, d and Y) of the glucose fermenters and the rumen environment (α, β_g, γ_A, γ_P and γ_B) that can lead to a greater numbers of lowest positive equal steady state glucose concentration in expression (5.46).

The final main result of the GHM$^{\theta}$ model is that changing rumen environments and/or biological parameters of glucose fermenters allows different types of glucose fermenters to co-exist with a shift in glucose fermentation pathways that can lead to differences in volatile fatty acids profiles and methane production. Note that by changing the rumen environment via changing α, β_g, γ_A, γ_P and γ_B, this could change substrate concentrations that could change θ_i so that $S_g^*(i)$ will be changed. With an example of two types of glucose fermenter, by increasing passage rate, it leads to less methane production and greater propionate production that agrees with the conceptual model postulated by Janssen [76] and a chemostat experiment conducted by Isaacson *et al.* [72]. By increas-

ing passage rate, the differences in estimated methane production from the GHM$^{\theta}$ model with two types of glucose fermenter is more noticeable than the HM model. This is because increasing passage rate reduces hydrogen generation rate by switching glucose fermentation pathways via thermodynamic terms. That is, passage rate indirectly affects methane production by directly affecting the amount of hydrogen generated from fermentation pathways. The reduction of methane production based on the GHM$^{\theta}$ model with two types of glucose fermenters is ≈ 2.74 %. That is less than 11% which was reported from animal experiment [132]. This can be improved in the future work such as by including more types of glucose fermenters and glucose fermentation pathways so that the GHM$^{\theta}$ model could potentially approximate realistic rumen function.

6.2 Future work

The GHM$^{\theta}$ model could be used to explore other anaerobic ecological systems in which microbes compete for the same growth limiting substrate, for example, food processing with microbes; waste treatment and anaerobic digesters. In wastewater treatment [56], methane is formed mainly from the breakdown of acetic acid (between 60 to 70%) and that formed from hydrogen is a smaller part (between 30 and 40%). Those microbes that degrade acetate cannot establish themselves in the rumen at high densities, because they grow too slowly to maintain a population due to the high passage rates in the rumen relative to rice paddies and wastewater systems [76]. The GHM$^{\theta}$ model (in particular expression (3.8)), could be used to model the rate of transformation of a substrate to products by methanogens and the effect of all substrate and product concentrations on the metabolism rate of that substrate in the wastewater treatment.

In reality, values of the biological parameters (n, q, K, m, d and Y) of the glucose fermenters and methanogens, and the rumen environment (α, β_g, γ_A, γ_P and γ_B) are not constant but occur over some range. Each parameter value can be sampled once. With sampled parameter values, whether there is a co-existence of glucose fermenters can be determined from expression (5.46). By repeating over many samplings, one can cal-

culate the likelihoods of observing co-existence of glucose fermenters.

It is assumed that the ΔG_{ATP} is the same for both methanogens and all types of glucose fermenters. From Chapter 3, there are differences in the rate of hydrogen metabolism at low hydrogen concentration if different values of ΔG_{ATP} are used. Different values of ΔG_{ATP} for methanogens and glucose fermenters [147], [159], [160] can be used to explore their impacts on the outcomes (e.g., whether different types of glucose fermenter can co-exist by altering ΔG_{ATP}) of the full model.

The GHM$^{\theta}$ model can be expanded by introducing more types of methanogens (there are more than one type of methanogens). The focus of this thesis is on the hydrogen-using carbon dioxide-reducing rumen methanogens. There are other types of methanogens which can use methanol or other methyl compounds. These different types of methanogens use different pathways to produce methane in the rumen. The biological parameters of these different types of methanogens can be different from that of the hydrogen-using carbon dioxide-reducing rumen methanogens. Competition among any number of types of methanogens could lead to different estimated methane production. The principles developed in this thesis could be extended to include these other types of methanogens. The generalized analytical results of co-existence for glucose fermenters from the GHM$^{\theta}$ (Section 5.4.3) can be adapted to explore the competition among any number of type of methanogens.

There is a great diversity in fermentation pathways found in bacteria (Appendix B). For the same glucose fermentation pathways, the ATP gained by different types of glucose fermenters (n_i) can also vary (Appendix C). The biological parameters of different types of glucose fermenters can be different. Based on the generalized analytical results of co-existence, the GHM$^{\theta}$ model is able to explore infinitely many different combinations of pathways and glucose fermenters that are capable of maintaining themselves in the rumen. Future work should consider a minimal selection of glucose fermenters in the GHM$^{\theta}$ model and their parameters may need to be adapted to determine how to ensure that the GHM$^{\theta}$ model approximates a realistic rumen function. Such GHM$^{\theta}$ model can produce realistic methane production, calculated by expres-

sion (3.15), and volatile fatty acids profiles and need to yield realistic response in the rumen such as by increasing passage rate, whether this would lead to less methane production and greater propionate production that agrees with the conceptual model postulated by Janssen [76] and a chemostat experiment conducted by Isaacson *et al.* [72]. Recall that changing the passage rate does not change the outcome of competitive exclusion when using the Monod growth rate model (or any other specific growth rate function that is a function of substrate only) [146]. In these models ([17], [29], [96], [140], [146], [183], [184]), only one microbe (among those competing for the same growth limiting substrate) can survive in the long term. From expression (5.46), changing the passage has the potential to cause co-existence of different types and/or mixtures of glucose fermenters and so different end product profiles and estimated methane production per mole of glucose fermented, as predicted by the GHM$^{\theta}$ model. Examples can be shown via simulations.

One assumption is that the pH value of the rumen is constant. A non-constant pH (i.e., $[H^+]$) can be used in θ_i by allowing pH to vary realistically in response to volatile fatty acid concentrations in the rumen. Changing θ_i via varying pH, could reduce the activity of glucose fermenters so that less glucose can be metabolized to hydrogen for methanogens; and also lead to varying VFA concentrations that can change the pH value of the rumen and a co-existence of different types of glucose fermenters. Reducing the activity of methanogens can be achieved by reducing the pH value of rumen. By modifying expression (3.9), the effect of pH value on the activity of methanogens and hydrogen metabolism can be explored that could lead to a better estimation of methane production.

The absorption rates of acetate, butyrate and propionate in the rumen are not constant, and vary as the pH value of the rumen varies, for example. Different absorption rates lead to different VFA concentrations that could change the value of θ_i. The GHM$^{\theta}$ model could be used to explore the impact of non-constant volatile fatty acid absorption rate on the co-existence. A temporal variation in absorption rates can change rumen environments (e.g., VFA concentration) that allows different types

of glucose fermenters to co-exist with a shift in glucose fermentation pathways.

Feed and microbes pass through the rumen as ruminants keep ingesting solid feed, drinking liquid and secreting saliva, with the flow of material out of the rumen being commonly described as the passage rate. That is, passage is linked to solid feed, liquid and saliva in the rumen so that passage is not constant, and varies as feed intake and rumen fill change during the day. The GHM$^{\theta}$ model could be used to explore the impact of non-constant passage rate on the co-existence. Short-term change in passage rate might allow even more glucose fermenters to co-exist. Another assumption is that the glucose generation rate is constant. The GHM$^{\theta}$ model can be expanded to explore the nature of feed digested, feeding level and feeding frequency (that leads to different glucose generation rates) on methane production in the rumen. In the rumen, the glucose generation rate depends on the ingesting solid feed. The breaking down of the feed into glucose does not occur infinitely quickly in the rumen (this is affected by the nature of the feed). Note that passage rate is dependent on the ingesting solid feed. That is, both rates of glucose generation and passage are dependent on the amount and nature of solid feed. In future investigations, based on the nature of feed digested, feeding level and feeding frequency, both rates of glucose generation and passage can be self adjusted by the GHM$^{\theta}$ model. From such an adapted model, the predicted effects of nature of feed digested, feeding level and feeding frequency on methane production need to be verified with data from experiments.

Glucose is one component of feed that enters the rumen. Other components of feed or substrate, e.g., different sugars, amino acids, etc. and the associated microbes, could be introduced by modifying the GHM$^{\theta}$ model. This can be achieved by constructing equations in the same form as equations (4.2) and (4.3). The analytical results from Chapter 5 are applicable to the GHM$^{\theta}$ model with different pathways for other sugars, amino acids, and other feed compounds, and their associated microbes. The effects of those substrate and feed compounds on methane production needed to be verified. Then, such models (adapted from the

GHM$^{\theta}$ model) can be integrated with models of whole rumen function or farm systems to address more complex assumptions and such models may help with reducing prediction errors of mechanistic modelling of enteric methane production. Existing empirical and mechanistic mathematical models of methane production from rumen have 20% to 50% prediction errors (37% [37] for Baldwin *et al.* [4]; 20% [37] for Dijkstra *et al.* [31]; 50% [82] for Moe and Tyrrell [114]; 20% [82] for Baldwin [5]). These existing models ([4], [5], [31], [114]) did not have a representation of the interaction between hydrogen and methanogen growth (i.e., hydrogen-methanogen dynamics). Such interaction is included in the GHM$^{\theta}$ model and can be modelled by employing an explicit expressions of the hydrogen pool (for modeling hydrogen feedback on fermentation pathways) and the methanogens population pool (for exploring strategies that directly target methanogens activity, e.g., inhibitors).

Ultimately, a mechanistic model with these elements could improve our ability to mathematically predict enteric methane production and support experimentation with animals for exploring mitigation strategies, at the methanogen cell level by exploring the effects of using inhibitors or vaccines and by altering the rumen environment. For example, inhibitors and vaccines can be simulated by decreasing q_m and/or increasing m_m and increasing d_m. Changes in methanogen parameters will have feedback on the selection of the glucose fermentation pathways and glucose fermenters via the hydrogen pool and θ_i, further modifying methane formation through favoring different pathways with different hydrogen stoichiometries by changing rumen environment. For example, by increasing the passage rate, this can shift fermentation pathways that leads to a lower hydrogen generation rate and methane production. The estimated methane production is calculated from expression (3.15) of the model. The model can be used to screen strategies that can reduce the magnitude of expression (3.15). Such methane mitigation strategies can then be verified by animal trials and laboratory experiments before implementing these strategies in the real world.

Appendix A

The full model equations

All the equations are listed to show the interactions among parameters and variables. This also demonstrates the bottom-up development of the mechanistic modelling of enteric methane production in the rumen.

A.1 The HM model

$$S_h' = -\frac{q_m S_h}{K_m + S_h} X_m - \alpha S_h + \beta_h \text{ (mol ml}^{-1}\text{ s}^{-1}\text{)} ,$$
$$X_m' = \Delta_m E_m X_m - \alpha X_m \text{ (cell ml}^{-1}\text{ s}^{-1}\text{)} ,$$

where

$$\Delta_m = \frac{n_m q_m S_h}{K_m + S_h} - m_m \text{ (mol}_{ATP}\text{ cell}^{-1}\text{ s}^{-1}\text{)} ,$$

and

$$E_m = \begin{cases} Y_m, & \text{if } \Delta_m(S_h) > 0 , \\ \frac{d_m}{m_m}, & \text{if } \Delta_m(S_h) \leq 0 . \end{cases}$$

Methane production

$$M = \frac{1}{4} \frac{q_m S_h}{K_m + S_h} X_m \text{ (mol ml}^{-1}\text{ s}^{-1}\text{)} .$$

Table A.1: Parameters used in the HM model.

Parameter	Description	Unit
α	passage rate through the rumen	s^{-1}
β_h	rate of hydrogen generation	mol ml^{-1} s^{-1}
n_m	ATP gained from metabolizing each mole of hydrogen	mol_{ATP} mol^{-1}
q_m	maximal rate at which a methanogen can metabolize hydrogen	mol $cell^{-1}$ s^{-1}
K_m	hydrogen concentration at half of q_m assuming no thermodynamic feedback	mol ml^{-1}
m_m	maintenance requirement of a methanogen	mol_{ATP} $cell^{-1}$ s^{-1}
d_m	death coefficient of methanogen	s^{-1}
Y_m	reproduction coefficient of methanogen	cell mol_{ATP}^{-1}

A.2 The HM$^\theta$ model

Here the thermodynamic term is incorporated to depict the effect of hydrogen concentration on the rate of hydrogen metabolism. The methane production pathway is

$$H_2 + \frac{1}{4}CO_2 \rightarrow \frac{1}{4}CH_4 + \frac{1}{2}H_2O \ ,$$

The HM$^\theta$ model is

$$\begin{aligned}
\theta_m &= \frac{[H_2O]^{\frac{1}{2}}[CH_4]^{\frac{1}{4}}}{S_h[CO_2]^{\frac{1}{4}}} \ e^{(\Delta G^o_{T_m} + n_m \ \Delta G_{ATP})/(\mathcal{R}T)} \ \text{(unitless)} \ , \\
S'_h &= -\frac{q_m S_h(1-\theta_m)}{K_m + S_h(1+\theta_m)} X_m - \alpha S_h + \beta_h \ \text{(mol } ml^{-1} \ s^{-1}) \ , \\
X'_m &= \Delta_m E_m X_m - \alpha X_m \ \text{(cell } ml^{-1} \ s^{-1}) \ ,
\end{aligned}$$

where

$$\Delta_m = \frac{n_m q_m S_h(1-\theta_m)}{K_m + S_h(1+\theta_m)} - m_m \ (mol_{ATP} \ cell^{-1} \ s^{-1}) \ ,$$

Table A.2: Additional parameters used in the HM$^\theta$ model.

Parameter	Description	Unit
$[H_2O]$	water concentration	mol ml^{-1}
$[CH_4]$	dissolved methane concentration in the rumen	mol ml^{-1}
$[CO_2]$	dissolved carbon dioxide in the rumen	mol ml^{-1}
$\Delta G^o_{T_m}$	Gibbs free energy of methane production at temperature T under standard conditions	kJ mol^{-1}
ΔG_{ATP}	energy required to generate one unit of ATP	kJ mol$^{-1}_{ATP}$
$\mathcal{R}$	ideal gas constant	kJ mol^{-1} K^{-1}
T	temperature	K

and

$$E_m = \begin{cases} Y_m, & \text{if } \Delta_m(S_h) > 0 \ , \\ \frac{d_m}{m_m}, & \text{if } \Delta_m(S_h) \leq 0 \ , \end{cases}$$

with methane production

$$M^\theta = \frac{1}{4} \frac{q_m S_h (1-\theta_m)}{K_m + S_h(1+\theta_m)} X_m \text{ (mol ml}^{-1} \text{ s}^{-1}) \ .$$

A.3 The GHM$^\theta$ model

Hydrogen is generated from glucose fermentation. Each type of glucose fermenter X_i, $i = 1, ..., nn$, is associated with a glucose fermentation pathway

$$\text{glucose} + w_{wt_i} H_2O \rightarrow w_{A_i} A + w_{P_i} P + w_{B_i} B + w_{h_i} H_2 + w_{cd_i} CO_2 + w_{H^+{}_i} H^+ \ .$$

The thermodynamic term θ_m affects the rates of hydrogen generation and metabolism. The generalized GHM$^\theta$ model is the HM$^\theta$ model with additional equations:

$$\theta_i = \frac{(S_A)^{w_{A_i}} (S_P)^{w_{P_i}} (S_B)^{w_{B_i}} (S_h)^{w_{h_i}} [CO_2]^{w_{cd_i}} [H^+]^{w_{H^+{}_i}}}{S_g [H_2O]^{w_{wt_i}}} \ e^{(\Delta G^o_{T_i} + n_i \ \Delta G_{ATP})/(\mathcal{R}T)} \text{ (unitless)} \ ,$$

$$S_g' = -\sum_{i=1}^{nn} \frac{q_i S_g(1-\theta_i)}{K_i + S_g(1+\theta_i)} X_i - \alpha S_g + \beta_g \text{ (mol ml}^{-1}\text{ s}^{-1}) ,$$
$$X_i' = \Delta_i E_i X_i - \alpha X_i \text{ (cell ml}^{-1}\text{ s}^{-1}) ,$$

3910 where

$$\Delta_i(S_g) = \frac{n_i q_i S_g(1-\theta_i)}{K_i + S_g(1+\theta_i)} - m_i \text{ (mol}_{ATP}\text{ cell}^{-1}\text{ s}^{-1}) ,$$

3911 and

$$E_i = \begin{cases} Y_i, & \text{if } \Delta_i(S_g) > 0 , \\ \frac{d_i}{m_i}, & \text{if } \Delta_i(S_g) \leq 0 . \end{cases}$$

3912

$$S_A' = \sum_{i=1}^{nn} w_{A_i} \frac{q_i S_g(1-\theta_i)}{K_i + S_g(1+\theta_i)} X_i - \gamma_A S_A - \alpha S_A \text{ (mol ml}^{-1}\text{ s}^{-1}) ,$$
$$S_P' = \sum_{i=1}^{nn} w_{P_i} \frac{q_i S_g(1-\theta_i)}{K_i + S_g(1+\theta_i)} X_i - \gamma_P S_P - \alpha S_P \text{ (mol ml}^{-1}\text{ s}^{-1}) ,$$
$$S_B' = \sum_{i=1}^{nn} w_{B_i} \frac{q_i S_g(1-\theta_i)}{K_i + S_g(1+\theta_i)} X_i - \gamma_B S_B - \alpha S_B \text{ (mol ml}^{-1}\text{ s}^{-1}) ,$$

3913 and

$$\beta_h = \sum_{i=1}^{nn} w_{h_i} \frac{q_i S_g(1-\theta_i)}{K_i + S_g(1+\theta_i)} X_i \text{ (mol ml}^{-1}\text{ s}^{-1}) .$$

Table A.3: Additional parameters used in the GHM$^{\theta}$ model.

Parameter	Description	Unit
$\gamma_A\ \gamma_P\ \gamma_B$	absorption rate of acetate, propionate and butyrate	s^{-1}
β_g	rate of glucose generation	mol ml^{-1} s^{-1}
n_i	ATP gained by glucose fermenter i metabolizing per mole of glucose	mol_{ATP} mol^{-1}
q_i	maximal rate at which glucose fermenter i can metabolize glucose	mol $cell^{-1}$ s^{-1}
K_i	glucose concentration at half of q_i assuming no thermodynamic feedback	mol ml^{-1}
m_i	maintenance requirement of glucose fermenter i	mol_{ATP} $cell^{-1}$ s^{-1}
d_i	death coefficient of glucose fermenter i	s^{-1}
Y_i	reproduction coefficient of glucose fermenter	cell mol_{ATP}^{-1}
$[H^+]$	hydrogen ion concentration	mol ml^{-1}
$\Delta G^o_{T_i}$	Gibbs free energy of glucose fermentation at temperature T under standard conditions	kJ mol^{-1}
$w_{A_i}\ w_{P_i}\ w_{B_i}$	moles of acetate, propionate and butyrate generated from each mole of glucose fermented by glucose fermenter i	unitless
$w_{wt_i}\ w_{cd_i}\ w_{H^+{}_i}$	moles of water, carbon dioxide and hydrogen ions generated from each mole of glucose fermented by glucose fermenter i	unitless
w_{h_i}	moles of hydrogen generated from each mole of glucose fermented by glucose fermenter i	unitless

Appendix B

Fermentation pathways

In the rumen, there is a diversity in fermentation pathways of glucose, glutamate, alanine and lactate etc [118]. There are more glucose fermentation pathways than those listed in Section 4.1. For example, five theoretical fermentation pathways

$$\begin{aligned}
&\text{glucose} + 2\ \mathrm{H_2O} \rightarrow 2\ A + 4\ \mathrm{H_2} + 2\ \mathrm{CO_2} + 2\ \mathrm{H^+}\ ,\\
&\text{glucose} + 2/3\ \mathrm{H_2O} \rightarrow 2/3\ A + 2/3\ B + 8/3\ \mathrm{H_2} + 2\ \mathrm{CO_2} + 4/3\ \mathrm{H^+}\ ,\\
&\text{glucose} \rightarrow B + 2\ \mathrm{H_2} + 2\ \mathrm{CO_2} + \mathrm{H^+}\ ,\\
&\text{glucose} \rightarrow A + P + \mathrm{H_2} + \mathrm{CO_2} + 2\ \mathrm{H^+}\ ,\\
&\text{glucose} \rightarrow 2/3\ A + 4/3\ P + 2/3\ \mathrm{CO_2} + 2/3\ \mathrm{H_2O} + 2\ \mathrm{H^+}\ ,
\end{aligned}$$

were identified to explore fermentation thermodynamics [76]. Here A, P and B, respectively, represent the volatile fatty acids: acetate, propionate and butyrate. In reality, there five pathways are points on a continuum glucose fermentation pathways.

$$\underset{2\ \mathrm{H_2}}{B} \longleftrightarrow \underset{8/3\ \mathrm{H_2}}{2/3\ A + 2/3\ B} \longleftrightarrow \underset{4\ \mathrm{H_2}}{2\ A} \longleftrightarrow \underset{\mathrm{H_2}}{A + P} \longleftrightarrow 2/3\ A + 4/3\ P$$

$$\xleftarrow{\text{more } B \text{ production}} \quad \underset{\text{production}}{\text{most } \mathrm{H_2}} \quad \xrightarrow{\text{more } P \text{ production}}$$

For simplicity, CO_2, H^+, and H_2O are not shown. Each pathway within this continuum regime could be associated with different types of glucose fermenters and different ATP yields (Appendix C) that may be considered in the GHM$^\theta$ model.

Appendix C

ATP yields from glucose fermentation

For the GHM$^{\theta}$ model, each glucose fermenter is assumed to be associated with one pathway. Each metabolic scheme for glucose fermentation will be considered in three steps: glucose uptake, fermentation to pyruvate, and further metabolism of pyruvate.

C.1 Glucose uptake

Four possible mechanisms of glucose uptake into the cell of glucose fermenters are considered, based on those reviewed by [73]. They are:

1. Glucose uptake coupled to the use of 1 ATP via an ABC transporter, resulting in 1 glucose transported from outside to inside the cell.

2. Glucose uptake coupled to the use of 1 cation (proton or sodium) via a symporter, resulting in 1 glucose transported from outside to inside the cell. The generation of the proton or sodium gradient to drive the symporter requires 1/3 ATP per cation, although this can vary from 3/8 to 3/11 [108].

3. Glucose uptake via a facilitated diffusion transport mechanism, resulting in 1 glucose transported from outside to inside the cell.

4. Glucose uptake coupled to conversion of 1 phosphoenolpyruvate (PEP) to 1 pyruvate using the phosphotransferase system (PTS), resulting in the uptake of 1 glucose from outside the cells to form 1 glucose-6-phosphate inside the cell.

C.2 Fermentation to pyruvate

For the numerical study of the GHM$^{\theta}$ model, it is assumed that glucose is fermented using the Embden-Meyerhof-Parnas pathway, as described by [49]. It also allows the variation that the ATP used in the phosphofructokinase (PFK) step may be replaced by the use of pyrophosphate (PPi), which has the net result of consuming 2 ATP in this step [75]. When glucose uptake is coupled to the use of PEP, no ATP is used in the activation of glucose to glucose-6-phosphate because that product is formed in the transport step, but 1 PEP is converted to pyruvate without formation of ATP at the PEP kinase step. The variations are therefore:

1. Glucose fermentation to 2 pyruvate using ATP at the PFK step, with the net gain of 2 ATP and 4 electrons. This can follow from glucose uptake mechanisms 1, 2, and 3.

2. Glucose fermentation to 2 pyruvate using PPi at the PFK step, with the net gain of 1 ATP and 4 electrons. This can follow from glucose uptake mechanisms 1, 2, and 3.

3. Glucose-6-phosphate fermentation to 2 pyruvate using ATP at the PFK step, with the net gain of 2 ATP and 4 electrons. This can follow from glucose uptake mechanism 4.

4. Glucose-6-phosphate fermentation to 2 pyruvate using PPi at the PFK step, with the net gain of 1 ATP and 4 electrons. This can follow from glucose uptake mechanism 4.

C.3 Further metabolism of pyruvate

The further metabolism of pyruvate can be oxidative (generating electrons) or reductive (using electrons). Overall, the metabolic schemes must balance electrons and carbons. For the purposes of these simulations, the following uses of pyruvate are considered (based on [49]):

1. Oxidation of pyruvate to acetate plus carbon dioxide, coupled to the generation of 1 ATP and 2 electrons.

2. Reduction of pyruvate to propionate, coupled with the use of 4 electrons. This is the case in the acrylate pathway of propionate formation.

3. Reduction of pyruvate to propionate, coupled with the use of 4 electrons and generation of 2/3 ATP [142]. This can occur in the succinate or randomizing pathway of propionate formation.

4. Oxidation of pyruvate to butyrate and carbon dioxide. Formally, this is described as 1 pyruvate being metabolized to 1/2 butyrate, 1 carbon dioxide, with no net formation or use of electrons, and generation of 1/2 ATP.

A complete metabolic scheme for any single glucose fermenters will have to balance carbon atoms in glucose and the various products (e.g., carbon dioxide, acetate, propionate, and butyrate), and the electrons derived from oxidations and used in reductions. Glucose is a 6-carbon compound, and pyruvate is a 3-carbon compound. The products of pyruvate metabolism considered here are carbon dioxide, acetate, propionate, and butyrate, with 1, 2, 3, and 4 carbons respectively. Lactate is another potential product, as are succinate, formate, ethanol and alanine. Excess electrons are used to generate hydrogen, with 2 electrons being used to generate 1 hydrogen. Hydrogen formation may not always be thermodynamically feasible if the prevailing hydrogen concentration is too high [34], and the GHM$^{\theta}$ model accounts for that, by penalizing glucose fermenters that use metabolisms that are unfavorable under the prevailing conditions (measured by θ_i). For each glucose fermentation pathway and

its associated glucose fermenters, X_i, there will be a net amount of ATP generated per glucose molecule fermented, n_i, that will be used in the numerical study. For instance, in Section 5.2, for glucose fermenter X_1 associated with pathway

$$\text{glucose} \rightarrow B + 2\ \text{H}_2 + 2\ \text{CO}_2 + \text{H}^+\ ,$$

$n_1 = 3\ \text{mol}_{ATP}\ \text{mol}^{-1}$ is used. This is the maximal ATP yield per mole of glucose fermented via glucose uptake mechanisms 3 or 4 (no ATP needed); followed by fermentation of glucose to pyruvate by variations 1 or 3 ($2\ \text{mol}_{ATP}\ \text{mol}^{-1}$ generated per mole of glucose fermented), and then metabolism of pyruvate to butyrate ($1\ \text{mol}_{ATP}\ \text{mol}^{-1}$ generated). However, n_1 could also be as low as $1\ \text{mol}_{ATP}\ \text{mol}^{-1}$, if glucose is fermented via glucose uptake mechanisms 1 (1 ATP required); followed by fermentation of glucose to pyruvate by variations 2 or 4 ($1\ \text{mol}_{ATP}\ \text{mol}^{-1}$ generated per mole of glucose fermented), and then metabolism of pyruvate to butyrate ($1\ \text{mol}_{ATP}\ \text{mol}^{-1}$ generated). Overall, the possible variety of glucose fermentation pathways and ATP yields is very large, and glucose is of course only one component of feed that enters the rumen.

Bibliography

[1] Alberty RA and Goldberg RN (1992) Standard thermodynamic formation properties for the adenosine 5'-triphosphate series. Biochemistry 31, 10610 – 10615.

[2] Aledo JC (2001) Metabolic pathways: does the actual Gibbs free-energy change affect the flux rate? Biochem Mol Biol Educ 29, 142 – 143.

[3] Axelsson J (1949) The amount of produced methane energy in the European metabolic experiments with adult cattle. Anu Rep Agric Coll Sweden. 16, 404 – 409.

[4] Baldwin RL, Thornley JHM and Beever DE (1987) Metabolism of the lactating cow: II. Digestive elements of a mechanistic model. J Dairy Res 54, 107 – 131.

[5] Baldwin RL (1995) Modeling ruminant digestion and metabolism. Chapman and Hall, London, UK.

[6] Bani Shahabadi M, Yerushalmi L and Haghighat F (2010) Estimation of greenhouse gas generation in wasterwater treatment plants - Model development and application. Chemosphere 78, 1085 – 1092.

[7] Beauchemin KA and McGinn SM (2005) Methane emissions from feedlot cattle fed barley or corn diets. J Anim Sci 83, 653 – 661.

[8] Beauchemin KA and McGinn SM (2006) Methane emissions from beef cattle: Effects of fumaric acid, essential oil and canola oil. J Anim Sci 84, 1489 – 1496.

4044 [9] Beltrami E (1987) Mathematics for dynamic modeling. Academic
4045 press, Inc. California, USA.

4046 [10] Benchaar C, Rivest J, Pomar C, Chiquette J (1998) Prediction
4047 of methane production from dairy cows using existing mechanistic
4048 models and regression equations. J Anim Sci 76, 617 – 627.

4049 [11] Blasing TJ and Smith K (2006) Recent Greenhouse Gas Concen-
4050 trations, Oak Ridge National Laboratory, United State Depart-
4051 ment of Energy. http://cdiac.ornl.gov/pns/current_ghg.html. Ac-
4052 cessed 06/03/2014.

4053 [12] Black JL, Beever DE, Faichney GJ Howarth BR, Graham NM
4054 (1981) Simulation of the effects of rumen function on the flow of
4055 nutrients from the stomach of sheep: Part 1 – description of a
4056 computer program. Agric Sys 6, 195 – 219.

4057 [13] Blaxter KL and Clapperton JL (1965) Prediction of the amount of
4058 methane produced by ruminants. Br J Nutr 19, 511 – 522.

4059 [14] Bratzler JW and Forbes EB (1940) The estimation of methane
4060 production by cattle. J Nutr 19, 611 – 613.

4061 [15] Buckel W and Thauer RK (2013) Energy conservation via elec-
4062 tron bifurcating ferredoxin reduction and proton/Na^+ translocat-
4063 ing ferredoxin oxidation. Biochimica et Biophysica Acta 1827, 94 –
4064 113.

4065 [16] Buddle BM, Denis M, Attwood GT, Altermann E, Janssen PH,
4066 Ronimus RS, Pinares-Patiño CS, Muetzel S, Wedlock DN (2011)
4067 Strategies to reduce methane emissions from farmed ruminants
4068 grazing on pasture. Vet J 188, 11 – 17.

4069 [17] Butler GJ and Wolkowicz GK (1985) A mathematical model of
4070 the chemostat with a general class of functions describing nutrient
4071 uptake. SIAM J Appl Math 45, 138 – 151.

4072 [18] Button DK (1991) Biochemical basis for whole-cell uptake kinet-
4073 ics: Specific affinity, oligotrophic capacity, and the meaning of the
4074 Michaelis constant. Appl Environ Microbiol 57, 2033 – 2038.

4075 [19] Campbell IM (1988) Catalysis at surfaces. Chapman and Hall.
4076 Springer Netherlands.

4077 [20] Cao M, Gregson K and Marshall S (1998) Global methane emission
4078 from wetlands and its sensitivity to climate change. Atmos Environ
4079 32, 3293 – 3299.

4080 [21] Chang R (2005) Physical chemistry for the biosciences. University
4081 Science Books. California, USA.

4082 [22] Christophersen CT, Wright ADG and Vercoe PE (2008) In vitro
4083 methane emission and acetate: propionate ratio are decreased when
4084 artificial stimulation of the rumen wall is combined with increasing
4085 grain diets in sheep. J Anim Sci 86, 384 – 389.

4086 [23] Clark H, Kelliher F and Pinares-Patiño CS (2011) Reducing CH_4
4087 emissions from grazing ruminants in New Zealand: challenges and
4088 opportunities. Asian-Australas J Anim Sci 24, 295 – 302.

4089 [24] Cord-Ruwisch R, Seitz HJ and Conrad R (1988) The capacity of
4090 hydrogenotrophic anaerobic bacteria to compete for traces of hy-
4091 drogen depends on the redox potential of the terminal electron
4092 acceptor. Arch Microbiol 149, 350 – 357.

4093 [25] Costello DJ, Greenfieldo PF and Lee PL (1991) Dynamic modelling
4094 of a single-stage high-rate anaerobic reactor – I. Model derivation.
4095 Water Res 25, 847 – 858.

4096 [26] Cottle DJ, Nolan JV and Wiedemann SG (2011) Ruminant enteric
4097 methane mitigation: a review. Anim Prod Sci 51, 491 – 514.

4098 [27] Czerkawski JW (1969) Methane production in ruminants and its
4099 significance. World Rev Nutr Diet 11, 240 – 282.

[28] Czerkawski JW and Breckenridge G (1969) Fermentation of various soluble carbohydrates by rumen micro-organisms with particular reference to methane production. Br J Nutr 23, 925 – 937.

[29] De Leenheer P, Li B and Smith HL (2003) Competition in the chemostat: some remarks. Can Appl Math Q 11, 229 – 230.

[30] Denman SE, Tomkin NW and McSweeney CS (2007) Quantitation and diversity analysis of ruminal methanogenic populations in response to the antimnthanogenic compound bromochloromethane. FEMS Microbiol ecol 62, 313 – 322.

[31] Dijkstra J, Neal HDSTC, Beever DE, France J (1992) Simulation of nutrient digestion, absorption and outflow in the rumen: Model description. J Nutr 122, 2239 – 2256.

[32] Dijkstra J, Boer H, van Bruchem J, Bruining M, Tamminga S (1993) Absorption of volatile fatty acids from the rumen of lactating dairy cows as influenced by volatile fatty acid concentration, pH and rumen liquid volume. Br J Nutr 69, 385 – 396.

[33] Dijkstra J (1994) Production and absorption of volatile fatty acids in the rumen. Livest Prod Sci 39, 61 – 69.

[34] Dolfing J (1988) Acetogenesis. In Zehnder AJB (eds) Biology of Anaerobic Microorganisms, pp 417 – 468. Wiley, New York, USA.

[35] Dziuk HE (1984) Digestion in the ruminant stomach. In Swenson MJ (eds) Dukes' physiology of domestic animals, pp 320 – 339. Cornell University Press, London, UK.

[36] El-Fadel M, Findikakis AN and Leckie JO (1989) A numerical model for methane production in managed sanitary landfills. Waste Manag Res 7, 31 – 42.

[37] Ellis JL, Bannink A, France J, Kebreab, E, Dijkstra J (2010) Evaluation of enteric methane prediction equations for dairy cows used in whole farm models. Glob Change Biol 16, 3246 – 3256.

[38] Ellis JL, Dijkstra J, Kebreab E, Bannink A, Odongo NE, McBride BW, France J (2008) Aspects of rumen microbiology central to mechanistic modelling of methane production in cattle. J Agri Sci 146, 213 – 233.

[39] Ellis JL, Kebreab E, Odongo NE, Beauchemin K, McGinn S, Nkrumah JD, Moore SS, Christopherson R, Murdoch GK, McBride BW, Okine EK, France J (2009) Modelling methane production from beef cattle using linear and nonlinear approaches. J Anim Sci 87, 1334 – 1345.

[40] Engel PC (1977) Enzyme kinetics (outline studies in biology). Chapman and Hall Ltd. London.

[41] Evans E (1981) An evaluation of the relationships between dietary parameters and rumen solid turnover rate. Can J Anim Sci 61, 91 – 103.

[42] Feist AM, Scholten JCM, Palsson BØ, Brockman FJ, Ideker T (2006) Modeling methanogenesis with a genome-scale metabolic reconstruction of *Methanosarcina barkeri*. Mol Syst Biol 2, 2006.0004.

[43] Fernando SC, Purvis II HT, Najar FZ, Sukharnikov LO, Krehbiel CR, Nagaraja TG, Roe BA, DeSilva U (2010) Rumen microbial population dynamics during adaptation to a high-grain diet. Appl Environ Microbiol 76, 7482 – 7490.

[44] Finlay BJ, Esteban G, Clarke KJ, Williams AG, Embley TM, Hirt RR (1994) Some rumen ciliates have endosymbiotic methanogens. FEMS Microbiol Lett 117, 157 – 162.

[45] Foley PA, Kenny DA, Callan JJ, Boland TM, OMara F P (2009). Effect of DL-malic acid supplementation on feed intake, methane emission, and rumen fermentation in beef cattle. J Anim Sci, 87, 1048 – 1057.

4157 [46] Fonty G, Joblin K, Chavarot M, Roux R, Naylor G, Michallon F
4158 (2007) Establishment and development of ruminal hydrogenotrophs
4159 in methanogen-free lambs. Appl Environ Microbiol 73, 6391 – 6403.

4160 [47] Gerber M and Span R (2008) An analysis of available mathematical
4161 models for anaerobic digestion of organic substances for production
4162 of biogas. Presented at international gas union research conference.
4163 Paris.

4164 [48] Goel G, Makkar HPS and Becker K (2008) Changes in microbial
4165 community structure, methanogenesis and rumen fermentation in
4166 response to saponin-rich fractions from different plant materials. J
4167 Appl Microbiol 105, 770 – 777.

4168 [49] Gottschalk G (1986) Bacterial metabolism, 2nd edition. Springer,
4169 New York, USA.

4170 [50] Goopy JP, Donaldson A, Hegarty R, Vercoe PE, Haynes F, Barnett
4171 M, Oddy HV (2014) Low-methane yield sheep have smaller rumens
4172 and shorter rumen retention time. Br J Nutr 111, 578 – 585.

4173 [51] Großkopf T and Soyer OS (2016) Microbial diversity arising from
4174 thermodynamic constraints. ISME J 10, 2725 – 2733.

4175 [52] Hackmann TJ and Spain, JN (2010) Invited review: Ruminant
4176 ecology and evolution: Perspectives useful to ruminant livestock
4177 research and production. J Dairy Sci 93, 1320 – 1334.

4178 [53] Haldane JBS (1930) Enzymes. Longmans. London.

4179 [54] Hammond KJ, Burke JL, Koolaard JP, Muetzel S, Pinares-Patiño
4180 CS, Waghorn GC (2013) Effects of feed intake on enteric methane
4181 emissions from sheep fed fresh white clover (*Trifolium repens*) and
4182 perennial ryegrass (*Lolium perenne*) forages. Anim Feed Sci Tech-
4183 nol 179, 121 – 132.

4184 [55] Henderson G, Cox F, Ganesh S, Jonker A, Young W, Global Ru-
4185 men Census Collaborators, Janssen PH (2015) Rumen microbial

community composition varies with diet and host, but a core microbiome is found across a wide geographical range. Sci Rep 5, 14567.

[56] Hill DT (1982) A comprehensive dynamic model for animal waste methanogenesis. T ASAE 25, 1374 – 1380.

[57] Hirsch MW, Smale S and Devaney RL (2013) Differential equations, dynamical systems, and an introduction to chaos. 3rd edition. Academic Press, San Diego, USA.

[58] Hoh CY and Cord-Ruwisch R (1996) A practical kinetic model that considers endproduct inhibition in anaerobic digestion processes by including the equilibrium constant. Biotechnol Bioeng. 51, 597 – 604.

[59] Holter JB and Young AJ (1992) Methane prediction in dry and lactating Holstein cows. J Dairy Sci 75, 2165 – 2175.

[60] Holzapfel-Pschorn A, Conrad R and Seiler W (1985) Production, oxidation and emission of methane in rice paddies. FEMS Microbiol Ecol 31, 343 – 351.

[61] Hristov AN, Oh J, Firkins JL, Dijkstra J, Kebreab E, Waghorn G, Makkar HPS, Adesogan AT, Yang W, Lee C, Gerber PJ, Henderson B, Tricarico JM (2013) Special topics mitigation of methane and nitrous oxide emissions from animal operations: I. A review of enteric methane mitigation options. J Anim Sci 91, 5045 – 5069.

[62] Hristov AN, Oh J, Giallongo F, Frederick TW, Harper MT, Weeks HL, Branco AF, Moate PJ, Deighton MH, Williams SRO, Kindermann M, Duval S (2015) An inhibitor persistently decreased enteric methane emission from dairy cows with no negative effect on milk production. Proc Natl Acad Sci USA 112, 10663 – 10668.

[63] Hsu SB, Hubbell S and Waltman P (1977) A mathematical theory for single-nutrient competition in continuous clutures of microorganisms. SIAM J Appl Math 32, 366 – 383.

[64] Hsu SB (1978) Limiting behavior for competing species. SIAM J Appl Math 34, 760 – 763.

[65] Huang Y, Sass RL and Fisher Jr. FM (1998) Model estimates of methane emission from irrigated rice cultivation of China. Glob Change Biol 4, 809 – 821.

[66] Huang Y, Zhang W, Zheng X, Li J, Yu Y (2004) Modeling methane emissions from rice paddies with various agricultural practice. J Geophys Res 109, D08113.

[67] Hungate RE (1966) The rumen and its microbes. Academic Press New York. NY, USA.

[68] Hungate RE (1967) Hydrogen as an intermediate in the rumen fermentation. Arch Mikrobiol 59, 158 – 164.

[69] Hungate RE, Reichl and Prins R (1971) Parameters of rumen fermentation in a continuously fed sheep: evidence of a microbial rumination pool. Appl Microbiol 22, 1104 – 1113.

[70] Hungate RE (1975) The rumen microbial ecosystem. Annu Rev Ecol Syst 6, 39 – 66.

[71] Intergovernmental Panel on Climate Change (2007) Climate change 2007: synthesis report. https://www.ipcc.ch/publications_and_data/publications_ipcc_fourth_assessment_report_synthesis_report.htm. Accessed 21/04/2015.

[72] Isaacson HR, Hinds FC, Bryant MP, Owens FN (1975) Efficiency of energy utilization by mixed rumen bacteria in continuous culture. J Dairy Sci 58, 1645 – 1659.

[73] Jahreis K, Pimentel-Schmitt EF, Brückner R, Titgemeyer F (2008) Ins and outs of glucose transport systems in eubacteria. FEMS Microbiol Rev 32, 891 – 907.

[74] Janssen PH, Schuhmann A, Bak F, Liesack W (1996) Disproportionation of inorganic sulfur compounds by *Desulfocapsa thiozymogenes* gen. nov., sp. nov. Arch Microbiol 166, 184 – 192.

[75] Janssen PH (1998) Pathway of glucose catabolism by strain VeGlc2, an anaerobe belonging to the *Verrucomicrobiales* lineage of bacterial descent. Appl Environ Microbiol 64, 4830 – 4833.

[76] Janssen PH (2010) Influence of hydrogen on rumen methane formation and fermentation balances through microbial growth kinetics and fermentation thermodynamics. Anim Feed Sci Technol 160, 1 – 22.

[77] Jeyanathan J, Martin C and Morgavi DP (2014) The use of direct-fed microbials for mitigation of ruminant methane emissions: a review. Animal 8, 250 – 261.

[78] Jin Q and Bethke CM (2007) The thermodynamics and kinetics of microbial metabolism. Am J Sci 307, 643 – 677.

[79] Johnson JMF, Franzluebbers AJ, Weyers SL, Reicosky DC (2007) Agricultural opportunities to mitigate greenhouse gas emissions. Environ Pollut 150, 107 – 124.

[80] Johnson KA and Johnson DE (1995) Methane emissions from cattle. J Anim Sci 73, 2483 – 2492.

[81] Kaster AK, Moll J, Parey K, Thauer RK (2011) Coupling of ferredoxin and heterodisulfide reduction via electron bifurcation in hydrogenotrophic methanogenic archaea. Proc Natl Acad Sci USA 108, 2981 – 2986.

[82] Kebreab E, Johnson KA, Arcgibeque SL, Pape D Wirth T (2008) Model for estimating enteric methane emissions from United States dairy and feedlot cattle. J Anim Sci 86, 2738 – 2748.

[83] Kittelmann S, Pinares-Patiño CS, Seedorf H, Kirk MR, Ganesh S, McEwan JC Janssen PH (2014) Two different bacterial community types are linked with the low-methane emission trait in sheep. PloS One 9, e103171.

[84] Kohn RA and Boston RC (2000) The role of thermodynamics in controlling rumen metabolism. In McNamara JP, France J and

4276 Beever, DE (eds) Modelling nutrient utilization in farm animals
4277 10 – 24. CAB International, Wallingford, UK.

4278 [85] Kolver ES and de Veth MJ (2002) Prediction of ruminal pH from
4279 pasture-based diets. J Dairy Sci 85, 1255 – 1266.

4280 [86] Konopka A, Zakharova T and Nakatsu C (2002) Effect of starvation
4281 length upon microbial activity in a biomass recycle reactor. J Ind
4282 Microbiol Biotechnol 29, 286 – 291.

4283 [87] Kovářová-Kova K and Egli T (1998) Growth kinetics of suspended
4284 microbial cells: from single-substrate-controlled growth to mixed-
4285 substrate kinetics. Appl Environ Microbiol 62, 646 – 666.

4286 [88] Kriss M (1930) Quantitative relations of the dry matter of the
4287 food consumed, the heat production, the gaseous outgo, and the
4288 insensible loss in body weight of cattle. J Agric Res 40, 283 – 295.

4289 [89] Kubitschek HE (1970) Introduction to research with continuous
4290 cultures. Prentice-Hall, Englewood Cliffs. New Jersey, USA.

4291 [90] Kumar S, Choudhury PK, Carro MD, Griffith GW, Dagar SS,
4292 Puniya M, Calabro S, Ravella SR, Dhewa T, Upadhyay RC, Sirohi
4293 SK, Kundu SS, Wanapat M, Puniya AK (2014) New aspects and
4294 strategies for methane mitigation from ruminants. Appl Microbiol
4295 Biotechnol 98, 31 – 44.

4296 [91] Leahy SC, Kelly WJ, Ronimus RS, Wedlock DN, Altermann E
4297 and Attwood GT (2013) Genome sequencing of rumen bacteria
4298 and archaea and its application to methane mitigation strategies.
4299 Animal 7, 235 – 243.

4300 [92] Legesse G, Small JA, Scott SL, Crow GH, Block HC, Alemu AW,
4301 Robins CD, Kebreab E (2011) Predictions of enteric methane emis-
4302 sions for various summer pasture and winter feeding strategies for
4303 cow calf production. Anim Feed Sci Technol 166, 678 – 687.

4304 [93] Leng RA (2014) Interactions between microbial consortia in
4305 biofilms: a paradigm shift in rumen microbial ecology and enteric
4306 methane mitigation. Anim Prod Sci 54, 519 – 543.

4307 [94] Li CS (2000) Modeling trace gas emissions from agricultural ecosys-
4308 tems. Nutr Cycl Agroecosys 58, 259 – 276.

4309 [95] Liu H, Wang J, Wang A, Chen J (2011) Chemical inhibitors of
4310 methanogenesis and putative applications. Appl Microbiol Biotech-
4311 nol 89, 1333 – 1340.

4312 [96] Liu S, Wang X, Wang L, Song H (2013) Competitive exclusion in
4313 delayed chemostat models with differential removal rates. SIAM J
4314 Appl Math 74, 634 – 648.

4315 [97] Liu Y, Lin Y-M and Yang S-F (2003) A thermodynamic interpre-
4316 tation of the Monod model. Current Microbiol 46, 233 – 234.

4317 [98] Liu Y (2007) Overview of some theoretical approaches for deriva-
4318 tion of the Monod model. Appl Microbial Biotechnol 73, 1241 –
4319 1250.

4320 [99] Lopez S, McIntosh FM, Wallace RJ, Newbold CJ (1999) Effect of
4321 adding acetogenic bacteria on methane production by mixed rumen
4322 microorganisms. Anim Feed Sci Technol 78, 1 – 9.

4323 [100] Lovley DR (1988) Hydrogen concentrations as an indicator of the
4324 predominant terminal electron-accepting reactions in aquatic sedi-
4325 ments. Geochim Cosmochim Acta 52, 2993 – 3003.

4326 [101] Martin C, Morgavi DP and Doreau M (2010) Methane mitigation
4327 in ruminants: from microbe to the farm scale. Animal 4, 351 – 365.

4328 [102] MATLAB (R2011b) Mathwork, Inc. Natick, MA, USA.

4329 [103] McAllister TA, Okine EK, Mathison GW, Cheng KJ (1996) Di-
4330 etary, environmental and microbiological aspects of methane pro-
4331 duction in ruminants. Can J Anim Sci 76, 231 – 243.

[104] McArthur JM and Miltimore JE (1961) Rumen gas analysis by gas-solid chromatography. Can J Anim Sci 41, 187 – 196.

[105] McCollum FT and Galyean ML (1985) Cattle grazing blue grama rangeland II. seasonal forage intake and digesta kinetics. J Range Manage 6, 543 – 546.

[106] McGinn SM and Beauchemin KA (2012) Dairy farm methane emissions using a dispersion model. J Environ Qual 41, 73 – 79.

[107] Meale SJ, McAllister TA, Beauchemin KA, Harstad OM, Chaves AV (2012) Strategies to reduce greenhouse gases from ruminant livestock. Acta Agric Scand A 62, 199 – 211.

[108] Meier T, Faraldo-Gomez JD and Börsch M (2011) ATP synthase a paradigmatic molecular machine. In Frank J (eds) Molecular machines in biology, pp 208 – 238. Cambridge University Press, Cambridge, UK.

[109] Mills JAN, Dijkstra J, Banink A, Cammell SS, Kebreab E, France J (2001) A mechanistic model of whole-tract digestion and methanogenesis in the lactating dairy cow: Model development, evaluation, and application. J Anim Sci 79, 1584 – 1579.

[110] Mills JAN, Kebreab E, Yates CM, Crompton LA, Cammell SB, Dhanoa MS, Agnew RE, France J (2003) Alternative approaches to predicting methane emissions from dairy cows. J Anim Sci 81, 3141 – 3150.

[111] Ministry of the Environment (2014) New zealand's 2020 emissions target. http://www.mfe.govt.nz/publications/climate/nz-2020-emissions-target/html/index.html. Accessed 15/03/2016.

[112] Ministry of the Environment (2016) New zealand's greenhouse gas inventory. http://www.mfe.govt.nz/climate-change/reporting-greenhouse-gas-emissions/nzs-greenhouse-gas-inventory. Accessed 11/10/2016.

[113] Moate PJ, Clarke T, Davis LH, Laby RH (1997) Rumen gases and bloat in grazing dairy cows. J Agr Sci 129, 459 – 469.

[114] Moe PW and Tyrrell HF (1979) Methane production in dairy cows. J Dairy Sci 62, 1583 – 1586.

[115] Monod J (1949) The growth of bacterial cultures. Annu Rev Microbiol 3, 317 – 394.

[116] Moraes LE, Strathe AB, Fadel JG, Casper DP, Kebreab E (2014) Prediction of enteric methane emissions from cattle. Glob Change Biol 20, 2140 – 2148.

[117] Morvay Y, Bannink A, France J, Kebreab E, Dijkstra J (2011) Evaluation of models to predict the stoichiometry of volatile fatty acid profiles in rumen fluid of lactating Holstein cows. J Dairy Sci 94, 3063 – 3080.

[118] Müller V (2001) Bacterial fermentation. eLS, DOI: 10.1038/npg.els.0001415.

[119] Murray RM, Bryant AM and Leng RA (1976) Rates of production of methane in the rumen and large intestine of sheep. Br J Nutr 36, 1 – 14.

[120] Neidhrdt F, Ingraham J and Schaechter M (1990) Physiology of the bacterial cell: a molecular approach. Sinauer Associates, USA.

[121] Newbold CJ, Lassalasl B and Jouany JP (1995) The importance of methanogens associated with ciliate protozoa in ruminal methane production *in vitro*. Lett Appl Microbiol 21, 230 – 234.

[122] Nickolas JT and Priscilla AU (2007) Methane generation in landfills. Renew Energ 32, 1243 – 1257.

[123] Oetzel GR (2003) Introduction to ruminal acidosis in dairy cattle. Presented at preconvention seminar 7: dairy herd problem investigation strategies. American association of bovine practitioners. 36th Annual Conference, September 15 – 17. Columbus, OH.

[124] Offner A and Sauvant D (2006) Thermodynamic modeling of ruminal fermentations. Anim Res 55, 343 – 365.

[125] Pacheco D, Waghorn G and Janssen PH (2014) Decreasing methane emissions from ruminants grazing forages: a fit with productive and financial realities? Anim Product Sci 54, 1141 – 1154.

[126] Pathak H, Li S and Wassmann R (2005) Greenhouse gas emissions from Indian rice fields: calibration and upscaling using the DNDC model. Biogeosciences 2, 113 – 123.

[127] Patra AK and Saxena J (2009) The effect and mode of action of saponins on microbial populations and fermentation in the rumen and ruminant production. Nutr Res Rev 22, 204 – 219.

[128] Patra AK (2012) Enteric methane mitigation technologies for ruminant livestock: a synthesis of current research and future directions. Environ Monit Assess 184, 1929 – 1952.

[129] Pavlostathis SG and Giraldo-Gomez E (1991) Kinetics of anaerobic treatment. Water Sci Technol 24, 35 – 59.

[130] Peters V and Conrad R (1996) Sequential reduction processed and initiation of CH_4 production upon flooding of oxic upland soils. Soil Biol Biochem 28, 371 – 382.

[131] Pinares-Patiño CS, Ebrahimi SH, McEwan JC, Clark H and Luo D (2011) Is rumen retention time implicated in sheep differences in methane emission? Proc NZ Soc Anim Prod 71, 219 – 222.

[132] Pinares-Patiño CS, McEwan JC, Dodds KG, Cardenas EA, Hegarty RS, Koolaard JP and Clark H (2011) Repeatability of methane emissions from sheep. Anim Feed Sci Technol 166, 210 – 218.

[133] Pirt SJ (1975) Principles of microbe and cell cultivation. Blackwell Scientific Publication. Oxford, UK.

[134] Plowman KM (1973) Enzyme kinetics. McGraw-Hill, New York.

[135] Ramin M and Huhtanen P (2013) Development of equations for predicting methane emissions from ruminants. J Dairy Sci 96, 2476 – 2493.

[136] Rea S, Bowman JP, Popovski S, Pimm C, Wright AG (2007) *Methanobrevibacter millerae* sp. nov. and *Methanobrevibacter olleyae* sp. nov., methanogens from the ovine and bovine rumen that can utilize formate for growth. Int J Syst Evol Microbiol 57, 450 – 456.

[137] Ripple WJ, Smith P, Haberl H, Montzka SA, McAlpine C, Boucher DH (2014) Ruminants, climate change and climate policy. Nature Clim Change 4, 2 – 5.

[138] Robinson JA, Strayer RF and Tiedje JM (1981) Method of measuring dissolved hydrogen in anaerobic ecosystems: application to the rumen. Appl Environ Microbiol 41, 545.

[139] Russell JB and Baldwin RL (1979) Comparison of substrate affinities among several rumen bacteria: a possible determinant of rumen bacterial competition. Appl Environ Microbiol 37, 531 – 536.

[140] Sari T (2010) A Lyapunov function for the chemostat with variable yields. C R Acad Sci Paris Ser I, 348 747 – 751.

[141] Sass RL, Fisher FM, Harcombe PA, Turner FT (1991) Mitigation of methane emissions from rice fields: possible adverse effects of incorporated rice straw. Glob Biogeochem Cy 5, 275 – 287.

[142] Schink B (1990) Conservation of small amounts of energy in fermenting bacteria. In Finn RK, Präve P (eds) Biotechnology focus 2, pp 63 – 89. Hanser, Munich, Germany.

[143] Scholten JC and Conrad R (2000) Energetics of syntrophic propionate oxidation in defined batch and chemostat cocultures. Appl Environ Microbiol 66, 2934 – 2942.

[144] Shangguan XJ, Wang MX, Shen RX, Wang YS, Wassmann R, Rennenber H, Seiler W, Xie XL, Wang WD, Xie KH (1994) The feature

of methane emission from a paddy field in the central China region. Sci Atmos Sin 18, 358 – 365.

[145] Shi W, Moon CD, Leahy SC, Kang D, Froula J, Kittelmann S, Fan C, Deutsch S, Gagic D, Seedorf H, Kelly WJ, Atua R, Sang C, Soni P, Li D, Pinares-Patiño CS, McEwan JC, Janssen PH, Chen F, Visel A, Wang Z, Attwood GT, Rubin E (2014) Methane yield phenotypes linked to differential gene expression in the sheep rumen microbiome. Genome Res 24, 1517 – 1525.

[146] Smith HL and Waltman P (1995) The theory of the chemostat: dynamics of microbial competition. Cambridge University Press. Cambridge, UK.

[147] Stouthamer AH (1979) The search for correlation between theoretical and experimental growth yields. In Quayle JR (eds) Microbial biochemistry, pp 1 – 47. University Park, Baltimore, USA.

[148] Statistics New Zealand (2014) New zealand in profile: 2014. http://www.stats.govt.nz/browse_for_stats/snapshots-of-nz/nz-in-profile-2014.aspx. Accessed 15/03/2016.

[149] Stewart AA, Little SM, Ominski KH, Wittenberg KM, Janzen HH (2009) Evaluating greenhouse gas mitigation practices in livestock systems: an illustration of a whole-farm approach. J Agric Sci 147, 367 – 382.

[150] Sun XZ, Hoskin SO, Zhang GG, Molano G, Muetzel S, Pinares-Patiño CS (2012) Sheep fed forage chicory (*Cichorium intybus*) or preennial ryegrss (*Lolium perenne*) have similar methane emissions. Anim Feed Sci Technol 172, 217 – 225.

[151] Sun XZ, Waghorn GC, Hoskin SO, Harrison SJ, Muetzel S, Pacheco D (2012) Methane emissions from sheep fed fresh brassicas (*Brassica* spp.) compared to perennial ryegrass (*Lolium perenne*). Anim Feed Sci Technol 174, 107 – 116.

4478 [152] Sun XZ, Henderson G, Cox F, Molano G, Harrison SJ, Luo D,
4479 Janssen PH, Pacheco D (2015) Lambs fed fresh winter forage rape
4480 (*Brassica napus* L.) emit less methane than those fed perennial
4481 ryegrass (*Lolium perenne* L.), and possible mechanism behind the
4482 difference. PLoS One 10, e0119697.

4483 [153] Subharat S, Shu D, Zheng T, Buddle BM, Janssen PH, Luo D,
4484 Wedlock DN (2015) Vaccination of cattle with a methanogen pro-
4485 tein produces specific antibodies in the saliva which are stable in
4486 the rumen. Vet Immunol Immunopathol 164, 201 – 207.

4487 [154] Sutton JD, Hart IC, Broster WH, Elliott RJ, Schuller E(1986)
4488 Feeding frequency for lactating cows: effects on rumen fermen-
4489 tation and blood metabolites and hormones. Brit J Nutr 56, 181 –
4490 192.

4491 [155] Takahashi J and Young BA (1991) Prophylactic effect of L-cysteine
4492 on nitrate-induced alteration in respiratory exchange and metabolic
4493 rate in sheep. Anim Feed Sci Technol 35, 105 – 113.

4494 [156] Takai Y (1970) The mechanism of methane fermentation in flooded
4495 paddy soil. Soil Sci Plant Nutr 16, 238 – 244.

4496 [157] Ten Brummeler E, Hulshoff Pol LW, Dolfing J, Lettinga G, Zehnder
4497 AJB (1985) Methanogenesis in un upflow anaerobic sludge blanket
4498 reactor at pH 6 on an acetate-propionate mixture. Appl Environ
4499 Microbiol 49, 1472 – 1477.

4500 [158] Tedeschi LO, Cavalcanti LFL, Fonseca MA, Herrero M, Thornton
4501 PK (2014) The evolution and evaluation of dairy cattle models for
4502 predicting milk production: an agricultural model intercomparison
4503 and improvement project (AgMIP) for livestock. Anim Product Sci
4504 54, 2052 – 2067.

4505 [159] Thauer RK, Jungermann K and Decker K (1977) Energy conser-
4506 vation in chemotrophic anaerobic Bacteria. Bacteriol Rev 41, 100
4507 – 180.

[160] Thauer RK, Kaster AK, Seedorf H, Buckel W, Hedderich R (2008) Methanogenic archaea: ecologically relevant differences in energy conservation. Nat Rev Microbiol 6, 579 – 591.

[161] Thompson S, Sawyer J, Bonam R, Valdivia JE (2009) Building a better methane generation model: validating models with methane recovery rates from 35 Canadian landfills. Waste Manage 29, 2085 – 2091.

[162] Tran QH and Uden G (1998) Changes in the proton potential and the cellular energetics of *Escherichia coli* during growth by aerobic and anaerobic respiration or by fermentation. Eur J Biochem 251, 538 – 543.

[163] Ulyatt MJ, Baldwin RL and Koong LJ (1767) The basis of nutritive value – A modelling approach. Proc NZ Soc Anim Prod 36, 140.

[164] Ungerfeld EM and Kohn RA (2006) The role of thermodynamics in the control of ruminal fermentation. In Sejrsen K, Hvelplund T and Nielsen MO (eds) Ruminant physiology: digestion, metabolism and impact of nutrition on gene expression, immunology and stress, pp 55 – 85. Wageningen Academic Publishers, Wageningen, the Netherlands.

[165] Ungerfeld EM, Kohn RA, Wallace RJ, Newbold CJ (2007) A meta-analysis of fumarate effects on methane production in ruminal batch cultures. J Anim Sci 85, 2556 – 2563.

[166] Ungerfeld EM (2013) A theoretical comparison between two ruminal electron sinks. Front Microbiol 4, 319.

[167] US Census Bureau (2016) US and world population clock. http://www.census.gov/popclock/. Accessed 15/03/2016.

[168] van Kessel JAS and Russell JB (1996) The effect of pH on ruminal methanogenesis. FEMS Microbiol Ecol 20, 205 – 210.

[169] van Lingen HJ, Plugge CM, Fadel JG, Kebreab E, Bannink A, Dijkstra J (2016) Thermodynamic driving force of hydrogen on rumen microbial metabolism: a theoretical investigation. PLoS One 11, e0161362.

[170] van Zijderveld SM, Gerrits WJJ, Dijkstra J, Newbold JR, Hulshof RBA, Perdok HB (2011) Persistency of methane mitigation by dietary nitrate supplementation in dairy cows. J Dairy Sci 94, 4028 – 4038.

[171] Varma A, Morbidelli, M and Wu H (1999) Parametric sensitivity in chemical systems. Cambridge University Press, New York.

[172] Vermunt J and Visser R (1987) Nitrate toxicity in cattle. NZ Vet J 35, 136 – 137.

[173] Vetharaniam I, Vibart RE, Hanigan MD, Janssen PH, Tavendale MH, Pacheco D (2015) A modified version of the Molly rumen model to quantify methane emissions from sheep. J Anim Sci 93, 3551 – 3563.

[174] Waghorn GC, Burke JL and Kolver ES (2007) Principles of feeding value. In Rattray PV, Brookes IM and Nicol AM (eds) Pasture and supplements for grazing animals, pp 35 – 59. New Zealand Society of Animal Production, Hamilton, NZ.

[175] Wallace RJ, Wood TA, Rowe A, Price J, Yanez DR, Williams SP, Newbold CJ (2006) Encapsulated fumaric acid as a means of decreasing ruminal methane emissions. Int Congr Ser 1293, 148 – 151.

[176] Walter KM, Zimov SA, Chanton JP, Verbyla D, Chapin, FS (2006) Methane bubbling from Siberian thaw lakes as a positive feedback to climate warming. Nature 443, 71 – 75.

[177] Wang M, Wang R, Xie TY, Janssen PH, Sun XZ, Beauchemin KA, Tan ZL, Gao M (2016) Shift in rumen fermentation and microbiota are associated with dissolved ruminal hydrogen concentrations in

4566 lactating dairy cows fed different types of carbohydrates. J Nutr
4567 DOI:10.3945/jn.116.232462.

4568 [178] Wilhelm E, Battino R, Wilcock RJ (1977) Low-pressure solubility
4569 of gases in liquid water. Chem Rev 77, 219 – 262.

4570 [179] Williams AG and Coleman GS (1992) The rumen protozoa.
4571 Springer-Verlag, London.

4572 [180] Williams YJ, Popovski S, Rea SM, Skillman LC, Toovey AF,
4573 Northwood KS, Wright ADG (2009) A vaccine against rumen
4574 methanogens can alter the composition of archaeal populations.
4575 Appl Environ Microbiol 75, 1860 – 1866.

4576 [181] Wolin MJ (1960) A theoretical rumen fermentation balance. J
4577 Dairy Sci 43, 1452 – 1459.

4578 [182] Wolin MJ (1979) The rumen fermentation: a model for microbial
4579 interactions in anaerobic ecosystems. Adv Microb Ecol 3, 49 – 77.

4580 [183] Wolkowicz GK and Lu Z (1992) Global dynamics of a mathematical
4581 model of competition in the chemostat: general response functions
4582 and differential death rates. SIAM J Appl Math 52, 222 – 233.

4583 [184] Wolkowicz GK and Xia H (1997) Global asymptotic behavior of a
4584 chemostat model with discrete delays. SIAM J Appl Math 57, 1019
4585 – 1043.

4586 [185] Wright ADG, Kennedy P, Neill CJO, Toovey AF, Popovski S, Rea
4587 SM, Pimm CL, Klein L (2004) Reducing methane emissions in
4588 sheep by immunization against rumen methanogens. Vaccine 22,
4589 3976 – 3985.

4590 [186] Zhang L, Huang X, Xue B, Peng Q, Wang Z, Yan T, Wang L (2015)
4591 Immunization against rumen methanogenesis by vaccination with
4592 a new recombinant protein. PloS One 10, e0140086.

4593 [187] Zhuang Q, Melack JM, Zimov S, Walter KM, Butenhoff CL, Khalil
4594 MAK (2009) Global methane emissions from wetlands, rice paddies
4595 and lakes. Eos Trans Amer Geophys Union 90, 37 – 38.